A Parametric Study on Soil-Structure Interaction Mechanisms through A 3D Finite Element Numerical Modelling of Palladium Drive Integral Abutment Bridge in Ontario

by

Yoon-Gi Min

A thesis
presented to the University of Waterloo
in fulfillment of the
thesis requirement for the degree of
Master of Applied Science
in
Civil Engineering

Waterloo, Ontario, Canada, 2013

Author's Declaration

I hereby declare that I am the sole author of this thesis. This is a true copy of the thesis, including any required final revisions as accepted by my examiners. I understand that my thesis may be made electronically available to the public.

Yoon-Gi Min

Abstract

The term "Integral Abutment Bridges" is used broadly all over the world these days. While the expansion joints used in bridges were once a scientifically proved cure to the problem of natural expansion and contraction, there are the excessive maintenance costs being accumulated annually due to the deterioration of essential functions from deicing chemicals and debris. This drawback triggered the advent of Integral Abutment Bridges. The performance of Integral Abutment Bridges at almost no extra costs in seasonal and daily cyclic contraction and expansion can be assessed as a monumental landmark of civil engineering technologies with respect to the massive budget reductions.

However, since Integral Abutment Bridges are destined to expand or contract under the laws of nature, the bridge design became more complicated and sophisticated in order to complement the removal of expansion joints. That is why numerous researchers are attracted to Integral Abutment Bridges with deep interests. Accordingly, in designing the piled abutments of Integral bridges, it is essential to precisely predict the bridge's behavior in advance. In particular, the design requires the comprehensive understanding on the mechanism of the soil-structure interaction, namely, the process regarding the nonlinear responses of the soils behind the abutments and around the piles.

Researchers have been broadly carried out during the last several decades on the behavior of piled bridge abutments. However, most of the studies have been analyzed with focus on structural elements or soils, respectively for the static and dynamic loads such as thermal variations and earthquake loads. In other words, structural researchers are mostly concerned with the structural effect of temperature-induced displacements while geotechnical research workers have been concentrating on the behavior of soils by the response of soil-structure systems.

This presented research developed 3D numerical models with 3 m, 4 m, 5 m, 6 m, 7 m, and 8 m-tall abutments in the bridge using the finite element analysis software MIDAS CIVIL that simulate the behaviors of Integral Abutment Bridges to study the soil-structure interaction mechanism. In addition, this work evaluated and validated the suitability to the limit of the abutment height in Ontario's recommendations for Integral Abutment Bridges by a parametric study under the combined static loading conditions. In order to be a balanced research in terms of a multidisciplinary study, this research analyzed key facts and issues related to soil-structure interaction mechanisms with both structural and geotechnical concerns. Moreover, the study established an explanatory diagram on soil-structure interaction mechanisms by cyclic thermal movements in Integral Abutment Bridges.

Keywords: Integral Abutment Bridges; soil-structure interaction; soil-structure interaction mechanisms; seasonal and daily cyclic contraction and expansion; cyclic thermal movements

Acknowledgements

I would like to express my sincere appreciation to my supervisor, Dr. Leo Rothenburg for his deep insight, guidance, and motivation from his lifetime's experience during this research. This study sparked off from four papers recommended by him when I was bewildered regarding a topic for my thesis. Without him, my thesis would have been put in the shade yet.

My sincerest thanks goes to Dr. Maria Anna Polak since her lecture and advice made my eyes opened about the finite element analysis and help me have an eye to the structural analysis. Her words of encouragement were very supportive during my MASc program.

My deepest thanks also goes to Dr. Giovanni Cascante for his integrity and erudition, for his dynamic leadership to make our geotechnical graduate students active, and for his amazing devotions to our school community.

My sincerest gratitude also goes to Dr. Dipanjan Basu for his profound insight for the research, for his high level of expertise regarding sustainability in geotechnical engineering, and for his contributions to research in North America.

My special thanks goes to my special friends: Mathieu Finas, Kamelia Atefi, Wei Zhang, María José, Bijan Mahbaz, Hassan Ali, Muhammad Irfan, and Fredy Alonso.

I would also like to acknowledge Dr. Wan Ho Song, Dr. Jeehye Lee, Dr. Miok Park, and PhD student Yujin Jung.

Most outstandingly, I would like to pay my innermost respect to my parents.

Lastly, I cannot thank my wife and children enough for being patient with the inconvenience for my program.

Dedication

I dedicate this thesis to

my parents, wife and children, friends, and mentors.

Table of Contents

List of Figures

List of Tables

Chapter 1 Introduction

1.1 Background

The term "Integral Abutment Bridges" is used broadly all over the world in the field of civil engineering. However, relying on the region and time frame, other terms such as integral bridge, integral bridge abutments, joint-less bridge, rigid-frame bridge or U-frame bridge have been emerging or are expected in use as a similar terminology (Horvath, 2000). The concept of conventional bridges with a series of functions by devices including expansion joints, roller supports, and abutment bearings to cope with cyclic thermal expansion and contraction, creep and shrinkage, has been inducing high maintenance costs due to material corrosion and deterioration by leakage of water containing salt or deicing chemicals through the joints. Thus, according to producing an effect opposite to what was intended in traditional bridges, Integral Abutment Bridges have become increasingly popular for limited budgets (Arockiasamy et al., 2004; Shah, 2007; Krier, 2009; and Faraji et al., 2001).

In the United States, since the Teens Run Bridge built was built in 1938 near Eureka in Gallia County, Ohio as the first integral bridge (Burke Jr, 2009), there are approximately 13000 integral abutment bridges, of which about 9000 are full integral abutment bridges, around 4000 are semi-integral abutment bridges (Maruri & Petro, 2005; NYSDOT, 2005). Meanwhile in Canada, several provinces along with Alberta, Quebec, Nova Scotia, and Ontario have integral abutment bridges. Especially Ontario limits its integral bridge span to less than 100 m and a 20-degree skew angle. They also recommend the abutment heights more than 6m should not be considered for integral abutment design, unless it is used in conjunction with the retained soil system. Ontario's recommendations for integral bridges are similar to those used by many US states. These feature a weak joint between the roadway deck and approach slab and a single row of vertical steel H piles (Kunin & Alampalli, 1999; Bakeer et al., 2005; and MTO, 1996). Moose Creek Bridge, one of the prefabricated bridges using precast concrete wall units and deck elements for integral abutment bridges, was built in 2004 in Ontario by the Ministry of Transportation of Ontario (Husain et al., 2005).

In the United States and Canada, overall the model of integral abutment bridges has confirmed to be successful economically in both initial construction and maintenance costs as well as satisfied technically in removing expansion joint problems. However, it does not yet possess a perfect liberty from annual maintenance caused by the bump at bridge approach slabs, decreasing a pavement ride quality for automobiles. Moreover, some maintenance operations for cracks or settlements are required by the excess movements during the winter and summer months. In order to increase the confidence in the design and construction of Integral Abutment Bridges, it is urgent and crucial that a comprehensive and exhaustive performance study be implemented (Horvath, 2000; Husain & Bagnariol, 2000).

1. 2 Research Motivation

Despite the successful performance of Integral Abutment Bridges, the literature indicates that there are primarily three geotechnical uncertainties in their inherent nature regarding their post-construction, in-service problems. It appears that the first one is relative movement between the bridge abutments and adjacent retained soil caused by the result of natural, seasonal thermal variations. The second one results from interaction phenomena occurring in the pile-soil system between vertical piles beneath the abutment wall and soil adjacent to them. The last one is the void created underneath approach slabs by the settled soil. (Horvath, 2000; Faraji et al., 2001)

The motivation for this research has been unsurprisingly generated from a trial to tackle three geotechnical uncertainties enumerated above in Integral Abutment Bridges. The leading motive for this research can be described as follows.

The investigation of geotechnical uncertainties:

This research is a more soil-oriented task congruous to be solved by geotechnical researchers because the major causes in post-construction, in-service problems for Integral Abutment Bridges come down to geotechnical issues.

The multidisciplinary study:

This study is a worthwhile attempt since it should be performed based on the key concepts and theories that civil engineers should know in both geotechnical and structural engineering branches.

The appropriateness of a new and creative contribution to knowledge:

This work is naturally considered as a fresh and contributive activity in terms of the development of knowledge due to evaluate and validate together with recommendations of several states in the USA over the suitability of some Ontario's recommendations through the original modelling of Palladium Drive Integral Abutment Bridge in Ontario.

1. 3 Research Scope and Objectives

The goal of this research is to evaluate and validate together with corresponding guidelines of several states in the USA over the suitability of the limit of the abutment height in Ontario's recommendations to the design for Integral Abutment Bridges by a parametric study through a 3D finite element numerical modelling.

(1) Comparisons to Ontario's recommendations and those of several states in USA

- The limit of the abutment height and wingwall length
- The limit of bridge length and skew

(2) Approach in multidisciplinary study

- Including approach in structural engineering
- Including approach in geotechnical engineering

(3) Modelling including 3m, 4m, 5m, 6m, 7m, 8m-Tall Abutment Bridges

- Including effects of the abutment height on the girder stress
- Including effects of the abutment height on the abutment stress
- Including effects of abutment height on the pile bending moment
- Including effects of the abutment height on the pile stress
- Including effects of the abutment height on the pile displacement

(4) Effects of the pile orientation (weak axis and strong axis)

(5) Effects of the soil stiffness (sand 1, sand 2, clay 1 and clay 2)

(6) Three dimensional finite element numerical modeling

(7) Constructing graphical analysis

The finite element code of MIDAS CIVIL (2013) was used in this study for the 3D numerical modeling.

1. 4 Thesis Organization

This thesis is divided into five chapters including this introductory one.

Chapter 2 explores the primary concepts and theories, and the previous works by accredited scholars and researchers through literature review.

Chapter 3 defines geometry data, material properties, limitations and assumptions for bridge analysis

Chapter 4 presents and reviews the results of the parametric study.

Chapter 5 creates conclusions and recommendations for future research.

Chapter 2 Literature Review

2.1 Introduction

This chapter explores the primary concepts and theories, and the previous works by accredited scholars and researchers regarding this research. The reason for doing so, as aforementioned in Section 1.2, is that the study should be implemented based on the key concepts and theories in both geotechnical and structural engineering branches. Therefore, a clear understanding on related knowledge in this multidisciplinary approach should be preceded in order to be a thorough, exhaustive, and in-depth work before full-fledged discussions are performed.

2.2 Integral Abutment Bridges (IABs)

Figure 2.1 shows the structural elements of an integral abutment bridge including the bridge system consisting of continuous deck-type superstructure, abutment, pile foundation, and the approach system. The basic concept of integral abutment bridges is the use of integral stub-type abutments supported on single rows of vertically driven flexible piles.

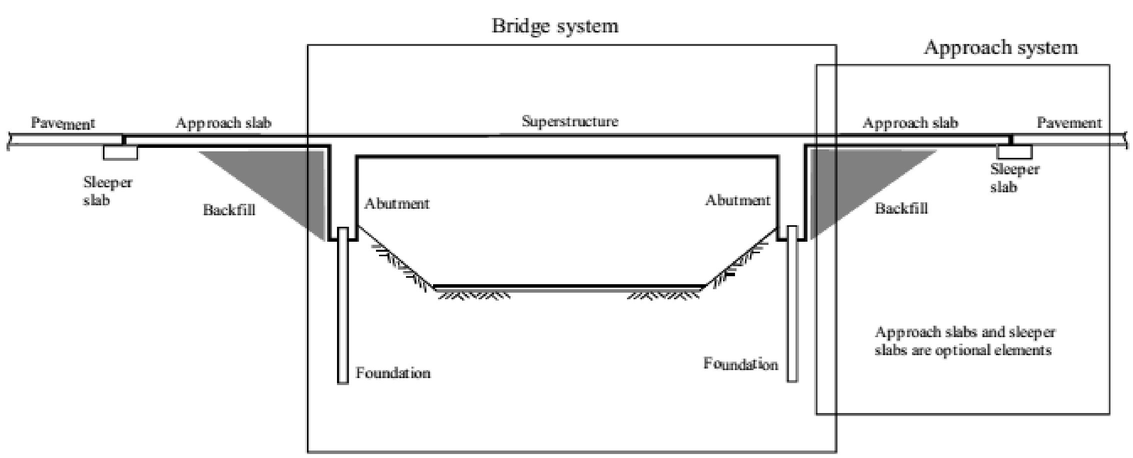

Figure 2.1: Simplified geometry of an integral abutment bridge (Arsoy, 2000)

2.3 The Problems of Integral Abutment Bridges

There are a number of limitations in the design of Integral Abutment Bridges owing to two main problems. Although the IAB concept has confirmed to be economical and technically successful in terms of eliminating expansion joint problems, it is not free from problems. Bridges are susceptible due to a complex soil-structure interaction mechanism involving relative movement between the bridge abutments and the backfill, and the piles and adjacent soil. One of the two major problems observed with IABs is the development of lateral earth pressures against the abutments. The other is the void development under approach slabs. (Horvath, 2000).

2.4 Soil-Structure Interaction

Soil-Structure Interaction can be divided into soil-abutment interaction and soil-pile interaction. Kim (2009) argues that the movement of the back-wall by expansion of the superstructure is resisted by the back-fill behind the abutment and the soil around piles. The soil imposes a compressive load on the backwall and abutment, resisting its displacement. The passive pressure on the structure significantly increases by its displacement. A change in backfill stiffness does not significantly affect IAB response. (Kim. 2009)

The lateral movement of piles is significantly affected by the soil stiffness around the piles. The stiffness of the supporting soil depends on the soil type. A reduction of soil stiffness causes an increase in horizontal displacement. Maximum horizontal displacement varies significantly when the pile orientation is changed. Therefore, the piles are often installed with their weak axis of bending parallel to the bridge centerline. (Arockiasamy et al. 2004; Wasserman, 2007)

2.5 Temperature Effects

A change in temperature causes a material to change in length. This fundamental property of materials is responsible for expansion and contraction of bridge superstructures. As the temperature increases, the bridge expands. As the temperature cools down, the bridge will contract to shorter. In conventional bridges, expansion joints exist between the superstructure and the abutment to accommodate these displacements. On the contrary, in integral abutment bridges, the expansion joints are eliminated and the superstructure is allowed to freely displace the bridge abutments. In this way, the pile and the approach fill are subjected to lateral loading and unloading due to the abutment displacements. The properties of the structure materials substantially affect the bridge responses to temperature effects. The bridge responses to the temperature loads are governed by many factors, such as types of soil adjacent to abutment, abutment displacements including translations and rotations, piles types and arrangements, and so on (Metzger, 1995; Bettinger, 2001; Arsoy et al., 2004; Shah, 2007; Shehu, 2009).

2.6 Nonlinear Analysis of Integral Bridges: Finite-Element Model (Faraji et al., 2001)

Falaji et al. (2001) illuminate several benefits of Integral abutment bridges (IABs), which are cost reduction, decreased corrosion and degradation, better maintenance, and enhanced capacity to seismic loading. However, the authors highlight the reaction of the soil-abutment system and soil-foundation piles as a largest uncertainty. In order to examine that issue, they created a full three dimensional finite-element model of IABs with three spans. They represented that the nonlinear soil response adjoining with abutments and piles is symbolized into the spring system behind abutments and next to supporting pile.

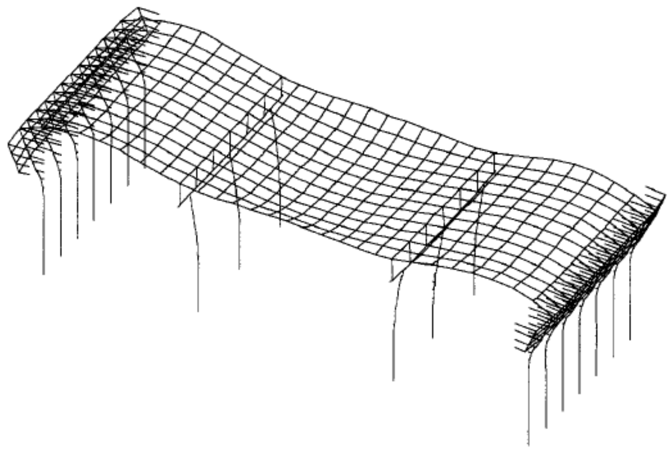

Figure 2.2: Deformed Shape of FE Mesh after Thermal Loading (Deflections Exaggerated), (Faraji et al., 2001)

As shown in Figure 2.2, they found that one of the most significant factors affecting the overall bridge behavior is the level of soil compaction behind the abutment wall. Thus, they recommended that non-compaction back system is necessary in IAB design.

2.7 Performance of Abutment–Backfill System under Thermal Variations IN INTEGRAL Bridges Built on Clay (Dicleli & Albhaisi, 2004)

In their study (2004), they indicate their interests for the maximum length limits and an extremely comprehensive abutment-backfill system. As expressed in Figure 2.3, the authors studied the performance of the abutment–backfill system under thermal variations through modeling of a six span slab-on-steel-girder integral bridge. They describe palpably and tangibly over the stiffness of the clay, widely using of stub abutments (less than 1.0 m below the deck soffit) in North America, the orientation of the piles supporting the abutment, and the connecting method between the abutment and the pile head.

In their study, they developed design guidelines to determine the maximum forces in integral bridge abutments as a function of the displacements by thermal variations.

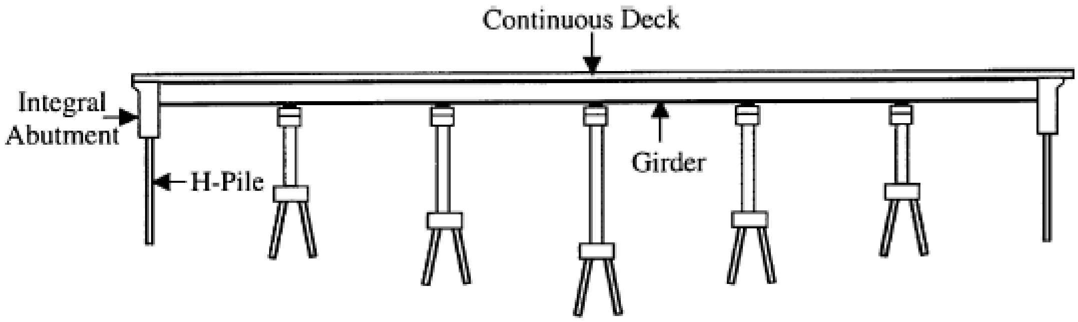

Figure 2.3: Six span slab-on-steel-girder integral bridge used in their study (Dicleli & Albhaisi, 2004)

The main findings drawn from their study are as follows:

- The stiffness of the clay substantially influences on the magnitude of the internal forces in the abutment, which is required to decrease for improving its capacity.
- Stub abutments are intensely required in integral bridges due to control the maximum length limit of integral bridges.
- Non-compacted backfill system is strongly recommended in the design of Integrated Abutment Bridges.
- The orientation of the piles supporting the abutment should be installed about their weak axis of bending to secure additional capacity against the flexural forces.
- The application of a pin joint between the abutment and the pile head has the validity because of the reduction of the flexural demand on the abutment.
- The variations in the abutment thickness within the dimensional limits (1–1.5 m), have only a insignificant effect on the distribution and intensity of the backfill pressure.

In conclusion, this paper is considerably trustworthy for the further research since they provide nonlinear modeling procedure in detail.

Chapter 3 Numerical Modeling of Integral Abutment Bridge

3.1 Introduction

The bridge site is located along Palladium Drive Interchange over Hwy 417 in the western suburb of Kanata, in Ottawa, Ontario as shown in Figure 3.1. The existing bridge, a two span prestressed concrete girder bridge was built in 1993. Figures 3.1 and 3.2 show two satellite views of Palladium Drive IAB with the length (73 m) and the width (20.4 m) (MTO, 1996).

Figure 3.1: Site Location of Palladium Drive IAB (taken from Google Maps)

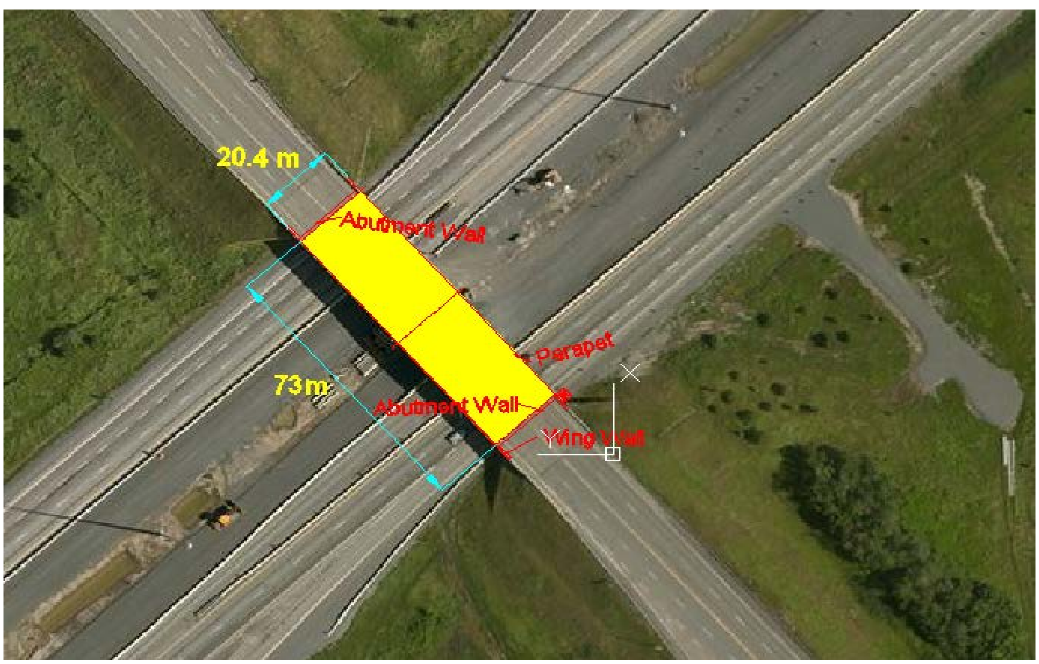

Figure 3.2: Aerial View of Palladium Drive IAB (taken from Bing Maps)

3.2 Limitations and Assumptions

Figure 3.3: Elevation View of Palladium Drive IAB (Husain & Bagnariol, 2000)

Palladium Drive IAB as shown in Figure 3.3 was chosen for this purpose due to a symmetrical integral bridge with no skew to save calculation time and to effectively reflect the abutment–backfill interaction effects under thermal variations by seasonal and daily temperature changes. This pre-stressed concrete girder bridge has the bridge deck to be 73 m long and 20.4 m wide with each span measuring 36.5 m, and each abutment supported by steel H-shaped piles according to the Ministry of Transportation of Ontario (MTO, 1996) .

For effective accomplishments of the research goal and the parametric study, the foundation soil is assumed to be either clay or sand. Accordingly, two different sand and clay stiffnesses are included in the presented study. For medium-stiff and stiff clay, corresponding values of the undrained shear strength (C_u) 40, 80 kPa and the soil strain at 50% of ultimate soil resistance (e_{50}) 0.01, 0.006, and for medium dense and dense sand, corresponding values of the coefficient of horizontal subgrade reaction, k, 6000, 12000 (kN/m^3) which were adopted from two references (Bowles, 1996; Reese et al, 2006), were used in this parametric study.

Furthermore, for the model with various abutment heights, the abutments and corresponding wingwalls are modified in 3 m, 4 m, 5 m, 6 m, 7m, and 8 m high, respectively. Thus, each abutment is supported on a single row of 15 H-shaped piles, as shown in Figures 3.4 and 3.5. Correspondingly, the length of H-shaped piles is revised in 17 m, 16 m, 15 m, 14 m, 13m, and 12 m long, respectively except that the top of the H-shaped piles was embedded 0.6 m into the abutment wall, according to variations of the abutment heights enumerated above. The water table is assumed to be at 1.1 m below its sub-road surface (- 6.9 m from the top of abutments).

3.3 Two Dimensional Geometry for 3D Modeling of Palladium Drive IAB

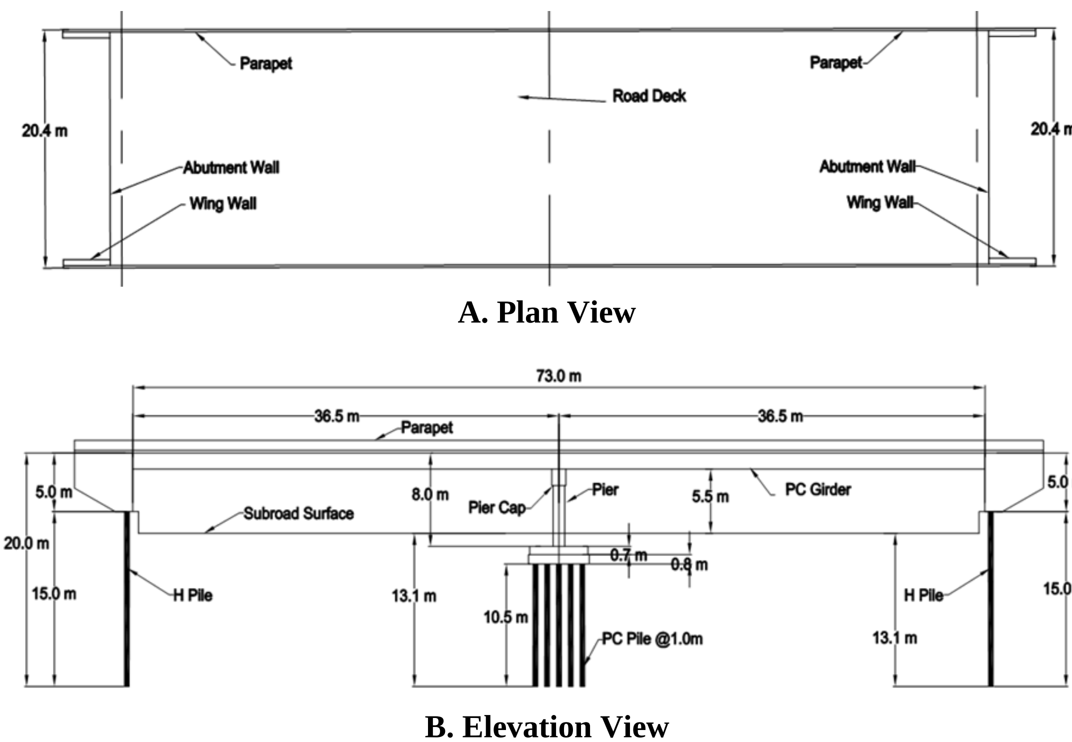

Figure 3.4: Plan and Elevation Views of Palladium Drive IAB

Figure 3.4 shows plan and elevation views of Palladium Drive IAB with 5-m-tall abutments and 5.5 m vertical clearance. The length of PC piles supporting four piers is 10.5m except that the top of the PC piles was embedded 0.4 m into the PC pile cap with 0.8 m thick.

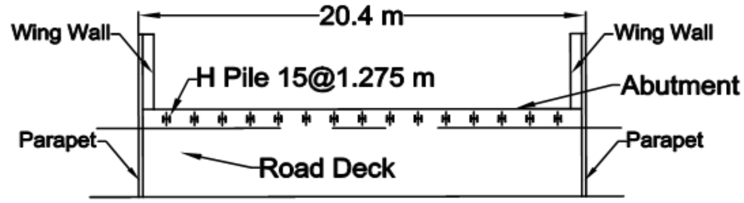

A. Plan View for H-shaped Piles

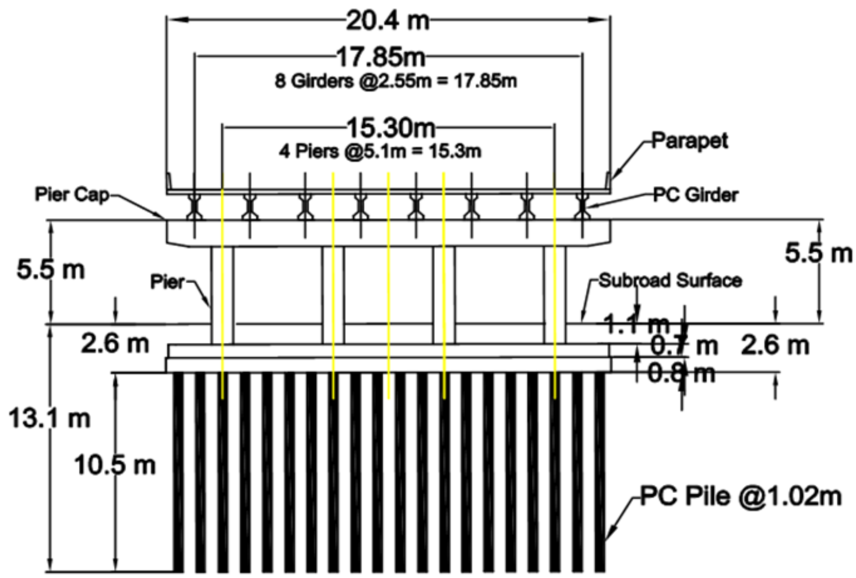

B. Section View for Center Piers

Figure 3.5: Plan View for H-shaped Piles and Section View for Center Piers

Figure 3.5.A indicates 15 H-shaped piles with spacing 1.275m embedded into the bottom of each abutment in weak axial direction. Figure 3.6 expresses eight pre-stressed concrete girders, its rigid-connected abutment, and its road deck including four traffic lanes with each 3.6 m wide. As shown in Figures 3.5 and 3.6, the bridge superstructure is a typical slab-on-girder, with a 225 mm reinforced concrete deck that is assumed fully composite with eight AASHTO (American Association of State Highway and Transportation Officials) Type IV pre-stressed concrete girders. This bridge model was created in the bridge finite element analysis software MIDAS CIVIL (2013).

Figure 3.6: Views for PC Girders and Road Deck of the bridge (taken from Google Maps)

3.4 Configuration of Main Elements of Palladium Drive IAB Model

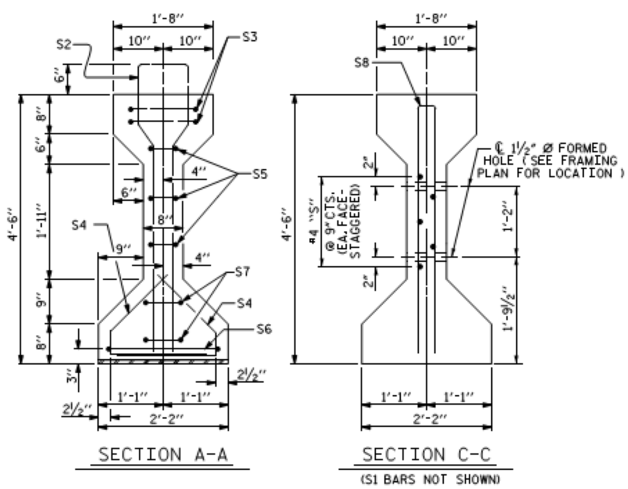

AASHTO Type IV (Source: NCDOT Website)

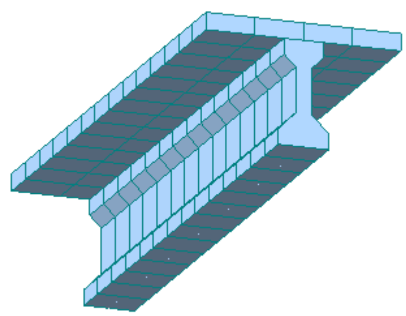

Composite girder

Figure 3.7: AASHTO Type IV PC Girder and Deck Slab

As shown in Figures 3.7 and 3.8, AASHTO Type IV pre-stressed concrete girder has 1371mm (4 feet 6 inch) deep, 508 mm (1 foot 8 inch) top wide, and 660.4 mm (2 feet 2 inch) bottom wide. This girder and slab create composite action between them. The deck slab in the elements exhibiting composite action has 0.225 m thick and 2.55m wide. Figure 3.9 displays that the substructure in each side consists of 15 steel H-shaped piles, an abutment, and two wingwalls.

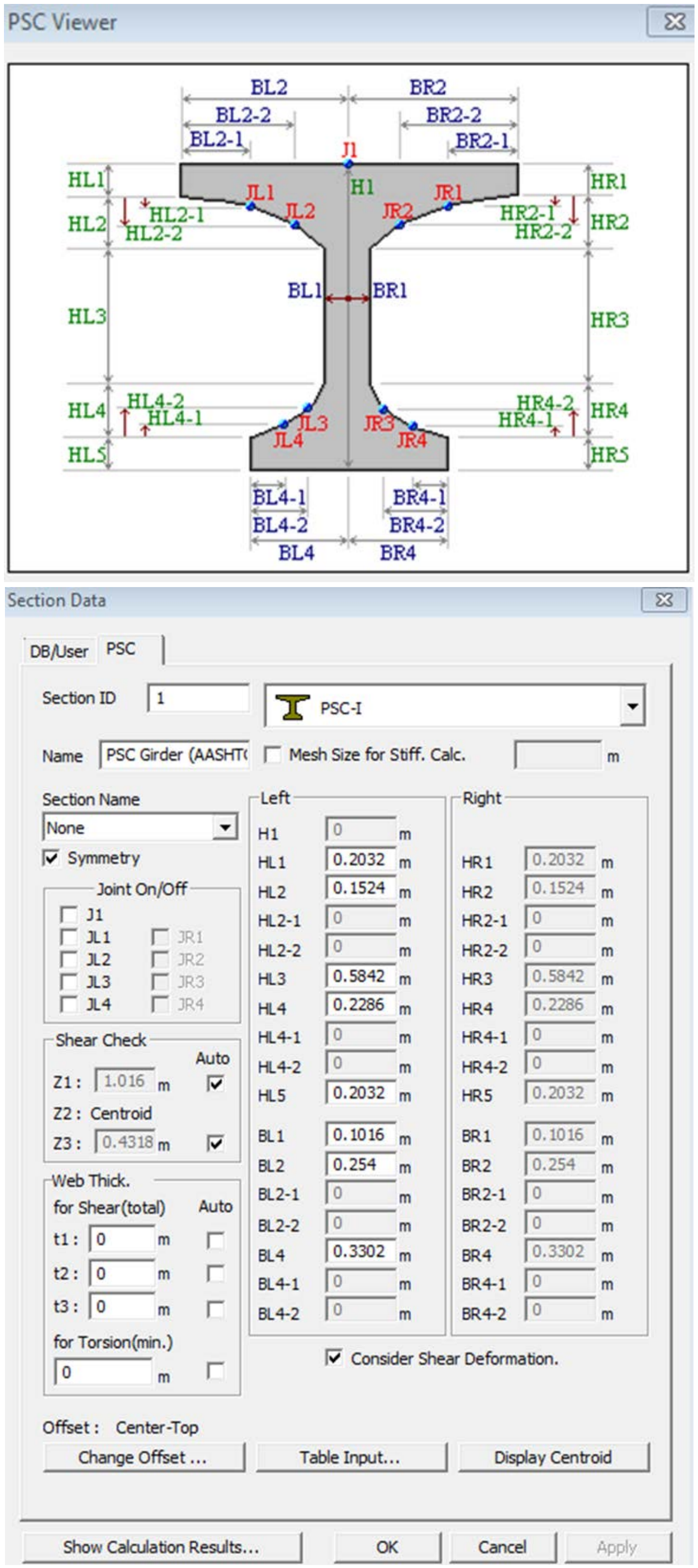

Figure 3.8: Built-In Database for AASHTO Type IV PC Girder in MIDAS CIVIL

Steel H-shaed Pile (HP 310*125)	Abutment (Thickness: 1 m)	Wing Wall (Thickness: 0.45 m)	Sub-Structure in Each Side
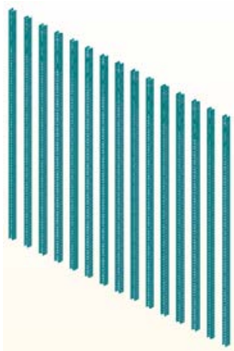	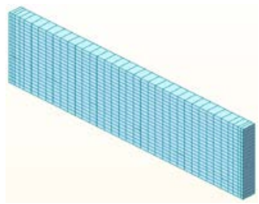	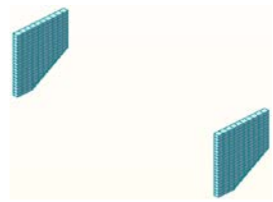	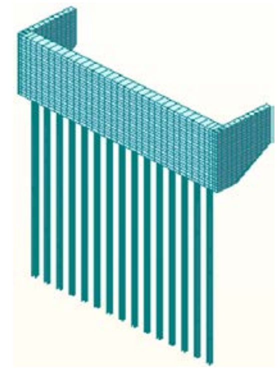

Figure 3.9: Configuration of 15 Steel H-shaped piles, an Abutment, and two Wingwalls

3.5 Material Properties

The material properties for soils used in this study were adopted from two References (Bowles, 1996; Reese et al, 2006). Concrete components were modeled using homogeneous, isotropic elements and are assumed linear-elastic. The non-linear behavior of the steel pile was assumed to be elastic perfectly plastic. The material properties used in this study are shown in Tables 3.1 and 3.2.

In Table 3.1, notations are as follows:

$\boldsymbol{\gamma_{unsat}}$ (Unsaturated unit weight), $\boldsymbol{\gamma_{sat}}$ (Saturated unit weight), $\boldsymbol{\gamma_{w}}$ (Water unit weight), $\boldsymbol{\gamma'}$ (Submerged unit weight), $\boldsymbol{\phi'}$ (Effective stress friction angle), $\mathbf{K_0}$ (Coefficient of earth pressure at rest), **e** (Void ratio in soils), $\mathbf{G_s}$ (Specific gravity of soil solids), $\boldsymbol{\gamma_d}$ (Dry unit weight), $\mathbf{e_{50}}$ (Soil strain at 50% of ultimate soil resistance), $\mathbf{C_u}$ (Undrained shear strength), and **k** (Coefficient of horizontal subgrade reaction).

Table 3.1: Material Properties for Soils

Soil Type	Sand 1	Sand 2	Clay 1	Clay 2
	Medium-Dense	Dense	Medium-stiff	Stiff
γ_{unsat} (kN/m^3)	19	20	18	19
γ_{sat} (kN/m^3)	20	21	19	20
γ_w (kN/m^3)	9.81	9.81	9.81	9.81
γ' (kN/m^3)	10.19	11.19	9.19	10.19
ϕ' (deg)	32	38	-	-
K_0	0.47	0.38	0.63	0.61
e_{50}	-	-	0.01	0.006
C_u (kPa)	-	-	40	80
k (kN/m^3)	6,000	12,000	4,500	9,500

Table 3.2: Material Properties for Structure

Elements	Strength f'c, (MPa = 10^6 N/m^2)	Young's Modulus E, (MPa = 10^6 N/m^2)	Poisson's Ratio	Coefficient of thermal expansion α, (1/°C)
PC Girder	50	3.02E+04	0.167	1.00E-05
Diaphragm	50	3.02E+04	0.167	1.00E-05
Deck Slab	40	2.78E+04	0.167	1.00E-05
Abutment & Wing wall	40	2.78E+04	0.167	1.00E-05
Piers & Pier Cap	50	3.02E+04	0.167	1.00E-05
PC Piles & Cap, Footing	50	3.02E+04	0.167	1.00E-05
Steel H-shaped Piles	400*	2.00E+05	0.3	1.20E-05

* Minimum Yield Strength

3.6 Loads

3.6.1 Ambient Temperature Load

This study utilizes the AASHTO LRFD (2012) recommended design temperature range of 0ºF to 80ºF (-18ºC to 27ºC) for concrete structures in cold climates as shown Table 3.3. Each reference temperature of 5 ºC (Summer) and 0 ºC (Winter) was assumed. The assumed reference temperature translates to a temperature rise (expansion) of + 22 degree and -18 degree fall (contraction).

Table 3.3: A Temperature Ranges (AASHTO LRFD, 2012)

Climate	Steel or Aluminum	Concrete	Wood
Moderate	0° to 120°F	10° to 80°F	10° to 75°F
Cold	-30° to 120°F	0° to 80°F	0° to 75°F

3.6.2 Temperature Gradient

The superstructure temperature gradient contributes considerably to superstructure stresses in IABs and is included in this study by using AASHTO LRFD (2012) as shown in Figure 3.10.

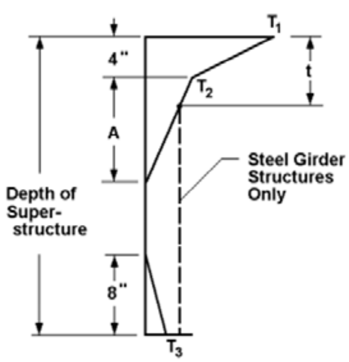

Zone	T_1 (°F)	°C	T_2 (°F)	°C
1	54	12.2	14	-10
2	46	7.8	12	-11.1
3	41	5	11	-11.7
4	38	3.3	9	-12.8

Figure 3.10: Vertical temperature gradient (AASHTO LRFD, 2012)

The vertical temperature gradient in concrete and steel superstructures with concrete decks was used as a zone 3 considering the interstate border as shown in Figures 3.10 and 3.11.

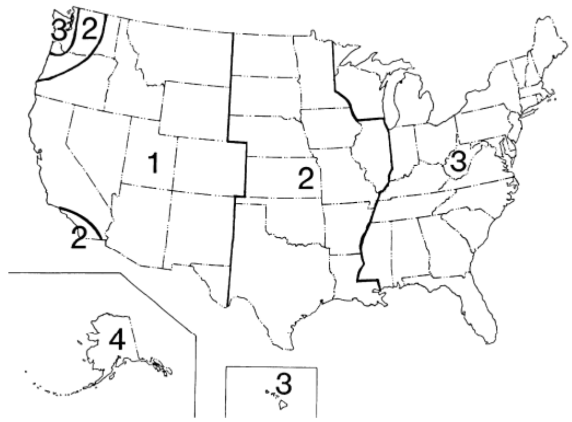

Figure 3.11: Solar Radiation Zones for the United States (AASHTO LRFD, 2012)

3.6.3 Earth Pressure

As stated in Chapter 2, passive earth pressure is the biggest as shown Figure 3.12. However, the earth pressure at rest was applied in this study for the normal condition.

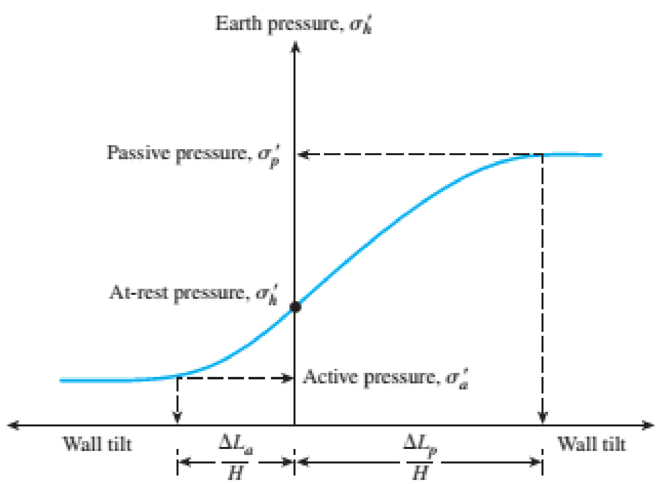

Figure 3.12: Variation of the magnitude of lateral earth pressure with wall tilt (Das, 2010)

The coefficient of earth pressure at rest K_0 is normally determined by the following empirical relationship (Jaky, 1944).

$$\mathbf{K_0} = 1 - \sin\phi' \quad (3\text{-}1)$$

3.6.4 Parapet Load

The elements of parapet were not developed in the model. Accordingly, as shown Figure 3.13, the parapet load is applied on both longitudinal edge nodes of the bridge deck as 10 kN/m.

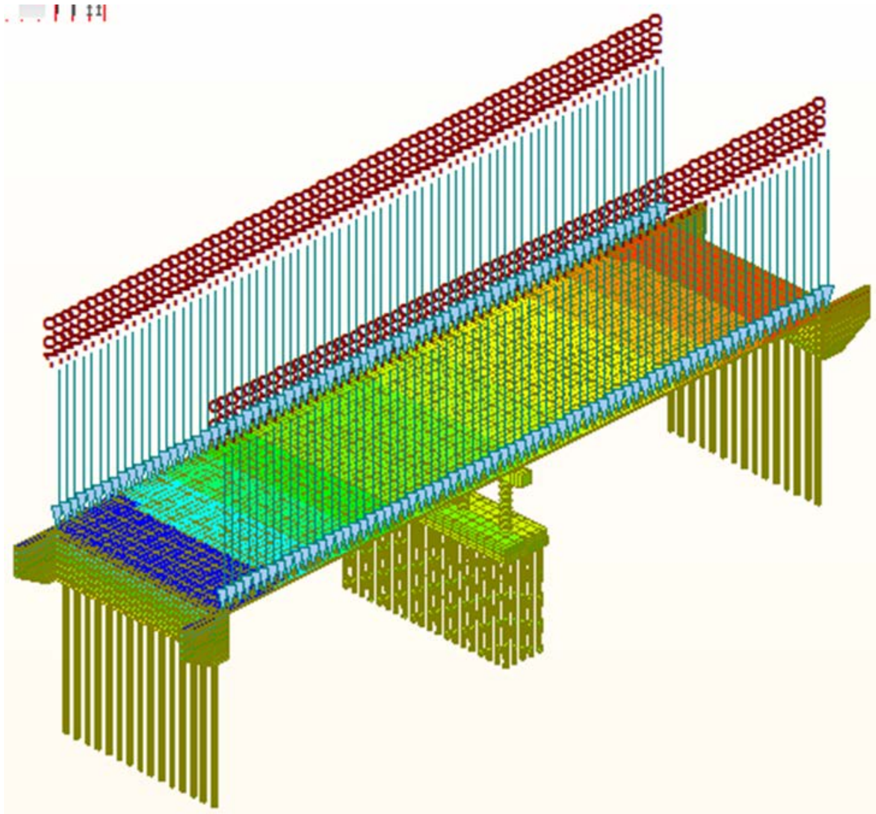

Figure 3.13: Parapet load (applied 10 kN/m)

3.6.5 Static Combination Load

In this study, to simulate real conditions in IABs, the static combination load was used as follows.

Load combination 1 (LCB 1) creates expansion. LCB 1 includes the following:

Self-Weight + Parapet Load + Earth Pressure at rest + Temperature Load (positive) + Temperature Gradient

Load combination 2 (LCB 2) creates contraction. LCB 2 includes the following:

Self-Weight + Parapet Load + Earth Pressure at rest + Temperature Load (negative) + Temperature Gradient

3.7 Compared Standards to Ontario's recommendations for IABs

Tables 3.4 and 3.5 contrast the limit of the abutment height, wingwall length, span length, and skew in Canada and USA. Ontario's recommendations for integral bridges are similar to those used by many US states in in terms of span length and skew whereas Ontario's are one and a half times more than those of US states with regard to the abutment height. Thus, this study evaluates six types of abutments with a height (3m, 4m, 5m, 6m, 7m, and 8m) for comparison.

Table 3.4: The limit of Abutment Height in Canada and USA

(Modified from Conboy & Stoothoff, 2005)

Provinces or States	Abutment Height Meters (feet)	Wingwall Length Meters (feet)	Note
Connecticut	2.44 (8)	-	Exclusion from application if used in conjunction with the retained soil system
Maine	3.66 (12)	3.05 (10)	
Massachusetts	3.96 (13)	3.05 (10)	
New Hampshire	-	-	
Vermont	3.96 (13)	3.05 (10)	
Ontario	6.0 (19.7)	7 (23.0)	

Table 3.5: The limit of Span Length and Skew in Canada and USA

(Modified from Conboy & Stoothoff, 2005)

Provinces or States	Span Length		Skew Angle (Degrees)
	Steel Meters (feet)	Concrete Meters (feet)	
Connecticut	-	-	20
Maine	70.0 (200)	100.6 (330)	30
Massachusetts	100.6 (330)	179.8 (590)	30
New Hampshire	91.4 (300)	182.9 (600)	-
Vermont	100.6 (330)	179.8 (590)	20
Ontario	100.0 (328)	100.0 (328)	20

3.8 Dimensions, Spacing, and Complete Images Figuration for Bridge Components

Figures 3.14 through 3.17 display dimensions, spacing, and complete images for bridge components used in this study. Further details for AASHTO Type IV pre-stressed concrete girder shown in Figure 3.14 are expressed in Figure 3.8.

Name	Configureration	Dimensions and Spacing
PC Girder	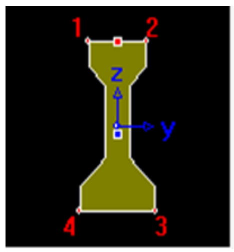	**Height: 1.371 m** **Width (Top): 0.508 m** **Width (Bottom): 0.6604 m** **Spacing (Trav.): 8@1.275 m** **Trav.: Traverse Direction** **(Refer to Figure 3.8 for further details)**
Diaphragm	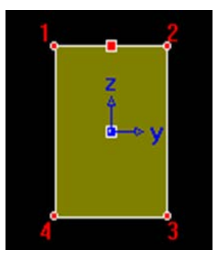	**Height: 1.371 m** **Width (Top): 1.0 m** **Width (Bottom): 1.0 m** **Spacing: 0 m** **(Only one on Pier Cap)**
Deck Slab	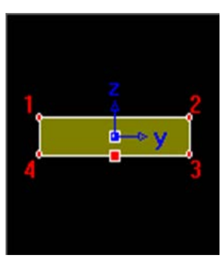	**Thickness: 0.225 m** **Width (Long.): 73.0 m** **Width (Trav.): 20.4 m** **Long.: Longitudinal Direction** **Trav.: Traverse Direction**

Figure 3.14: Dimensions and Spacing for Bridge Components (A)

Name	Configureration	Dimensions and Spacing
Abutment	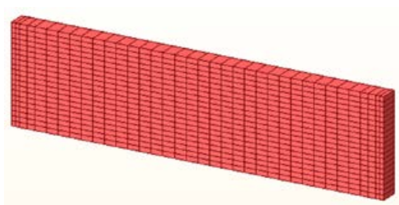	**Height: 5.0 m (For 5m-Tall Abutment)** **Width (Trav.): 20.4 m** **Thickness: 1.0 m** **Spacing (Long.): 2@73.0 m (Center to Center)** **Long.: Longitudinal Direction** **Trav.: Traverse Direction**
Wingwall	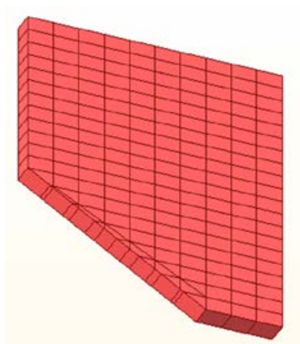	**Height (Left)*: 3.0 m (For 5m-Tall Abutment)** **Height: (Right)*: 5.0 m (For 5m-Tall Abutment)** **Width (Top): 5.0 m** **Width (Bottom): 1.5 m** **Thickness: 0.45 m** **Spacing: 19.95 m at Each Abutment** **(Center to Center, Symmetrical)** *** : Variable depending on Abutment Hight,** **Abutment Height 3m: 1 m (Left), 3 m (Right)** **Abutment Height 4m: 2 m (Left), 4 m (Right)** **Abutment Height 6m: 4 m (Left), 6 m (Right)** **Abutment Height 7m: 5 m (Left), 7 m (Right)** **Abutment Height 8m: 6 m (Left), 8 m (Right)**
Pier		**Height: 5.129 m** **Diameter: 1.0 m** **Spacing: 4@2.55 m**
Pier Cap	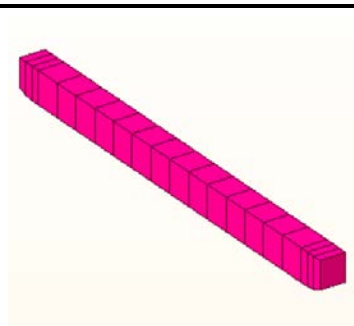	**Height: 1.4 m (1.2 m at tapered ends)** **Width (Top): 1.2 m** **Width (Bottom): 1.2 m** **Length: 20.4 m** **Spacing: 0 m** **(Only one on Piers)**

Figure 3.15: Dimensions and Spacing for Bridge Components (B)

Name	Configureration	Dimensions and Spacing
PC Piles	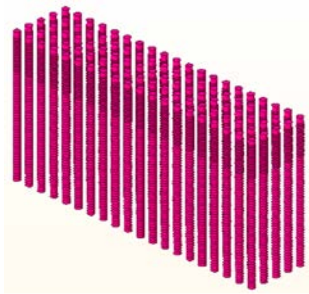	Length: 10.5 m (Except Embedded 0.4 m into the Pile Cap) Diameter: 0.45 m Spacing (Long.): 5@1.0 m Spacing (Trav.): 20@1.02 m Long.: Longitudinal Direction Trav.: Traverse Direction
PC Pile Cap	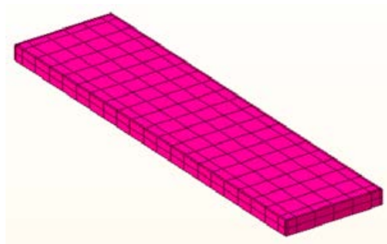	Thickness: 0.8 m Width (Long.): 5.2 m Width (Trav.): 20.58 m Long.: Longitudinal Direction Trav.: Traverse Direction
Footing	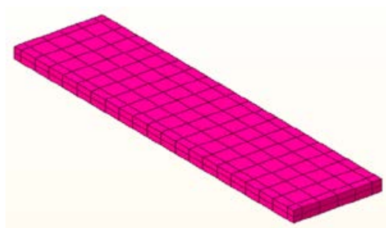	Thickness: 0.7 m Width (Long.): 5.0 m Width (Trav.): 20.38 m Long.: Longitudinal Direction Trav.: Traverse Direction
Steel H-shaped Piles	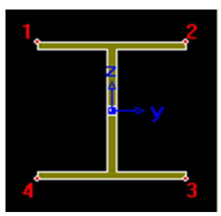 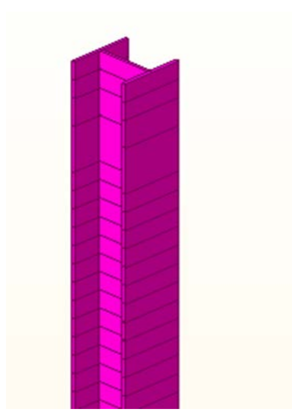	Height: 0.312 m Width (Top): 0.312 m Width (Bottom): 0.312 m Thickness (Web): 0.0174 m Thickness (Flange): 0.0174 m Length*: 15.0 m (For 5 m-Tall Abutment, Except Embedded 0.6 m) Spacing (Trav.): 15@1.275 m (Symmetrical at Each Abutment) Trav.: Traverse Direction * : Variable depending on Abutment Hight, Abutment Height 3m: 17 m (Except Embedded 0.6 m) Abutment Height 4m: 16 m (Except Embedded 0.6 m) Abutment Height 6m: 14 m (Except Embedded 0.6 m) Abutment Height 7m: 13 m (Except Embedded 0.6 m) Abutment Height 8m: 12 m (Except Embedded 0.6 m)

Figure 3.16: Dimensions and Spacing for Bridge Components (C)

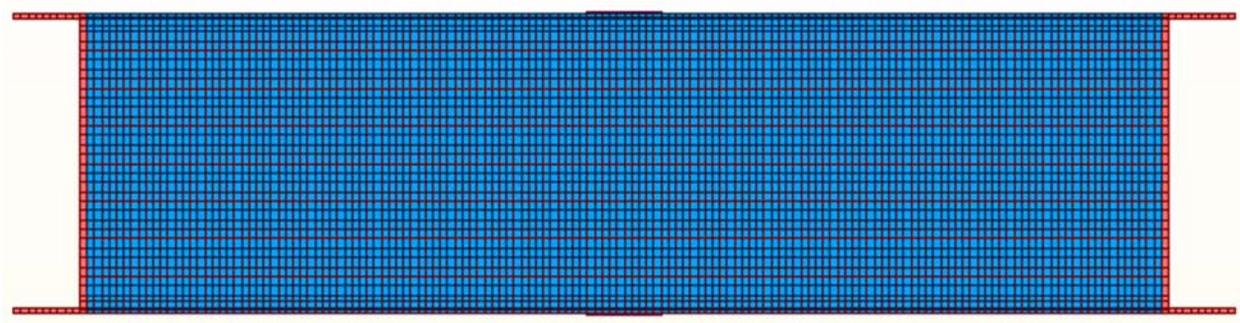

A. Plan View of 5 m-Tall Abutment Bridge Model

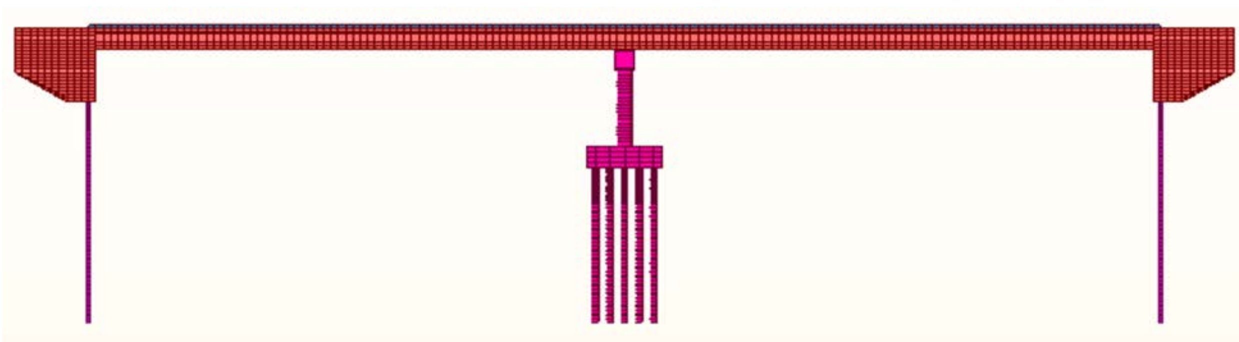

B. Front Elevation View of 5 m-Tall Abutment Bridge Model

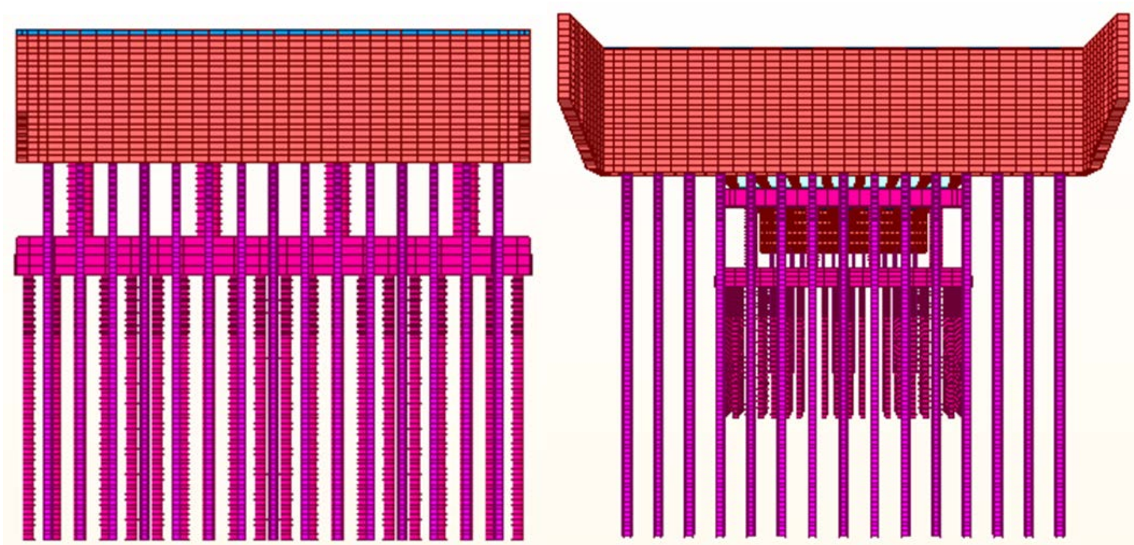

C. Side Elevation View and Perspective View of 5 m-Tall Abutment Bridge Model

Figure 3.17: Panorama of 5 m-Tall Abutment Bridge Model

3.9 Variations of Abutment Height in Palladium Drive IAB Model

Figures 3.18 and 3.19 show the models with 3 m, 4 m, 5 m, 6 m, 7m, and 8 m-tall abutment, respectively. As described in Figure 3.15, wingwalls were modified in high according to abutment height, respectively.

Abutment Height	Isometric View
3 m-Tall Abutment **(H pile: 17 m long)**	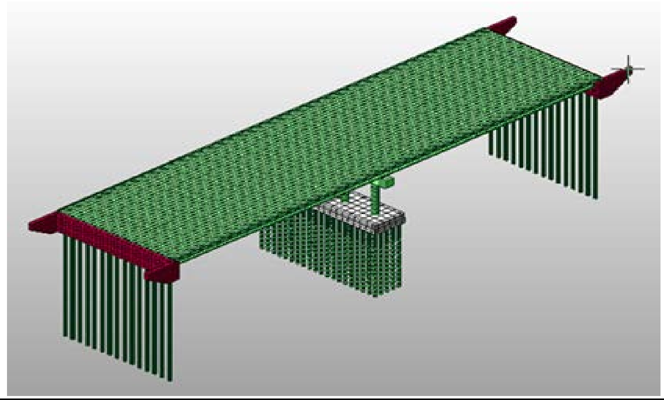
4 m-Tall Abutment **(H pile: 16 m long)**	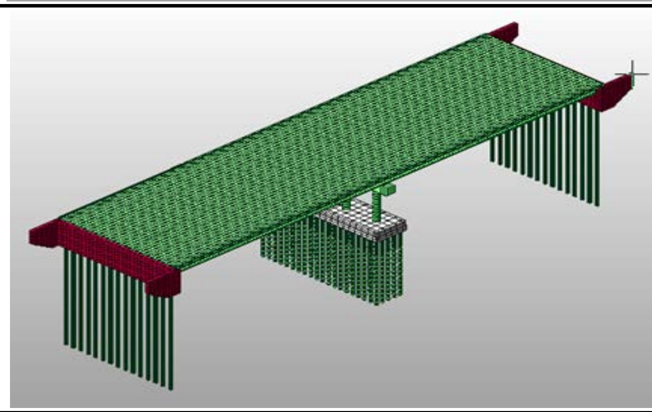
5 m-Tall Abutment **(H pile: 15 m long)**	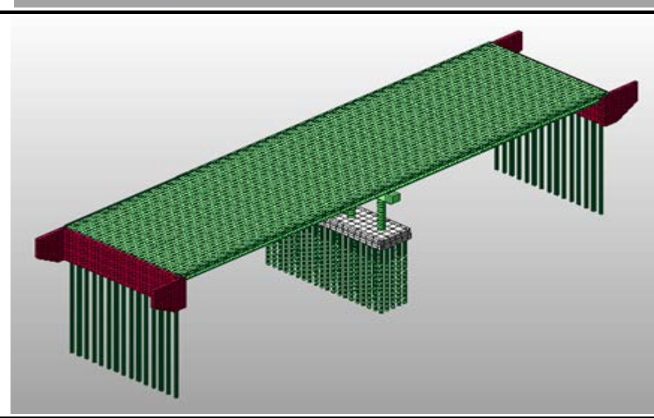

Figure 3.18: Completed Geometry of 3 m, 4m, 5m Tall Models

Abutment Height	Isometric View
6 m-Tall Abutment **(H pile: 14 m long)**	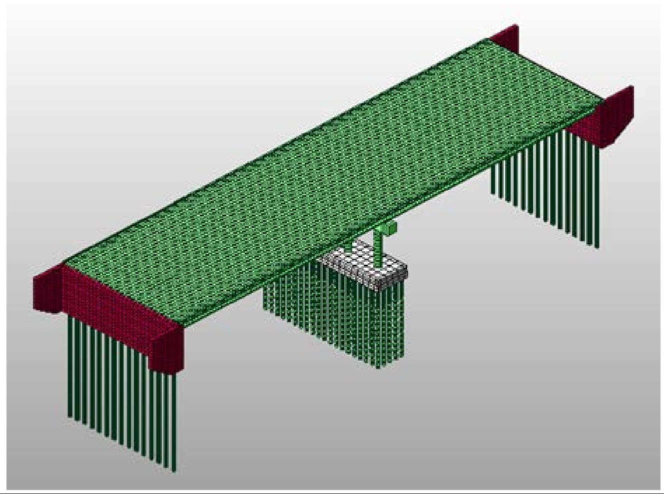
7 m-Tall Abutment **(H pile: 13 m long)**	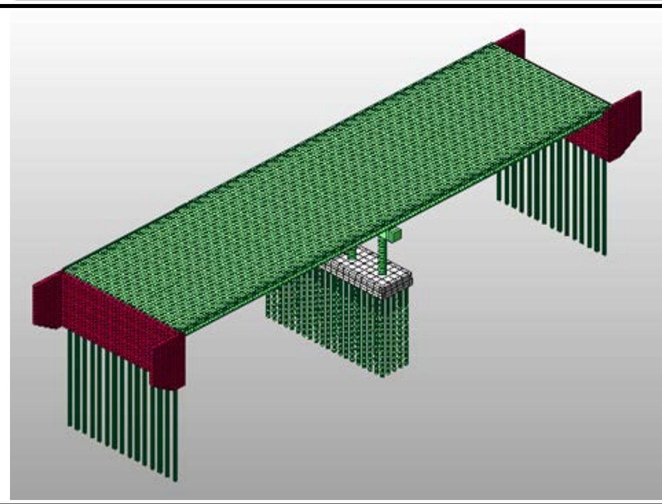
8 m-Tall Abutment **(H pile: 12 m long)**	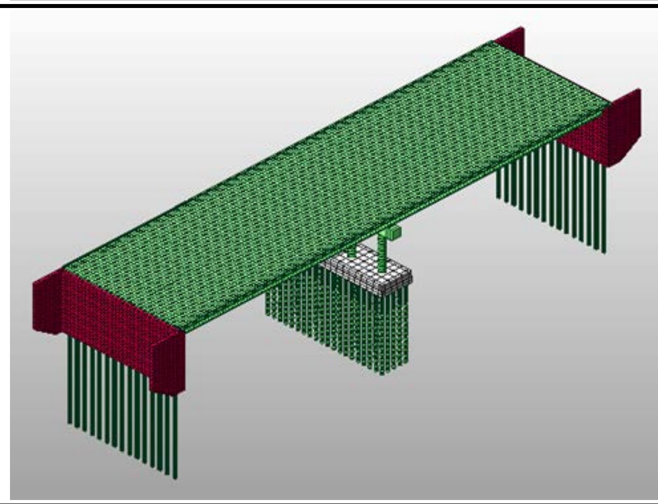

Figure 3.19: Completed Geometry of 6 m, 7m, 8m Tall Models

Chapter 4 Parametric Study Results and Reviews

4.1 Introduction

This chapter lays out the results from the parametric study performed using the 3D numerical models mentioned in Chapter 3. The results of the parametric study are illustrated colorfully to exactly represent to the prediction of IAB behavior. Seven important matters are as in the following sections: (1) Girder Stress, (2) Abutment Stress, (3) Pile Moment, (4) Pile Stress, and (5) Pile Displacement, (6) Soil-Abutment Interaction, and (7) Soil-Pile Interaction.

4.2 Girder Stress

Figures 4.1 and 4.2, show the maximum combined girder stress induced by expansion or contraction cases.

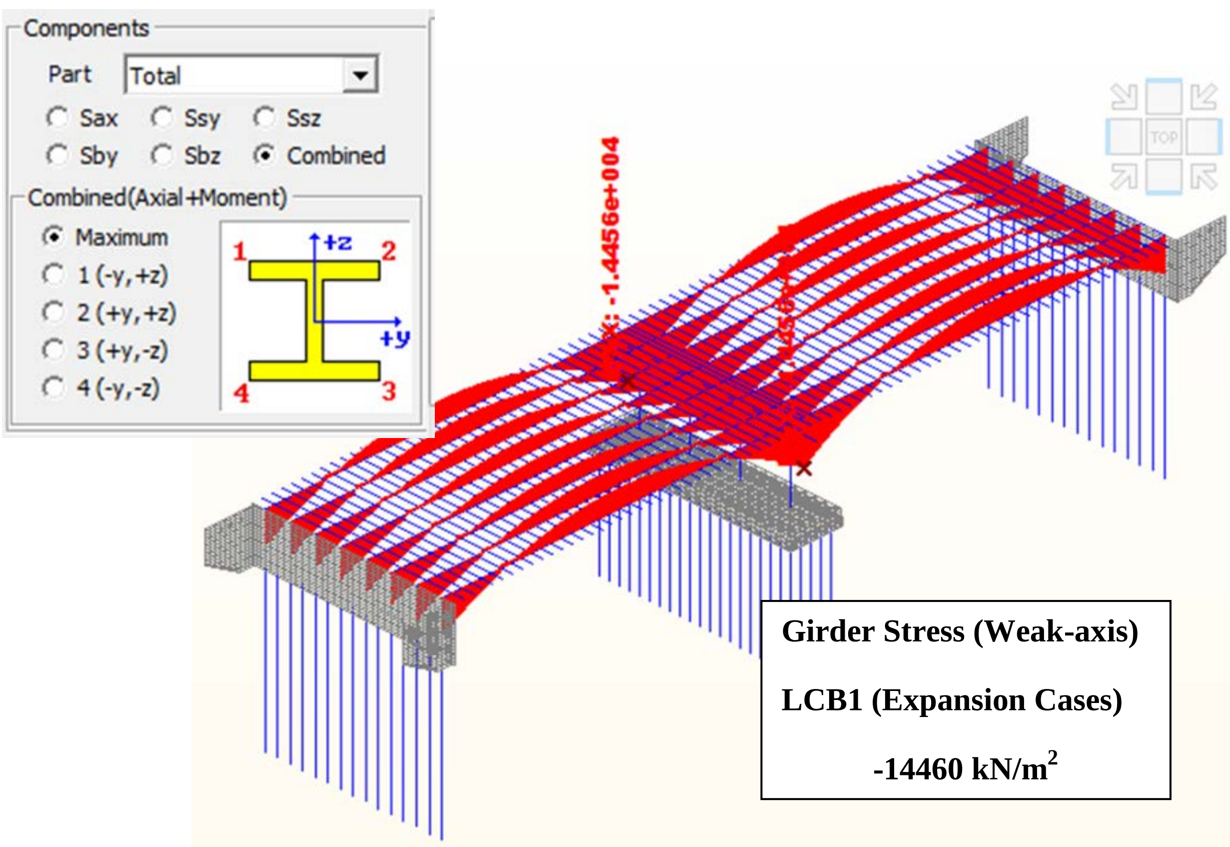

Figure 4.1: Girder Stress in 5m-Tall Abutment with Sand 1 & Weak-Axis by LCB 1 (Expansion)

In Figure 4.1,

where Sax: Axial stress in the element's local x-direction (Local x-direction: element's axial direction)

Ssy: Shear stress in the element's local y-direction

Ssz: Shear stress in the element's local z-direction

Sby: Normal stress resulting from the moment (Mz) about the element's local z-axis

Sbz: Normal stress resulting from the moment (My) about the element's local y-axis

Combined: Combined stress (Combined stress: Sax ± Sby ± Sbz)

Maximum (Axial+Moment): Combined stress representing the absolute largest among combined stresses at 1, 2, 3 and 4 (the location 1, 2, 3 and 4 shown in the Section Shape of the Section Data window)

1(-y,+z): combined stress at 1

2(+y,+z): combined stress at 2

3(+y,-z): combined stress at 3

4(-y,-z): combined stress at 4

The noticeable difference between expansion and contraction cases is the magnitude of compressive stress generated at both ends of bridge girder. Expansion creates higher compressive (-) stress at both ends of girder than contraction does. On the other hand, contraction produces higher tensile (+) stress in the middle of the span than expansion does in Figures 4.1 and 4.2.

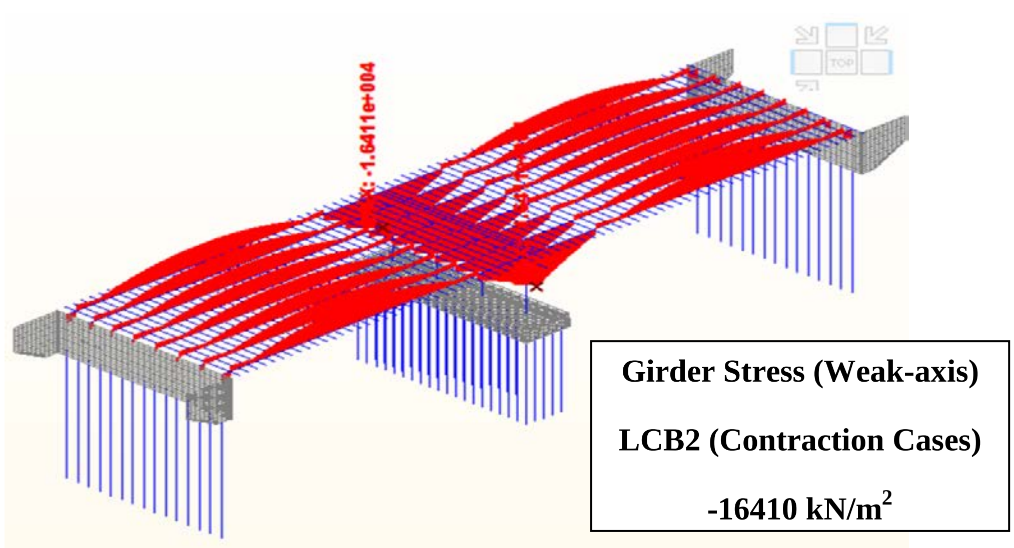

Figure 4.2: Girder Stress in 5m-Tall Abutment with Sand 1 & Weak-Axis by LCB 2 (Contraction)

Figure 4.2 expresses that the higher compressive stress in contraction cases occurs on the piers compared with expansion cases. Figures 4.3 through 4.6 and Tables 4.1 through 4.4 show the maximum combined girder stress with regard to: (1) abutment height; (2) soil types; (3) pile orientation, for both expansion and contraction cases.

The abutment height has a negative influence on the maximum combined girder stress, as discovered from Figures 4.3 and 4.4 and Tables 4.1 and 4.2. As the abutment height increases in strong axial direction there is up to a 3 % reduction (6m-Tall Abutment: 97 %) in the maximum combined girder stress by expansion cases whereas the maximum combined girder stress in strong axial direction under contraction cases shows up to an 10.1 % attenuation along with the rise of the abutment height (Tables 4.1a and 4.2a).

In weak axial direction, as the abutment height increases there is up to a 4.6 % reduction (6m-Tall Abutment: 95.4 %) in the maximum combined girder stress by expansion cases whereas the maximum combined girder stress with weak axial direction under contraction cases shows up to an 11 % drop along with the rise of the abutment height (Tables 4.1a and 4.2a).

In addition, pile orientation has a bit of influence on the maximum combined girder stress between 3m and 6m due to the difference of weak and strong axis bending.

Table 4.1: Values of Girder Stress by abutment height & pile orientation in LCB 1 (Expansion)

Girder Stress: LCB1 (Expansion Cases) Unit: kN/m^2 (Absolute Value)		
Abutment Height	**Strong-axis**	**Weak-axis**
3 m	**1.487E+04**	**1.513E+04**
4 m	**1.451E+04**	**1.462E+04**
5 m	**1.441E+04**	**1.446E+04**
6 m	**1.442E+04**	**1.443E+04**
7 m	**1.445E+04**	**1.445E+04**
8 m	**1.450E+04**	**1.449E+04**

Table 4.1a: Reduction Rate in Girder Stress by abutment height & pile orientation in LCB 1 (Expansion)

Reduction Rate in Girder Stress: LCB1 (Expansion Cases) Reference: 3 m		
Abutment Height	Strong-axis	Weak-axis
3 m	100.0%	100.0%
4 m	97.6%	96.6%
5 m	96.9%	95.6%
6 m	97.0%	95.4%
7 m	97.2%	95.5%
8 m	97.5%	95.8%

Table 4.2: Values of Girder Stress by abutment height & pile orientation in LCB 2 (Contraction)

Girder Stress: LCB2 (Contraction Cases) Unit: kN/m^2 (Absolute Value)		
Abutment Height	Strong-axis	Weak-axis
3 m	1.728E+04	1.749E+04
4 m	1.674E+04	1.689E+04
5 m	1.631E+04	1.641E+04
6 m	1.599E+04	1.605E+04
7 m	1.573E+04	1.577E+04
8 m	1.554E+04	1.556E+04

Table 4.2a: Reduction Rate in Girder Stress by abutment height & pile orientation in LCB 2 (Contraction)

Reduction Rate in Girder Stress: LCB2 (Contraction Cases) Reference: 3 m		
Abutment Height	Strong-axis	Weak-axis
3 m	100.0%	100.0%
4 m	96.9%	96.6%
5 m	94.4%	93.8%
6 m	92.5%	91.8%
7 m	91.0%	90.2%
8 m	89.9%	89.0%

In addition, as exposed in Tables 4.1b and 4.2b, the pile orientation has a bit of influence on the maximum combined girder stress in both expansion and contraction cases due to the difference of weak and strong axis bending.

As a change in the pile orientation follows from strong axial direction to weak axial direction, the maximum combined girder stress slightly increases in expansion cases. However, if the abutment height exceeds 6 m, the maximum combined girder stress decreases adversely when an alteration in the pile orientation from strong axial direction to weak axial direction occurs, as shown in Tables 4.1 and 4.1b. This indicates that a variation in pile orientation has not an influence on the maximum combined girder stress due to the increase of the self-weight and stiffness of the abutment if the abutment height surpasses 6 m.

On the other hand, if a change in the pile orientation follows from strong axial direction to weak axial direction, the maximum combined girder stress slightly increases in contraction cases. However, as the abutment height increase, the effects of a change in the pile orientation declines since the increase rate of the maximum combined girder stress decreases by gradual steps as exposed in Tables 4.2 and 4.2b. As is in the expansion cases, this also shows that a variation in pile orientation has not an influence on the maximum combined girder stress due to the increase of the self-weight and stiffness of the abutment if the abutment height rises.

Overall, in both expansion and contraction cases, there is a very distinct difference in terms of the trend on the maximum combined girder stress.

The trend on the maximum combined girder stress in expansion cases decrease and then slightly increases as the abutment height increase while the maximum combined girder stress in contraction cases steadily decreased when the abutment height rises.

Table 4.1b: Variation Rate in Girder Stress by abutment height & pile orientation in LCB 1 (Expansion)

Variation Rate in Girder Stress: LCB1 (Expansion Cases) Reference: Strong Axis		
Abutment Height	Strong-axis	Weak-axis
3 m	100.0%	101.7%
4 m	100.0%	100.8%
5 m	100.0%	100.3%
6 m	100.0%	100.1%
7 m	100.0%	100.0%
8 m	100.0%	99.9%

Table 4.2b: Variation Rate in Girder Stress by abutment height & pile orientation in LCB 2 (Contraction)

Variation Rate in Girder Stress: LCB2 (Contraction Cases) Reference: Strong Axis		
Abutment Height	Strong-axis	Weak-axis
3 m	100.0%	101.2%
4 m	100.0%	100.9%
5 m	100.0%	100.6%
6 m	100.0%	100.4%
7 m	100.0%	100.3%
8 m	100.0%	100.1%

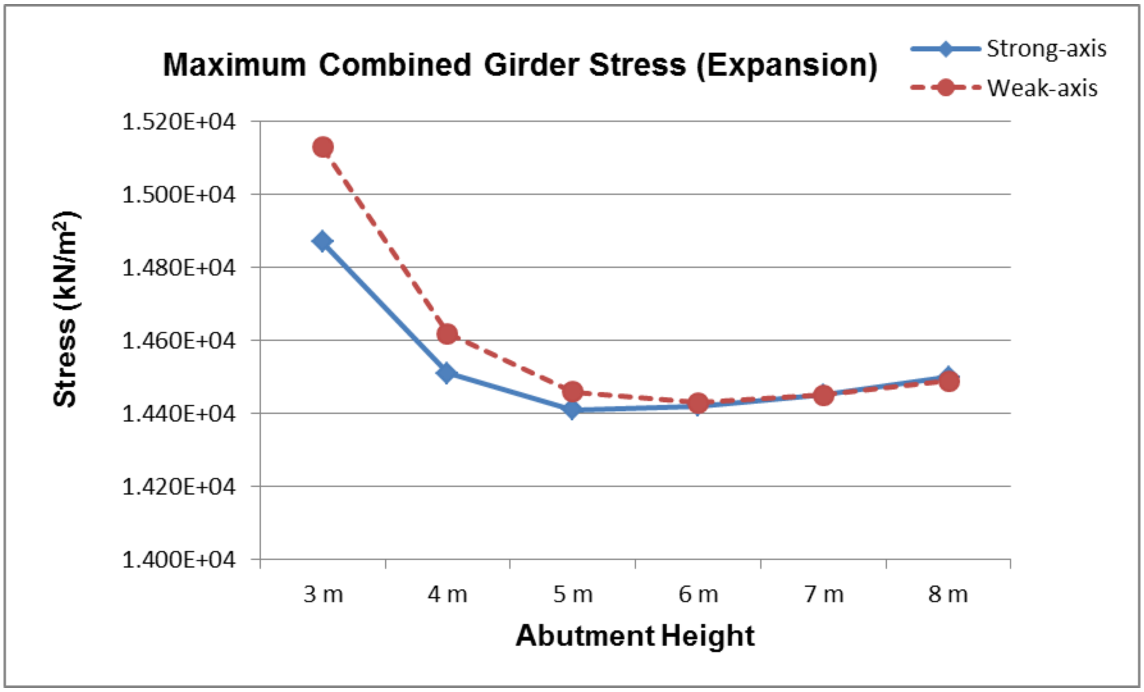

Figure 4.3: Girder Stress by abutment height and pile orientation in LCB 1 (Expansion)

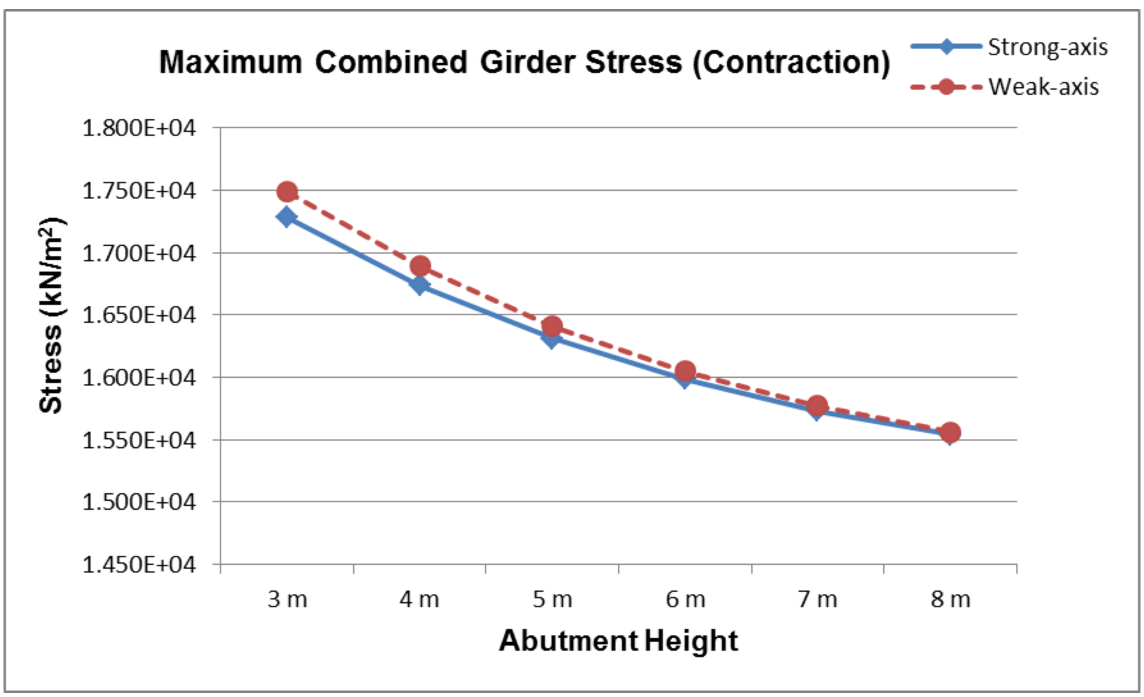

Figure 4.4: Girder Stress by abutment height and pile orientation in LCB 2 (Contraction)

The maximum combined girder stress obtained by soil types displays a similar trend for expansion and contraction cases as shown in Figures 4.5 and 4.6 , and Tables 4.3 through 4.4a.

As exposed in Tables 4.3 and 4.3a, when the soil stiffness from sand 1 to sand 2 increases in the strong axial direction, there is a 1.2 % reduction in the maximum combined girder stress by expansion cases. Similarly, the maximum combined girder stress in the weak axial direction is reduced by 1.4 % with the rise of the soil stiffness from sand 1 to sand 2 under expansion cases.

On the other hand, as the soil stiffness from clay 1 to clay 2 increases in the strong axial direction there is a 3.0 % reduction in the maximum combined girder stress by expansion cases. In the same way, the maximum combined girder stress in the weak axial direction is reduced by 3.8 % with the rise of the soil stiffness from clay 1 to clay 2 under expansion cases as uncovered in Table 4.3a.

Table 4.3: Values of Girder Stress by soil types & pile orientation in LCB 1 (Expansion)

Girder Stress: LCB1 (Expansion Cases) Unit: kN/m^2 (Absolute Value)		
Soil Types	**Strong-axis**	**Weak-axis**
Sand 1	**1.4410E+04**	**1.4460E+04**
Sand 2	**1.4240E+04**	**1.4260E+04**
Clay 1	**1.5110E+04**	**1.5380E+04**
Clay 2	**1.4650E+04**	**1.4800E+04**

Table 4.3a: Reduction Rate in Girder Stress by soil types & pile orientation in LCB 1 (Expansion)

Reduction Rate in Girder Stress: LCB1 (Expansion Cases) Reference: Sand 1, Clay 1		
Soil Types	**Strong-axis**	**Weak-axis**
Sand 1	**100.0%**	**100.0%**
Sand 2	**98.8%**	**98.6%**
Clay 1	**100.0%**	**100.0%**
Clay 2	**97.0%**	**96.2%**

As shown in Tables 4.4 and 4.4a, when the soil stiffness from sand 1 to sand 2 increases in the strong axial direction, there is a 1.5 % reduction in the maximum combined girder stress by contraction cases. Similarly, the maximum combined girder stress in the weak axial direction is reduced by 1.6 % with the rise of the soil stiffness from sand 1 to sand 2 under contraction cases.

On the other hand, as the soil stiffness from clay 1 to clay 2 increases in the strong axial direction there is a 2.1 % reduction in the maximum combined girder stress by contraction cases. In the same way, the maximum combined girder stress in the weak axial direction is reduced by 2.5 % with the rise of the soil stiffness from clay 1 to clay 2 under contraction cases as uncovered in Table 4.4a.

Table 4.4: Values of Girder Stress by soil types & pile orientation in LCB 2 (Contraction)

Girder Stress: LCB2 (Contraction Cases) Unit: kN/m^2 (Absolute Value)		
Soil Types	**Strong-axis**	**Weak-axis**
Sand 1	**1.6310E+04**	**1.6410E+04**
Sand 2	**1.6070E+04**	**1.6150E+04**
Clay 1	**1.6770E+04**	**1.7020E+04**
Clay 2	**1.6420E+04**	**1.6600E+04**

Table 4.4a: Reduction Rate in Girder Stress by soil types & pile orientation in LCB 2 (Contraction)

Reduction Rate in Girder Stress: LCB2 (Contraction Cases) Reference: Sand 1, Clay 1		
Soil Types	**Strong-axis**	**Weak-axis**
Sand 1	**100.0%**	**100.0%**
Sand 2	**98.5%**	**98.4%**
Clay 1	**100.0%**	**100.0%**
Clay 2	**97.9%**	**97.5%**

In addition, the pile orientation has a bit of influence on the maximum combined girder stress in both expansion and contraction cases as a change in the pile orientation follows from strong axial direction to weak axial direction in soils of all types.

As shown in Tables 4.3b and 4.4b, the maximum combined girder stress has a similar trend for expansion and contraction cases. However, the maximum combined girder stress in the abutment with clayed soils is affected more than in that with sandy soils.

Table 4.3b: Increase Rate in Girder Stress by soil types & pile orientation in LCB 1 (Expansion)

Increase Rate in Girder Stress: LCB1 (Expansion Cases) Reference: Strong Axis		
Soil Types	**Strong-axis**	**Weak-axis**
Sand 1	**100.0%**	**100.3%**
Sand 2	**100.0%**	**100.1%**
Clay 1	**100.0%**	**101.8%**
Clay 2	**100.0%**	**101.0%**

Table 4.4b: Increase Rate in Girder Stress by soil types & pile orientation in LCB 2 (Contraction)

Increase Rate in Girder Stress: LCB2 (Contraction Cases) Reference: Strong Axis		
Soil Types	**Strong-axis**	**Weak-axis**
Sand 1	**100.0%**	**100.6%**
Sand 2	**100.0%**	**100.5%**
Clay 1	**100.0%**	**101.5%**
Clay 2	**100.0%**	**101.1%**

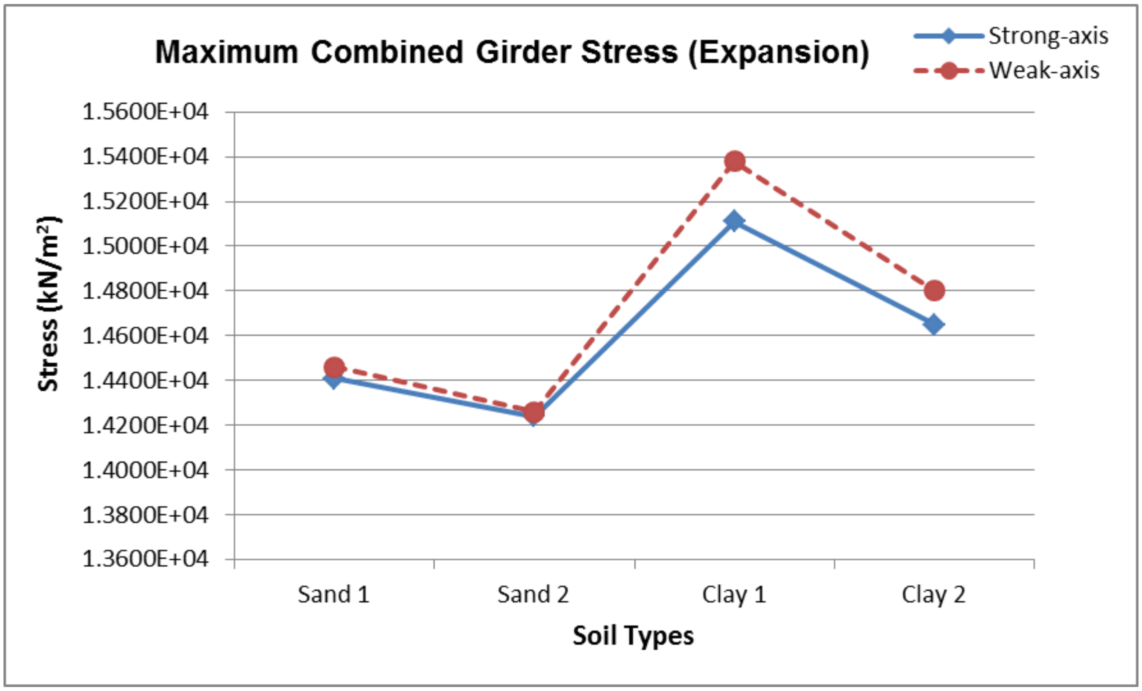

Figure 4.5: Girder Stress by soil types and pile orientation in LCB 1 (Expansion)

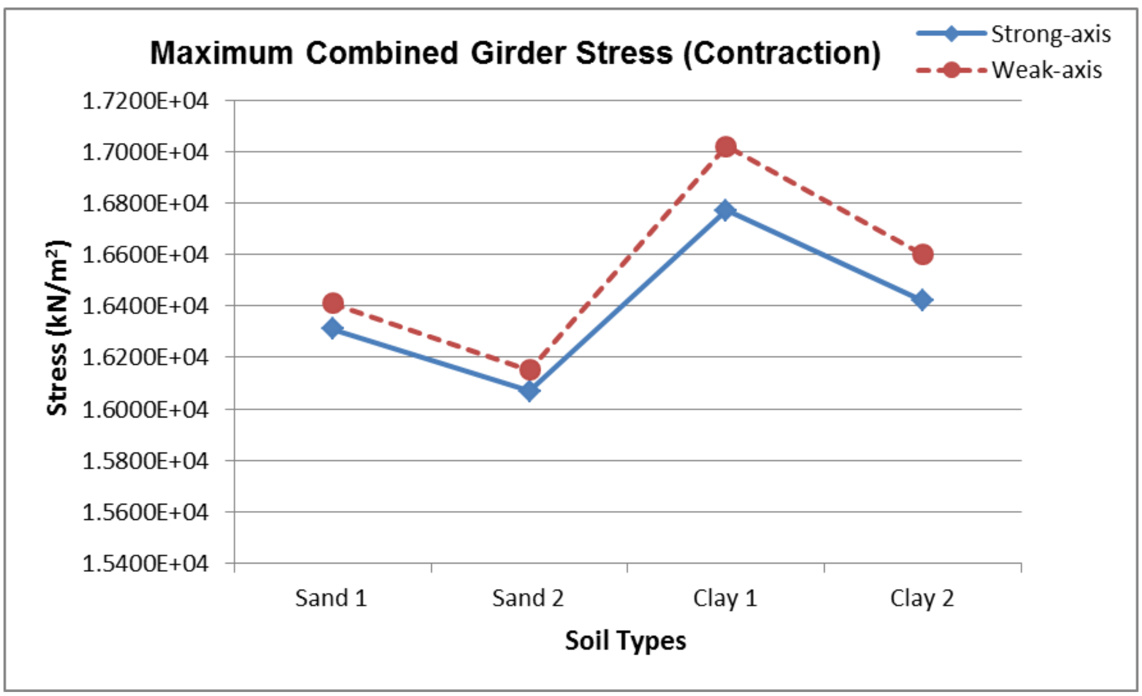

Figure 4.6: Girder Stress by soil types and pile orientation in LCB 2 (Contraction)

4.3 Abutment Stress

Figure 4.7 expresses the maximum principal stress on the top of abutment induced by expansion. The noticeable difference between expansion and contraction cases is detected in the rotated abutment as shown in Figures 4.7 and 4.12. In this sense, the manner of abutment movement is predominantly rotation about their bottom although there is a horizontal dislocation as well.

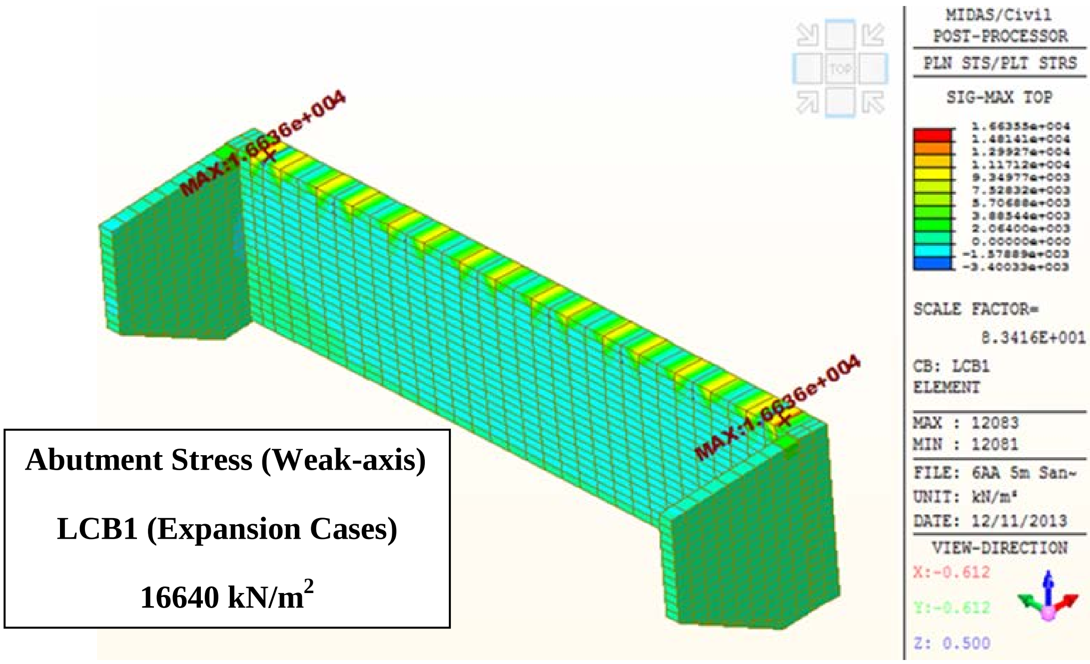

Figure 4.7: Abutment Stress in 5m-Tall Abutment with Sand 1 & Weak-Axis by LCB 1 (Expansion)

Figures 4.8 through 4.11 represent cutting line diagrams for the distribution of the maximum principal stress on the top of abutment induced by expansion. Figure 4.9 shows the distribution of abutment stress at center vertically cutting line from Figure 4.8. As exposed in Figure 4.10, the diagram of abutment stress at top horizontally cutting line is symmetrical within the width (20.4 m) of abutment. Similarly, the distribution of the maximum principal stress weakened at the bottom of abutment has perfect bilateral symmetry as shown in Figure 4.11.

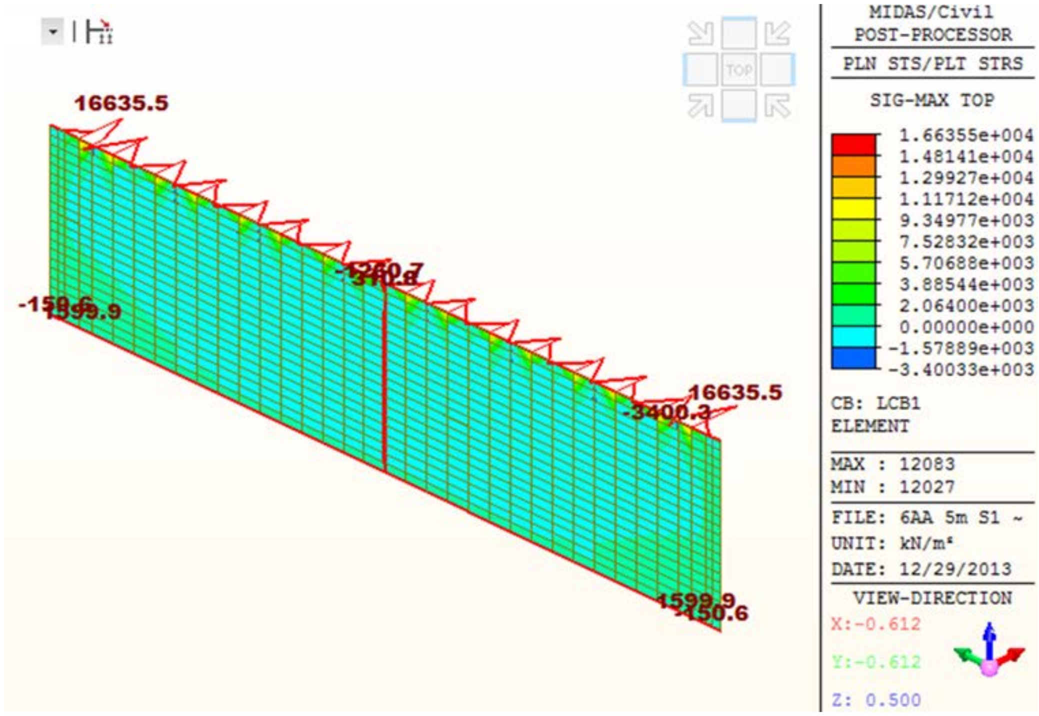

Figure 4.8: Distribution and Cutting Lines of Abutment Stress in 5m-Tall Abutment by LCB 1 (Expansion)

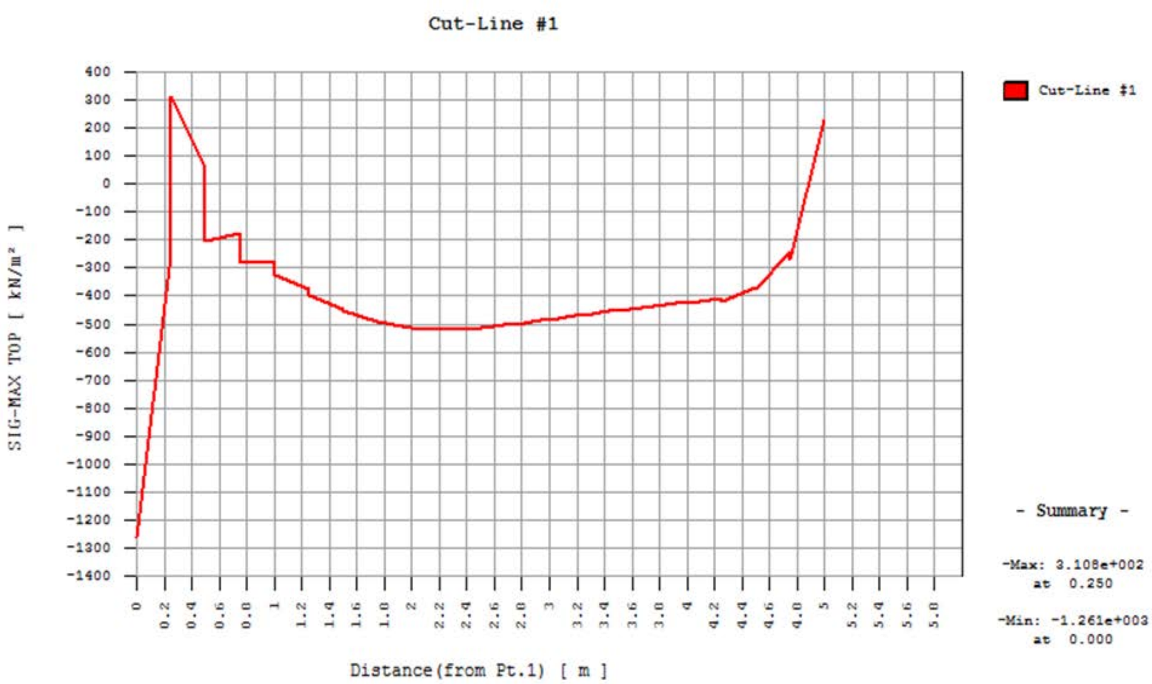

Figure 4.9: Diagram of Abutment Stress at Center Vertically Cutting Line from Figure 4.8

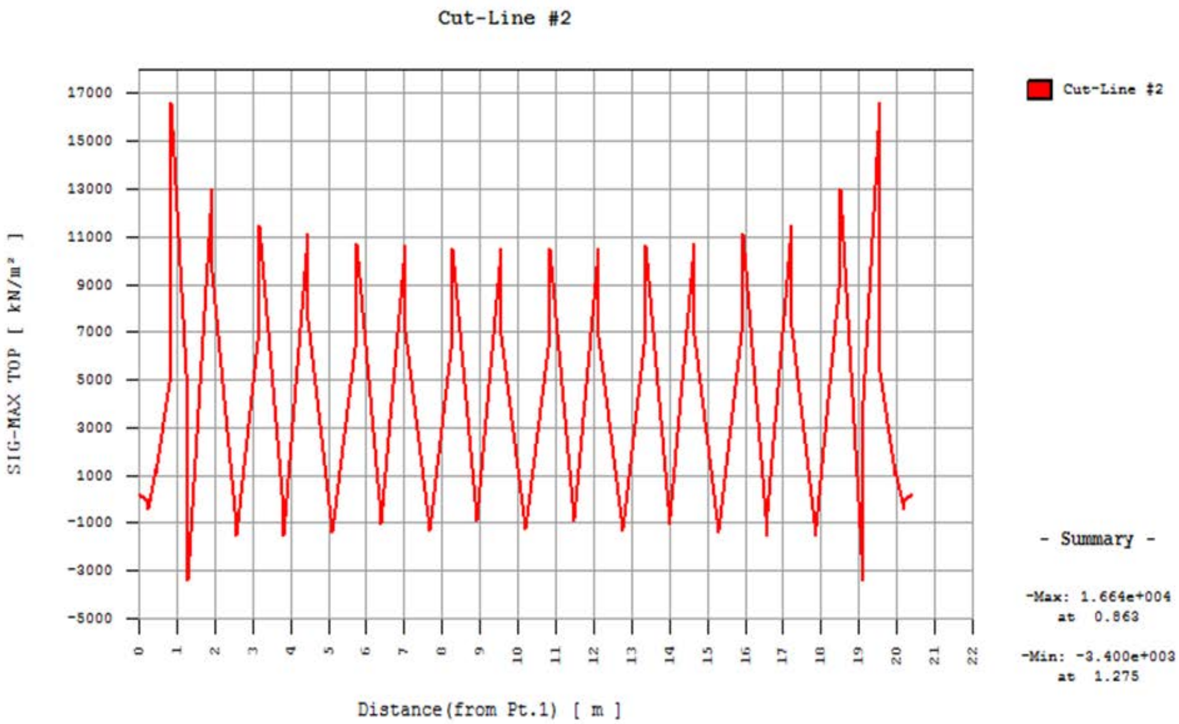

Figure 4.10: Diagram of Abutment Stress at Top Horizontally Cutting Line from Figure 4.8

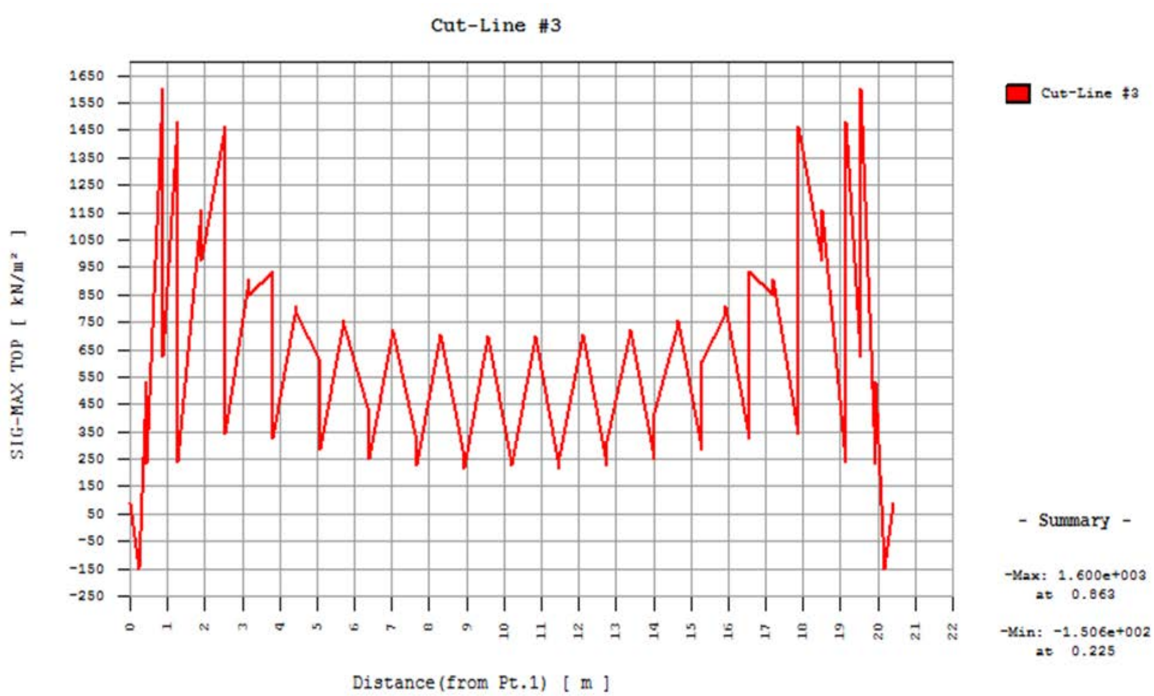

Figure 4.11: Diagram of Abutment Stress at Bottom Horizontally Cutting Line from Figure 4.8

The maximum principal stress are greatest at the top of each abutment as predicted.

Figures 4.7 and 4.12 express a symmetrical stress of both-side concrete abutments at the abutment-girder connection in both expansion and contraction cases. The present study evaluated Sig-Max (Maximum Principal Stress) in the concrete region.

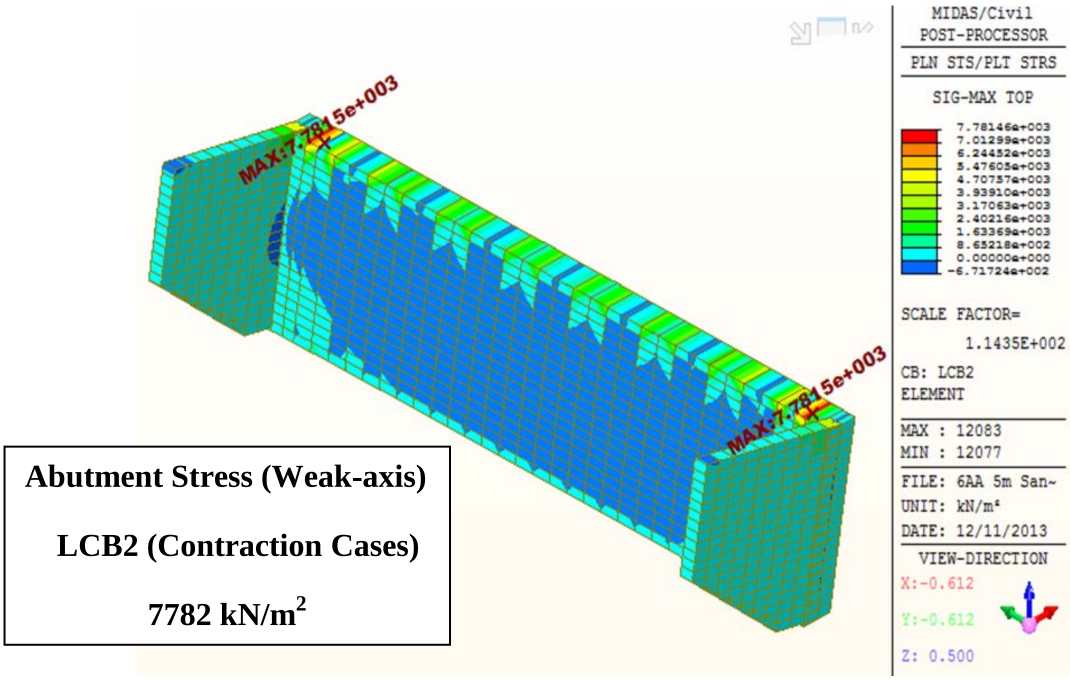

Figure 4.12: Abutment Stress in 5m-Tall Abutment with Sand 1 & Weak-Axis by LCB 2 (Contraction)

Figures 4.13 through 4.16 also represent cutting line diagrams for the distribution of the maximum principal stress on the top of abutment induced by contraction. Figure 4.14 shows the distribution of abutment stress at center vertically cutting line from Figure 4.13. As exposed in Figure 4.15, the diagram of abutment stress at top horizontally cutting line is symmetrical within the width (20.4 m) of abutment. Similarly, the distribution of the maximum principal stress weakened at the bottom of abutment has perfect bilateral symmetry as shown in Figure 4.16.

As exposed in Figures 4.15 and 4.16, the maximum principal stress in abutment is biggest at both sides of abutment. This indicates that the maximum principal stress in abutment is affected substantially by the girder.

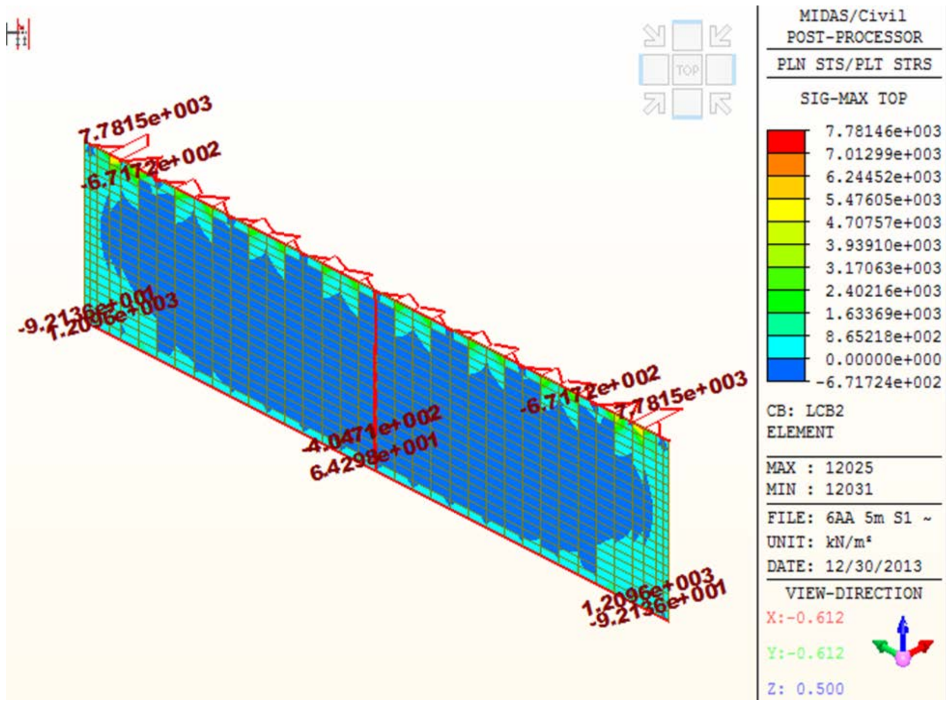

Figure 4.13: Distribution and Cutting Lines of Abutment Stress in 5m-Tall Abutment by LCB 2 (Contraction)

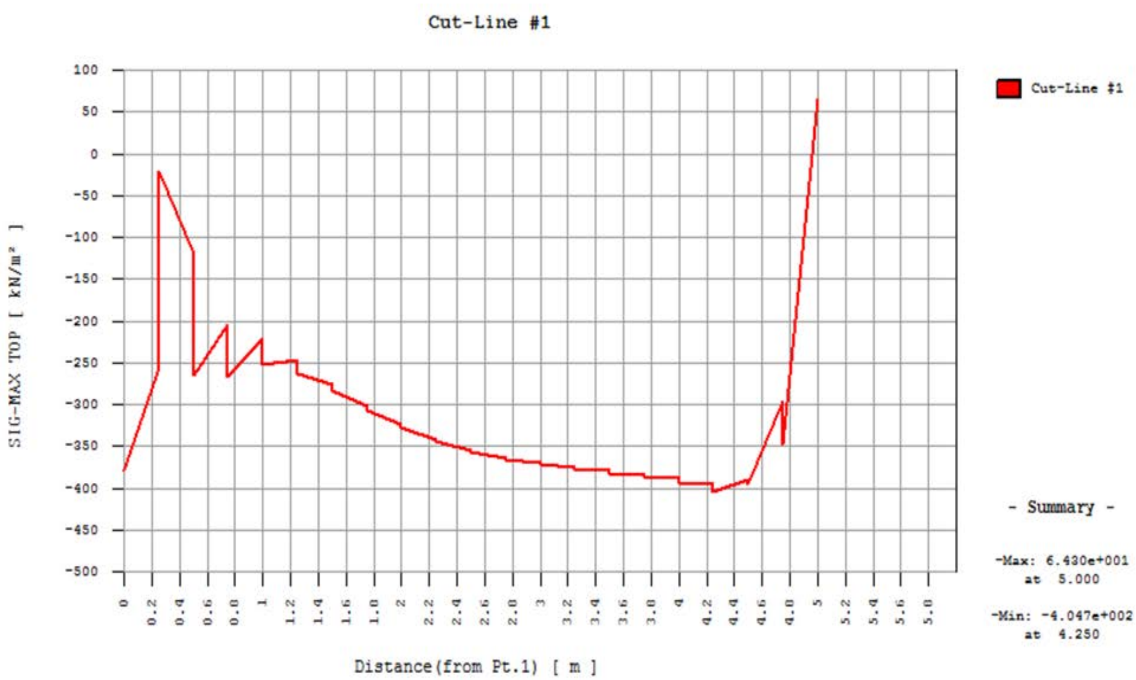

Figure 4.14: Diagram of Abutment Stress at Center Vertically Cutting Line from Figure 4.13

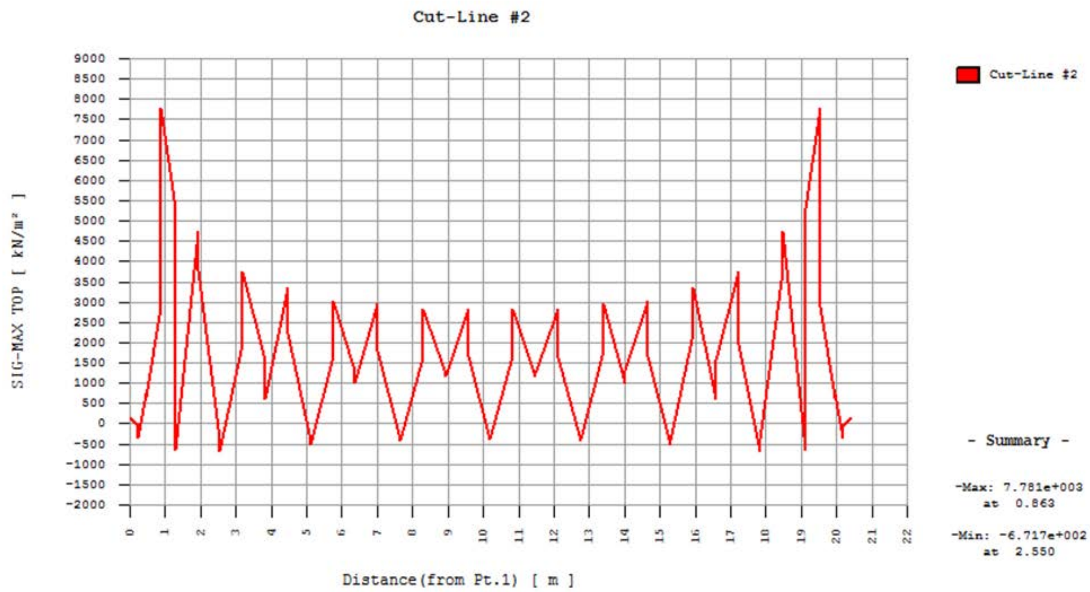

Figure 4.15: Diagram of Abutment Stress at Top Horizontally Cutting Line from Figure 4.13

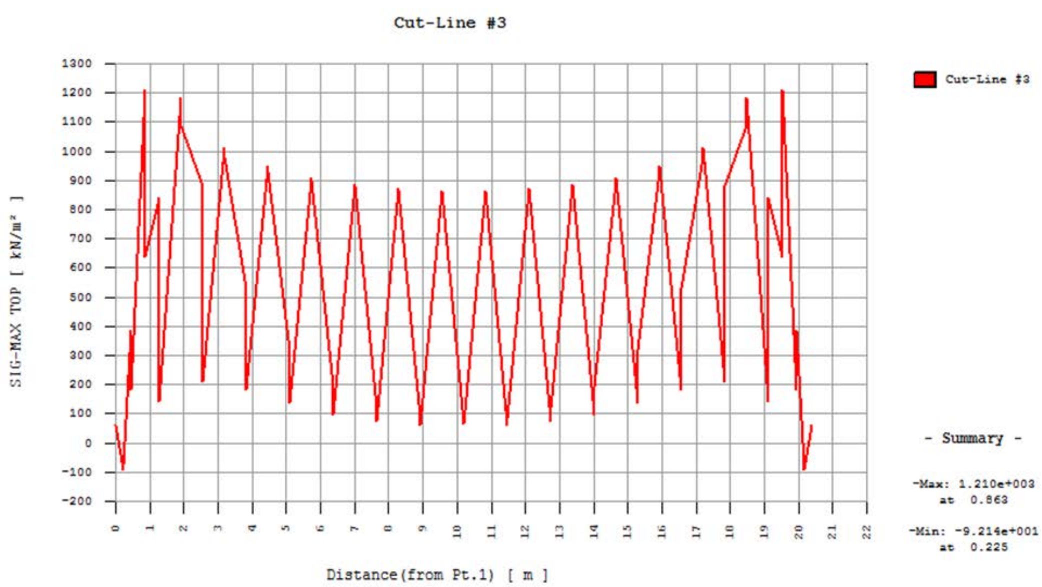

Figure 4.16: Diagram of Abutment Stress at Bottom Horizontally Cutting Line from Figure 4.13

Figures 4.17 through 4.20 show the concrete stress at the abutment-girder connection with regard to: (1) abutment height, (2) soil types, and (3) pile orientation, for both expansion and contraction cases.

The abutment stress increases meaningfully as the abutment height increases as shown Figures 4.16 and 4.17, contrary to the case of girder stress.

The abutment height has a positive influence on the abutment stress, as discovered from Figures 4.16 and 4.17 and Tables 4.5a and 4.6a. As the abutment height increases in strong axial direction there is up to a 6.1 % increase (5m-Tall Abutment: 106.1 %) in the maximum principal abutment stress by expansion cases whereas the maximum principal abutment stress in strong axial direction under contraction cases shows up to an 83.4 % increase along with the rise of the abutment height (Tables 4.5a and 4.6a).

In weak axial direction, there is up to a 11.3 % increase (5m and 6m-Tall Abutment: 111.3 %) in the maximum principal abutment stress by expansion cases when the abutment height increases. On the other hand, the maximum principal abutment stress with weak axial direction under contraction cases shows up to an 103 % surge along with the rise of the abutment height (Tables 4.5a and 4.6a).

Table 4.5: Values of Abutment Stress by abutment height & pile orientation in LCB 1 (Expansion)

Abutment Stress: LCB1 (Expansion Cases) Unit: kN/m^2 (Absolute Value)		
Abutment Height	**Strong-axis**	**Weak-axis**
3 m	**1.583E+04**	**1.495E+04**
4 m	**1.666E+04**	**1.628E+04**
5 m	**1.680E+04**	**1.664E+04**
6 m	**1.670E+04**	**1.664E+04**
7 m	**1.651E+04**	**1.651E+04**
8 m	**1.631E+04**	**1.633E+04**

Table 4.5a Increase Rate in Abutment Stress by abutment height & pile orientation in LCB 1 (Expansion)

Increase Rate in Abutment Stress: LCB1 (Expansion Cases) Reference: 3 m		
Abutment Height	Strong-axis	Weak-axis
3 m	100.0%	100.0%
4 m	105.2%	108.9%
5 m	106.1%	111.3%
6 m	105.5%	111.3%
7 m	104.3%	110.4%
8 m	103.0%	109.2%

Table 4.6: Values of Abutment Stress by abutment height & pile orientation in LCB 2 (Contraction)

Abutment Stress: LCB2 (Contraction Cases) Unit: kN/m^2 (Absolute Value)		
Abutment Height	Strong-axis	Weak-axis
3 m	5.446E+03	4.883E+03
4 m	6.928E+03	6.522E+03
5 m	8.046E+03	7.782E+03
6 m	8.873E+03	8.703E+03
7 m	9.498E+03	9.385E+03
8 m	9.987E+03	9.911E+03

Table 4.6a: Increase Rate in Abutment Stress by abutment height & pile orientation in LCB 2 (Contraction)

Increase Rate in Abutment Stress: LCB2 (Contraction Cases) Reference: 3 m		
Abutment Height	Strong-axis	Weak-axis
3 m	100.0%	100.0%
4 m	127.2%	133.6%
5 m	147.7%	159.4%
6 m	162.9%	178.2%
7 m	174.4%	192.2%
8 m	183.4%	203.0%

In addition, as exposed in Tables 4.5b and 4.6b, the pile orientation has a bit of influence on the maximum principal abutment stress in both expansion and contraction cases due to the difference of weak and strong axis bending.

As a change in the pile orientation follows from strong axial direction to weak axial direction, the maximum principal abutment stress slightly decreases in expansion cases. However, if the abutment height exceeds 6 m, the maximum principal abutment stress decreases less when an alteration in the pile orientation from strong axial direction to weak axial direction occurs, as shown in Tables 4.5 and 4.5b. This indicates that a variation in pile orientation has not an influence on the maximum principal abutment stress due to the increase of the self-weight and stiffness of the abutment if the abutment height surpasses 6 m.

On the other hand, if a change in the pile orientation follows from strong axial direction to weak axial direction, the maximum principal abutment stress more decreases in contraction cases. However, as the abutment height increase, the effects of a change in the pile orientation declines since the increase rate of the maximum principal abutment stress decreases by gradual steps as exposed in Tables 4.6 and 4.6b. As is in the expansion cases, this also shows that a variation in pile orientation has not an influence on the maximum principal abutment stress due to the increase of the self-weight and stiffness of the abutment if the abutment height rises.

Overall, in both expansion and contraction cases, there is a very distinct difference in terms of the trend on the maximum principal abutment stress.

The trend on the maximum principal abutment stress in expansion cases shows a decreasing tendency after increasing. On the other hand, the maximum principal abutment stress in contraction cases steadily increases when the abutment height rises.

Table 4.5b: Variation Rate in Abutment Stress by abutment height & pile orientation in LCB 1 (Expansion)

Variation Rate in Abutment Stress: LCB1 (Expansion Cases) Reference: Strong Axis		
Abutment Height	**Strong-axis**	**Weak-axis**
3 m	**100.0%**	**94.4%**
4 m	**100.0%**	**97.7%**
5 m	**100.0%**	**99.0%**
6 m	**100.0%**	**99.6%**
7 m	**100.0%**	**100.0%**
8 m	**100.0%**	**100.1%**

Table 4.6b: Variation Rate in Abutment Stress by abutment height & pile orientation in LCB 2 (Contraction)

Variation Rate in Abutment Stress: LCB2 (Contraction Cases) Reference: Strong Axis		
Abutment Height	**Strong-axis**	**Weak-axis**
3 m	**100.0%**	**89.7%**
4 m	**100.0%**	**94.1%**
5 m	**100.0%**	**96.7%**
6 m	**100.0%**	**98.1%**
7 m	**100.0%**	**98.8%**
8 m	**100.0%**	**99.2%**

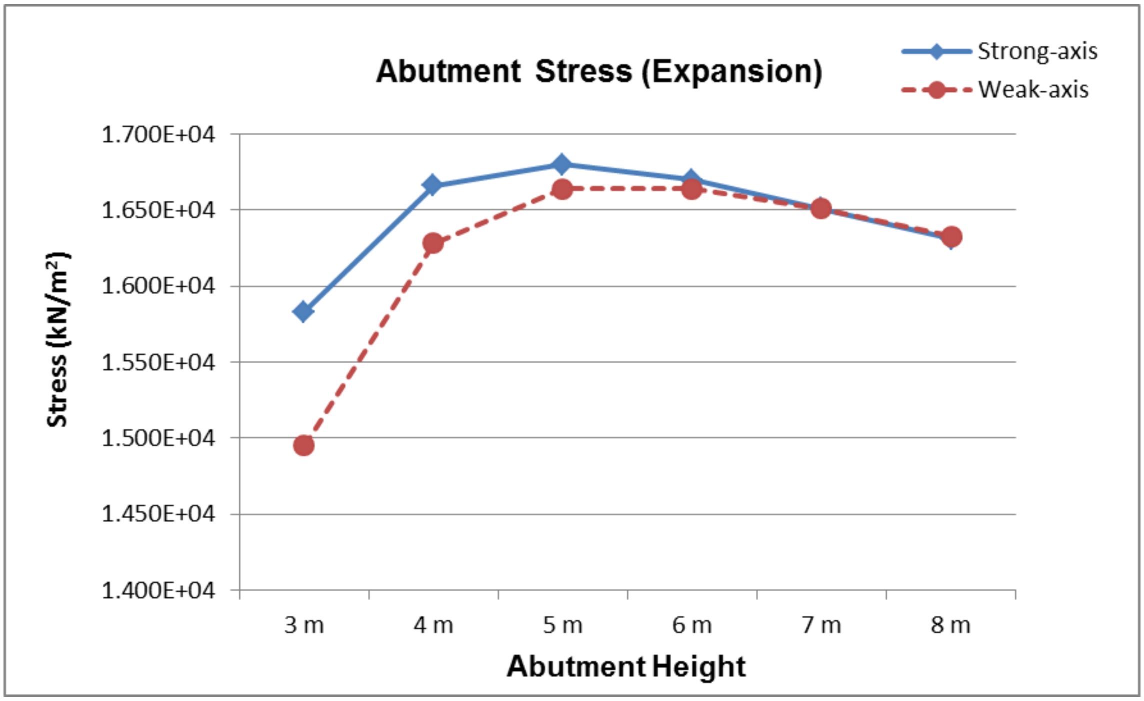

Figure 4. 17: Abutment Stress by abutment height and pile orientation in LCB 1 (Expansion)

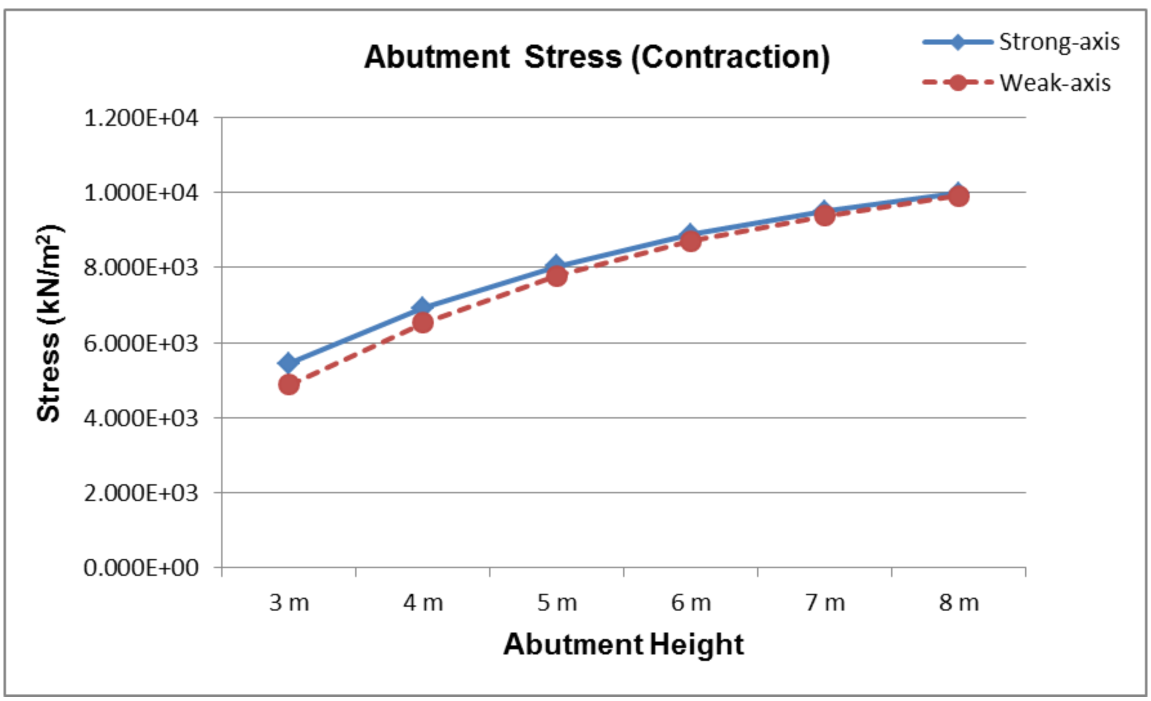

Figure 4.18: Abutment Stress by abutment height and pile orientation in LCB 2 (Contraction)

The maximum principal abutment stress obtained by soil types displays a similar trend for expansion and contraction cases as shown in Figures 4.18 and 4.19 , and Tables 4.7 through 4.8b. As exposed in Tables 4.7 and 4.7a, when the soil stiffness from sand 1 to sand 2 increases in the strong axial direction, there is a 2.9 % increase in the maximum principal abutment stress by expansion cases. Similarly, the maximum principal abutment stress in the weak axial direction is added by 3.5 % with the rise of the soil stiffness from sand 1 to sand 2 under expansion cases.

On the other hand, as the soil stiffness from clay 1 to clay 2 increases in the strong axial direction there is an 11.0 % increase in the maximum principal abutment stress by expansion cases. In the same way, the maximum principal abutment stress in the weak axial direction is increased by 14.6 % with the rise of the soil stiffness from clay 1 to clay 2 under expansion cases as uncovered in Table 4.7a.

As shown in Tables 4.8 and 4.8a, when the soil stiffness from sand 1 to sand 2 increases in the strong axial direction, there is a 1.1 % increase in the maximum principal abutment stress by contraction cases. Similarly, the maximum principal abutment stress in the weak axial direction is reduced by 2.2 % with the rise of the soil stiffness from sand 1 to sand 2 under contraction cases.

On the other hand, as the soil stiffness from clay 1 to clay 2 increases in the strong axial direction there is an 8.2 % increase in the maximum principal abutment stress by contraction cases. In the same way, the maximum principal abutment stress in the weak axial direction is increased by 12.9 % with the rise of the soil stiffness from clay 1 to clay 2 under contraction cases as uncovered in Table 4.8a.

In addition, the pile orientation has a bit of influence on the maximum principal abutment stress in both expansion and contraction cases as a change in the pile orientation follows from strong axial direction to weak axial direction in soils of all types.

As shown in Tables 4.7b and 4.8b, the maximum principal abutment stress has a similar trend for expansion and contraction cases. However, the maximum combined girder stress in the abutment with clayed soils is affected more than in that with sandy soils.

Table 4.7: Values of Abutment Stress by soil types & pile orientation in LCB 1 (Expansion)

Abutment Stress: LCB1 (Expansion Cases) Unit: kN/m^2 (Absolute Value)		
Soil Types	**Strong-axis**	**Weak-axis**
Sand 1	**1.6800E+04**	**1.6640E+04**
Sand 2	**1.7280E+04**	**1.7220E+04**
Clay 1	**1.4400E+04**	**1.3480E+04**
Clay 2	**1.5990E+04**	**1.5450E+04**

Table 4.7a Increase Rate in Abutment Stress by soil types & pile orientation in LCB 1 (Expansion)

Increase Rate in Abutment Stress: LCB1 (Expansion Cases) Reference: Sand 1, Clay 1		
Soil Types	**Strong-axis**	**Weak-axis**
Sand 1	**100.0%**	**100.0%**
Sand 2	**102.9%**	**103.5%**
Clay 1	**100.0%**	**100.0%**
Clay 2	**111.0%**	**114.6%**

Table 4.7b Reduction Rate in Abutment Stress by soil types & pile orientation in LCB 1 (Expansion)

Reduction Rate in Abutment Stress: LCB1 (Expansion Cases) Reference: Strong Axis		
Soil Types	**Strong-axis**	**Weak-axis**
Sand 1	**100.0%**	**99.0%**
Sand 2	**100.0%**	**99.7%**
Clay 1	**100.0%**	**93.6%**
Clay 2	**100.0%**	**96.6%**

Table 4.8: Values of Abutment Stress by soil types & pile orientation in LCB 2 (Contraction)

Abutment Stress: LCB2 (Contraction Cases) Unit: kN/m^2 (Absolute Value)		
Soil Types	**Strong-axis**	**Weak-axis**
Sand 1	8.0460E+03	7.7820E+03
Sand 2	8.1380E+03	7.9530E+03
Clay 1	7.1490E+03	6.3740E+03
Clay 2	7.7380E+03	7.1950E+03

Table 4.8a Increase Rate in Abutment Stress by soil types & pile orientation in LCB 2 (Contraction)

Increase Rate in Abutment Stress: LCB2 (Contraction Cases) Reference: Sand 1, Clay 1		
Soil Types	**Strong-axis**	**Weak-axis**
Sand 1	100.0%	100.0%
Sand 2	101.1%	102.2%
Clay 1	100.0%	100.0%
Clay 2	108.2%	112.9%

Table 4.8b Reduction Rate in Abutment Stress by soil types & pile orientation in LCB 2 (Contraction)

Reduction Rate in Abutment Stress: LCB2 (Contraction Cases) Reference: Strong Axis		
Soil Types	**Strong-axis**	**Weak-axis**
Sand 1	100.0%	96.7%
Sand 2	100.0%	97.7%
Clay 1	100.0%	89.2%
Clay 2	100.0%	93.0%

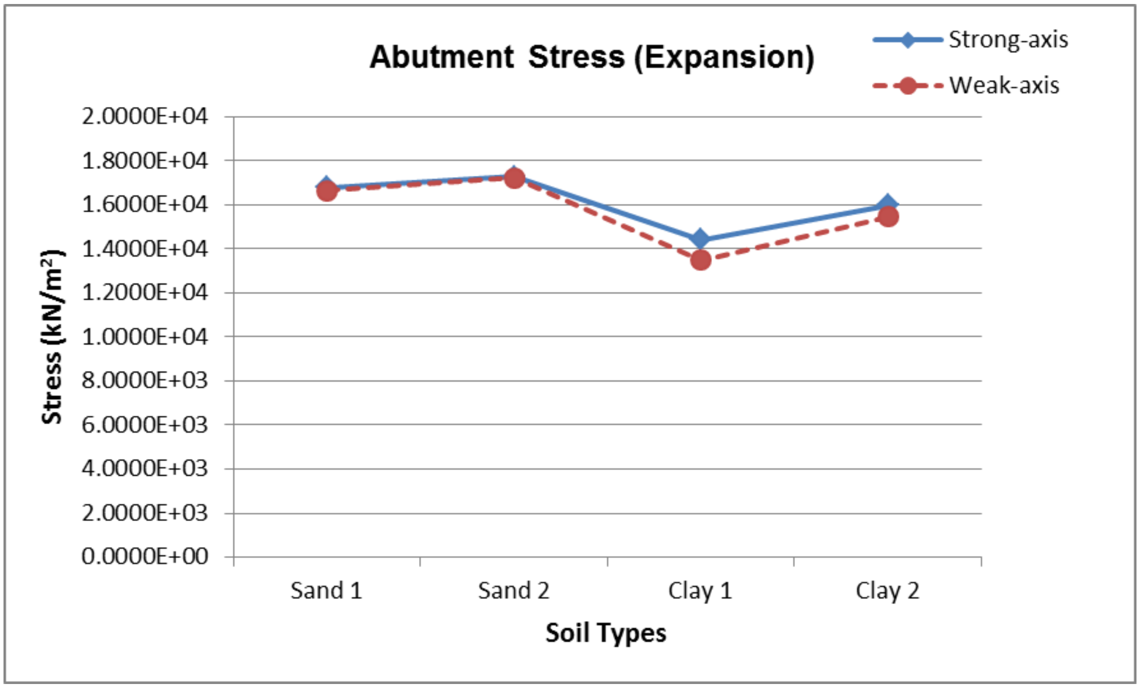

Figure 4.19: Abutment Stress by soil types and pile orientation in LCB 1 (Expansion)

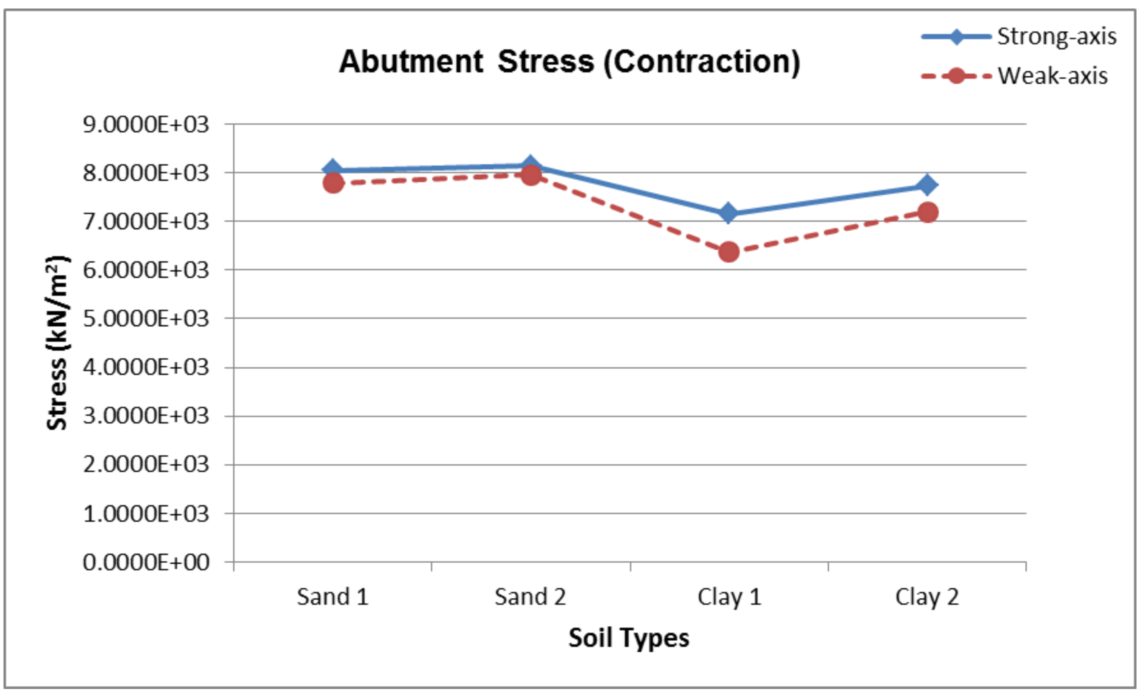

Figure 4.20: Abutment Stress by soil types and pile orientation in LCB 2 (Contraction)

4.4 Pile Moment

Figures 4.21 and 4.22 indicate the maximum pile bending moment induced by both expansion and contraction. Steel H-shaped piles were embedded 0.6 m into the abutment. Thus, the maximum pile bending moment occurs at the pile-abutment connection that there is the bottom of abutment in both expansion and contraction cases. The noticeable difference between expansion and contraction cases does not discover in the pile moment. The contraction creates a slightly higher pile bending moment at the pile-abutment connection than the expansion does.

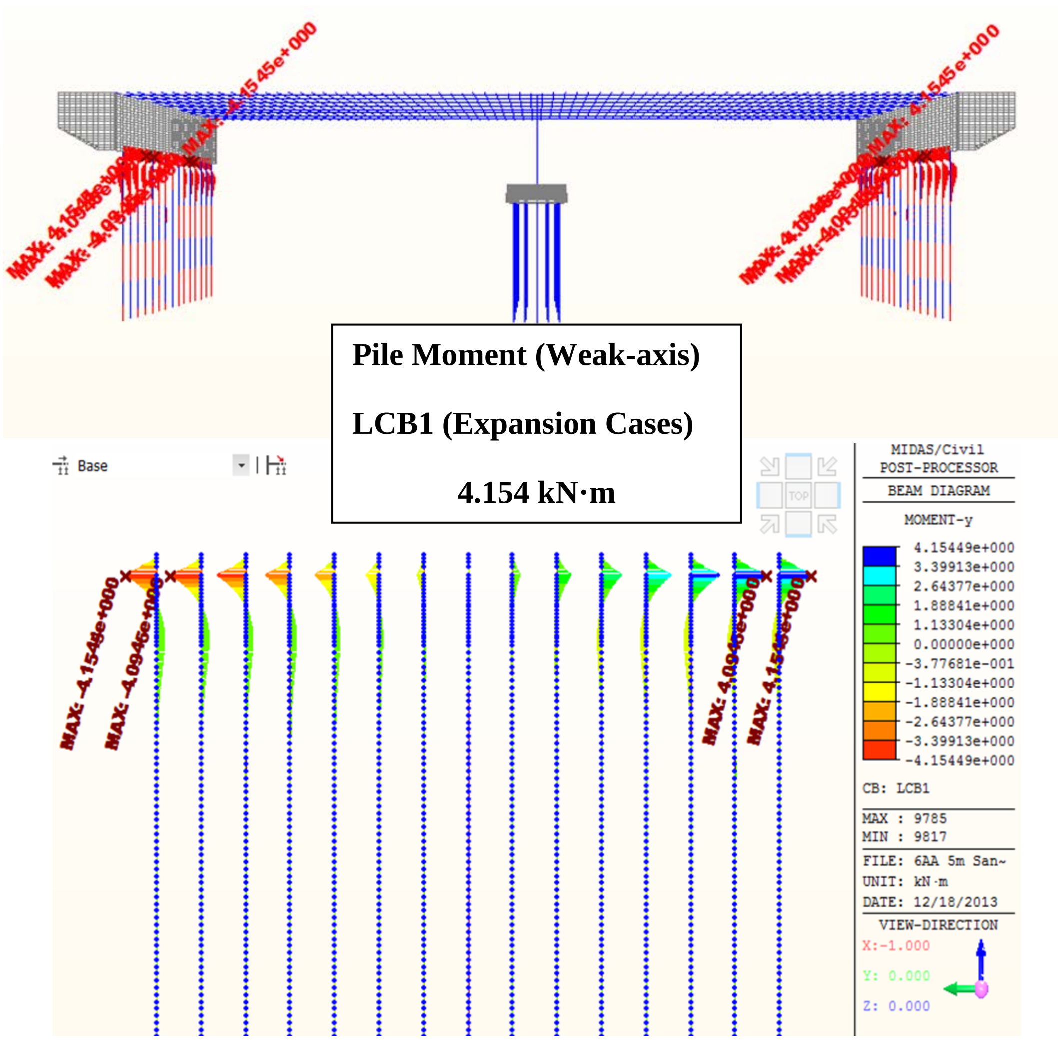

Figure 4.21: Pile Moment in 5m-Tall Abutment with Sand 1 & Weak-Axis by LCB 1 (Expansion)

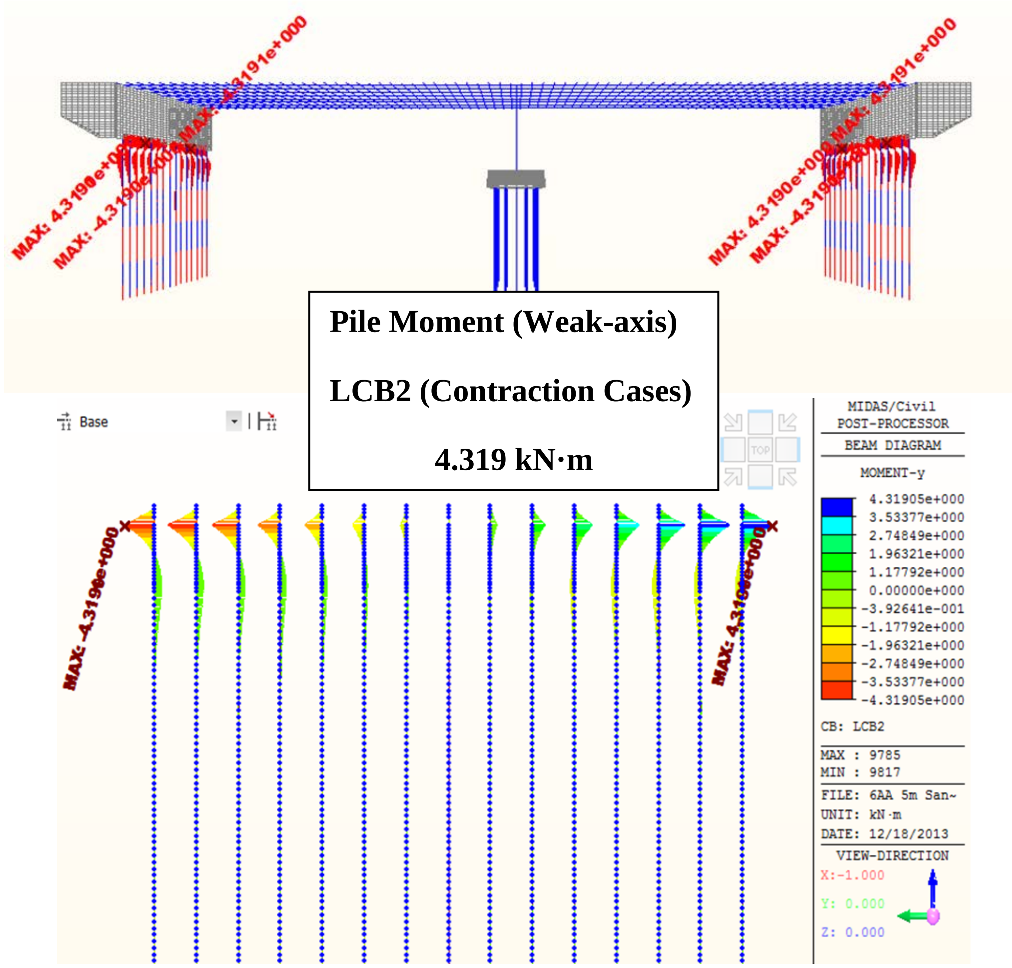

Figure 4.22: Pile Moment in 5m-Tall Abutment with Sand 1 & Weak-Axis by LCB 2 (Contraction)

As noticed from Figures 4.23 and 4.24, the abutment height has a significant influence on pile moment in the strong axial orientation since there is up to an 83.4 % reduction (6m-Tall Abutment: 17.6 %) in pile moment when the abutment height increases for expansion cases while up to a 48.5 % reduction (8m-Tall Abutment: 51.5 %) is discovered in contraction cases. On the other hand, the weak axial orientation also has a negative influence, up to a 66.4 % reduction (8m-Tall Abutment: 33.6 %) on the pile moment when the abutment height increases under the expansion cases. There is a 71.5 % reduction (8m-Tall Abutment: 28.5 %) on pile moment in contraction case when the abutment height increases.

Table 4.9: Values of Pile Moment by abutment height & pile orientation in LCB 1 (Expansion)

Pile Moment: LCB1 (Expansion Cases) Unit: kN·m (Absolute Value)		
Abutment Height	Strong-axis	Weak-axis
3 m	2.501E+02	7.498E+00
4 m	1.501E+02	5.461E+00
5 m	8.254E+01	4.154E+00
6 m	4.397E+01	3.321E+00
7 m	4.417E+01	2.813E+00
8 m	5.082E+01	2.521E+00

Table 4.9a: Reduction Rate in Pile Moment by abutment height & pile orientation in LCB 1 (Expansion)

Reduction Rate in Pile Moment: LCB1 (Expansion Cases) Reference: 3 m		
Abutment Height	Strong-axis	Weak-axis
3 m	100.0%	100.0%
4 m	60.0%	72.8%
5 m	33.0%	55.4%
6 m	17.6%	44.3%
7 m	17.7%	37.5%
8 m	20.3%	33.6%

Table 4.10: Values of Pile Moment by abutment height & pile orientation in LCB 2 (Contraction)

Pile Moment: LCB2 (Contraction Cases) Unit: kN·m (Absolute Value)		
Abutment Height	Strong-axis	Weak-axis
3 m	1.692E+02	7.575E+00
4 m	1.643E+02	5.631E+00
5 m	1.471E+02	4.319E+00
6 m	1.263E+02	3.383E+00
7 m	1.060E+02	2.692E+00
8 m	8.719E+01	2.160E+00

Table 4.10a: Reduction Rate in Pile Moment by abutment height & pile orientation in LCB 2 (Contraction)

Reduction Rate in Pile Moment: LCB2 (Contraction Cases) Reference: 3 m		
Abutment Height	Strong-axis	Weak-axis
3 m	100.0%	100.0%
4 m	97.1%	74.3%
5 m	86.9%	57.0%
6 m	74.6%	44.7%
7 m	62.6%	35.5%
8 m	51.5%	28.5%

Table 4.9b: Variation Rate in Pile Moment by abutment height & pile orientation in LCB 1 (Expansion)

Variation Rate in Pile Moment: LCB1 (Expansion Cases) Reference: Strong Axis		
Abutment Height	Strong-axis	Weak-axis
3 m	100.0%	3.0%
4 m	100.0%	3.6%
5 m	100.0%	5.0%
6 m	100.0%	7.6%
7 m	100.0%	6.4%
8 m	100.0%	5.0%

Table 4.10b: Variation Rate in Pile Moment by abutment height & pile orientation in LCB 2 (Contraction)

Variation Rate in Pile Moment: LCB2 (Contraction Cases) Reference: Strong Axis		
Abutment Height	Strong-axis	Weak-axis
3 m	100.0%	4.5%
4 m	100.0%	3.4%
5 m	100.0%	2.9%
6 m	100.0%	2.7%
7 m	100.0%	2.5%
8 m	100.0%	2.5%

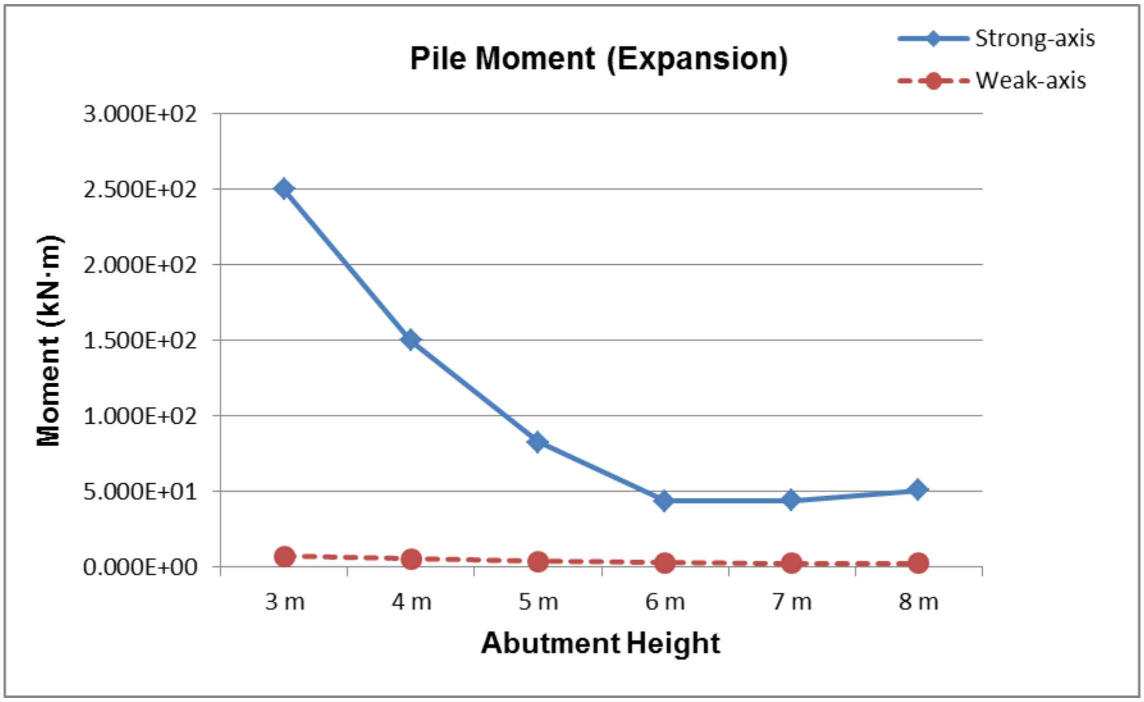

Figure 4.23: Pile Moment by abutment height and pile orientation in LCB 1 (Expansion)

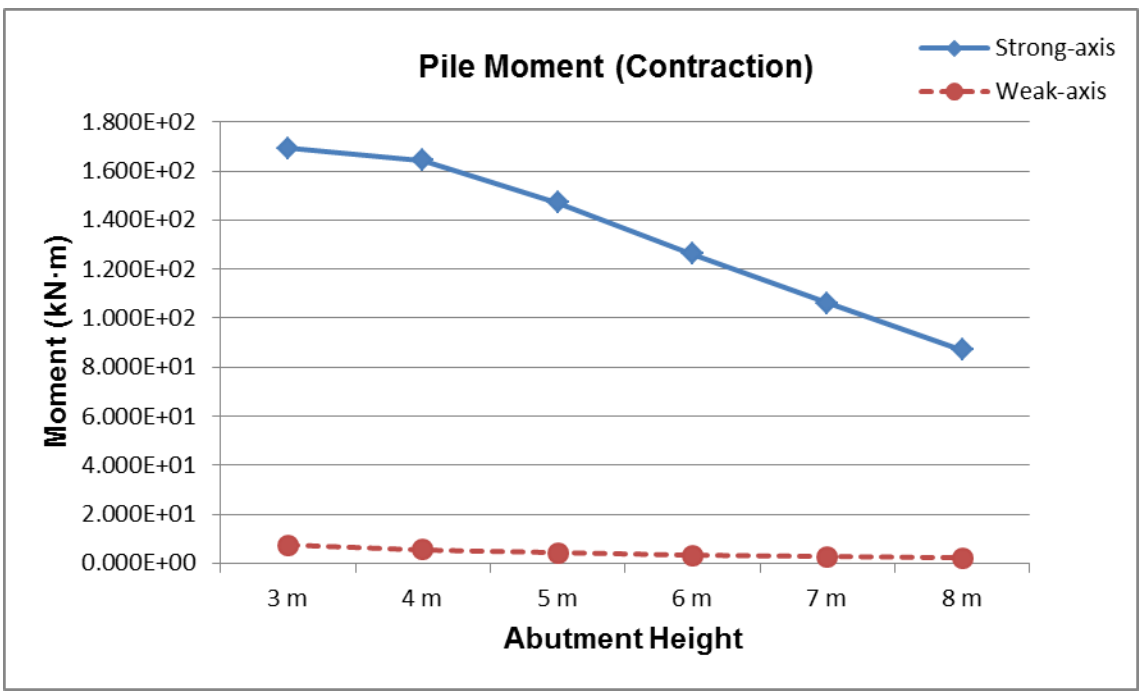

Figure 4.24: Pile Moment by abutment height and pile orientation in LCB 2 (Contraction)

As exposed in Tables 4.11 and 4.11a, when the soil stiffness from sand 1 to sand 2 increases in the strong axial direction, there is a 28.8 % reduction in the maximum pile bending moment by expansion cases. Similarly, the maximum pile bending moment in the weak axial direction is added by 13.6 % with the rise of the soil stiffness from sand 1 to sand 2 under expansion cases.

On the other hand, as the soil stiffness from clay 1 to clay 2 increases in the strong axial direction there is a 17.8 % decrease in the maximum pile bending moment by expansion cases. On the contrary, the maximum pile bending moment in the weak axial direction is increased by 32.0 % with the rise of the soil stiffness from clay 1 to clay 2 under expansion cases as uncovered in Table 4.11a.

As shown in Tables 4.12 and 4.12a, when the soil stiffness from sand 1 to sand 2 increases in the strong axial direction, there is a 10 % increase in the maximum pile bending moment by contraction cases. Similarly, the maximum pile bending moment in the weak axial direction is increased by 12.3 % with the rise of the soil stiffness from sand 1 to sand 2 under contraction cases.

On the other hand, as the soil stiffness from clay 1 to clay 2 increases in the strong axial direction there is a 9.8 % increase in the maximum pile bending moment by contraction cases. In the same way, the maximum pile bending moment in the weak axial direction is increased by 31.6 % with the rise of the soil stiffness from clay 1 to clay 2 under contraction cases as uncovered in Table 4.12a.

In addition, the pile orientation has a significant influence on the maximum pile bending moment in both expansion and contraction cases as a change in the pile orientation follows from strong axial direction to weak axial direction in soils of all types.

As shown in Tables 4.11b and 4.12b, the maximum pile bending moment has an opposing trend for expansion and contraction cases in the strong axial direction. As observed in Figures 4.25 and 4.26, if a change in the pile orientation follows from strong axial direction to weak axial direction, the maximum pile bending moment abruptly decreases in both the expansion and contraction cases.

Table 4.11: Values of Pile Moment by soil types & pile orientation in LCB 1 (Expansion)

Pile Moment: LCB1 (Expansion Cases) Unit: kN·m (Absolute Value)		
Soil Types	Strong-axis	Weak-axis
Sand 1	8.2540E+01	4.1540E+00
Sand 2	5.8730E+01	4.7200E+00
Clay 1	1.3580E+02	2.7930E+00
Clay 2	1.1160E+02	3.6880E+00

Table 4.11a: Variation Rate in Pile Moment by soil types & pile orientation in LCB 1 (Expansion)

Variation Rate in Pile Moment: LCB1 (Expansion Cases) Reference: Sand 1, Clay 1		
Soil Types	Strong-axis	Weak-axis
Sand 1	100.0%	100.0%
Sand 2	71.2%	113.6%
Clay 1	100.0%	100.0%
Clay 2	82.2%	132.0%

Table 4.11b Variation Rate in Pile Moment by soil types & pile orientation in LCB 1 (Expansion)

Variation Rate in Pile Moment: LCB1 (Expansion Cases) Reference: Strong Axis		
Soil Types	Strong-axis	Weak-axis
Sand 1	100.0%	5.0%
Sand 2	100.0%	8.0%
Clay 1	100.0%	2.1%
Clay 2	100.0%	3.3%

Table 4.12: Values of Pile Moment by soil types & pile orientation in LCB 2 (Contraction)

Pile Moment: LCB2 (Contraction Cases) Unit: kN·m (Absolute Value)		
Soil Types	Strong-axis	Weak-axis
Sand 1	1.4710E+02	4.3190E+00
Sand 2	1.6180E+02	4.8500E+00
Clay 1	1.3460E+02	2.9070E+00
Clay 2	1.4780E+02	3.8260E+00

Table 4.12a: Variation Rate in Pile Moment by soil types & pile orientation in LCB 2 (Contraction)

Variation Rate in Pile Moment: LCB2 (Contraction Cases) Reference: Sand 1, Clay 1		
Soil Types	Strong-axis	Weak-axis
Sand 1	100.0%	100.0%
Sand 2	110.0%	112.3%
Clay 1	100.0%	100.0%
Clay 2	109.8%	131.6%

Table 4.12b Variation Rate in Pile Moment by soil types & pile orientation in LCB 2 (Contraction)

Variation Rate in Pile Moment: LCB2 (Contraction Cases) Reference: Strong Axis		
Soil Types	Strong-axis	Weak-axis
Sand 1	100.0%	2.9%
Sand 2	100.0%	3.0%
Clay 1	100.0%	2.2%
Clay 2	100.0%	2.6%

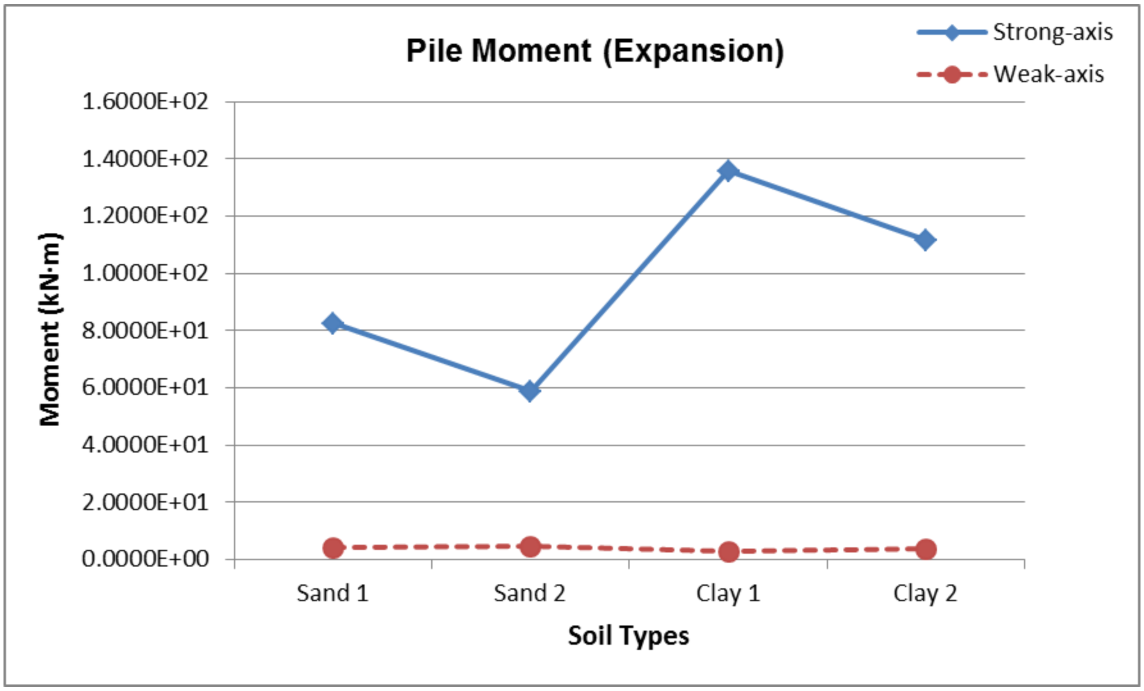

Figure 4.25: Pile Moment by soil types and pile orientation in LCB 1 (Expansion)

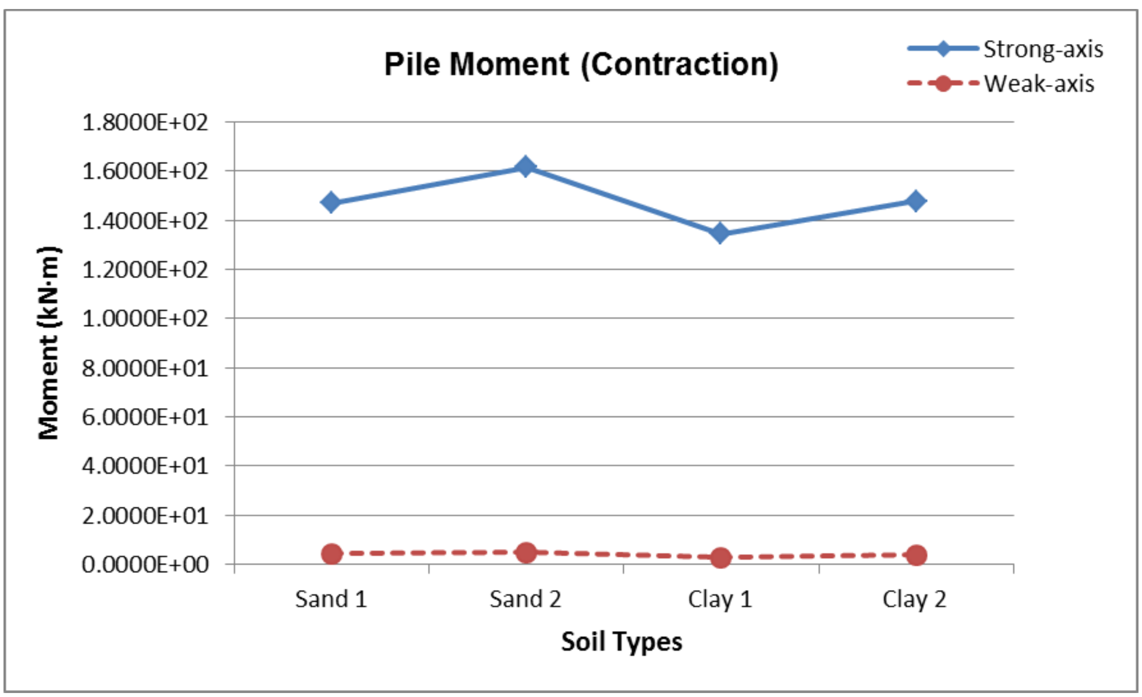

Figure 4.26: Pile Moment by soil types and pile orientation in LCB 2 (Contraction)

4.5 Pile Stress

Figures 4.27 and 4.29 indicate the maximum combined pile stress induced by both expansion and contraction. As expected, since Steel H-shaped piles were embedded 0.6 m into the abutment, the maximum pile stress occurs at the pile-abutment connection that there is the bottom of abutment in both expansion and contraction cases. The noticeable difference between expansion and contraction cases does not discover in pile stress. The contraction creates a slightly higher pile stress at the pile-abutment connection than the expansion does.

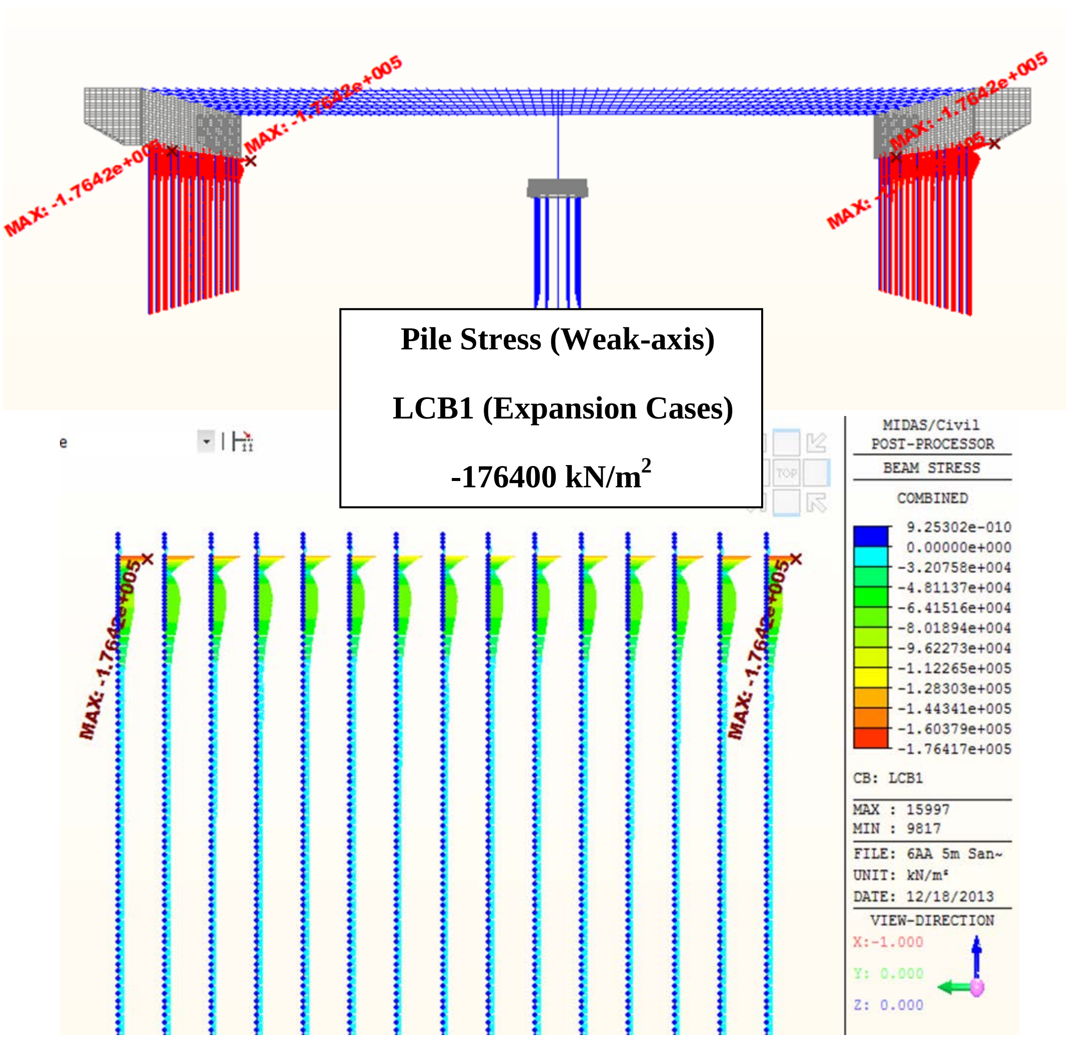

Figure 4.27: Pile Stress in 5m-Tall Abutment with Sand 1 & Weak-Axis by LCB 1 (Expansion)

Figures 4.28 and 4.30 display the variation of the maximum combined pile stress including that the maximum pile stress occurs at the pile-abutment connection in both expansion and contraction.

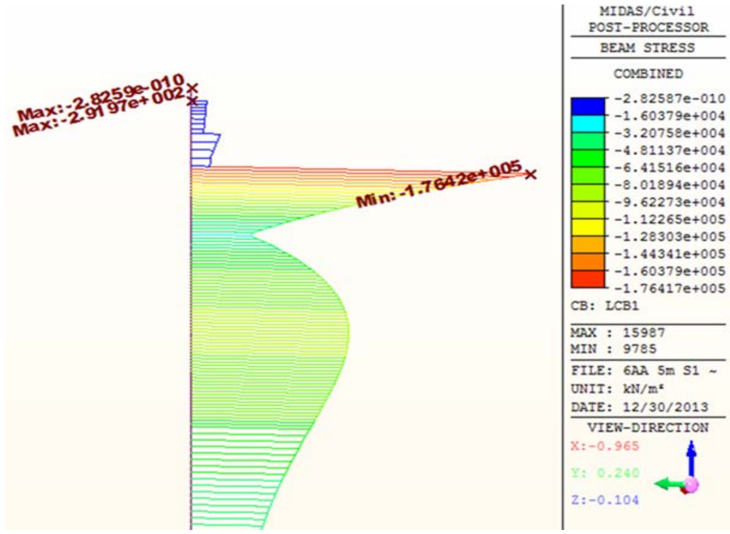

Figure 4.28: Pile Stress in 5m-Tall Abutment with Sand 1 & Weak-Axis by LCB 1 (Expansion)

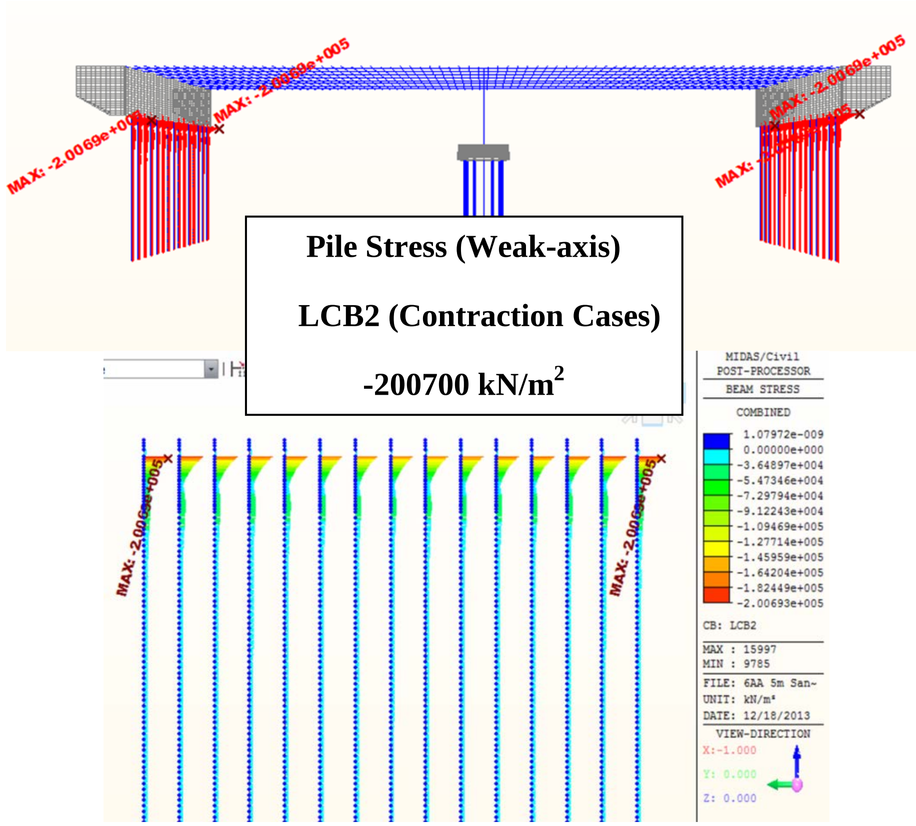

Figure 4.29: Pile Stress in 5m-Tall Abutment with Sand 1 & Weak-Axis by LCB 2 (Contraction)

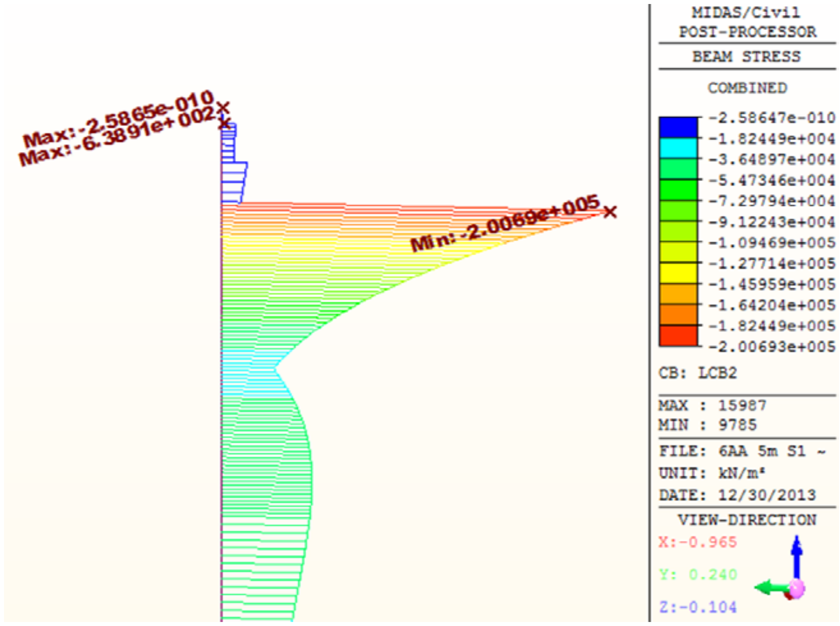

Figure 4.30: Pile Stress in 5m-Tall Abutment with Sand 1 & Weak-Axis by LCB 2 (Contraction)

As observed from Figures 4.31 and 4.32, the abutment height has a significant influence on the pile stress in weak axis orientation contrary to the case of pile moment, since there is up to an 81.4% reduction (8m-Tall Abutment: 18.6 %) in the pile stress when the abutment height increases for expansion cases while up to a 33.7 % reduction (8m-Tall Abutment: 66.3 %) is detected in contraction cases. On the other hand, the strong axis orientation has a slightly lower influence on the pile stress than the weak axis orientation when the abutment height increases, since there is up to a 64.1 % reduction (8m-Tall Abutment: 35.9 %) in the pile stress when the abutment height increases for expansion cases while up to a 33.3 % reduction (8m-Tall Abutment: 66.7 %) is detected in contraction cases.

In addition, as exposed in Tables 4.13b and 4.14b, the pile orientation has a substantially positive influence on the maximum combined pile stress in both expansion and contraction cases due to the difference of weak and strong axis bending.

Table 4.13: Values of Pile Stress by abutment height & pile orientation in LCB 1 (Expansion)

Pile Stress: LCB1 (Expansion Cases) Unit: kN/m^2 (Absolute Value)		
Abutment Height	**Strong-axis**	**Weak-axis**
3 m	1.788E+05	3.822E+05
4 m	1.208E+05	2.636E+05
5 m	8.158E+04	1.764E+05
6 m	5.570E+04	1.118E+05
7 m	5.677E+04	6.472E+04
8 m	6.418E+04	7.094E+04

Table 4.13a: Reduction Rate in Pile Stress by abutment height & pile orientation in LCB 1 (Expansion)

Reduction Rate in Pile Stress: LCB1 (Expansion Cases) Reference: 3 m		
Abutment Height	**Strong-axis**	**Weak-axis**
3 m	100.0%	100.0%
4 m	67.6%	69.0%
5 m	45.6%	46.2%
6 m	31.2%	29.3%
7 m	31.8%	16.9%
8 m	35.9%	18.6%

Table 4.14: Values of Pile Stress by abutment height & pile orientation in LCB 2 (Contraction)

Pile Stress: LCB2 (Contraction Cases) Unit: kN/m^2 (Absolute Value)		
Abutment Height	**Strong-axis**	**Weak-axis**
3 m	1.294E+05	2.104E+05
4 m	1.263E+05	2.158E+05
5 m	1.168E+05	2.007E+05
6 m	1.059E+05	1.798E+05
7 m	9.562E+04	1.591E+05
8 m	8.634E+04	1.396E+05

Table 4.14a: Reduction Rate in Pile Stress by abutment height & pile orientation in LCB 2 (Contraction)

Reduction Rate in Pile Stress: LCB2 (Contraction Cases) Reference: 3 m		
Abutment Height	Strong-axis	Weak-axis
3 m	100.0%	100.0%
4 m	97.6%	102.6%
5 m	90.3%	95.4%
6 m	81.8%	85.5%
7 m	73.9%	75.6%
8 m	66.7%	66.3%

Table 4.13b: Variation Rate in Pile Stress by abutment height & pile orientation in LCB 1 (Expansion)

Variation Rate in Pile Stress: LCB1 (Expansion Cases) Reference: Strong Axis		
Abutment Height	Strong-axis	Weak-axis
3 m	100.0%	213.8%
4 m	100.0%	218.2%
5 m	100.0%	216.2%
6 m	100.0%	200.7%
7 m	100.0%	114.0%
8 m	100.0%	110.5%

Table 4.14b: Variation Rate in Pile Stress by abutment height & pile orientation in LCB 2 (Contraction)

Variation Rate in Pile Stress: LCB2 (Contraction Cases) Reference: Strong Axis		
Abutment Height	Strong-axis	Weak-axis
3 m	100.0%	162.6%
4 m	100.0%	170.9%
5 m	100.0%	171.8%
6 m	100.0%	169.8%
7 m	100.0%	166.4%
8 m	100.0%	161.7%

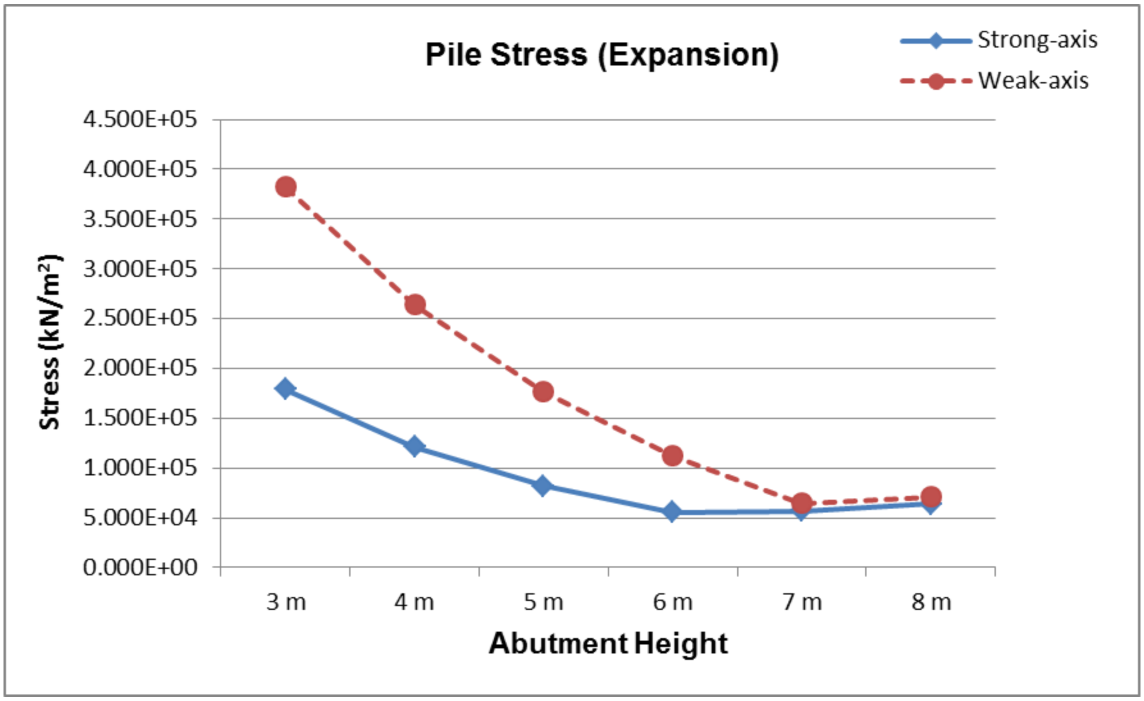

Figure 4.31: Pile Stress by abutment height and pile orientation in LCB 1 (Expansion)

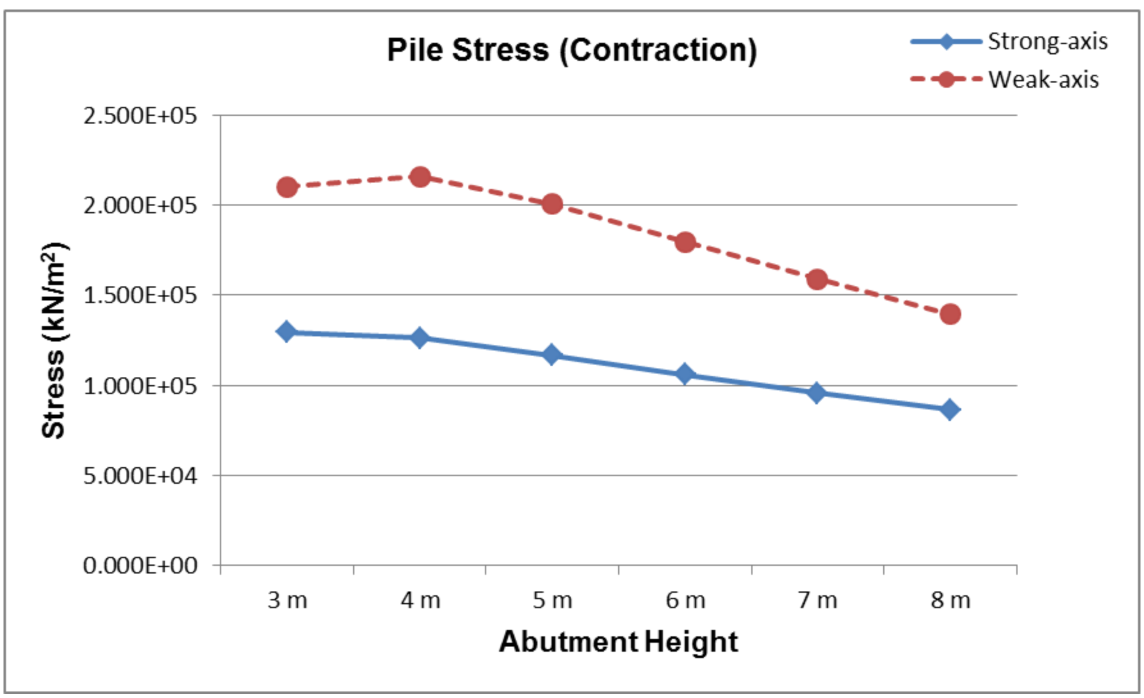

Figure 4.32: Pile Stress by abutment height and pile orientation in LCB 2 (Contraction)

As shown in Figures 4.33 and 4.34, there is an opposite tendency between expansion and contraction cases. In expansion cases, the soil stiffness has a negative influence on the maximum pile stress while the maximum pile stress increases when the soil stiffness increases in contraction cases as exposed in Tables 4.15a and 4.16a.

Table 4.15: Values of Pile Stress by soil types & pile orientation in LCB 1 (Expansion)

Pile Stress: LCB1 (Expansion Cases) Unit: kN/m^2 (Absolute Value)		
Soil Types	Strong-axis	Weak-axis
Sand 1	8.1580E+04	1.7640E+05
Sand 2	6.9050E+04	1.5470E+05
Clay 1	1.0970E+05	2.1900E+05
Clay 2	9.7490E+04	2.0760E+05

Table 4.15a: Variation Rate in Pile Stress by soil types & pile orientation in LCB 1 (Expansion)

Variation Rate in Pile Stress: LCB1 (Expansion Cases) Reference: Sand 1, Clay 1		
Soil Types	Strong-axis	Weak-axis
Sand 1	100.0%	100.0%
Sand 2	84.6%	87.7%
Clay 1	100.0%	100.0%
Clay 2	88.9%	94.8%

Table 4.15b: Variation Rate in Pile Stress by soil types & pile orientation in LCB 1 (Expansion)

Variation Rate in Pile Stress: LCB1 (Expansion Cases) Reference: Strong Axis		
Soil Types	Strong-axis	Weak-axis
Sand 1	100.0%	216.2%
Sand 2	100.0%	224.0%
Clay 1	100.0%	199.6%
Clay 2	100.0%	212.9%

Table 4.16: Values of Pile Stress by soil types & pile orientation in LCB 2 (Contraction)

Pile Stress: LCB2 (Contraction Cases) Unit: kN/m^2 (Absolute Value)		
Soil Types	Strong-axis	Weak-axis
Sand 1	1.1680E+05	2.0070E+05
Sand 2	1.2640E+05	2.2040E+05
Clay 1	1.0740E+05	1.8200E+05
Clay 2	1.1650E+05	2.0440E+05

Table 4.16a: Variation Rate in Pile Stress by soil types & pile orientation in LCB 2 (Contraction)

Variation Rate in Pile Stress: LCB2 (Contraction Cases) Reference: Sand 1, Clay 1		
Soil Types	Strong-axis	Weak-axis
Sand 1	100.0%	100.0%
Sand 2	108.2%	109.8%
Clay 1	100.0%	100.0%
Clay 2	108.5%	112.3%

Table 4.16b: Variation Rate in Pile Stress by soil types & pile orientation in LCB 2 (Contraction)

Variation Rate in Pile Stress: LCB2 (Contraction Cases) Reference: Strong Axis		
Soil Types	Strong-axis	Weak-axis
Sand 1	100.0%	171.8%
Sand 2	100.0%	174.4%
Clay 1	100.0%	169.5%
Clay 2	100.0%	175.5%

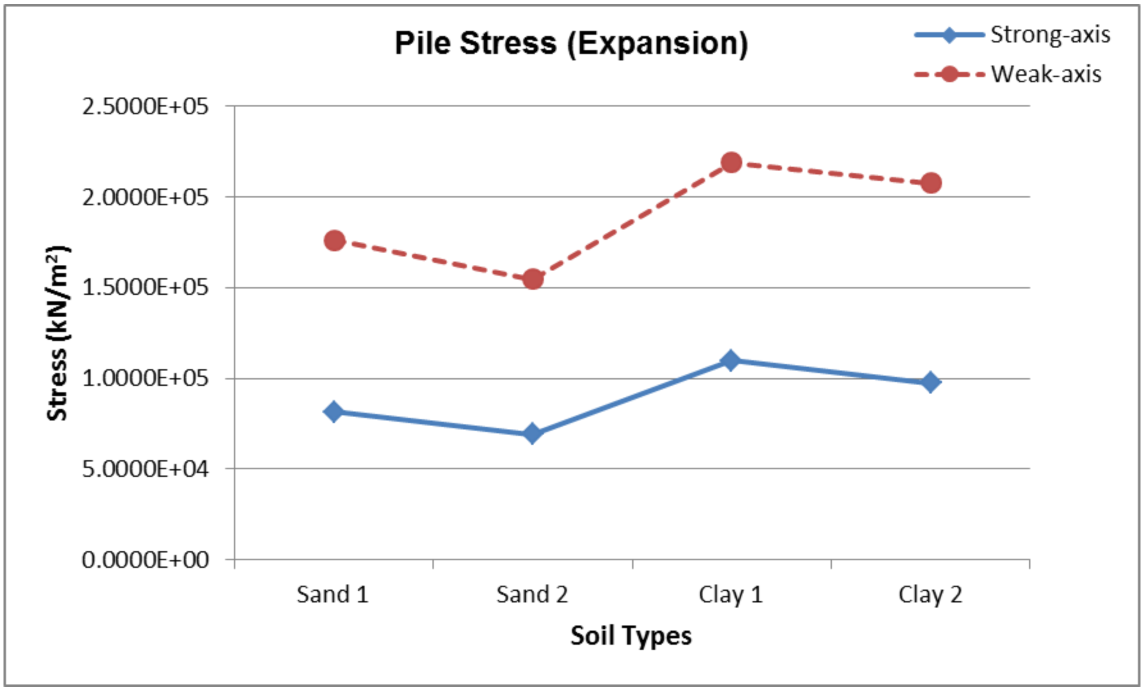

Figure 4.33: Pile Stress by soil types and pile orientation in LCB 1 (Expansion)

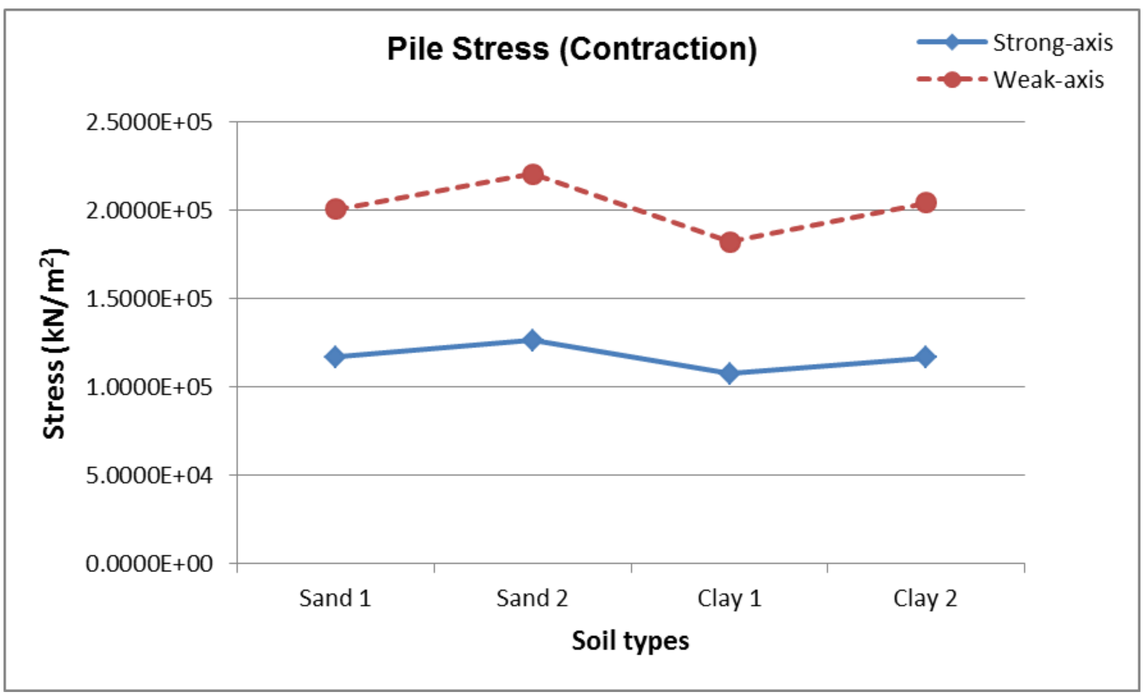

Figure 4.34: Pile Stress by soil types and pile orientation in LCB 2 (Contraction)

4.6 Pile Displacement

Figures 4.35 and 4.36 indicate the maximum pile head displacement induced by both expansion and contraction cases. As expected, the maximum pile displacement occurs at the pile head, the end of pile embedded 0.6 m into the abutment in expansion cases. However, in contraction cases, the maximum pile displacement does not occur at the pile head. The maximum pile displacement occurs at 0.3 m below the bottom of the abutment in contraction cases but it will be displayed later in Figure 4.55.

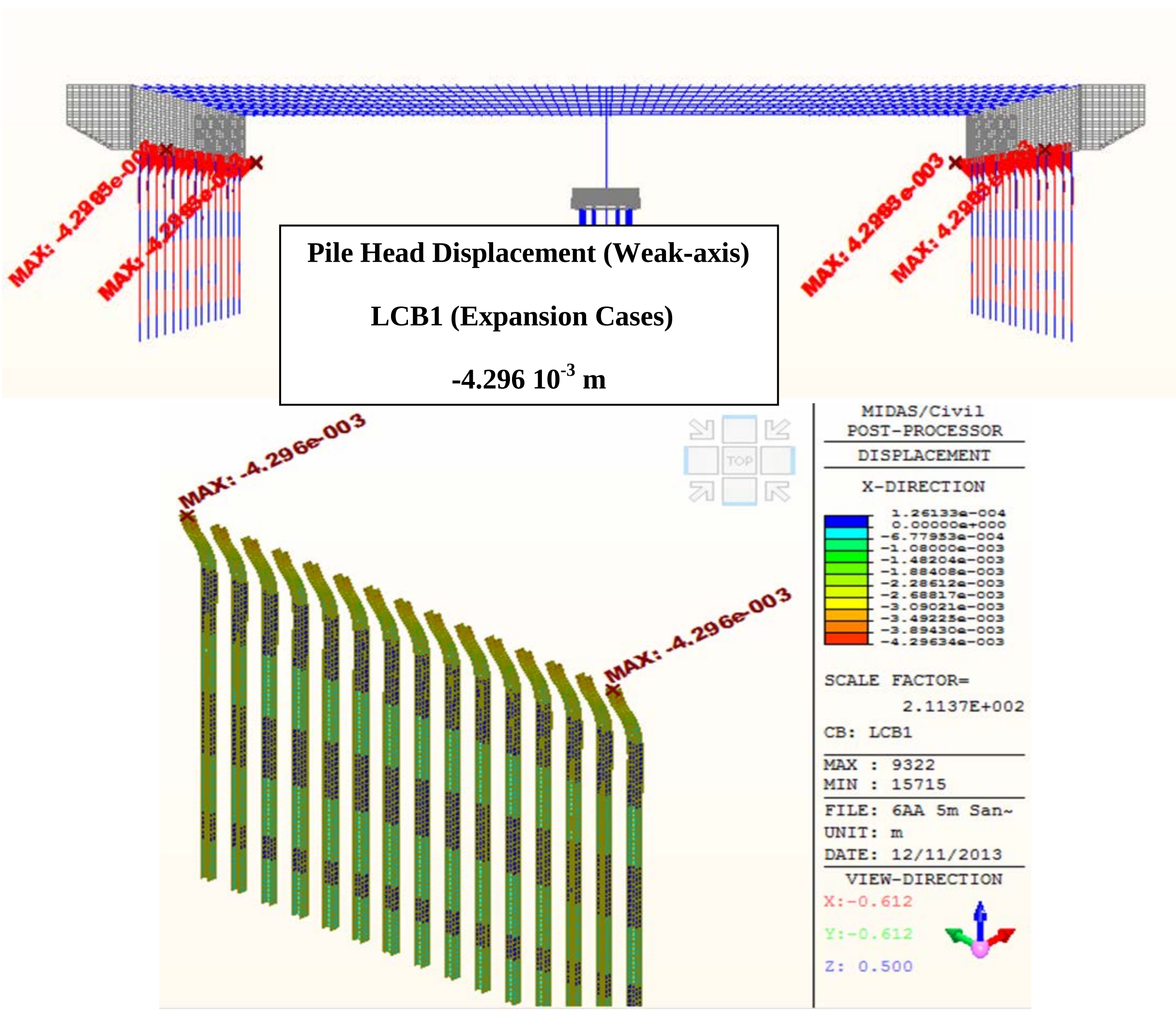

Figure 4.35: Pile Head Displacement in 5m-Tall Abutment with Sand 1 & Weak-Axis by LCB 1 (Expansion)

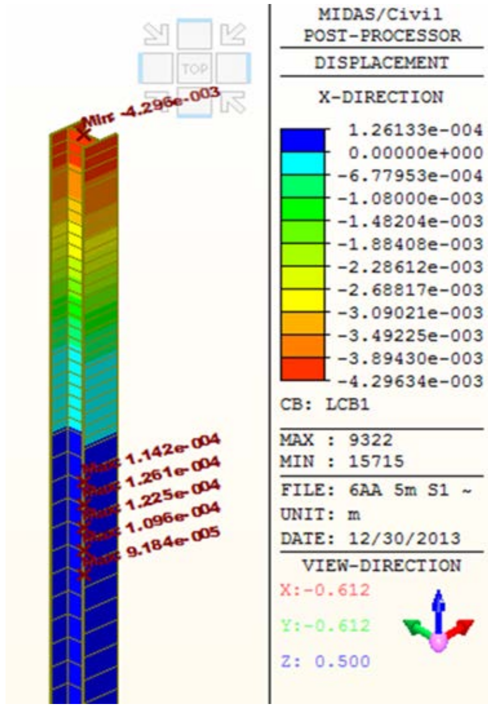

Figure 4.36: Pile Displacement in 5m-Tall Abutment with Sand 1 & Weak-Axis by LCB 1 (Expansion)

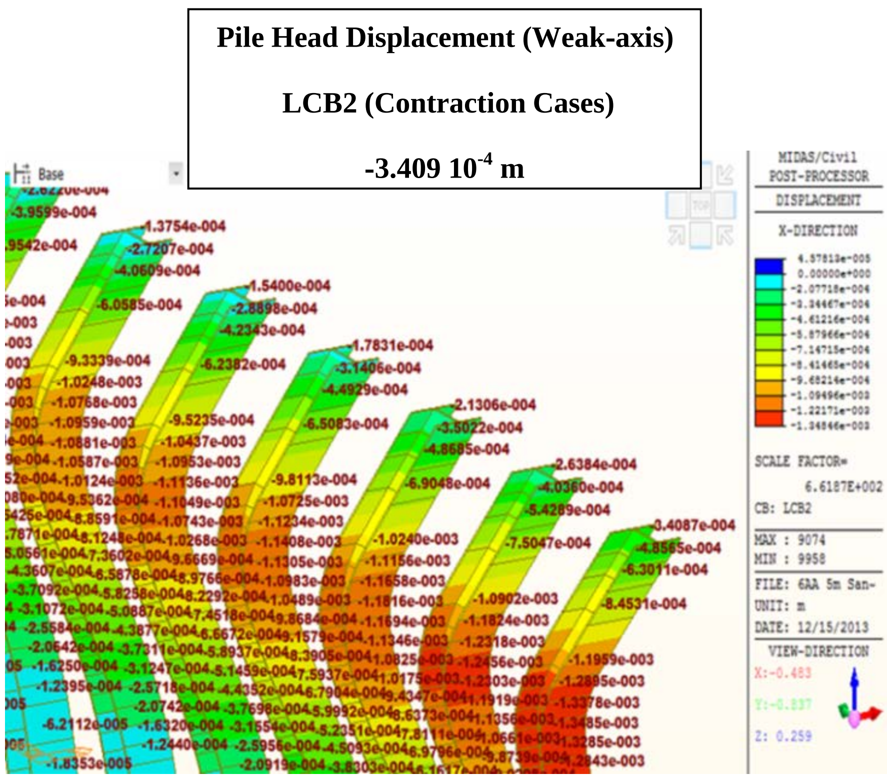

Figure 4.37: Pile Displacement in 5m-Tall Abutment with Sand 1 & Weak-Axis by LCB 2 (Contraction)

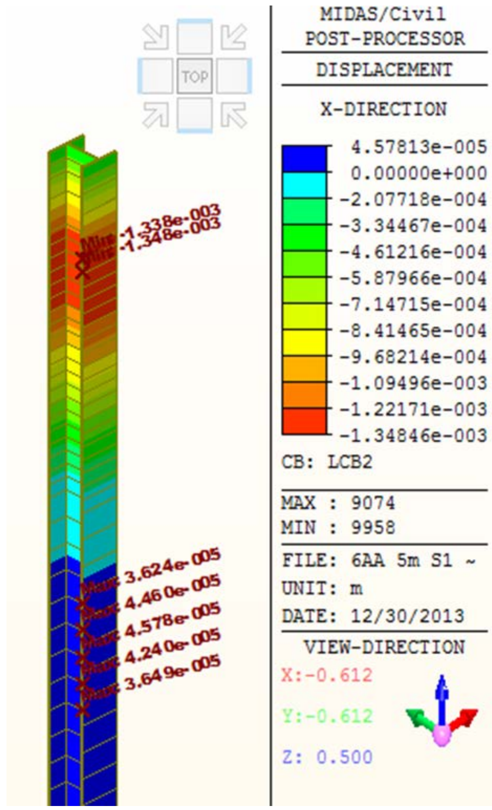

Figure 4.38: Pile Displacement in 5m-Tall Abutment with Sand 1 & Weak-Axis by LCB 2 (Contraction)

As shown from Figures 4.39 and 4.40, the abutment height has a significant influence on the pile head displacement in the weak axis orientation, since there is up to a 79 % reduction (8m-Tall Abutment: 21.0 %) in the pile head displacement when the abutment height increases for expansion cases while up to a 68.5 % reduction (8m-Tall Abutment: 31.5 %) is detected in contraction cases. On the other hand, the strong axis orientation has a slightly lower or higher influence on the pile head displacement than the weak axis orientation when the abutment height increases, since there is up to a 76.6 % reduction (8m-Tall Abutment: 23.4 %) in the pile head displacement when the abutment height increases for expansion cases while up to a 89.5 % reduction (8m-Tall Abutment: 10.5 %) is detected in contraction cases.

Table 4.17: Values of Pile Head Displacement by abutment height & pile orientation in LCB 1 (Expansion)

Pile Head Displacement: LCB1 (Expansion Cases) Unit: m (Absolute Value)		
Abutment Height	Strong-axis	Weak-axis
3 m	7.005E-03	7.656E-03
4 m	5.355E-03	5.770E-03
5 m	4.057E-03	4.296E-03
6 m	3.044E-03	3.162E-03
7 m	2.250E-03	2.290E-03
8 m	1.641E-03	1.606E-03

Table 4.17a: Reduction Rate in Pile Head Displacement by abutment height & pile orientation in LCB 1 (Expansion)

Reduction Rate in Pile Head Displacement: LCB1 (Expansion Cases) Reference: 3 m		
Abutment Height	Strong-axis	Weak-axis
3 m	100.0%	100.0%
4 m	76.4%	75.4%
5 m	57.9%	56.1%
6 m	43.5%	41.3%
7 m	32.1%	29.9%
8 m	23.4%	21.0%

Table 4.18: Values of Pile Head Displacement by abutment height & pile orientation in LCB 2 (Contraction)

Pile Head Displacement: LCB2 (Contraction Cases) Unit: m (Absolute Value)		
Abutment Height	Strong-axis	Weak-axis
3 m	1.595E-03	1.130E-03
4 m	6.689E-04	2.383E-04
5 m	2.291E-04	3.409E-04
6 m	2.341E-05	4.306E-04
7 m	1.818E-04	4.180E-04
8 m	1.668E-04	3.556E-04

Table 4.18a: Reduction Rate of Pile Head Displacement by abutment height & pile orientation in LCB 2 (Contraction)

Reduction Rate in Pile Head Displacement: LCB2 (Contraction Cases) Reference: 3 m		
Abutment Height	**Strong-axis**	**Weak-axis**
3 m	100.0%	100.0%
4 m	41.9%	21.1%
5 m	14.4%	30.2%
6 m	1.5%	38.1%
7 m	11.4%	37.0%
8 m	10.5%	31.5%

Table 4.17b: Reduction Rate in Pile Head Displacement by abutment height & pile orientation in LCB 1 (Expansion)

Variation Rate in Pile Head Displacement: LCB1 (Expansion Cases) Reference: Strong Axis		
Abutment Height	**Strong-axis**	**Weak-axis**
3 m	100.0%	109.3%
4 m	100.0%	107.7%
5 m	100.0%	105.9%
6 m	100.0%	103.9%
7 m	100.0%	101.8%
8 m	100.0%	97.9%

Table 4.18b: Reduction Rate of Pile Head Displacement by abutment height & pile orientation in LCB 2 (Contraction)

Variation Rate in Pile Head Displacement: LCB2 (Contraction Cases) Reference: Strong Axis		
Abutment Height	**Strong-axis**	**Weak-axis**
3 m	100.0%	70.8%
4 m	100.0%	35.6%
5 m	100.0%	148.8%
6 m	100.0%	1839.4%
7 m	100.0%	229.9%
8 m	100.0%	213.2%

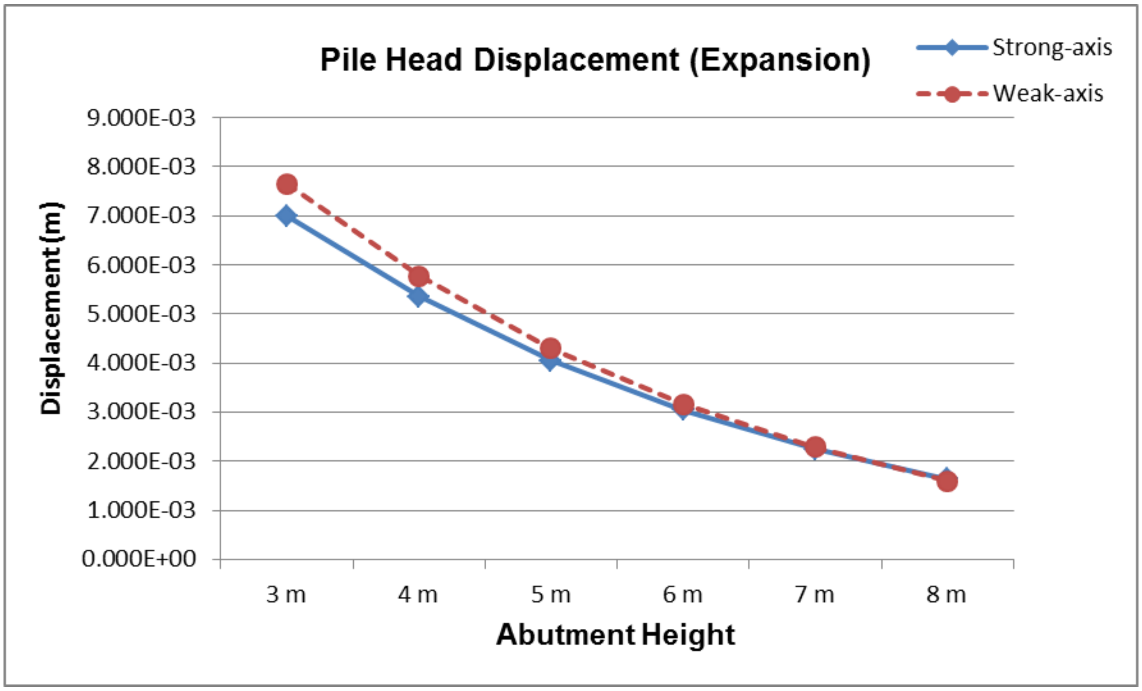

Figure 4.39: Pile Head Displacement by abutment height and pile orientation in LCB 1 (Expansion)

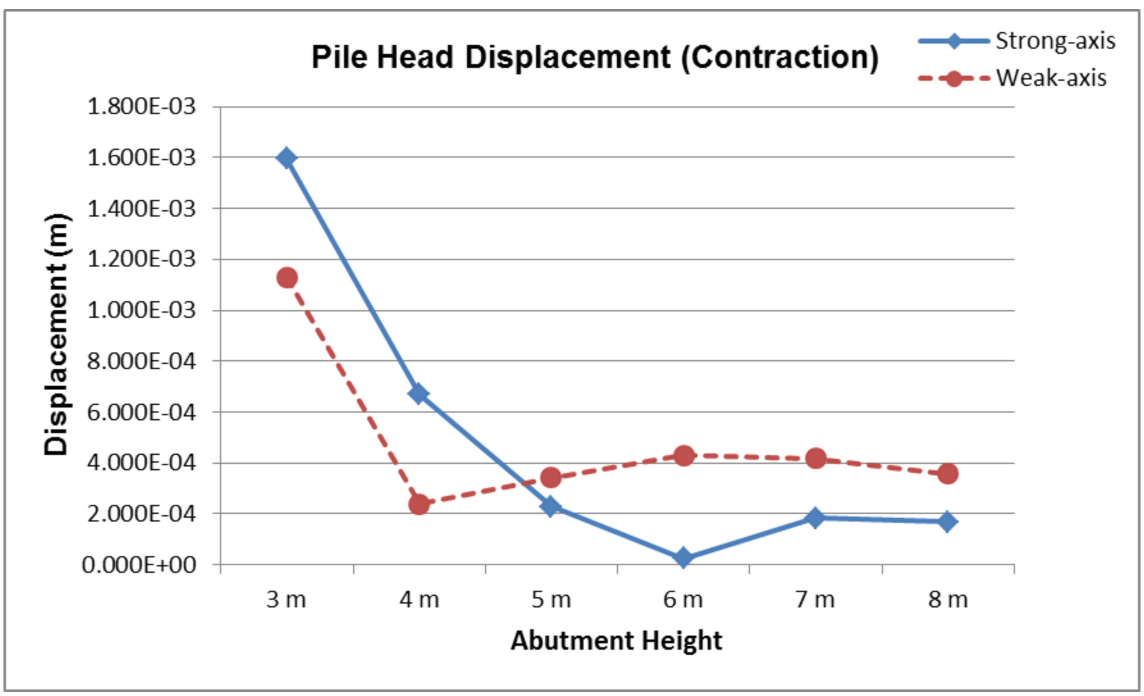

Figure 4.40: Pile Head Displacement by abutment height and pile orientation in LCB 2 (Contraction)

As shown in Figures 4.41 and 4.42, the difference of the soil stiffness has a negative influence on the pile head displacement when the soil stiffness increases in both expansion and contraction cases. As a result, the reduction in pile head displacement according to a growth of the abutment height is attributed to a weakened mobility by its augmented self–weight and an enlarged soil passive pressure by its increased surface area in the taller abutment.

Table 4.19: Values of Pile Head Displacement by soil types & pile orientation in LCB 1 (Expansion)

Pile Head Displacement: LCB1 (Expansion Cases) Unit: m (Absolute Value)		
Soil Types	**Strong-axis**	**Weak-axis**
Sand 1	**4.0570E-03**	**4.2960E-03**
Sand 2	**3.4110E-03**	**3.5150E-03**
Clay 1	**7.3450E-03**	**8.6080E-03**
Clay 2	**5.1780E-03**	**5.9290E-03**

Table 4.19a: Variation Rate in Pile Head Displacement by soil types & pile orientation in LCB 1 (Expansion)

Variation Rate in Pile Head Displacement: LCB1 (Expansion Cases) Reference: Sand 1, Clay 1		
Soil Types	**Strong-axis**	**Weak-axis**
Sand 1	**100.0%**	**100.0%**
Sand 2	**84.1%**	**81.8%**
Clay 1	**100.0%**	**100.0%**
Clay 2	**70.5%**	**68.9%**

Table 4.19b: Variation Rate in Pile Head Displacement by soil types & pile orientation in LCB 1 (Expansion)

Variation Rate in Pile Head Displacement: LCB1 (Expansion Cases) Reference: Strong Axis		
Soil Types	**Strong-axis**	**Weak-axis**
Sand 1	**100.0%**	**105.9%**
Sand 2	**100.0%**	**103.0%**
Clay 1	**100.0%**	**117.2%**
Clay 2	**100.0%**	**114.5%**

Table 4.20: Values of Pile Head Displacement by soil types & pile orientation in LCB 2 (Contraction)

Pile Head Displacement: LCB2 (Contraction Cases) Unit: m (Absolute Value)		
Soil Types	Strong-axis	Weak-axis
Sand 1	2.2910E-04	3.4090E-04
Sand 2	2.4100E-04	2.1310E-04
Clay 1	1.1360E-03	2.2200E-03
Clay 2	4.0210E-04	1.1550E-03

Table 4.20a: Variation Rate in Pile Head Displacement by soil types & pile orientation in LCB 2 (Contraction)

Variation Rate in Pile Head Displacement: LCB2 (Contraction Cases) Reference: Sand 1, Clay 1		
Soil Types	Strong-axis	Weak-axis
Sand 1	100.0%	100.0%
Sand 2	105.2%	62.5%
Clay 1	100.0%	100.0%
Clay 2	35.4%	52.0%

Table 4.20b: Variation Rate in Pile Head Displacement by soil types & pile orientation in LCB 2 (Contraction)

Variation Rate in Pile Head Displacement: LCB2 (Contraction Cases) Reference: Strong Axis		
Soil Types	Strong-axis	Weak-axis
Sand 1	100.0%	148.8%
Sand 2	100.0%	88.4%
Clay 1	100.0%	195.4%
Clay 2	100.0%	287.2%

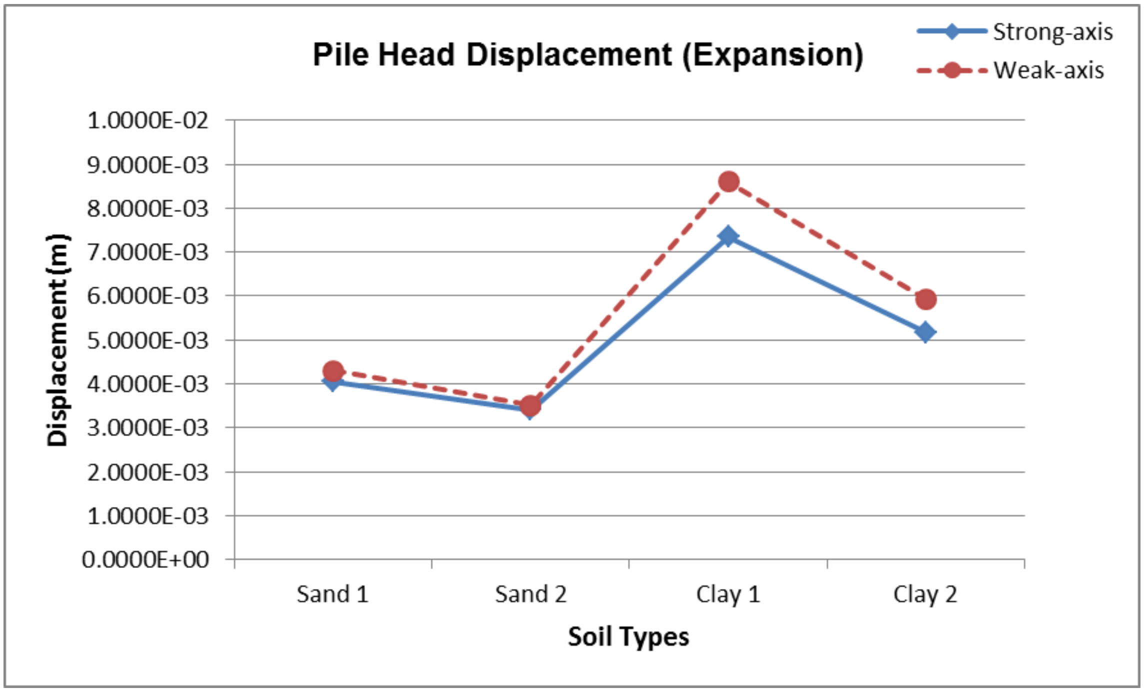

Figure 4.41: Pile Displacement by soil types and pile orientation in LCB 1 (Expansion)

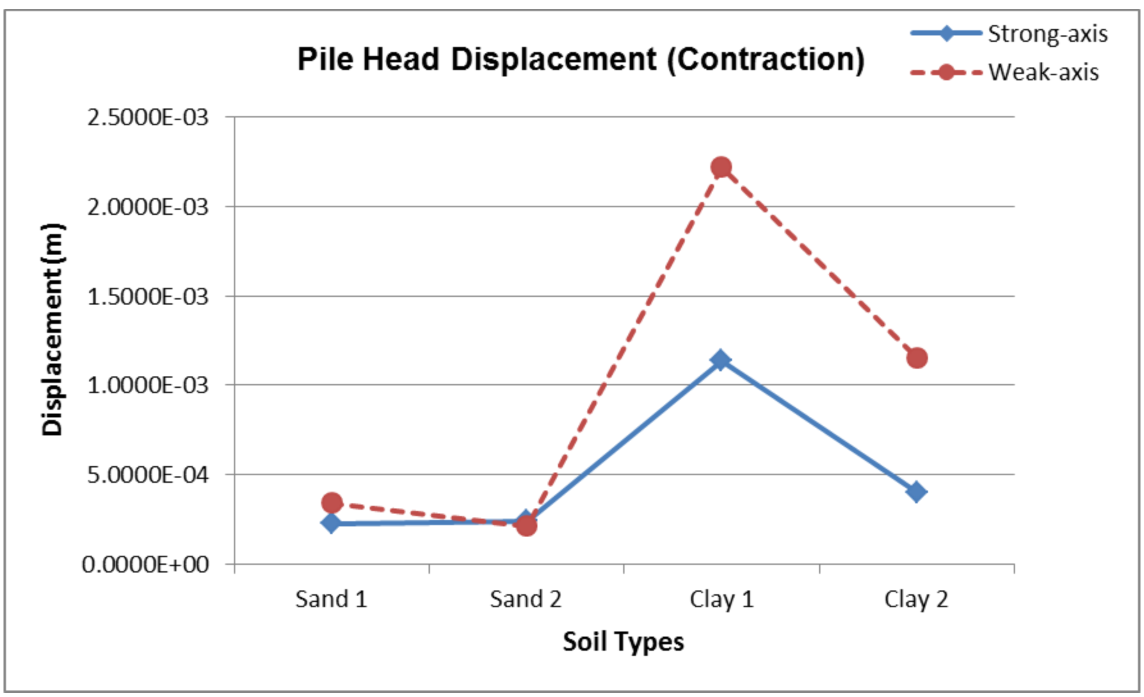

Figure 4.42: Pile Displacement by soil types and pile orientation in LCB 2 (Contraction)

4.7 Soil Abutment Interaction

As shown in Figure 4.43, the soil springs for integral abutments were created according to MIDAS CIVIL CODE (2013). The input data for 5 m–tall abutment without a strip footing was entered as displayed in Table 4.21. The input data for 3 m, 4 m, 6 m, 7 m, 8 m-tall abutments was applied with only those for sand 1 in both strong and weak axial directions to avoid excessive computation time in this study.

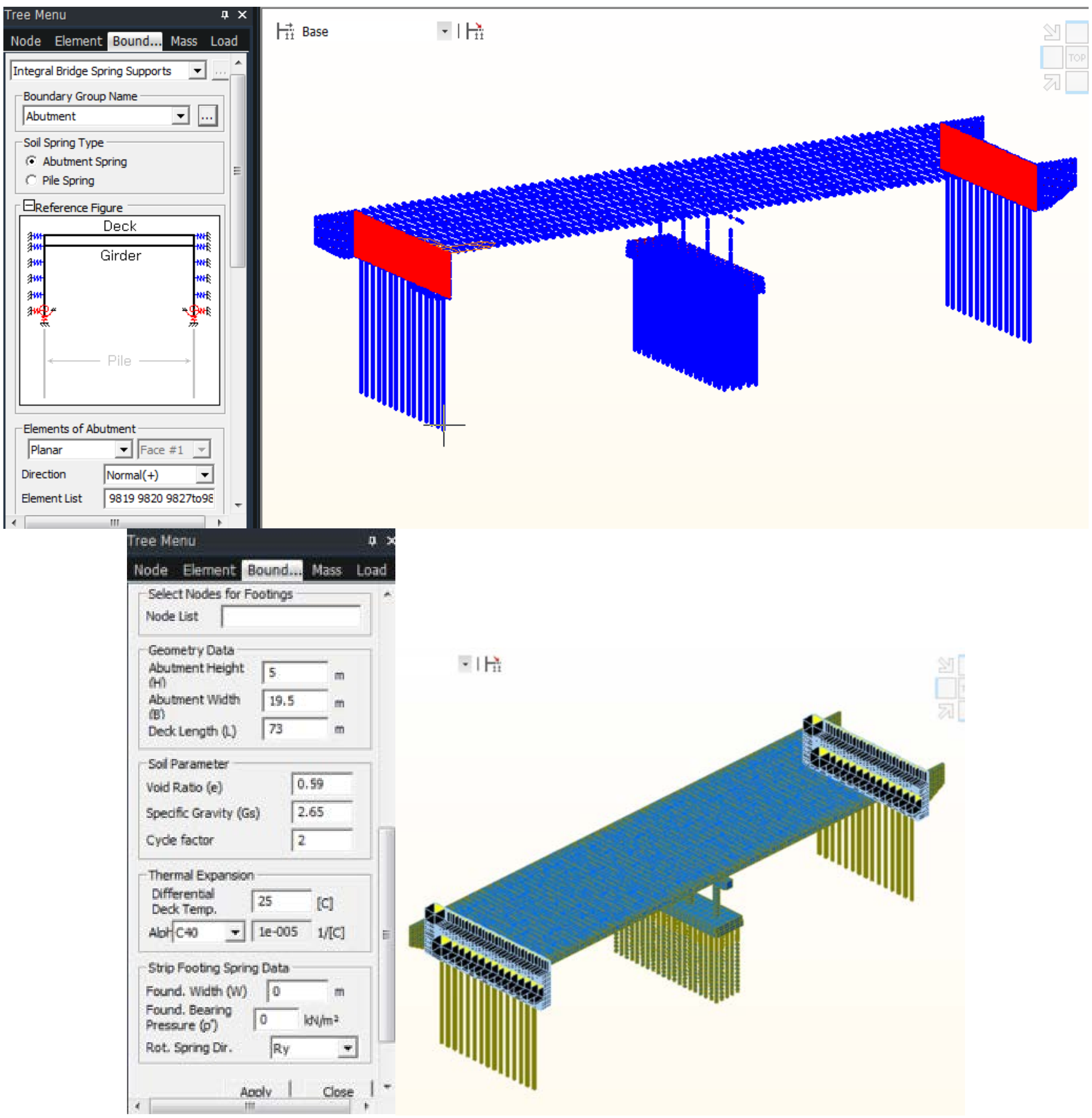

Figure 4.43: Procedure for Creating of Soil Springs on Abutments

Table 4.21: Input Data for 5 m-Tall Abutment

Geometry Data	**Abutment Height (H)**	**5 m**
	Abutment Width (B)	**19.5 m**
	Deck Length (L)	**73 m**
Soil Parameter	**Void Ratio e)**	**Sand 1: 0.59** **Sand 2: 0.45** **Clay 1: 0.76** **Clay 2: 0.59**
	Specific Gravity (Gs)	**2.65**
	Cycle factor (fcyc):	**2**
Thermal Extension	**Differential Deck Temperature**	**25**
	α: Thermal expansion coefficient of deck	**1.00E-05**

The interaction between the abutment wall and backfill soil has a hyperbolic relationship as experimentally observed, and verified with finite element analysis by other researchers. Thus, nonlinear springs for abutment were created by the lateral stress-displacement relationship for the abutment backfill of Integral Abutment Bridges in the bridge finite element analysis software MIDAS CIVIL.

The stiffness per unit area for abutment in the software MIDAS CIVIL is calculated using the method established by Broms (1971).

Stiffness per unit area:

$$K_s = 3.5\ G_{eq} / \ [H \times (B/H)^{0.5}] \qquad (4\text{-}1)$$

$$G_{eq} = p_{atm}\ 600\ f_{cyc}\ F\ (\mathrm{e})\ (p'/\ p_{atm})^{0.5}\ (2.5H \times\ 0.001/\Delta)^{\ 0.5} \qquad \text{for } 75\times10^{-6} < \Delta/H < 0.025$$

$$p' = 1.5\ \gamma_{fill}\ (H/2) - u = 1.5g \times \rho_d \times (H/2)$$

$$\rho_{d} = G_s\ \rho_w\ /\ (1+e)$$

Where:

f_{cyc} : Cycle Factor (=2)

G_{eq}: Equivalent shear modulus of the backfill

F (e) void ratio function: $\frac{(2.17-e)^2}{(1+e)}$

p_{atm}: Atmospheric pressure (100000 N/m^2)

e: void ratio (=0.59)

B: width of the bridge (=19.5 m, except wingwall thickness)

H: full height of the abutment (=5 m)

L: Deck Length (=73 m)

Δ: lateral displacement $\Delta = \frac{\alpha \times \Delta T \times L}{4}$

γ_{fill}: Unit weight of backfill (=19 kN/m^3)

G_s: Specific gravity of soils (=2.65)

ρ_w : Density of water (=1000 N/m^3)

u: Average pore pressure (=0)

g: Gravity acceleration (=9.806 m/sec^2)

Table 4.22: Soil stiffness for 5 m-Tall Abutment with Sand1

Node	Type	Stiffness (kN/m)
10052	Comp.-only	272.12
10053	Comp.-only	272.12
10136	Comp.-only	272.12
10137	Comp.-only	272.12
12316	Comp.-only	272.12
12389	Comp.-only	272.12
15611	Comp.-only	272.12
15684	Comp.-only	272.12
10057	Comp.-only	544.25
10058	Comp.-only	544.25
10131	Comp.-only	544.25
10132	Comp.-only	544.25
10142	Comp.-only	544.25
10143	Comp.-only	544.25
10230	Comp.-only	544.25
10231	Comp.-only	544.25
10240	Comp.-only	544.25
10241	Comp.-only	544.25
10332	Comp.-only	544.25
10333	Comp.-only	544.25
10342	Comp.-only	544.25
10343	Comp.-only	544.25
10438	Comp.-only	544.25
10439	Comp.-only	544.25

Table 4.22 shows the soil stiffness calculated for 5 m-Tall Abutment with Sand1 and Weak-Axis. For two abutments, 1584 soil springs was created.

4.8 Soil Pile Interaction

As shown Figure 4.44 and 4.45, the soil springs for H piles and PC piles were created according to MIDAS CIVIL CODE (2013). Table 4.23 shows the input data for H piles and PC piles in 5 m-Tall Abutment with Sand1.

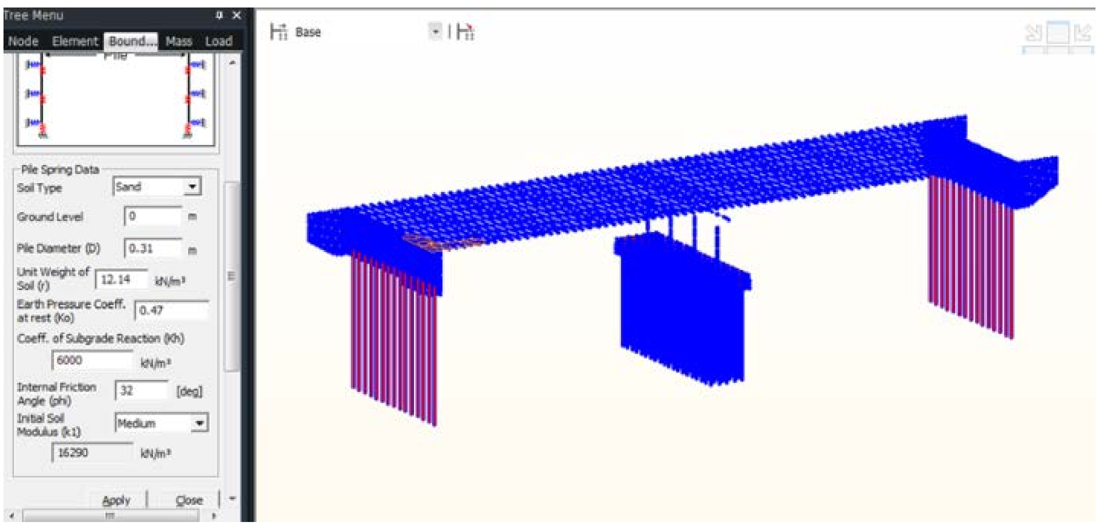

Figure 4.44: Procedure for Creating of Soil Springs on H Piles

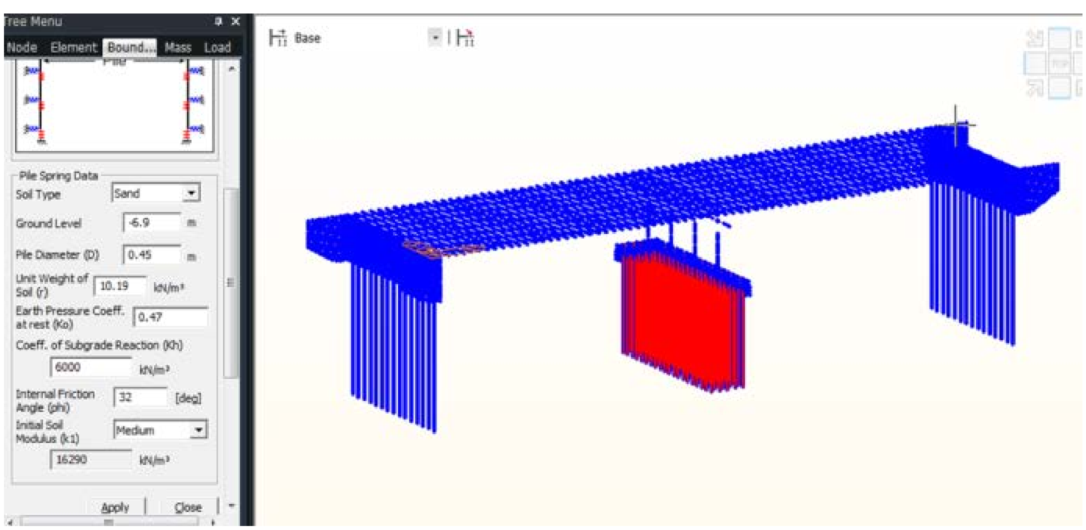

Figure 4.45: Procedure for Creating of Soil Springs on PC Piles

Table 4.23: Input Data for Soil Springs on H Piles and PC Piles with Sand1

Input Data for Soil Springs on H Piles and PC Piles with Sand1		H Pile	PC Pile
Geometry Data	Ground Level (Z)	0 m	-6.9 m
	Pile Diameter(D)	0.31 m	0.45 m
Soil Parameter	Unit Weight of Soil(γ) kN/m^3	3 m-Tall: 12.83 4 m-Tall: 12.51 5 m-Tall: 12.14 6 m-Tall: 11.73 7 m-Tall: 11.25 8 m-Tall: 10.68	10.19
	Earth Pressure Coeff. at rest(K_0)	0.47	0.47
	Coeff. of Subgrade Reaction(K_h) kN/m^3	6000	6000
	Internal Friction Angle (Φ)	32	32
	Initial Soil Modulus(k1) kN/m^3	16290	16290

Table 4.24: Input Data for Soil Springs on H Piles and PC Piles with Sand2

Input Data for Soil Springs on H Piles and PC Piles with Sand2		H Pile	PC Pile
Geometry Data	Ground Level (Z)	0 m	-6.9 m
	Pile Diameter(D)	0.31 m	0.45 m
Soil Parameter	Unit Weight of Soil(γ) kN/m^3	12.95	11.19
	Earth Pressure Coeff. at rest(K_0)	0.38	0.38
	Coeff. of Subgrade Reaction(K_h) kN/m^3	12000	12000
	Internal Friction Angle (Φ)	38	38
	Initial Soil Modulus(k1) kN/m^3	33930	33930

For sand, the soil stiffnesses for piles in the software MIDAS CIVIL are calculated using the method established by Reese et al (1974). The ultimate resistance of sand varies from a value determined by equation (4-2) at shallow depths to a value determined by equation (4-3) at large depths.

$X < X_t$

$$P_u = A\gamma X\,[c_1 + c_2 + c_3 - c_4] \qquad (4\text{-}2)$$

$c_1 = [K_0 X \tan\varphi' \sin\beta]/[\tan(\beta - \varphi') \cos\alpha]$

$c_2 = [\tan\beta / \tan(\beta - \varphi')] [D + X \tan\beta \tan\alpha]$

$c_3 = K_0 X \tan\beta (\tan\varphi' \sin\beta - \tan\alpha)$

$c_4 = K_a D$

$X > X_t$

$$P_u = AD [c_5 + c_6] \quad (4\text{-}3)$$

$c_5 = K_a \gamma X(\tan^8\beta - 1)$

$c_6 = K_a \gamma X \tan\varphi' \tan^4\beta$

Where:

P_u: Ultimate resistance per unit length

A : Empirical adjustment factor, which accounts for differences in static and cyclic behavior

γ : Total Unit weight of soil

X : Depth below soil surface

K_0 : Coefficient of earth pressure at rest

φ' : Angle of internal friction of sand

β : $45° + \varphi'/2$

α : $\varphi'/2$

K_a: Rankine minimum active earth pressure coefficient

D: Pile diameter

$Y_u = 3D/80$

$P_m = (B/A) P_u$

A, B: Non-dimensional empirical adjustment factors to account for difference in static and cyclic behavior

$Y_m = D/60$

$Y_k = [P_m / (k_1 X Y_m)^{1/n}]^{n/n-1}$

$P_k = k_1 X Y_k$

$n = [P_m (Y_u - Y_m)] / [Y_m (P_u - P_m)]$

k_1= Initial soil modulus

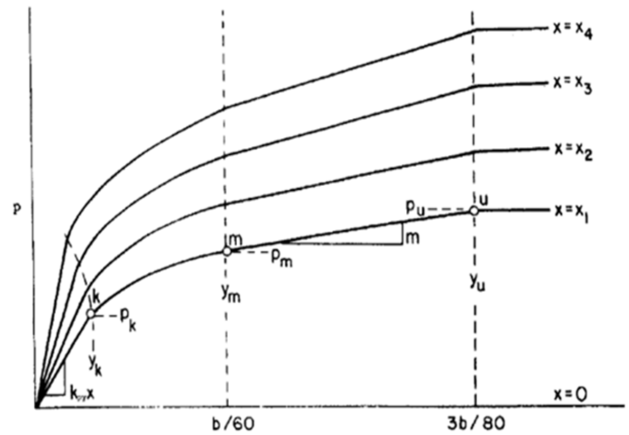

Figure 4.46: Characteristic shape of a family of p-y curves for static and cyclic loading in sand (Reese et al, 2006)

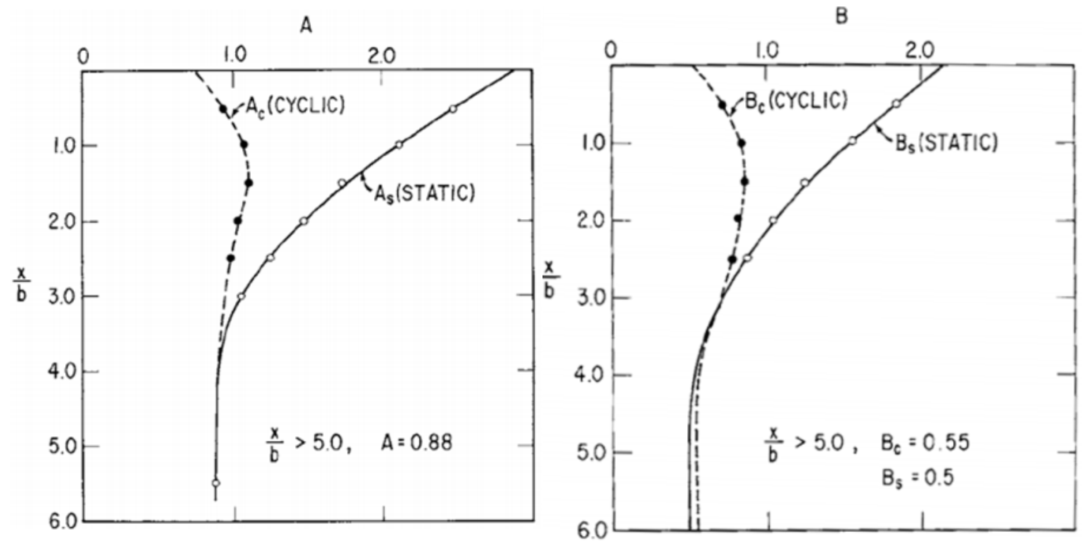

Figure 4.47: Values of coefficients A, B for static and cyclic loading in sand (Reese et al, 2006)

The soil stiffnesses calculated for H piles and PC piles with 5 m-tall abutment in both strong and weak-axis are as shown in Table 4.25.

For the lateral springs (p- y curves), 18,360 non-linear springs (multi-linear springs) were created. For the vertical springs (tangent springs, f-z curves) and point springs (tip springs, q-z curves), 9,180 linear springs were generated as shown in Figure 4.48.

Table 4.25: Soil stiffnesses calculated for Soil Springs on H Piles and PC Piles with Sand1

Node	Type	SDz (kN/m)	Multi-Linear Type	by (kN)	cx (m)	cy (kN)	dx (m)	dy (kN)	ex (m)	ey (kN)	fx (m)	fy (kN)
1	Multi-Linear	0	Symmetric	96.7	0.01	123.16	0.02	197.05	0.03	197.05	0.04	197.05
1	Multi-Linear	0	Symmetric	96.7	0.01	123.16	0.02	197.05	0.03	197.05	0.04	197.05
1	Linear	574.4681	Unsymmetric	0	0	0	0	0	0	0	0	0
2	Multi-Linear	0	Symmetric	96.7	0.01	123.16	0.02	197.05	0.03	197.05	0.04	197.05
2	Multi-Linear	0	Symmetric	96.7	0.01	123.16	0.02	197.05	0.03	197.05	0.04	197.05
2	Linear	574.4681	Unsymmetric	0	0	0	0	0	0	0	0	0
3	Multi-Linear	0	Symmetric	96.7	0.01	123.16	0.02	197.05	0.03	197.05	0.04	197.05
3	Multi-Linear	0	Symmetric	96.7	0.01	123.16	0.02	197.05	0.03	197.05	0.04	197.05
3	Linear	574.4681	Unsymmetric	0	0	0	0	0	0	0	0	0
4	Multi-Linear	0	Symmetric	96.7	0.01	123.16	0.02	197.05	0.03	197.05	0.04	197.05
4	Multi-Linear	0	Symmetric	96.7	0.01	123.16	0.02	197.05	0.03	197.05	0.04	197.05
4	Linear	574.4681	Unsymmetric	0	0	0	0	0	0	0	0	0
5	Multi-Linear	0	Symmetric	96.7	0.01	123.16	0.02	197.05	0.03	197.05	0.04	197.05
5	Multi-Linear	0	Symmetric	96.7	0.01	123.16	0.02	197.05	0.03	197.05	0.04	197.05
5	Linear	574.4681	Unsymmetric	0	0	0	0	0	0	0	0	0
6	Multi-Linear	0	Symmetric	142.42	0.01	154.32	0.01	246.91	0.02	246.91	0.02	246.91
6	Multi-Linear	0	Symmetric	142.42	0.01	154.32	0.01	246.91	0.02	246.91	0.02	246.91
6	Linear	395.7447	Unsymmetric	0	0	0	0	0	0	0	0	0

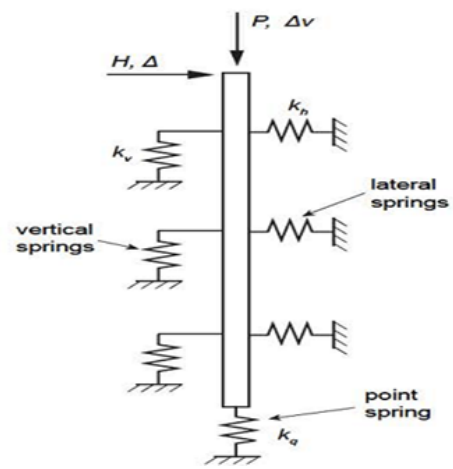

Figure 4.48: Design of Soil-Pile System (Greimann et al., 1987)

Table 4.26: Input Data for Soil Springs on H Piles and PC Piles with Clay1

Input Data for Soil Springs on H Piles and PC Piles with Clay1		H Pile	PC Pile
Geometry Data	Ground Level (Z)	0 m	-6.9 m
	Pile Diameter(D)	0.31 m	0.45 m
Soil Parameter	Unit Weight of Soil(γ) kN/m^3	11.19	9.19
	Earth Pressure Coeff. at rest(K_0)	0.63	0.63
	Coeff. of Subgrade Reaction(K_h) kN/m^3	4500	4500
	Undrained shear strength, Cu (kPa)	40	40
	Soil Strain e_{50}	0.01	0.01

Table 4.27: Input Data for Soil Springs on H Piles and PC Piles with Clay2

Input Data for Soil Springs on H Piles and PC Piles with Clay2		H Pile	PC Pile
Geometry Data	Ground Level (Z)	0 m	-6.9 m
	Pile Diameter(D)	0.31 m	0.45 m
Soil Parameter	Unit Weight of Soil(γ) kN/m^3	12.14	10.19
	Earth Pressure Coeff. at rest(K_0)	0.61	0.61
	Coeff. of Subgrade Reaction(K_h) kN/m^3	9500	9500
	Undrained shear strength, Cu (kPa)	80	80
	Soil Strain e_{50}	0.006	0.006

For clay, the stiffnesses for piles in the software MIDAS CIVIL are calculated using the method established by Matlock (1970). The ultimate resistance (P_u) of stiff clay increases from 3 C_u to 9 C_u as the depth X increases from 0 to X_R.

$$P_u = D[3C_u + \gamma X + JC_u X/D] \quad \text{for } X \le X_R$$

$$P_u = 9C_u D \quad \text{for } X \ge X_R$$

Where:

P_u: Ultimate resistance per unit length

γ: Total Unit weight of soil

X: Depth below soil surface

D: Pile diameter

C_u: Undrained shear strength

J: Dimensionless empirical constant (0.25 for stiff clay)

X_R: Depth below soil surface to bottom of reduced resistance zone

$$X_R = 6D / [\gamma X / C_u + J]$$

Table 4.28: Soil stiffnesses calculated for Soil Springs on H Piles and PC Piles with Clay1

Node	Type	SDz (kN/m)	Multi-Linear Type	by (kN)	cx (m)	cy (kN)	dx (m)	dy (kN)	ex (m)	ey (kN)	fx (m)	fy (kN)
1	Multi-Linear	0	Symmetric	3.89	0.01	8.1	0.03	11.66	0.09	16.2	0.11	16.2
1	Multi-Linear	0	Symmetric	3.89	0.01	8.1	0.03	11.66	0.09	16.2	0.11	16.2
1	Linear	321.4286	Unsymmetric	0	0	0	0	0	0	0	0	0
2	Multi-Linear	0	Symmetric	3.89	0.01	8.1	0.03	11.66	0.09	16.2	0.11	16.2
2	Multi-Linear	0	Symmetric	3.89	0.01	8.1	0.03	11.66	0.09	16.2	0.11	16.2
2	Linear	321.4286	Unsymmetric	0	0	0	0	0	0	0	0	0
3	Multi-Linear	0	Symmetric	3.89	0.01	8.1	0.03	11.66	0.09	16.2	0.11	16.2
3	Multi-Linear	0	Symmetric	3.89	0.01	8.1	0.03	11.66	0.09	16.2	0.11	16.2
3	Linear	321.4286	Unsymmetric	0	0	0	0	0	0	0	0	0
4	Multi-Linear	0	Symmetric	3.89	0.01	8.1	0.03	11.66	0.09	16.2	0.11	16.2
4	Multi-Linear	0	Symmetric	3.89	0.01	8.1	0.03	11.66	0.09	16.2	0.11	16.2
4	Linear	321.4286	Unsymmetric	0	0	0	0	0	0	0	0	0
5	Multi-Linear	0	Symmetric	3.89	0.01	8.1	0.03	11.66	0.09	16.2	0.11	16.2
5	Multi-Linear	0	Symmetric	3.89	0.01	8.1	0.03	11.66	0.09	16.2	0.11	16.2
5	Linear	321.4286	Unsymmetric	0	0	0	0	0	0	0	0	0
6	Multi-Linear	0	Symmetric	2.68	0.01	5.58	0.02	8.04	0.06	11.16	0.08	11.16
6	Multi-Linear	0	Symmetric	2.68	0.01	5.58	0.02	8.04	0.06	11.16	0.08	11.16
6	Linear	221.4286	Unsymmetric	0	0	0	0	0	0	0	0	0

4.9 Summary and In-depth Reviews

This section summarizes and reviews the results of the parametric study. The reviews progress in the following subsections: (1) Girder Stress, (2) Abutment Stress, (3) Pile Moment, (4) Pile Stress, and (5) Pile Displacement, (6) Soil-Structure Interaction.

4.9.1 Girder Stress

As shown in Figure 4.49, the expansion creates higher compressive stress at both ends of the girder than the contraction does. On the contrary, the contraction produces larger compressive stress at the middle of the edge girder due to the stress concentration than the expansion does. Similarly, the contraction generates higher tensile (+) stress in the middle of the span than the expansion (Figure 4.51).

The abutment height has some negative influence on the maximum combined girder stress in weak axial direction, since there is up to a 4.6 % reduction in the bottom girder stress in expansion cases when the abutment height increases whereas girder bottom stress show an 11 % drop in contraction cases (Tables 4.1a and 4.2a).

Figures 4.49 and 4.50 express the stress variations at the left end of the edge girder under both expansion and contraction cases. The maximum combined compressive stress at the left end of the edge girder in expansion cases is higher than in contraction.

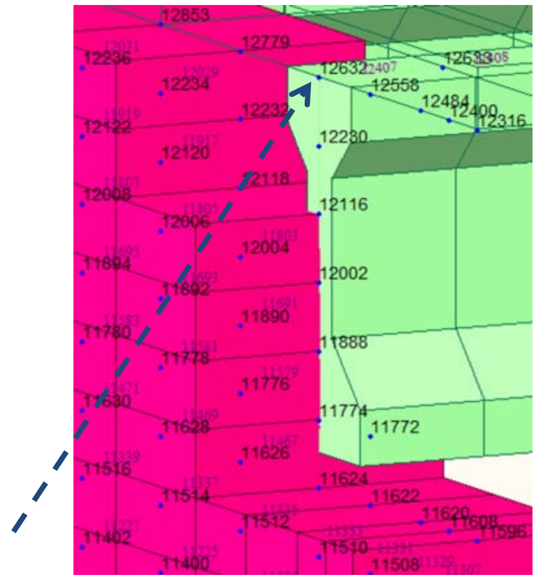

A. Node (12632) at the left end on the top of the edge girder

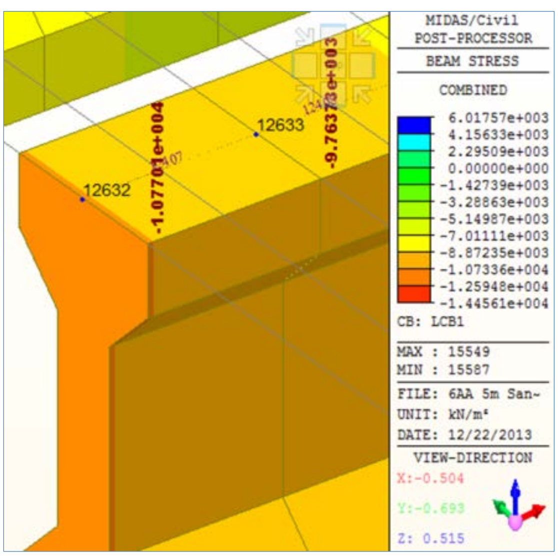

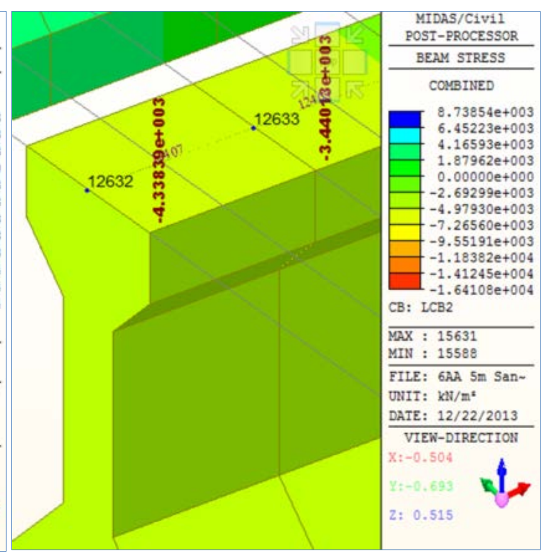

B. Stress in LCB 1 **C. Stress in LCB 2**

Figure 4.49: Stress Variations at the left end of the edge girder by LCB 1 or LCB 2

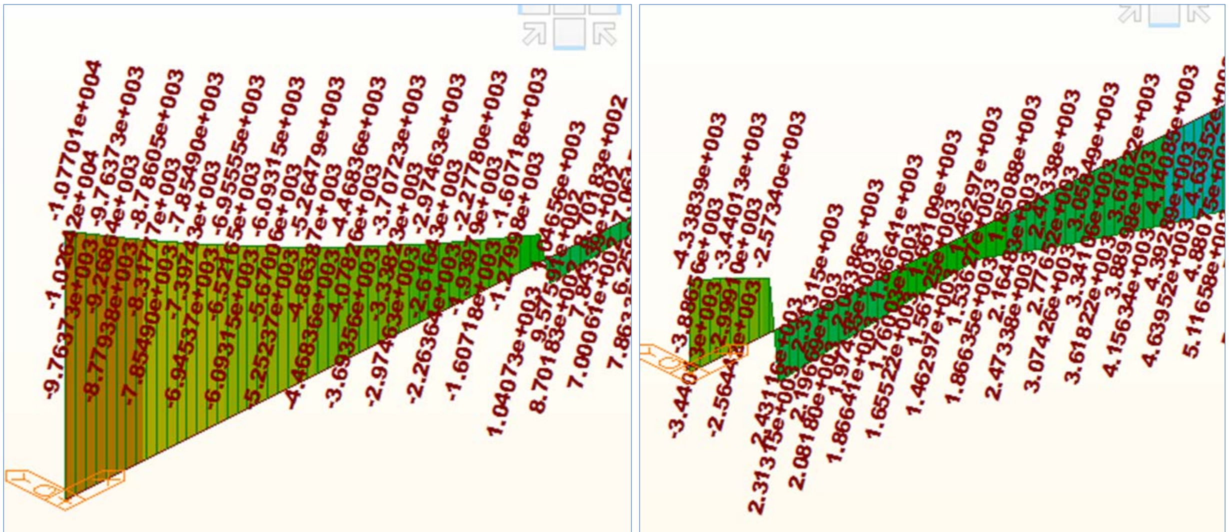

Beam Stress at a Node (12632) in Expansion	Beam Stress at a Node (12632) in Contraction
-10770 kN/m^2 (Compressive Stress)	-4338 kN/m^2 (Compressive Stress)

A. Beam Stress Diagram in LCB 1 **B. Beam Stress Diagram LCB 2**

Figure 4.50: Compared Stress Values at the left end of the edge girder by LCB 1 or LCB 2

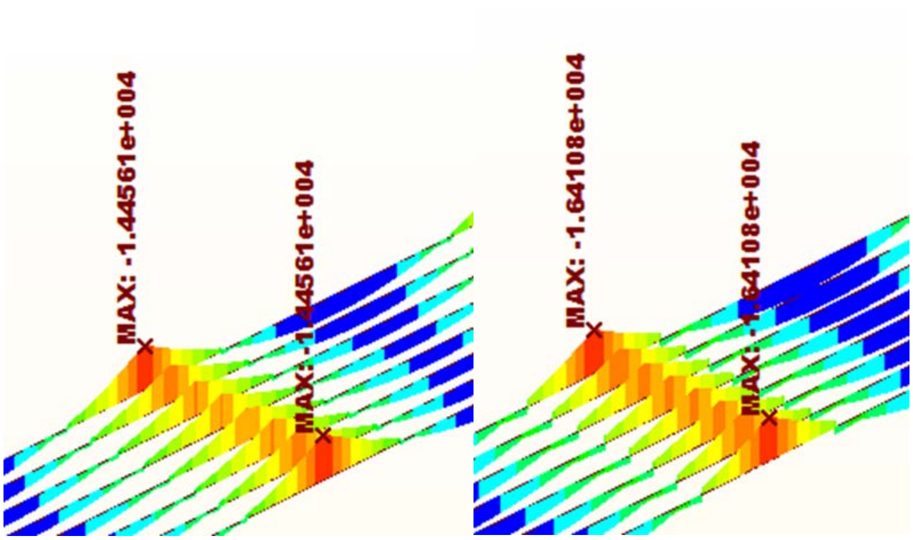

A. Stress in LCB 1 **B. Stress in LCB 2**

Figure 4.51: Stress Variation at the middle of the edge girder by LCB 1 or LCB 2

In weak axial direction, the maximum combined girder stress increases up to 6.4 % in clayed soils more than in sand. In addition, pile orientation has a bit of influence for the girder stress between 3m and 6m and has an effect with clayed soils due to the difference of weak and strong axis bending.

Overall, the maximum combined girder stress decreases slightly by the increase of the abutment height and increases a little more in contraction cases and clayed soils.

4.9.2 Abutment Stress

Figure 4.52 indicates the maximum principal stress generated in the element (12083) on the top of the abutment. At the same time, the manner of abutment movement is predominantly rotation about their bottom although there is a horizontal dislocation as well. The total horizontal displacements are greatest at the top of each abutment as predicted.

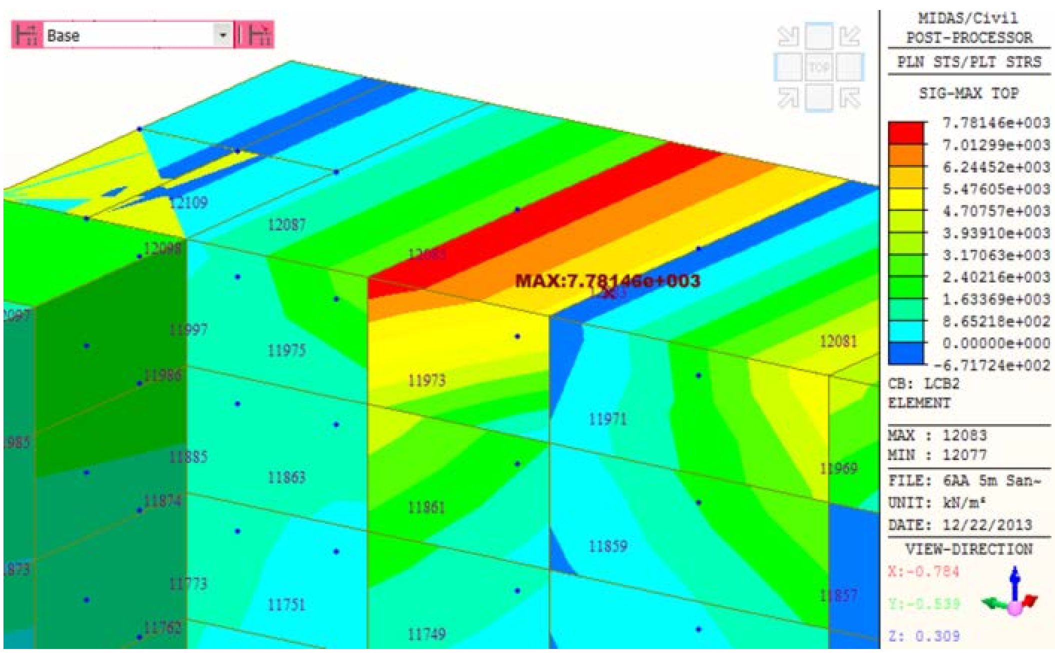

Figure 4.52: Abutment Stress in 5m-Tall Abutment with Sand 1 & Weak-Axis by LCB 2 (Contraction)

The abutment stress (the maximum principal stress) increases meaningfully as the abutment height increases (Figures 4.17 and 4.18), contrary to the case of girder stress.

On the other hand, the soil types and the difference of weak and strong axis bending have not an influence on the abutment stress.

Overall, the abutment stress increases expressively by the increase of the abutment height and remains unaffected by the soil types and the difference of weak and strong axis bending.

4.9.3 Pile Moment

As shown in Figures 4.22 and 4.53, the maximum pile bending moment occurs at the pile-abutment connection (Node: 10066, Element: 9785) that there is the bottom of abutment in both expansion and contraction cases.

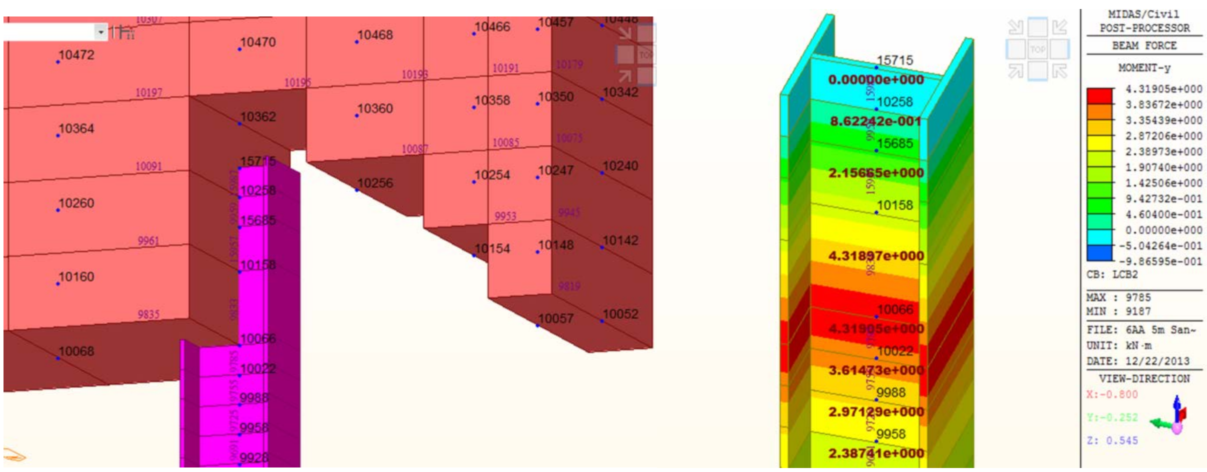

Figure 4.53: Maximum Pile Moment generated at the pile-abutment connection by LCB 2 (Contraction)

The abutment height has a negative and significant influence on the pile moment in strong axis orientation since there is up to an 83.4 % reduction in the pile moment when the abutment height increases for expansion cases while up to a 48.5 % reduction is discovered in contraction cases.

However, the weak axis orientation has not an influence on the pile moment when the abutment height increases (Figures 4.23 and 4.24).

The difference of the soil stiffness has not an influence on the pile moment in weak axis orientation. Only strong axis orientation has an influence on the pile moment when the soil stiffness increases (Figures 4.25 and 4.26).

Overall, the abutment height has a negative and significant influence on the pile moment in strong axis orientation. However, the weak axis orientation has not an influence on pile moment with the increase of the abutment height.

4.9.4 Pile Stress

As revealed in Figures 4.27 and 4.54, the maximum pile stress occurs at the pile-abutment connection (Node: 10066, Element: 9785) that there is the bottom of abutment in both expansion and contraction cases, since steel H-shaped piles were embedded 0.6 m into the abutment.

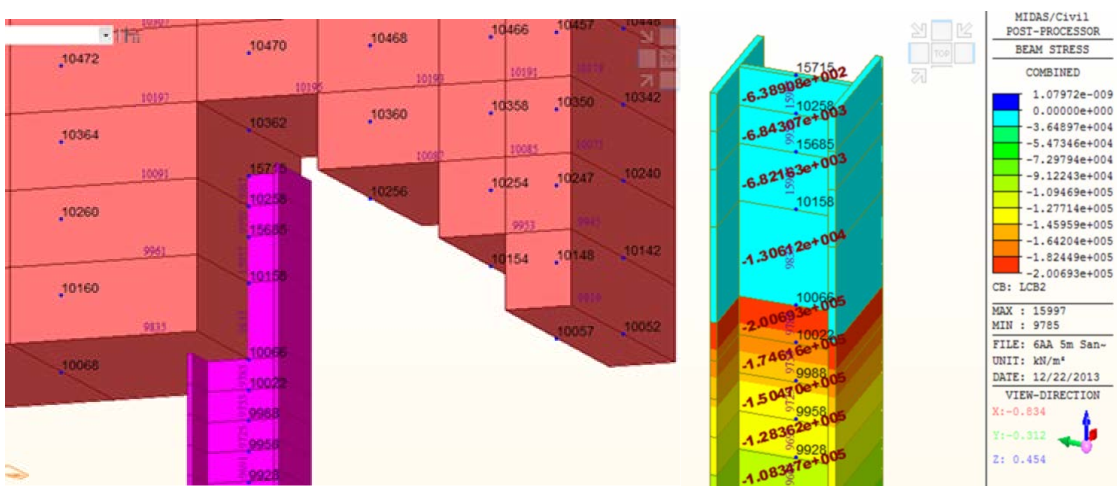

Figure 4. 54: Maximum Pile Stress generated at the pile-abutment connection by LCB 2 (Contraction)

The abutment height has a negative and significant influence on the pile stress in the weak axis orientation contrary to the case of the pile moment, since there is up to an 81.4 % reduction in pile stress for expansion cases while up to a 33.7 % reduction in contraction cases.

The strong axis orientation has a slightly lower influence on the pile stress than the weak axis orientation when the abutment height increases. The difference of the soil stiffness has not an influence on the pile stress in contraction cases. Only in expansion cases, the soil stiffness has a negative influence on pile stress when the soil stiffness increases.

Overall, the abutment height has a negative and significant influence on the pile stress in the weak axis orientation contrary to the case of pile moment. The difference of the soil stiffness has a small influence on the pile stress.

4.9.5 Pile Displacement

As exposed in Figures 4.35, 4.36, and 4.55, the maximum pile displacement occurs at the pile head, the end of pile embedded 0.6 m into the abutment in expansion cases. However, in the contraction cases, the maximum pile displacement does not occur at the pile head. The maximum pile displacement occurs at 0.3 m (Node: 9958) below the bottom of abutment in the contraction cases as demonstrated in Figure 4.55.

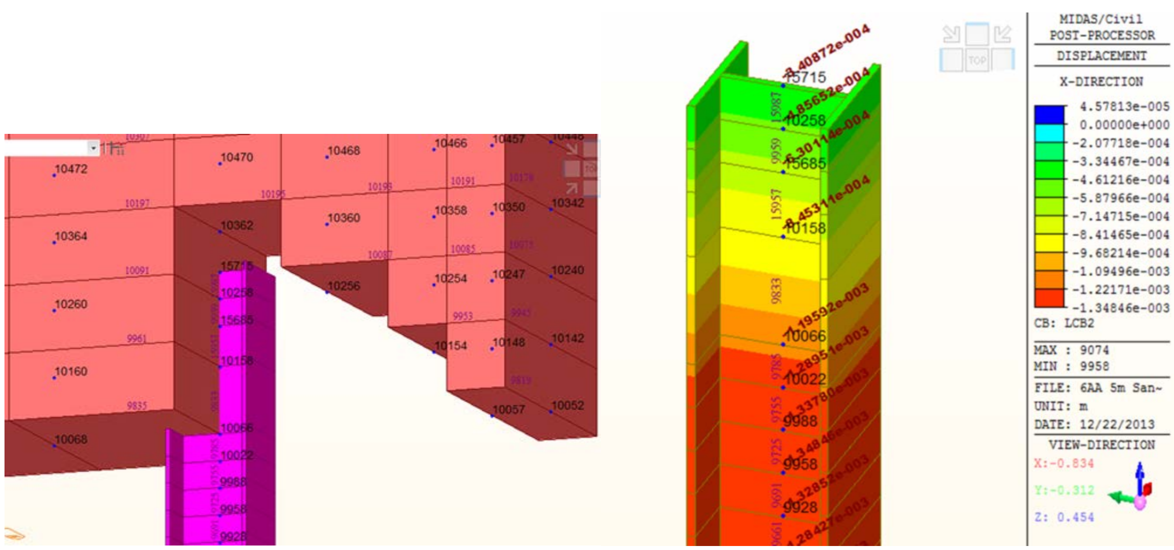

Figure 4.55: Maximum Pile Displacement generated by LCB 2 (Contraction)

In consequence, the abutment height has a negative and significant influence on the pile displacement in the weak axis orientation, since there is up to a 79 % reduction in the pile displacement when the abutment height increases for expansion cases while up to a 68.5 % reduction is detected in contraction cases. On the other hand, the strong axis orientation has a slightly lower or higher influence on the pile displacement than the weak axis orientation when the abutment height increases, since there is up to a 76.6 % reduction in pile displacement when the abutment height increases for expansion cases while up to a 89.5 % reduction is detected in contraction cases. The increase of the soil stiffness has a negative influence on the pile head displacement in both expansion and contraction cases.

Overall, the abutment height has a negative and significant influence on the pile displacement in the weak axis orientation. The difference of the soil stiffness has not an influence on the pile displacement. The increase of the soil stiffness has a negative influence on the pile displacement in both expansion and contraction cases. As a result, the reduction in the pile head displacement according to a growth of the abutment height is attributed to a weakened mobility by its augmented self–weight and an enlarged soil passive pressure by its increased surface area in the taller abutment.

4.9.6 Soil-Structure Interaction

The soil springs for integral abutments and piles were created according to MIDAS CIVIL CODE (2013). For the soil stiffness of two abutments, 1584 soil springs were created in 5 m-tall abutment with sand1 and weak-axis. The soil springs for H piles and PC piles in 5 m-tall abutment with sand1 and weak-axis are as follows. For the lateral springs (p- y curves), 18,360 non-linear springs (multi-linear springs) were created. For the vertical springs (tangent springs, f-z curves) and point springs (tip springs, q-z curves), 9,180 linear springs were generated.

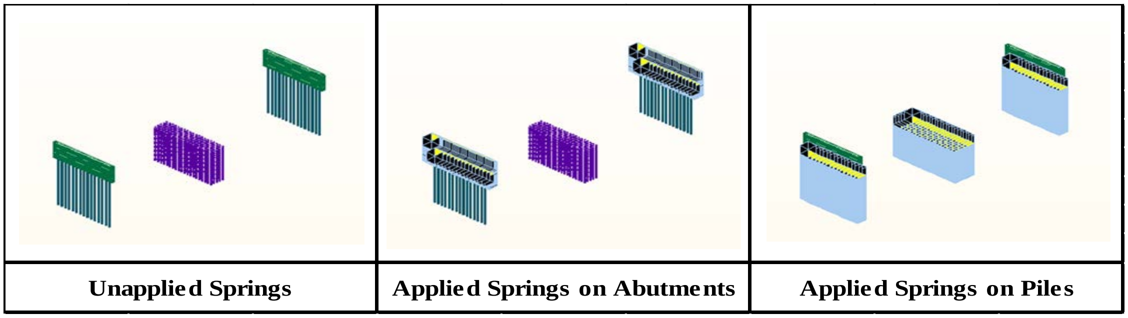

Figure 4.56: Soil Springs applied on Abutments and Piles

As shown in Table 4.29, the springs applied on models in this study are introduced through iterative processes. According to the increase of the abutment height, the length of H piles decreases. Thus, the spring quantity varies depending on the length of H piles and the abutment surface area. However, the length of PC piles has a fixed size.

Table 4.29: Springs Applied on Models with sand1 in this study

Abutment Height		Spring Quantity (EA)	Springs Applied on Models	H Pile Length (m)	PC Pile Length (m)
3 m	Abument Springs	992	Linear : 9480 Comp/Tens : 992 Multi-Linear : 18960	17	10.5
	Lateral Springs	18960			
	Tangent Springs	9350			
	Tip Springs	130			
4 m	Abument Springs	1288	Linear : 9330 Comp/Tens : 1288 Multi-Linear : 18660	16	10.5
	Lateral Springs	18660			
	Tangent Springs	9200			
	Tip Springs	130			
5 m	Abument Springs	1584	Linear : 9180 Comp/Tens : 1584 Multi-Linear : 18360	15	10.5
	Lateral Springs	18360			
	Tangent Springs	9050			
	Tip Springs	130			
6 m	Abument Springs	1880	Linear : 9030 Comp/Tens : 1880 Multi-Linear : 18060	14	10.5
	Lateral Springs	18060			
	Tangent Springs	8900			
	Tip Springs	130			
7 m	Abument Springs	2176	Linear : 8880 Comp/Tens : 2176 Multi-Linear : 17760	13	10.5
	Lateral Springs	17760			
	Tangent Springs	8750			
	Tip Springs	130			
8 m	Abument Springs	2472	Linear : 8730 Comp/Tens : 2472 Multi-Linear : 17460	12	10.5
	Lateral Springs	17460			
	Tangent Springs	8600			
	Tip Springs	130			

Figure4.57 represents soil-structure interaction mechanisms under cyclic thermal movements. The retained soil wedge behind each abutment moves downward and toward the abutment during the annual winter contraction. The void is then created under the approach slab by the settled soil. As a result, the lateral earth pressure increases due to the retracted position of the abutment. Finally this helps lead to eventual Ultimate Limit State failure of abutments. (Horvath, 2000; Faraji et al., 2001)

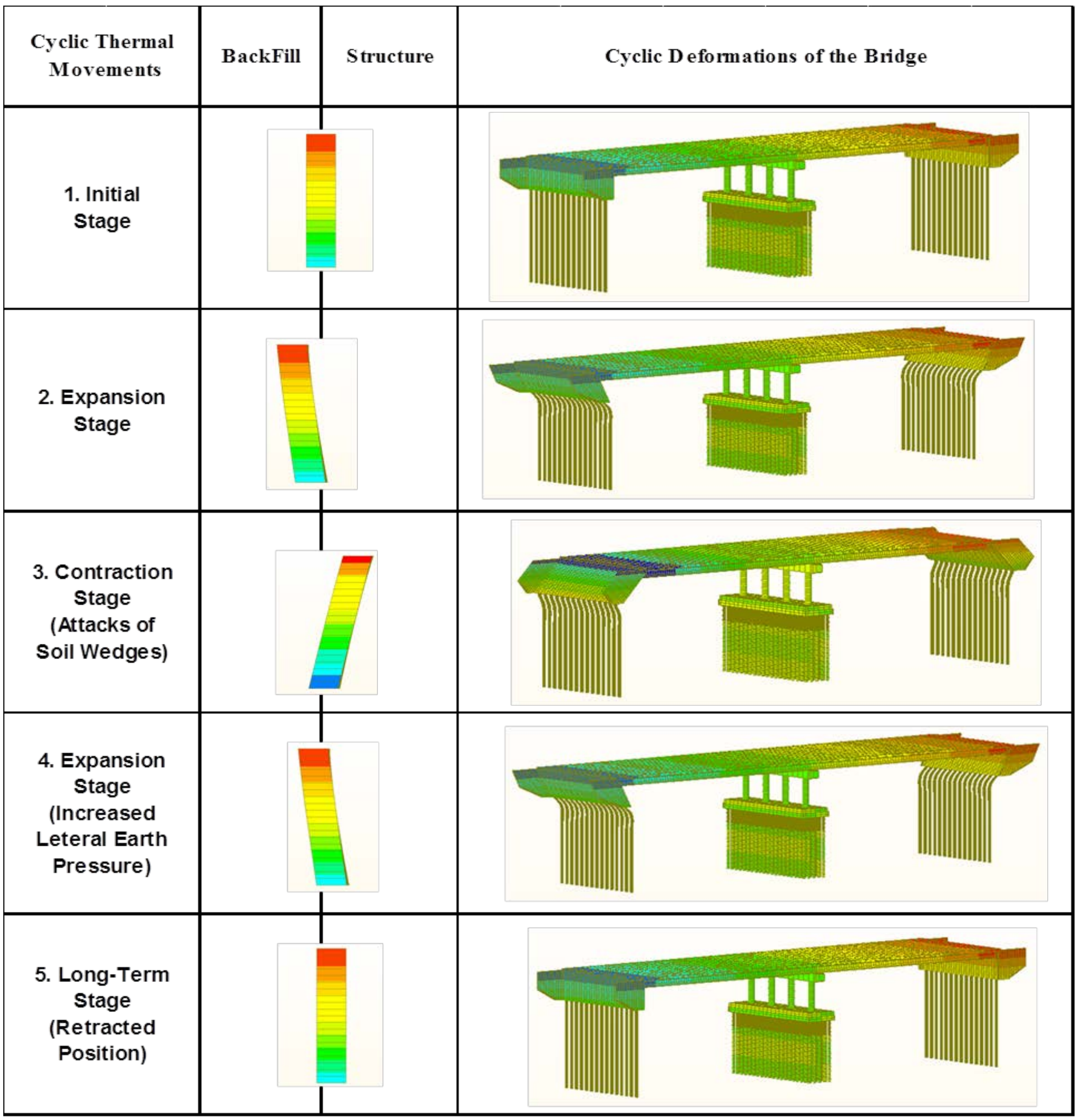

Figure 4.57: Soil-Structure Interaction Mechanisms under Cyclic Thermal Movements

Chapter 5 Conclusions and Future Research

5.1 Overview

The presented study was performed to evaluate and validate together with recommendations of several states in the USA over the suitability of the limit of the abutment height in Ontario's recommendations to the design for Integral Abutment Bridges through the original modelling of Palladium Drive Integral Abutment Bridge in Ontario.

The primary results of the parametric study are as follows.

- The girder stress decreases slightly by the increase of the abutment height and increase a little more in the contraction cases and clayed soils.
- The abutment stress increases expressively by the increase of the abutment height and remains unaffected by soil types and the difference of weak and strong axis bending.
- The abutment height has a negative and significant influence on the pile moment in the strong axis orientation. The weak axis orientation has not an influence on the pile moment with the increase of the abutment height.
- The abutment height has a negative and significant influence on the pile stress in the weak axis orientation contrary to the case of the pile moment. The difference of the soil stiffness has not an influence on the pile stress.
- The abutment height has a negative and significant influence on pile displacement in weak axis orientation. The difference of the soil stiffness has not an influence on pile stress.
- The increase of the soil stiffness has a negative influence on pile displacement in both expansion and contraction cases.
- The strong axis orientation has a higher influence on the pile moment compared to the weak axis orientation whereas the weak axis orientation has a larger influence on the pile stress than the strong axis orientation.

5.2 Conclusions

The conclusions drawn from this parametric study are as in the following.

(1) In terms of the maximum combined girder stress, the increase of the abutment height has a reduction effect on the girder stress until 6 m-tall abutment in expansion cases (Figure 4.3).

(2) The maximum combined girder stress is influenced negatively by the increase of the soil stiffness (Figures 4.5 & 4.6).

(3) The abutment stress is affected positively until 6 m-tall abutment in expansion cases by the increase of the abutment height (Figure 4.17).

(4) The pile moment is influenced negatively by the increase of the abutment height until 6 m-tall abutment (Figure 4.23).

(5) The pile stress is influenced negatively by the increase of the abutment height until 6 m-tall abutment in the strong axis orientation and until 7 m-tall abutment in the weak axis orientation (Figure 4.31).

(6) The pile head displacement is influenced negatively by the increase of the abutment height until 6 m-tall abutment in strong axis orientation and until 4 m-tall abutment in weak axis orientation (Figure 4.40).

(7) The increase of the soil stiffness has no effect on the pile moment in weak axis orientation. Girder stress and pile displacement are influenced negatively by the increase of the soil stiffness. (Figures 4.5, 4.6, 4.41, and 4.42).

(8) The strong axis orientation has a higher influence on the pile moment compared to the weak axis orientation whereas the weak axis orientation has a larger influence on the pile stress than the strong axis orientation (Figures 4.23, 4.24, 4.33, and 4.34).

(9) Overall, the limit of the abutment height (6 m) in Ontario compared to several states in USA, are assessed to be appropriate since the inflection point generally occurs at 6 m tall as shown in Figures 4.2, 4.17, 4.23, and 4.31.

5.3 Recommendations for future research

The following recommendations are made by the results achieved in this study

- Future studies are required including seismic analyses.
- Future studies are required including more than 3 spans in Integral Abutment Bridges.
- Future studies are required including bump effects regarding problems of approach slab.
- Future studies are required including the effects of wingwall length on bridge performances.
- Future studies are required including the best location of the construction joint in integral abutments.
- Future studies are required including the best location of the construction joint in integral abutments.
- Future studies are required including the effects of properties of diverse soils on bridge performances.

References

American Association of State Highway and Transportation Officials. (2012). AASHTO LRFD Bridge Design Specifications, Washington, D.C, USA.

Arockiasamy M., Butrieng N. and Sivakumar M., (2004), State-of-the-Art of Integral Abutment Bridges: Design and Practice, Journal of Bridge Engineering, 9, 5, 497-506.

Arsoy S., (2000), Experimental and Analytical Investigations of Piles and Abutments of Integral Bridges, Thesis: Ph.D., Virginia Polytechnic Institute and State University, VA, USA.

Bakeer R.M., Mattei N.J., Almalik B.K., Carr S.P. and Homes D., (2005), Evaluation of DOTD Semi-Integral Bridge and Abutment System, FHWA/LA.05/397, Department of Civil and Environmental Engineering, Tulane University, New Orleans, Louisiana, USA.

Bettinger C., (2001), Effects of Thermal Expansion on a Skewed Semi-Integral Bridge, Thesis: Master of Science, Ohio University, Athens, Ohio, USA.

Bowles J.E., (1996), Foundation Analysis and Design, McGraw-Hill, NY, USA.

Broms, B. B. and Ingleson, I. (1971). "Earth pressure against the abutments of a rigid frame bridge", Géotechnique, The Institution of Civil Engineers, London, U.K., Vol. 21, No. 1, pp. 15-28.

Burke Jr M.P., (2009), Integral and Semi-Integral Bridges, Wiley-Blackwell, Oxford, UK.

Conboy, D.W, Stoothoff E. J., 2005, Integral Abutment Design and Construction: The New England Experience, THE 2005 – FHWA CONFERENCE, Maryland, USA. 59 - 60.

Das B. M.., 2010, Principles of Geotechnical Engineering 7th, Cengage Learning, USA.

Dicleli M. and Albhaisi S.M., (2004), Performance of Abutment-Backfill System under Thermal Variations in Integral Bridges Built on Clay, Engineering Structures, 26, 7, 949-962.

Faraji S., Ting J.M., Crovo D.S. and Ernst H., (2001), Nonlinear Analysis of Integral Bridges: Finite-Element Model, Journal of Geotechnical and Geoenvironmental Engineering, 127, 454.

Greimann L.F., Abendroth R.E., Johnson D.E. and Ebner P.B., (1987), Pile Design and Tests for Integral Abutment Bridges, Iowa DOT Project HR-273, Department of Civil Engineering, Engineering Research Institute, Iowa State University, Ames , Iowa, USA.

Horvath, John S. (2000). "Integral-Abutment Bridges: Problems and Innovative Solutions Using EPS Geofoam and Other Geosynthetics." Manhattan College Research Report No. CE/GE-00-2, Manhattan College, Civil Engineering Department, Bronx, NY, USA.

Husain I., Bagnariol D., (2000), Performance of Integral Abutment Bridges. Report BO-99-04, Ministry of Transportation Ontario, Toronto, Ontario, Canada

Husain I., Huh B., Low J. and McCormick M., (2005), Moose Creek Bridge - Case Study of a Prefabricated Integral Abutment Bridge in Canada. Integral Abutment and Jointless Bridges (IAJB 2005), Baltimore, Maryland, 148-160.

JAKY, J. (1944). "The Coefficient of Earth Pressure at Rest, "Journal of the Society of Hungarian Architects and Engineers, Vol. 7, 355–358.

Kim, W. and J.A. Laman (2009). Load and Resistance Factor Design for Integral Abutment Bridges. Ph.D. Dissertation. The Pennsylvania State University, PA, USA.

Krier D., (2009), Modeling of Integral Abutment Bridges Considering Soil-Structure Interaction Effects, Thesis: Ph.D., The University of Oklahoma, Norman, OK, USA.

Kunin J. and Alampalli S., (1999), Integral Abutment Bridges: Current Practice in the United States and Canada, Special Report 132, New York State Department of Transportation, Albany, NY, USA.

Maruri R., Petro S., 2005, Integral Abutments and Jointless Bridges (IAJB) 2004 Survey Summary, Federal Highway Administration (FHWA)/Constructed Facilities Center (CFC) at West Virginia University.

Metzger A.T., (1995), Measurement of the Abutment Forces of a Skewed Semi-Integral Bridge as a Result of Ambient Temperature Change, Thesis: Master of Science, Ohio University, Athens, Ohio, USA.

Ministry Of Transportation Ontario, (1996), INTEGRAL ABUTMENT BRIDGES MANUAL, Report SO-96-01, Ministry of Transportation Ontario, Toronto, Ontario, Canada.

NYSDOT Bridge Manual –3rd Edition, 2005, New York State Department of Transportation, Albany, NY, USA.

Reese, L. C., Cox, W. R., and Koch, F. D. (1974). ‘‘Analysis of Laterally Loaded Piles in Sand,’’ Proceedings, Offshore Technology Conference, Houston, TX, Vol. II, Paper No. 2080, pp. 473–484.

Reese L. C., Isenhower W. M., Wang S. T, (2006), Analysis and Design of Shallow and Deep Foundations, John Wiley & Sons, Inc., New Jersey, USA and Canada.

Shah B.R., (2007), 3D Finite Element Analysis of Integral Abutment Bridges Subjected to Thermal Loading, Thesis: Master of Science, Kansas State University, Manhattan, Kansas, USA.

Shehu J., (2009), Evaluation of the Foundation and Wingwalls of Skewed Semi-Integral Bridges with Wall Abutments, Thesis: Master of Science, Ohio University, Athens, Ohio, USA.

Wasserman E.P., (2007), Integral Abutment Design (Practices in the United States). 1st U.S. - Italy Seismic Bridge Workshop, Pavia, Italy.

References (Websites)

Midas IT, Civil 2013 Online Manual, http://manual.midasuser.com/EN_Common/Civil/805/index.htm

North Carolina Department of Transportation: https://connect.ncdot.gov/resources/Structures /Pages/Structure-Standards.aspx

Prestress Services Industries LLC: http: //www.prestressservices.com/products

SteelConstruction.info: http://www.steelconstruction.info/Bridges_-_initial_design

Appendix

Table of Analysis Results

1. The Effects depending on Abutment Height

1.1. Girder Stress (Pile Orientation: Strong-Axis, Expansion Case)

1.2. Girder Stress (Pile Orientation: Strong-Axis, Contraction Case)

1.3. Girder Stress (Pile Orientation: Weak-Axis, Expansion Case)

1.4. Girder Stress (Pile Orientation: Weak-Axis, Contraction Case)

1.5. Abutment Stress (Pile Orientation: Strong-Axis, Expansion Case)

1.6. Abutment Stress (Pile Orientation: Strong-Axis, Contraction Case)

1.7. Abutment Stress (Pile Orientation: Weak-Axis, Expansion Case)

1.8. Abutment Stress (Pile Orientation: Weak-Axis, Contraction Case)

1.9. Pile Moment (Pile Orientation: Strong-Axis, Expansion Case)

1.10. Pile Moment (Pile Orientation: Strong-Axis, Contraction Case)

1.11. Pile Moment (Pile Orientation: Weak-Axis, Expansion Case)

1.12. Pile Moment (Pile Orientation: Weak-Axis, Contraction Case)

1.13. Pile Stress (Pile Orientation: Strong-Axis, Expansion Case)

1.14. Pile Stress (Pile Orientation: Strong-Axis, Contraction Case)

1.15. Pile Stress (Pile Orientation: Weak-Axis, Expansion Case)

1.16. Pile Stress (Pile Orientation: Weak-Axis, Contraction Case)

1.17. Pile Head Displacement (Pile Orientation: Strong-Axis, Expansion Case)

1.18. Pile Head Displacement (Pile Orientation: Strong-Axis, Contraction Case)

1.19. Pile Head Displacement (Pile Orientation: Weak-Axis, Expansion Case)

1.20. Pile Head Displacement (Pile Orientation: Weak-Axis, Contraction Case)

2. The Effects depending on Soil Types

2.1. Girder Stress (Pile Orientation: Strong-Axis, Expansion Case)

2.2. Girder Stress (Pile Orientation: Strong-Axis, Contraction Case)

2.3. Girder Stress (Pile Orientation: Weak-Axis, Expansion Case)

2.4. Girder Stress (Pile Orientation: Weak-Axis, Contraction Case)

2.5. Abutment Stress (Pile Orientation: Strong-Axis, Expansion Case)

2.6. Abutment Stress (Pile Orientation: Strong-Axis, Contraction Case)

2.7. Abutment Stress (Pile Orientation: Weak-Axis, Expansion Case)

2.8. Abutment Stress (Pile Orientation: Weak-Axis, Contraction Case)

2.9. Pile Moment (Pile Orientation: Strong-Axis, Expansion Case)

2.10. Pile Moment (Pile Orientation: Strong-Axis, Contraction Case)

2.11. Pile Moment (Pile Orientation: Weak-Axis, Expansion Case)

2.12. Pile Moment (Pile Orientation: Weak-Axis, Contraction Case)

2.13. Pile Stress (Pile Orientation: Strong-Axis, Expansion Case)

2.14. Pile Stress (Pile Orientation: Strong-Axis, Contraction Case)

2.15. Pile Stress (Pile Orientation: Weak-Axis, Expansion Case)

2.16. Pile Stress (Pile Orientation: Weak-Axis, Contraction Case)

2.17. Pile Head Displacement (Pile Orientation: Strong-Axis, Expansion Case)

2.18. Pile Head Displacement (Pile Orientation: Strong-Axis, Contraction Case)

2.19. Pile Head Displacement (Pile Orientation: Weak-Axis, Expansion Case)

2.20. Pile Head Displacement (Pile Orientation: Weak-Axis, Contraction Case)

1. The Effects depending on Abutment Height

1.1. Girder Stress (Pile Orientation: Strong-Axis, Expansion Case)

Girder Stress (strong-axis) LCB1 (Expansion Case) Unit: kN/m^2	
3 m-Tall	-14870
4 m-Tall	-14510
5 m-Tall	-14410
6 m-Tall	-14420
7 m-Tall	-14450
8 m-Tall	-14500

<table>
<tr><td rowspan="2">Abutment</td><td colspan="2">Girder Stress (strong-axis) Unit: kN/m²</td></tr>
<tr><td>LCB1 (Expansion)</td><td>-1.487E+04</td></tr>
<tr><td>3 m-Tall</td><td colspan="2">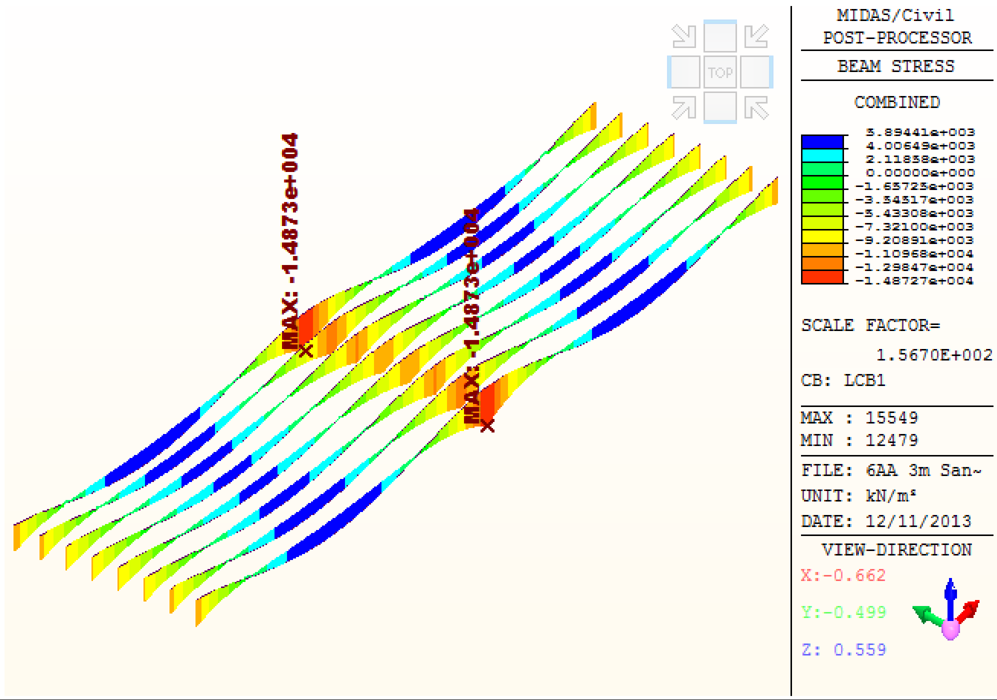
</td></tr>
<tr><td rowspan="2">Abutment</td><td colspan="2">Girder Stress (strong-axis) Unit: kN/m²</td></tr>
<tr><td>LCB1 (Expansion)</td><td>-1.451E+04</td></tr>
<tr><td>4 m-Tall</td><td colspan="2">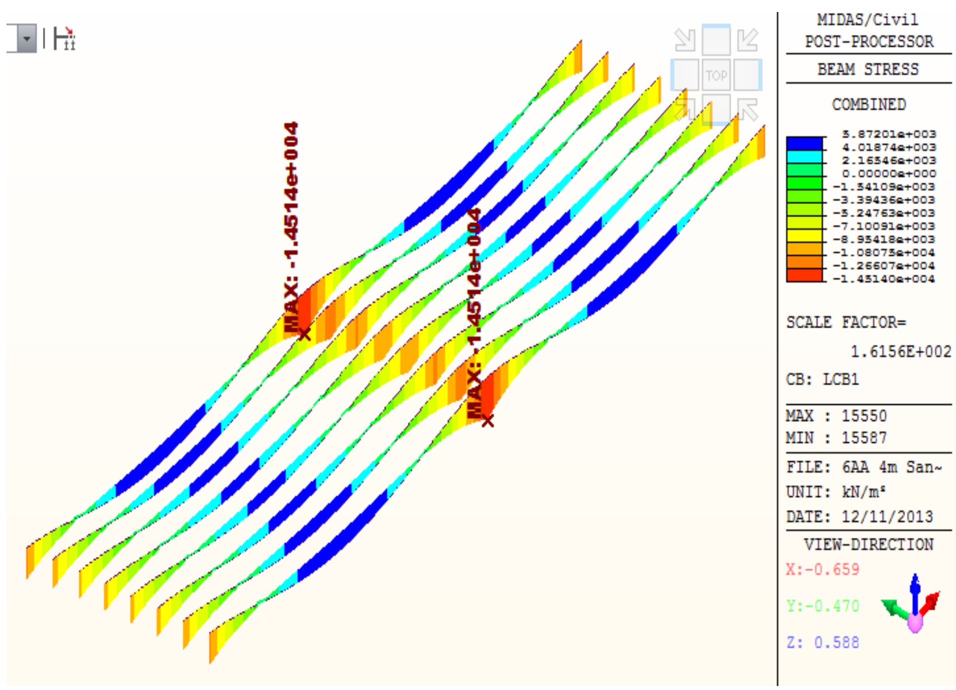
</td></tr>
</table>

<table>
<tr><td rowspan="2">Abutment</td><td colspan="2">Girder Stress (strong-axis) Unit: kN/m^2</td></tr>
<tr><td>LCB1 (Expansion)</td><td>-1.441E+04</td></tr>
<tr><td>5 m-Tall</td><td colspan="2">
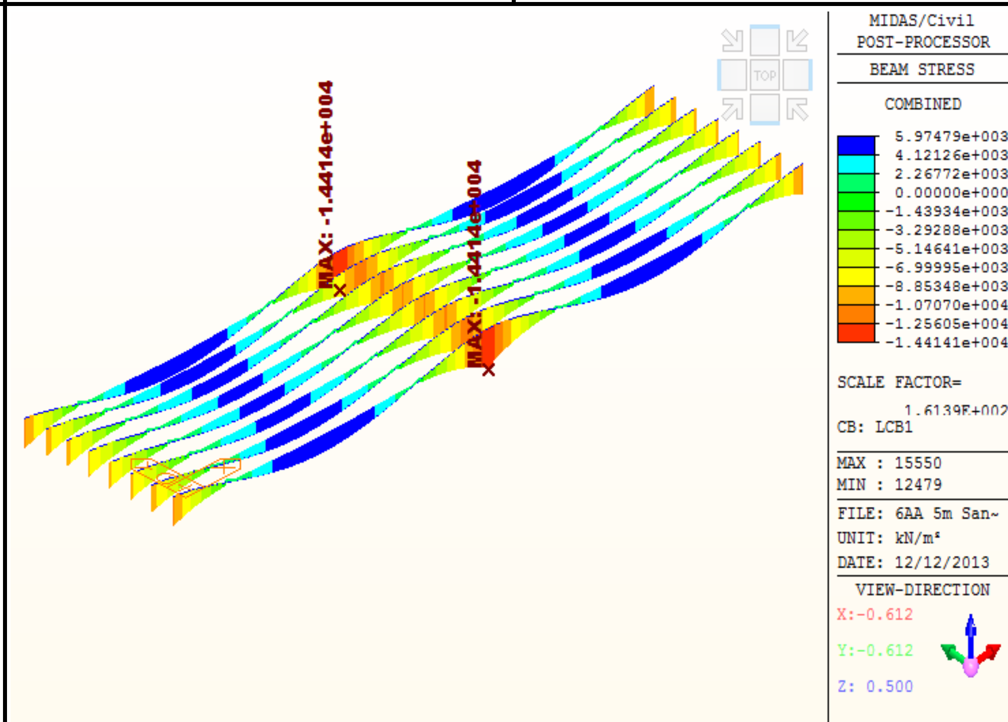

</td></tr>
</table>

<table>
<tr><td rowspan="2">Abutment</td><td colspan="2">Girder Stress (strong-axis) Unit: kN/m^2</td></tr>
<tr><td>LCB1 (Expansion)</td><td>-1.442E+04</td></tr>
<tr><td>6 m-Tall</td><td colspan="2">
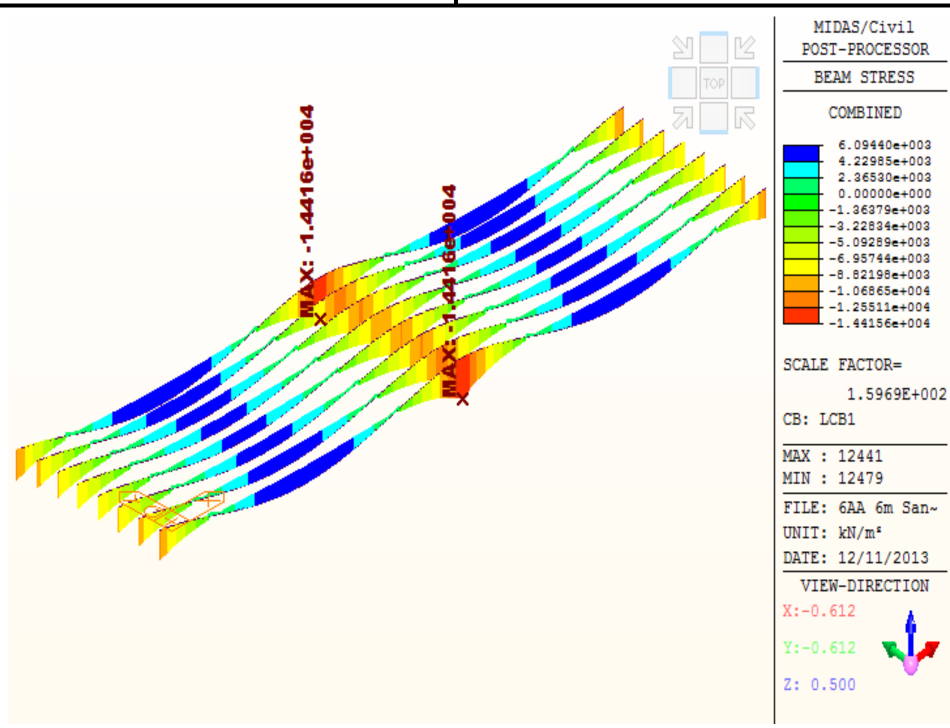

</td></tr>
</table>

<table>
<tr><td rowspan="2">Abutment</td><td colspan="2">Girder Stress (strong-axis) Unit: kN/m^2</td></tr>
<tr><td>LCB1 (Expansion)</td><td>-1.445E+04</td></tr>
<tr><td>7 m-Tall</td><td colspan="2">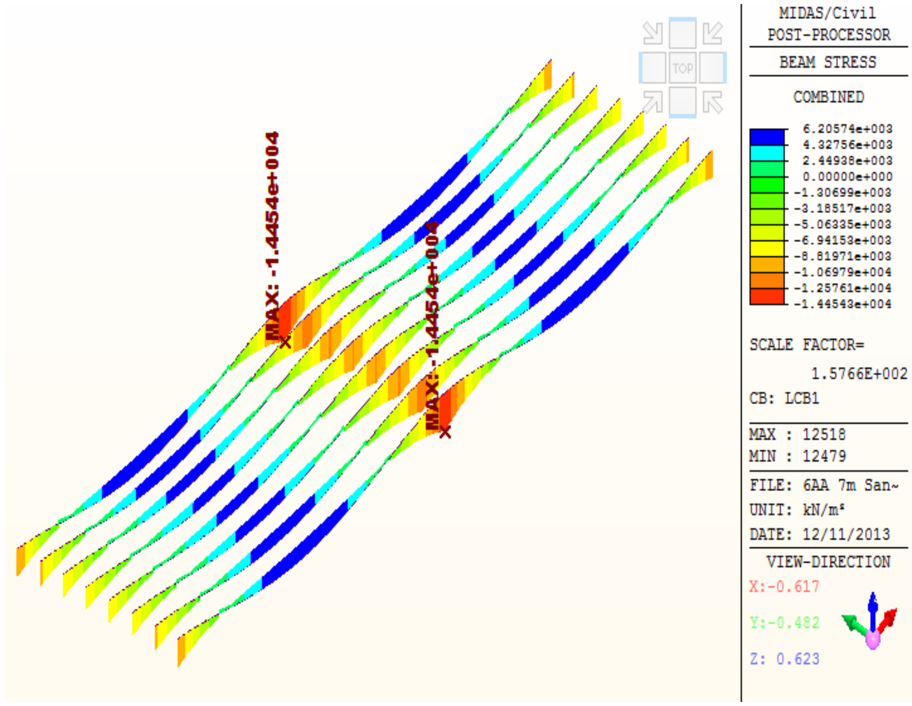
</td></tr>
<tr><td rowspan="2">Abutment</td><td colspan="2">Girder Stress (strong-axis) Unit: kN/m^2</td></tr>
<tr><td>LCB1 (Expansion)</td><td>-1.450E+04</td></tr>
<tr><td>8 m-Tall</td><td colspan="2">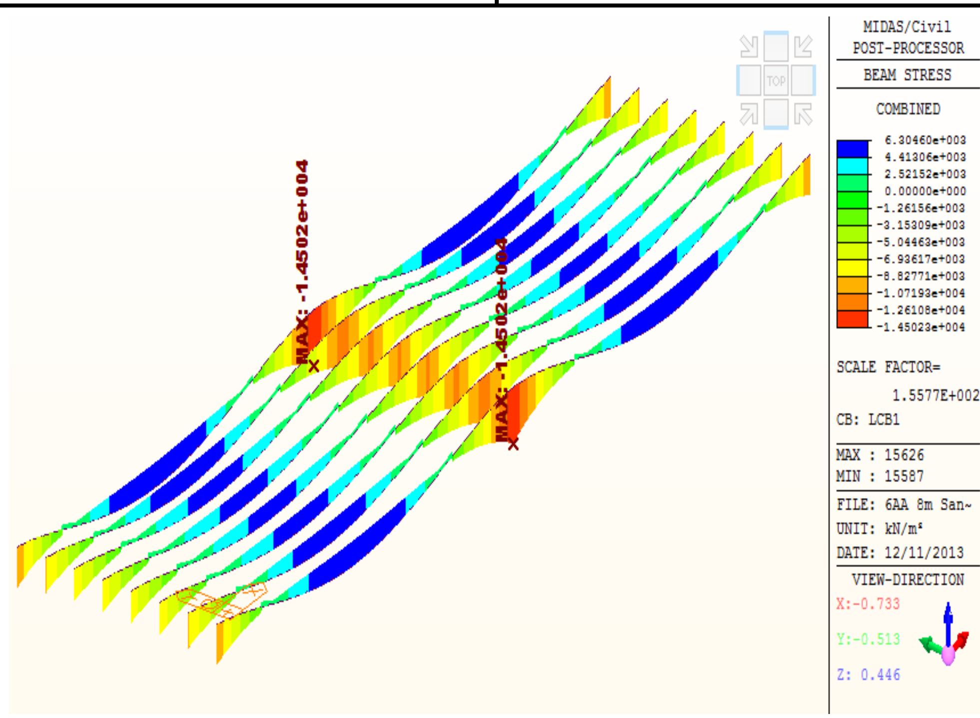
</td></tr>
</table>

1. The Effects depending on Abutment Height

1.2. Girder Stress (Pile Orientation: Strong-Axis, Contraction Case)

Girder Stress (strong-axis) LCB2 (Contraction Case) Unit: kN/m^2	
3 m-Tall	-17280
4 m-Tall	-16740
5 m-Tall	-16310
6 m-Tall	-15990
7 m-Tall	-15730
8 m-Tall	-15540

Abutment	Girder Stress (strong-axis) Unit: kN/m^2	
	LCB2 (Contraction)	-1.728E+04

3 m-Tall

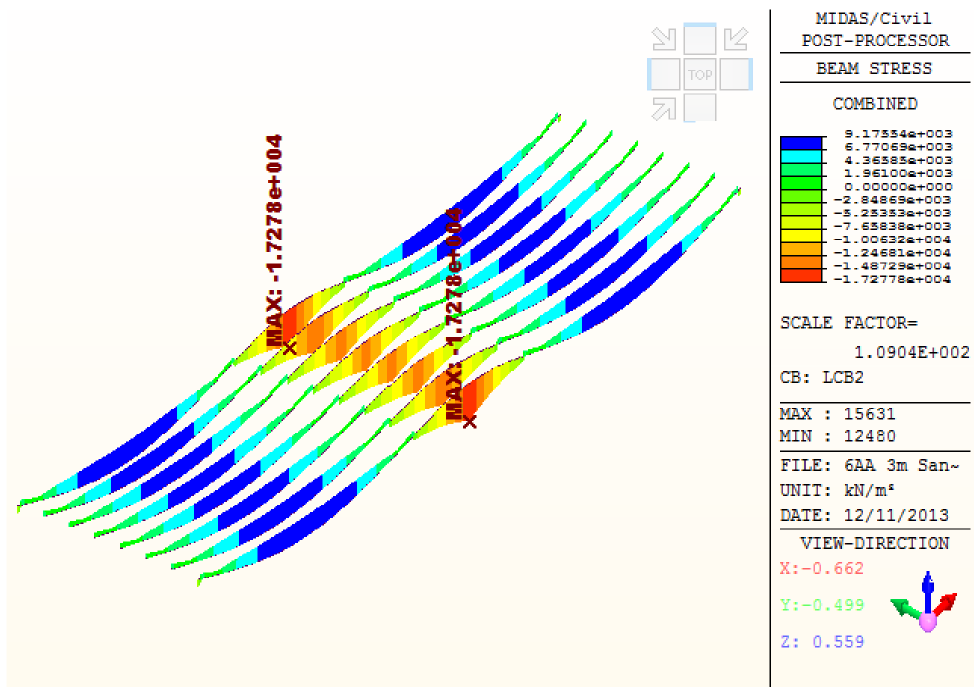

Abutment	Girder Stress (strong-axis) Unit: kN/m^2	
	LCB2 (Contraction)	-1.674E+04

4 m-Tall

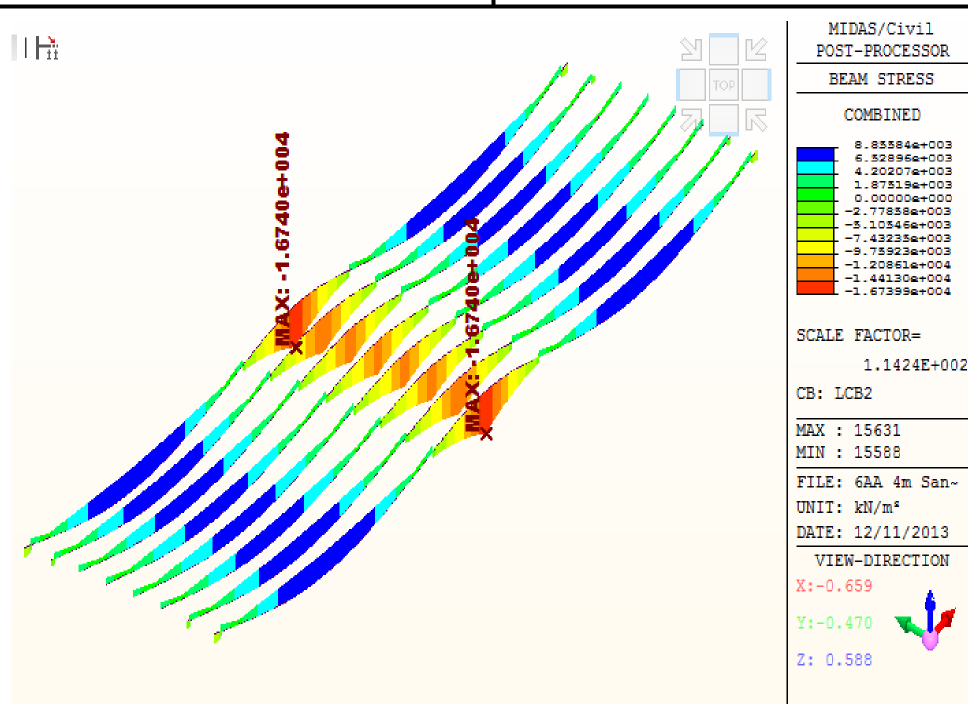

Abutment	Girder Stress (strong-axis) Unit: kN/m^2	
	LCB2 (Contraction)	-1.631E+04
5 m-Tall		

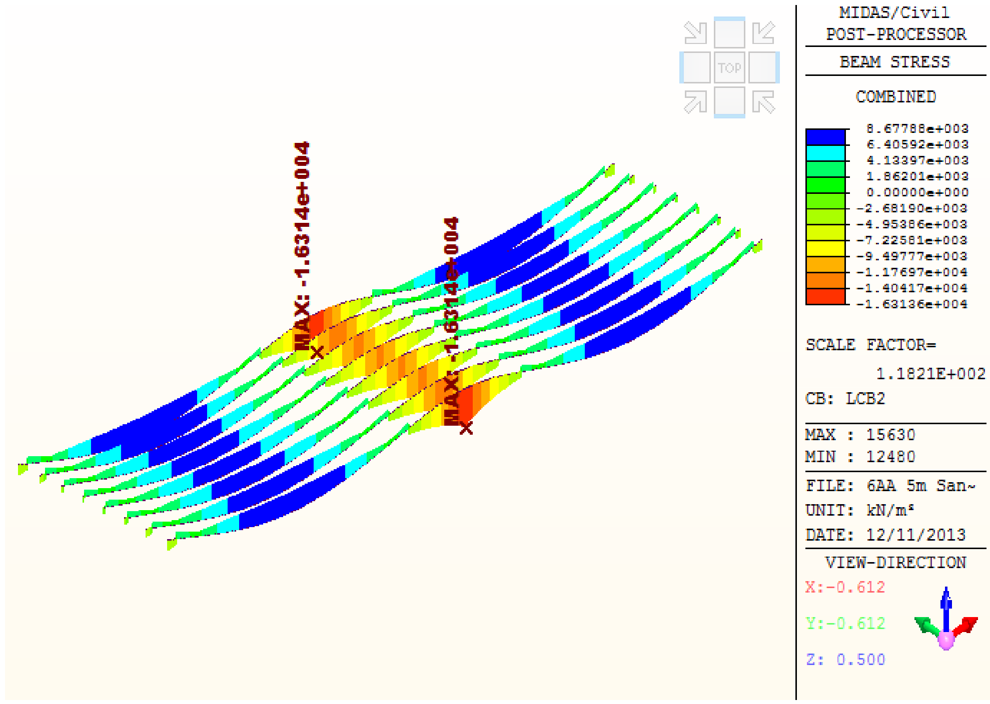

Abutment	Girder Stress (strong-axis) Unit: kN/m^2	
	LCB2 (Contraction)	-1.599E+04
6 m-Tall		

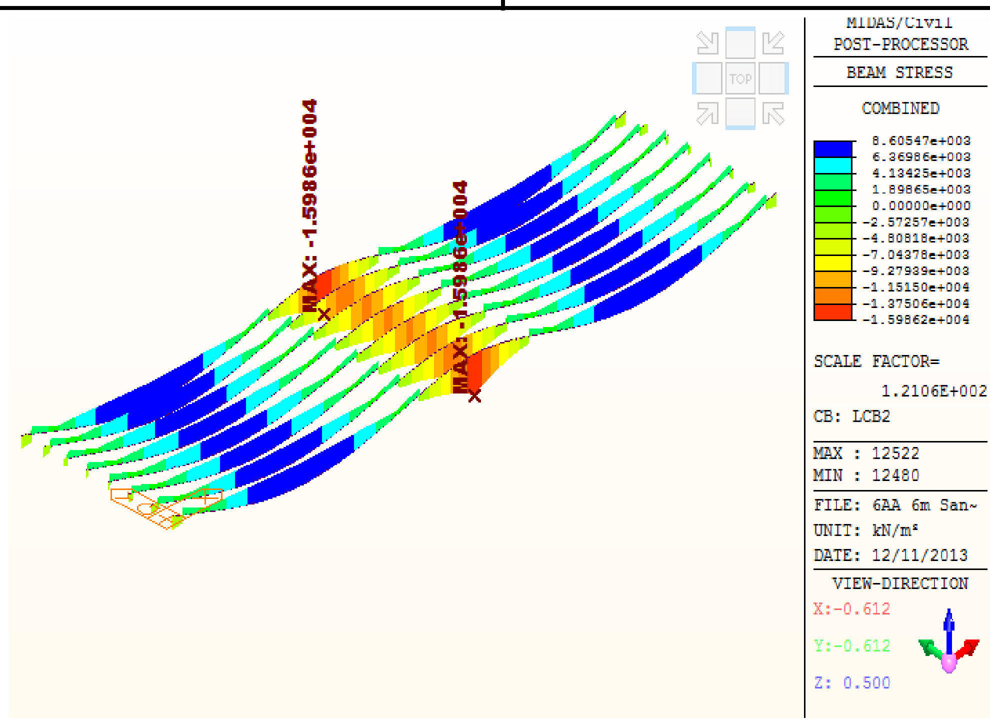

Abutment	Girder Stress (strong-axis) Unit: kN/m^2	
	LCB2 (Contraction)	-1.573E+04
7 m-Tall		

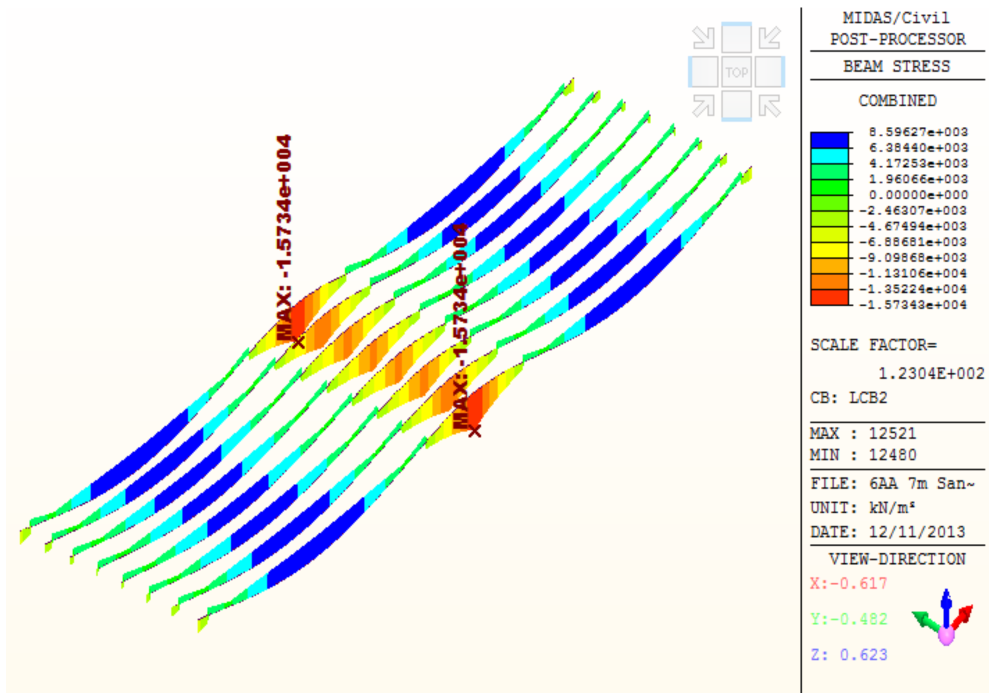

Abutment	Girder Stress (strong-axis) Unit: kN/m^2	
	LCB2 (Contraction)	-1.554E+04
8 m-Tall		

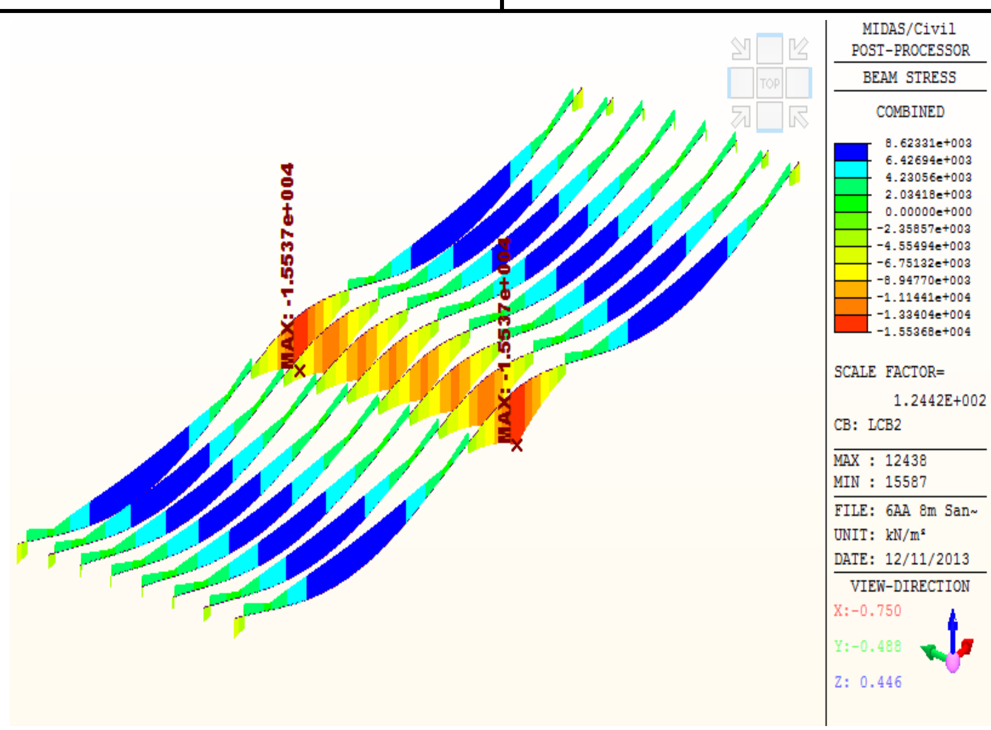

1. The Effects depending on Abutment Height

1.3. Girder Stress (Pile Orientation: Weak-Axis, Expansion Case)

Girder Stress (weak-axis) LCB1 (Expansion Case) Unit: kN/m^2	
3 m-Tall	-15130
4 m-Tall	-14620
5 m-Tall	-14460
6 m-Tall	-14430
7 m-Tall	-14450
8 m-Tall	-14490

Abutment	Girder Stress (weak-axis) Unit: kN/m^2	
	LCB1 (Expansion)	-1.513E+04
3 m-Tall	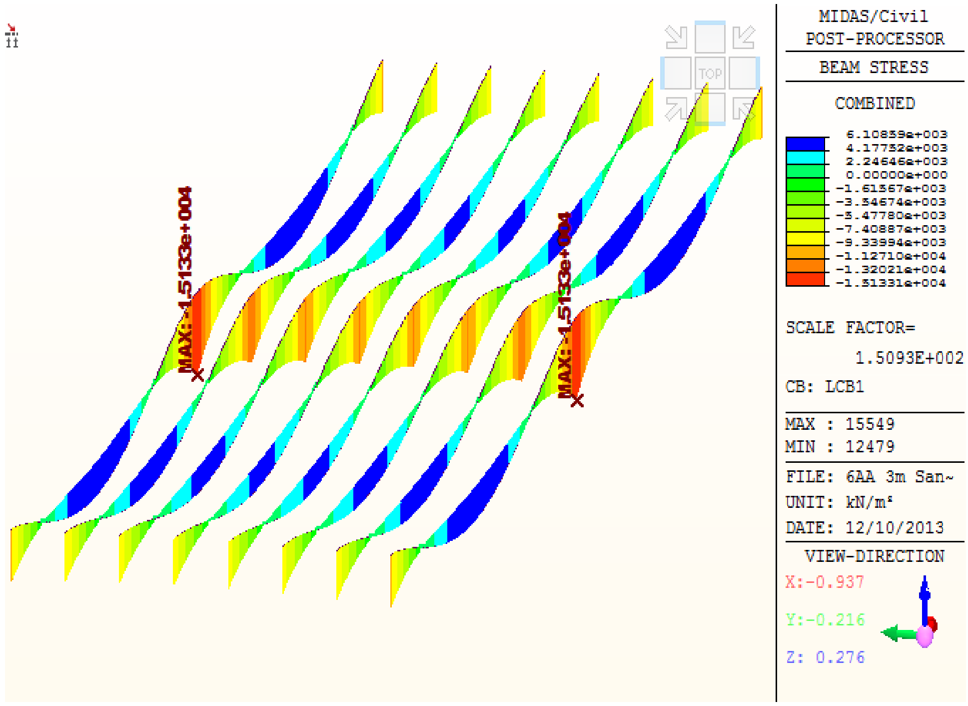	

Abutment	Girder Stress (weak-axis) Unit: kN/m^2	
	LCB1 (Expansion)	-1.462E+04
4 m-Tall	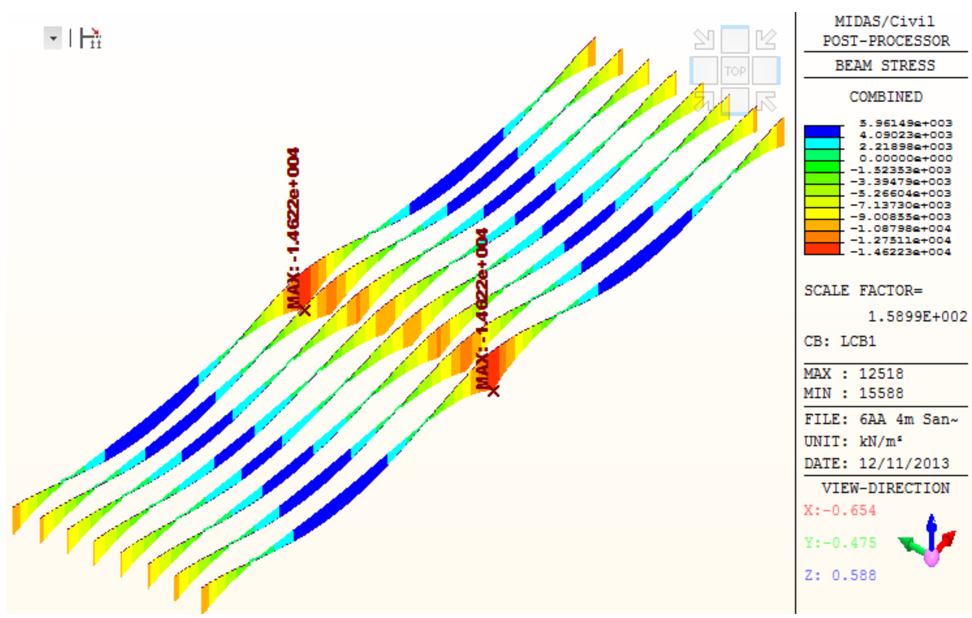	

<table>
<tr><td rowspan="2">Abutment</td><td colspan="2">Girder Stress (weak-axis) Unit: kN/m^2</td></tr>
<tr><td>LCB1 (Expansion)</td><td>-1.446E+04</td></tr>
<tr><td>5 m-Tall</td><td colspan="2">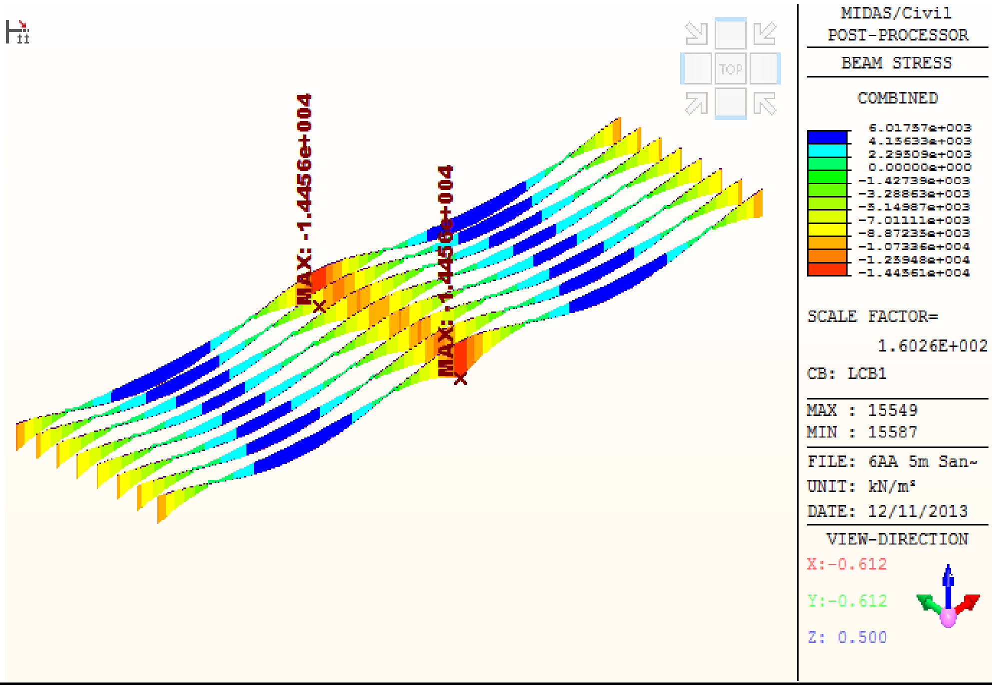
</td></tr>
<tr><td rowspan="2">Abutment</td><td colspan="2">Girder Stress (weak-axis) Unit: kN/m^2</td></tr>
<tr><td>LCB1 (Expansion)</td><td>-1.443E+04</td></tr>
<tr><td>6 m-Tall</td><td colspan="2">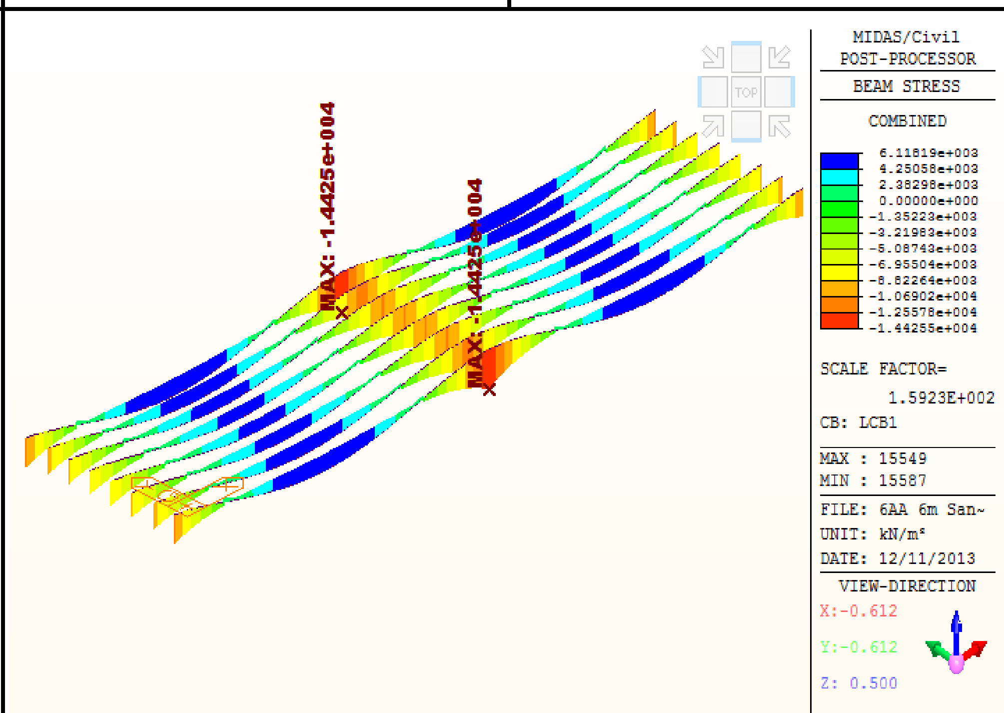
</td></tr>
</table>

Abutment	Girder Stress (weak-axis) Unit: kN/m^2	
	LCB1 (Expansion)	-1.445E+04
7 m-Tall	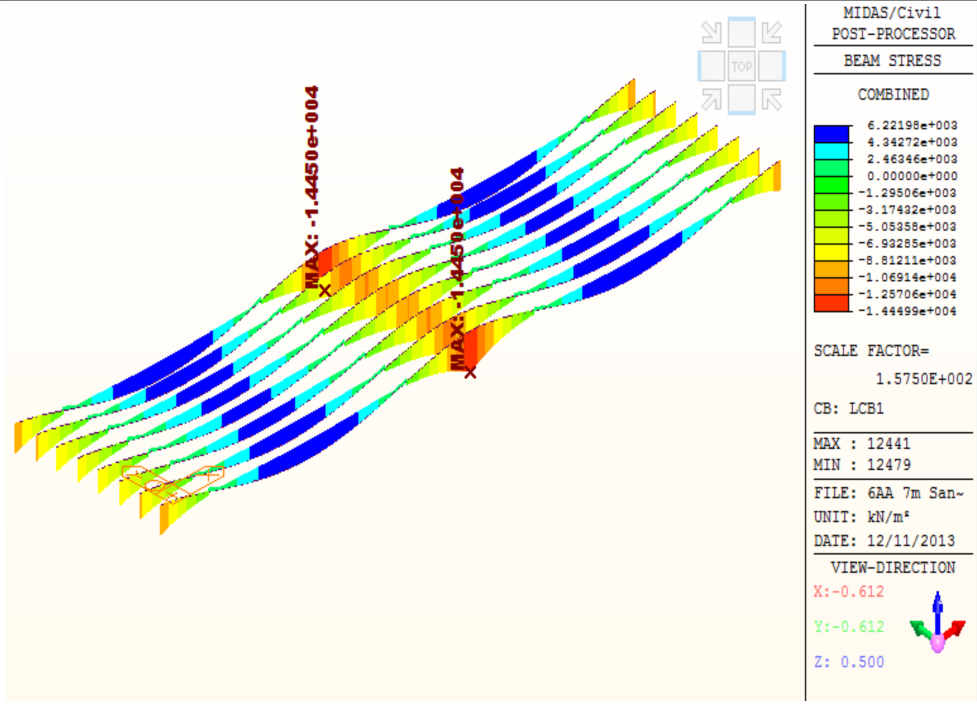	
Abutment	Girder Stress (weak-axis) Unit: kN/m^2	
	LCB1 (Expansion)	-1.449E+04
8 m-Tall	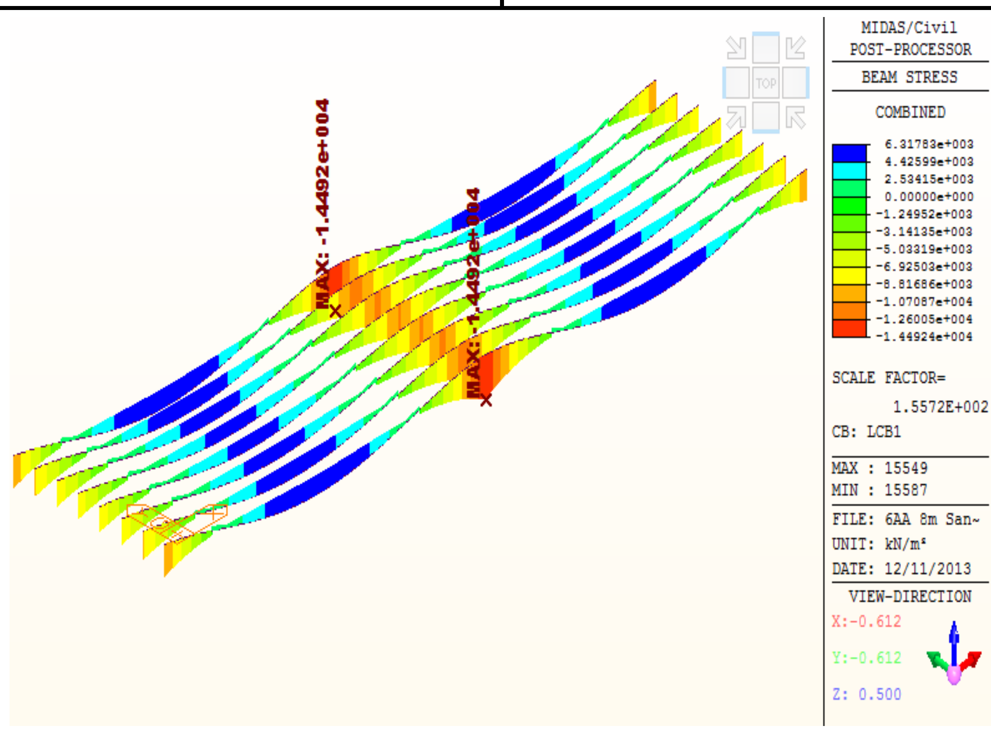	

1. The Effects depending on Abutment Height

1.4. Girder Stress (Pile Orientation: Weak-Axis, Contraction Case)

Girder Stress (weak-axis) LCB2 (Contraction Case) Unit: kN/m^2	
3 m-Tall	**-17490**
4 m-Tall	**-16890**
5 m-Tall	**-16410**
6 m-Tall	**-16050**
7 m-Tall	**-15770**
8 m-Tall	**-15560**

Abutment	Girder Stress (weak-axis) Unit: kN/m^2	
	LCB2 (Contraction)	-1.749E+04
3 m-Tall	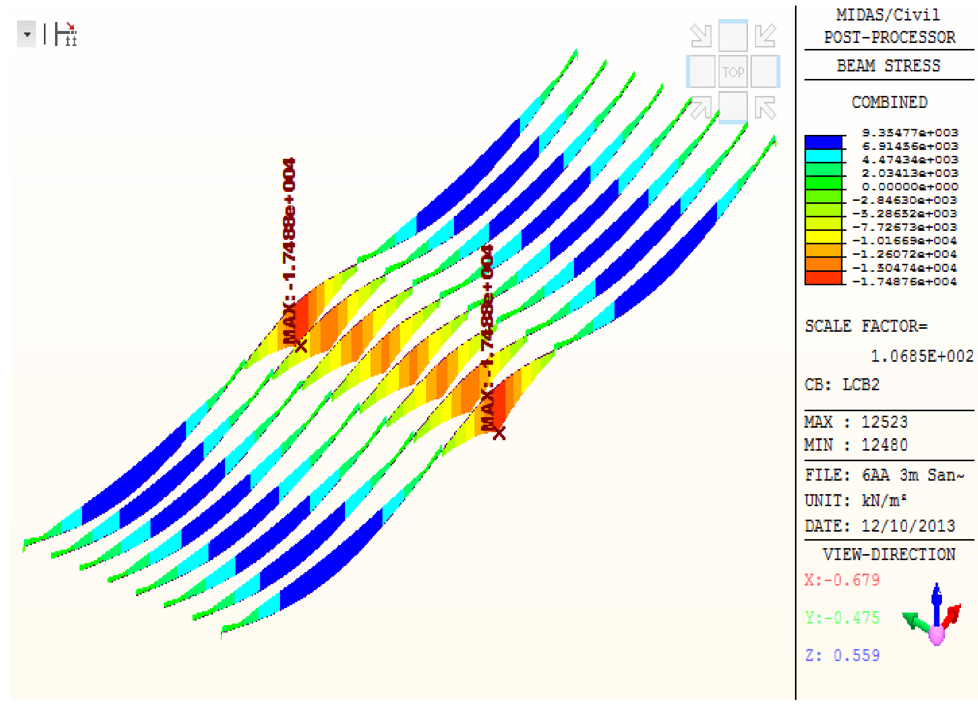	

Abutment	Girder Stress (weak-axis) Unit: kN/m^2	
	LCB2 (Contraction)	-1.689E+04
4 m-Tall	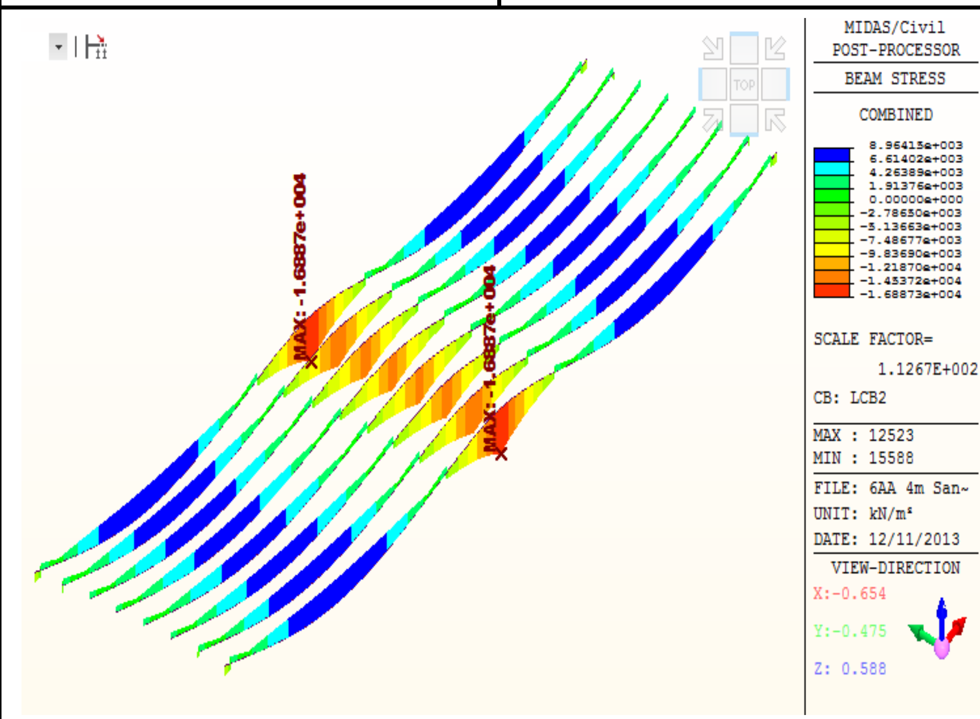	

<table>
<tr><td rowspan="2">Abutment</td><td colspan="2">Girder Stress (weak-axis) Unit: kN/m²</td></tr>
<tr><td>LCB2 (Contraction)</td><td>-1.641E+04</td></tr>
<tr><td>5 m-Tall</td><td colspan="2">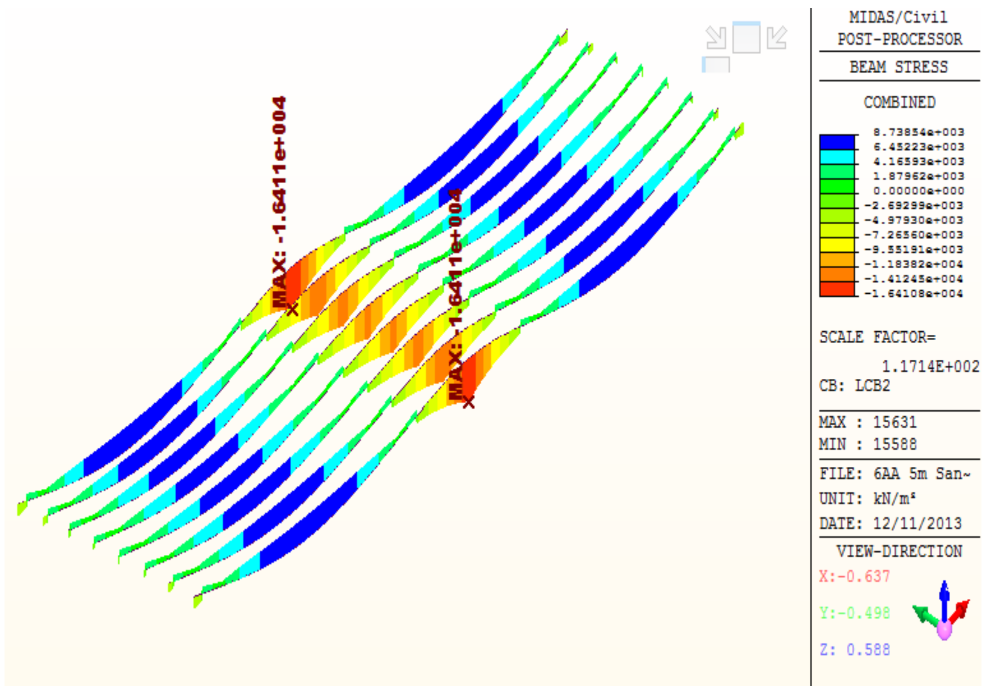
</td></tr>
</table>

<table>
<tr><td rowspan="2">Abutment</td><td colspan="2">Girder Stress (weak-axis) Unit: kN/m²</td></tr>
<tr><td>LCB2 (Contraction)</td><td>-1.605E+04</td></tr>
<tr><td>6 m-Tall</td><td colspan="2">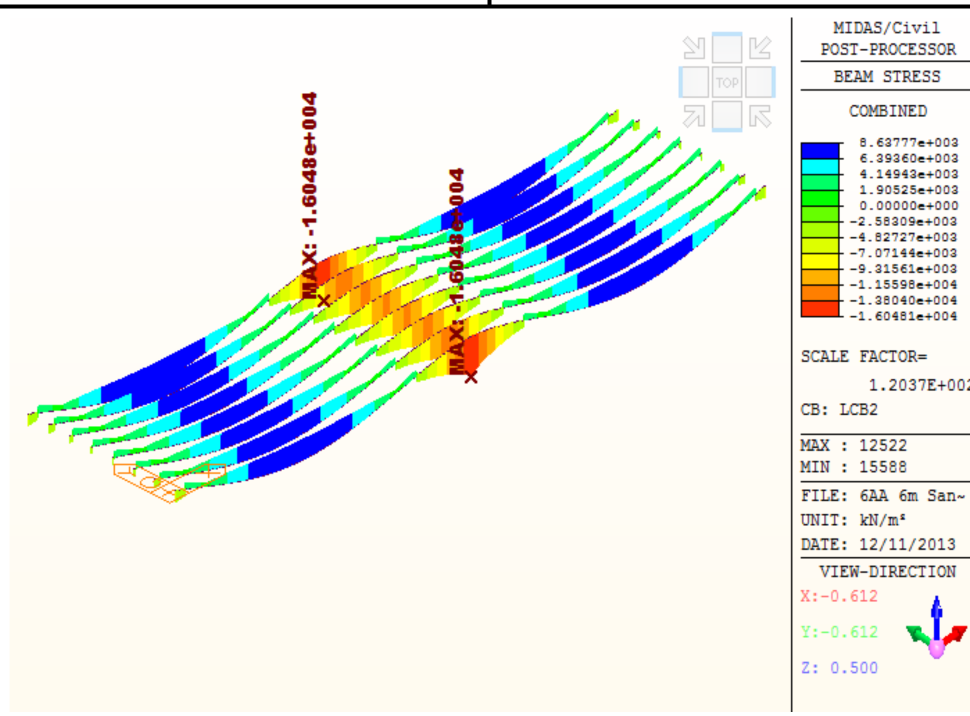
</td></tr>
</table>

<table>
<tr><td rowspan="2">Abutment</td><td colspan="2">Girder Stress (weak-axis) Unit: kN/m²</td></tr>
<tr><td>LCB2 (Contraction)</td><td>-1.577E+04</td></tr>
<tr><td>7 m-Tall</td><td colspan="2">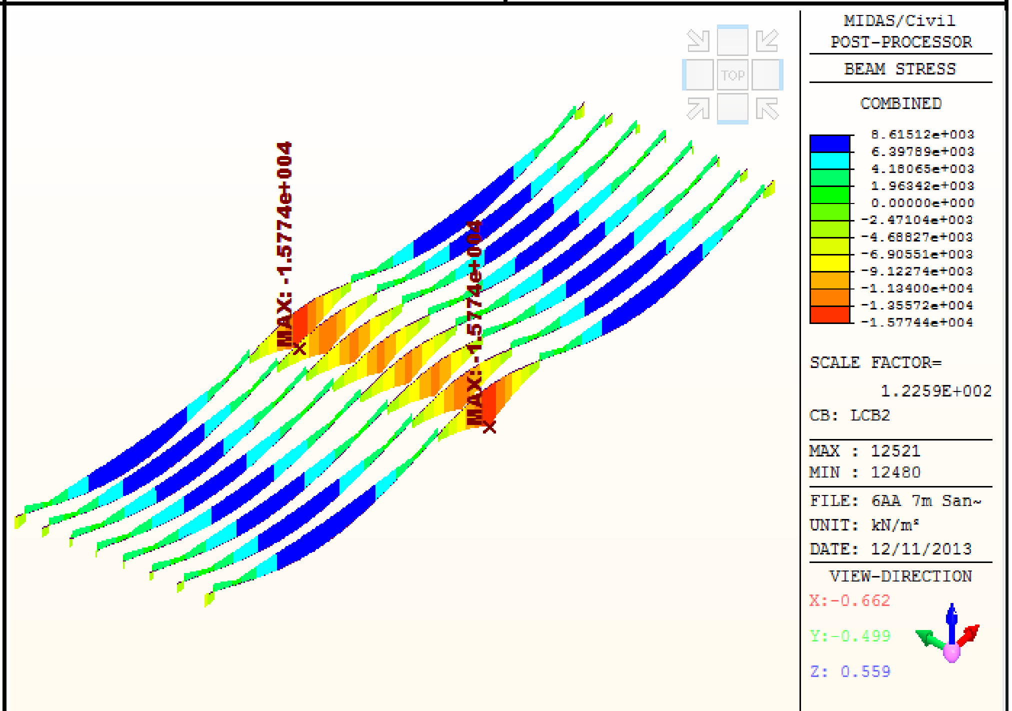
</td></tr>
<tr><td rowspan="2">Abutment</td><td colspan="2">Girder Stress (weak-axis) Unit: kN/m²</td></tr>
<tr><td>LCB2 (Contraction)</td><td>-1.556E+04</td></tr>
<tr><td>8 m-Tall</td><td colspan="2">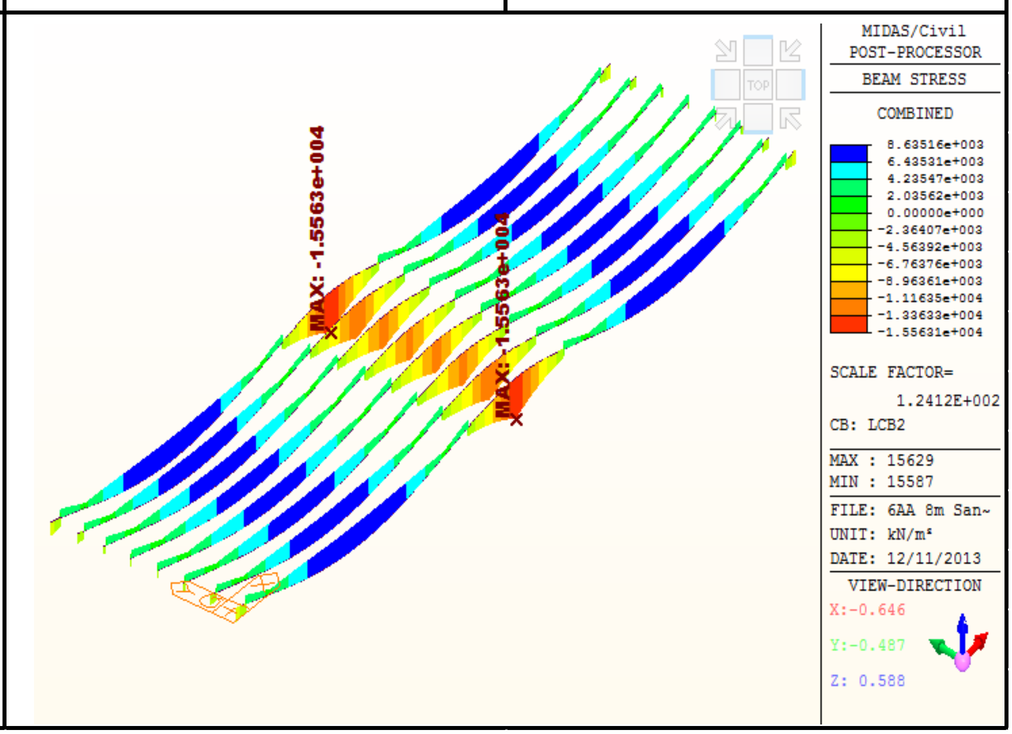
</td></tr>
</table>

1. The Effects depending on Abutment Height

1.5. Abutment Stress (Pile Orientation: Strong-Axis, Expansion Case)

Abutment Stress (strong-axis) LCB1 (Expansion Case) Unit: kN/m^2	
3 m-Tall	15830
4 m-Tall	16660
5 m-Tall	16800
6 m-Tall	16700
7 m-Tall	16510
8 m-Tall	16310

<table>
<tr><td rowspan="2">Abutment</td><td colspan="2">Abutment Stress (strong-axis) Unit: kN/m^2</td></tr>
<tr><td>LCB1 (Expansion)</td><td>1.583E+04</td></tr>
<tr><td>3 m-Tall</td><td colspan="2">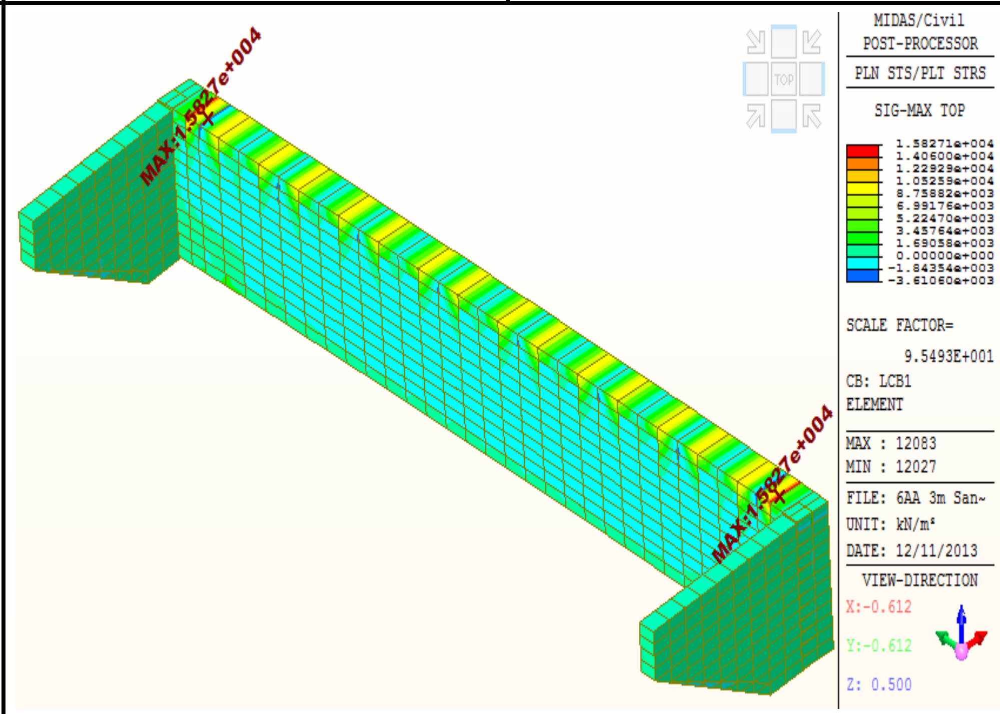
</td></tr>
<tr><td rowspan="2">Abutment</td><td colspan="2">Abutment Stress (strong-axis) Unit: kN/m^2</td></tr>
<tr><td>LCB1 (Expansion)</td><td>1.666E+04</td></tr>
<tr><td>4 m-Tall</td><td colspan="2">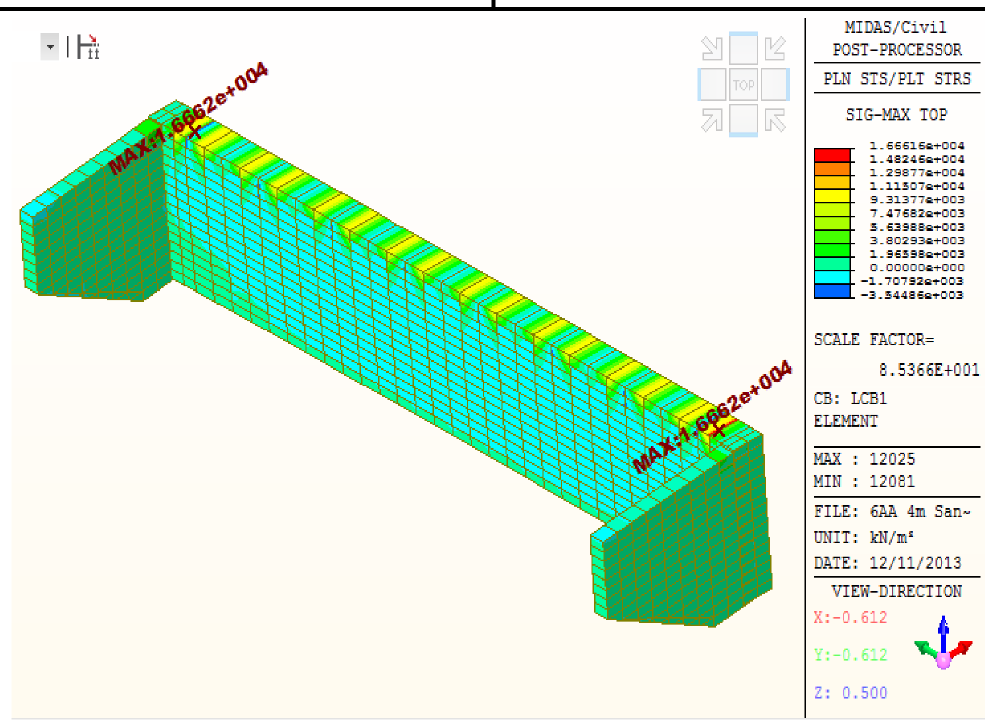
</td></tr>
</table>

Abutment	Abutment Stress (strong-axis) Unit: kN/m^2	
	LCB1 (Expansion)	1.680E+04
5 m-Tall	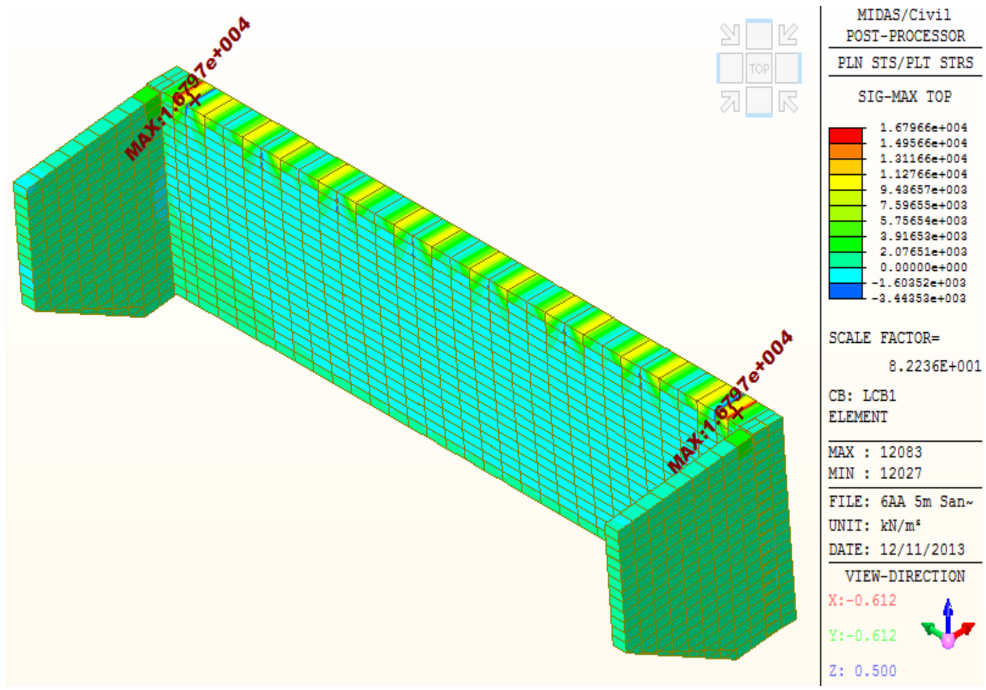	
Abutment	Abutment Stress (strong-axis) Unit: kN/m^2	
	LCB1 (Expansion)	1.670E+04
6 m-Tall	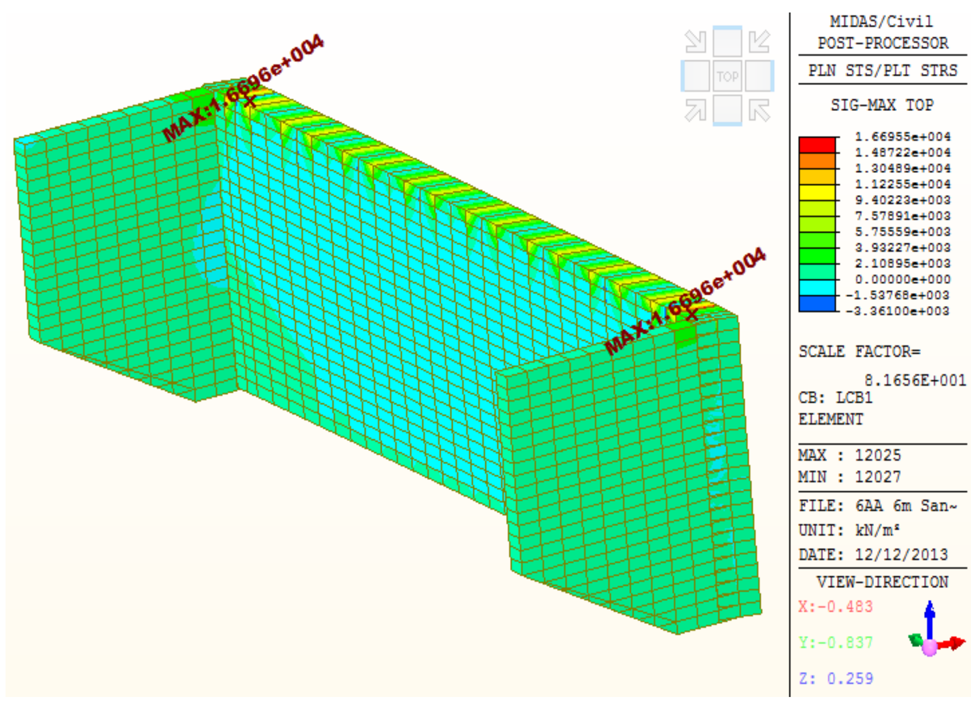	

<table>
<tr><td rowspan="2">Abutment</td><td colspan="2">Abutment Stress (strong-axis) Unit: kN/m^2</td></tr>
<tr><td>LCB1 (Expansion)</td><td>1.651E+04</td></tr>
<tr><td>7 m-Tall</td><td colspan="2">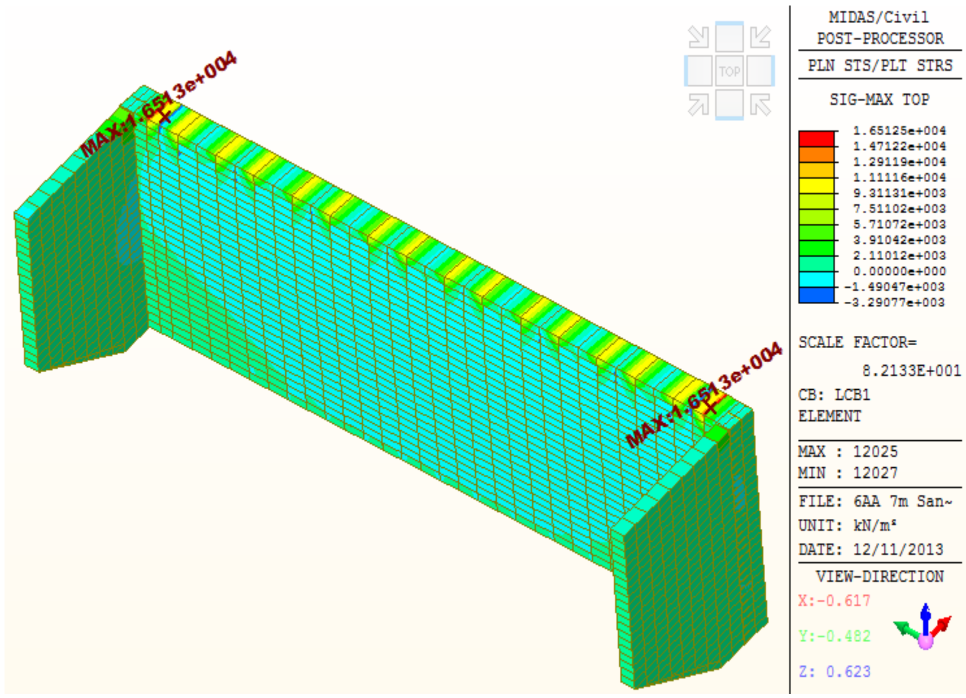
</td></tr>
<tr><td rowspan="2">Abutment</td><td colspan="2">Abutment Stress (strong-axis) Unit: kN/m^2</td></tr>
<tr><td>LCB1 (Expansion)</td><td>1.631E+04</td></tr>
<tr><td>8 m-Tall</td><td colspan="2">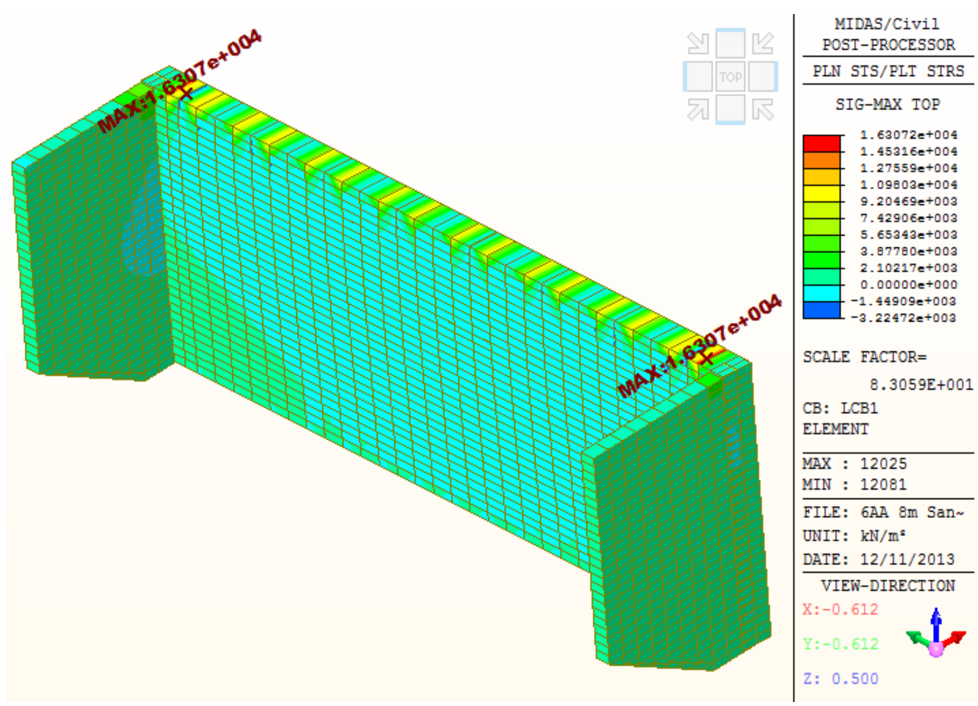
</td></tr>
</table>

1. The Effects depending on Abutment Height

1.6. Abutment Stress (Pile Orientation: Strong-Axis, Contraction Case)

Abutment Stress (strong-axis) LCB2 (Contraction Case) Unit: kN/m^2	
3 m-Tall	5446
4 m-Tall	6928
5 m-Tall	8046
6 m-Tall	8873
7 m-Tall	9498
8 m-Tall	9987

<table>
<tr><td rowspan="2">Abutment</td><td colspan="2">Abutment Stress (strong-axis) Unit: kN/m^2</td></tr>
<tr><td>LCB2 (Contraction)</td><td>5.446E+03</td></tr>
<tr><td>3 m-Tall</td><td colspan="2">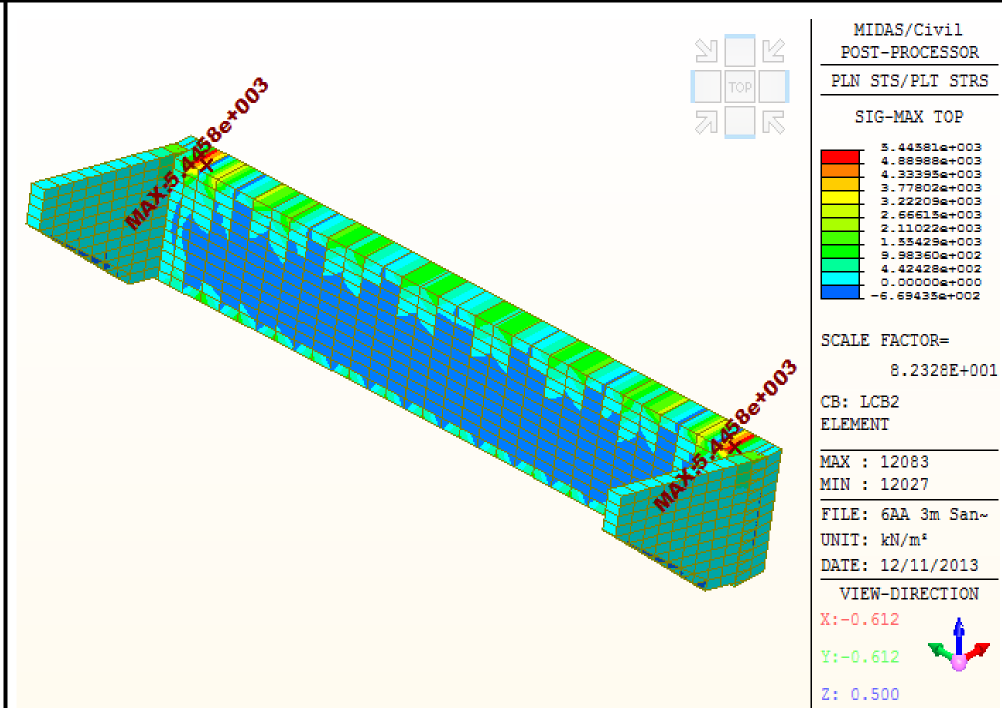
</td></tr>
<tr><td rowspan="2">Abutment</td><td colspan="2">Abutment Stress (strong-axis) Unit: kN/m^2</td></tr>
<tr><td>LCB2 (Contraction)</td><td>6.928E+03</td></tr>
<tr><td>4 m-Tall</td><td colspan="2">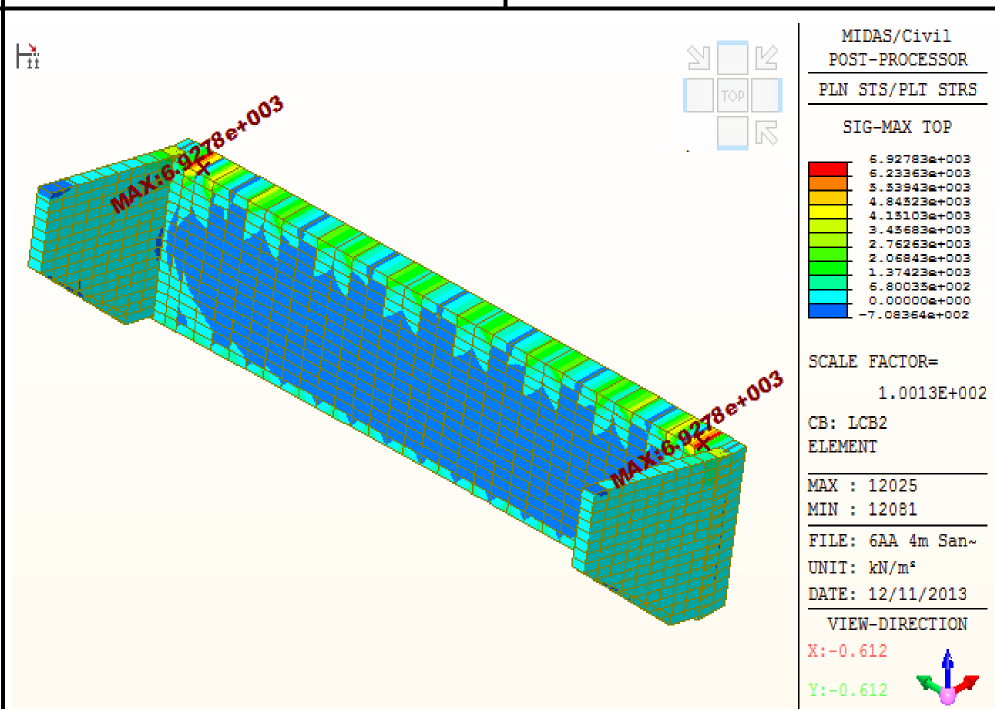
</td></tr>
</table>

<table>
<tr><td rowspan="2">Abutment</td><td colspan="2">Abutment Stress (strong-axis) Unit: kN/m^2</td></tr>
<tr><td>LCB2 (Contraction)</td><td>8.046E+03</td></tr>
<tr><td>5 m-Tall</td><td colspan="2">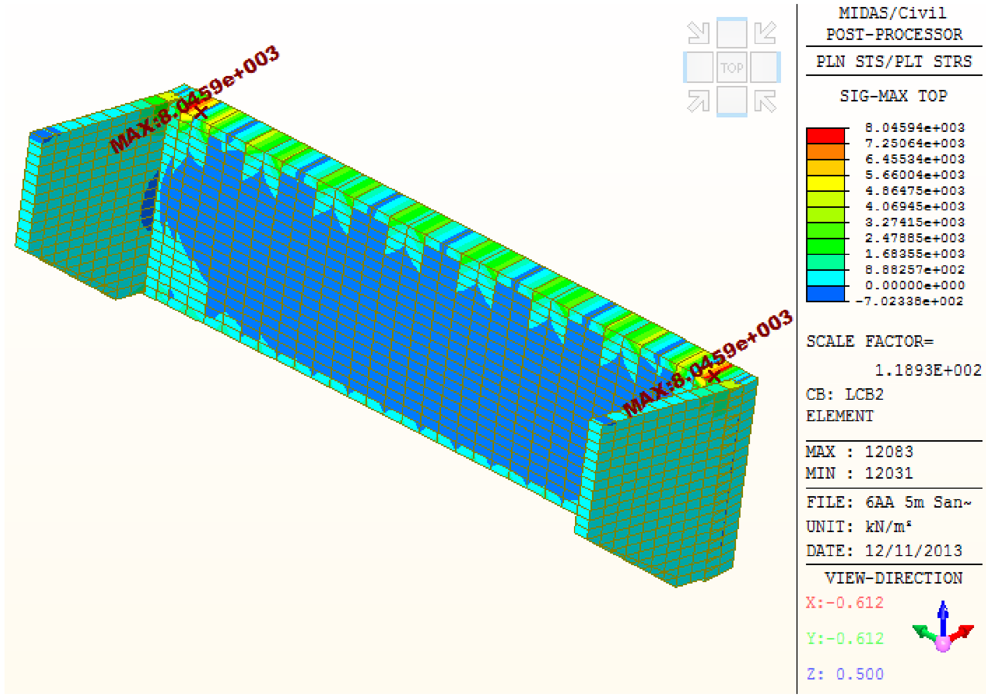
</td></tr>
<tr><td rowspan="2">Abutment</td><td colspan="2">Abutment Stress (strong-axis) Unit: kN/m^2</td></tr>
<tr><td>LCB2 (Contraction)</td><td>8.873E+03</td></tr>
<tr><td>6 m-Tall</td><td colspan="2">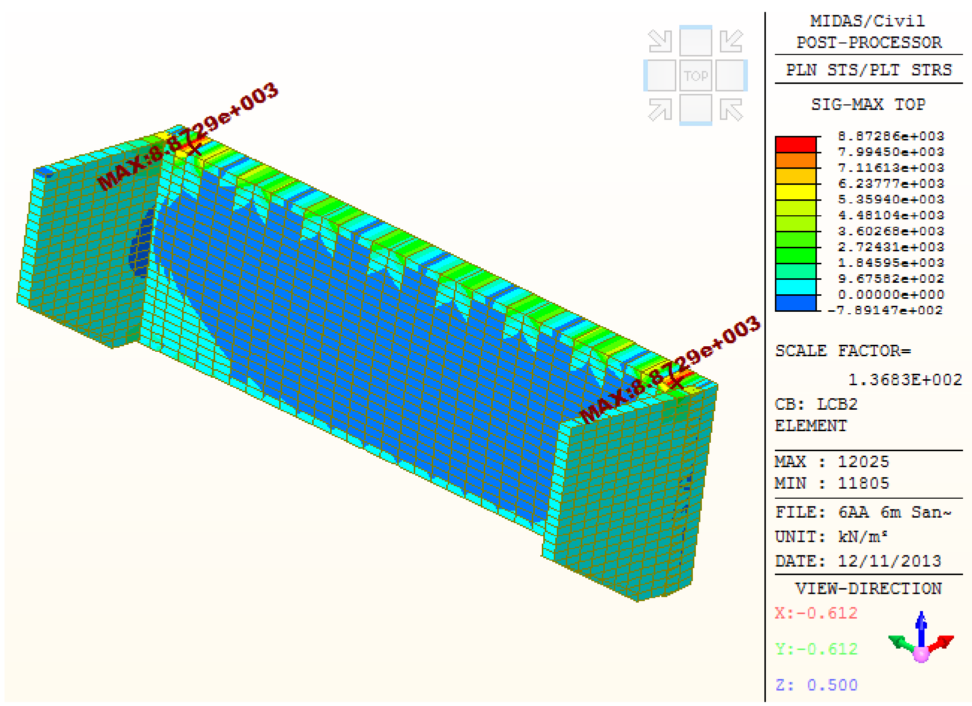
</td></tr>
</table>

Abutment	Abutment Stress (strong-axis) Unit: kN/m^2	
	LCB2 (Contraction)	9.498E+03
7 m-Tall	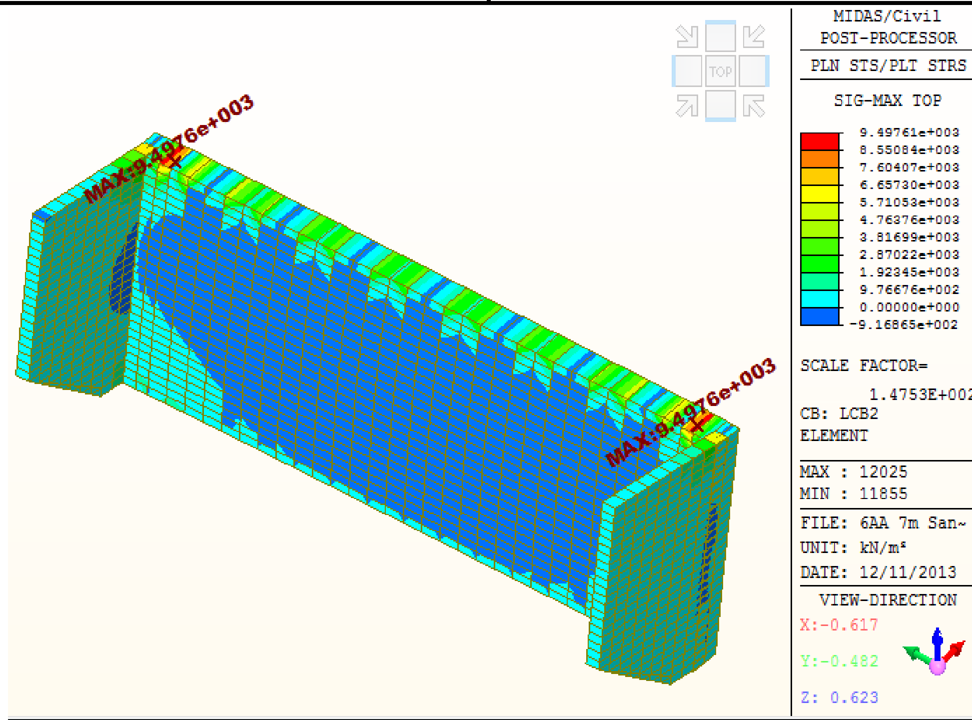	

Abutment	Abutment Stress (strong-axis) Unit: kN/m^2	
	LCB2 (Contraction)	9.987E+03
8 m-Tall	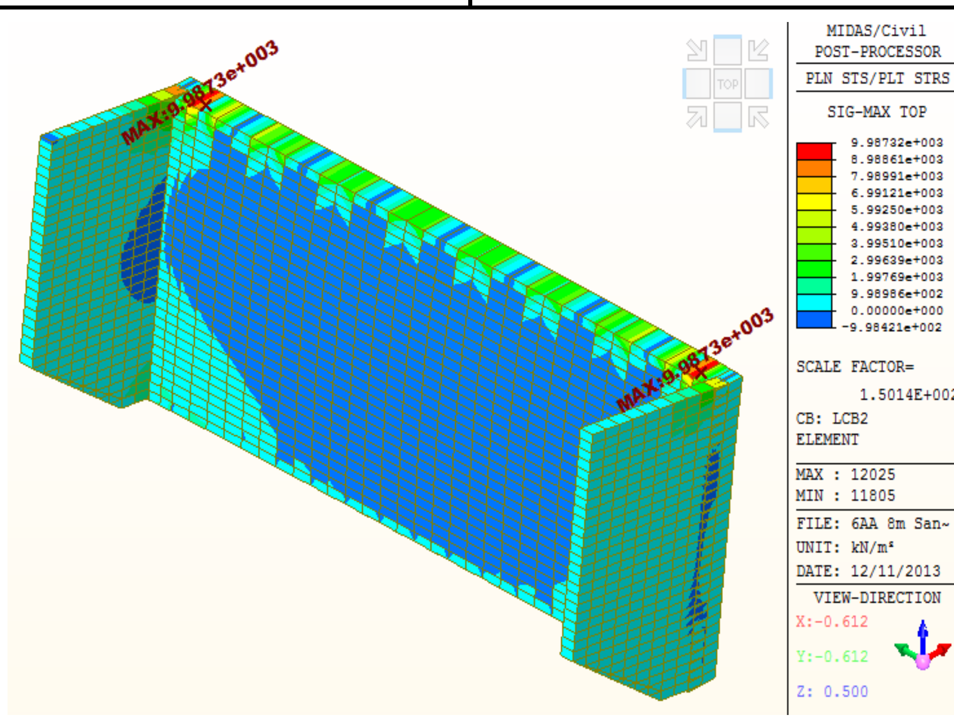	

1. The Effects depending on Abutment Height

1.7. Abutment Stress (Pile Orientation: Weak-Axis, Expansion Case)

Abutment Stress (weak-axis) LCB1 (Expansion Case) Unit: kN/m^2	
3 m-Tall	14950
4 m-Tall	16280
5 m-Tall	16640
6 m-Tall	16640
7 m-Tall	16510
8 m-Tall	16330

<table>
<tr><td rowspan="2">Abutment</td><td colspan="2">Abutment Stress (weak-axis) Unit: kN/m^2</td></tr>
<tr><td>LCB1 (Expansion)</td><td>1.495E+04</td></tr>
<tr><td>3 m-Tall</td><td colspan="2">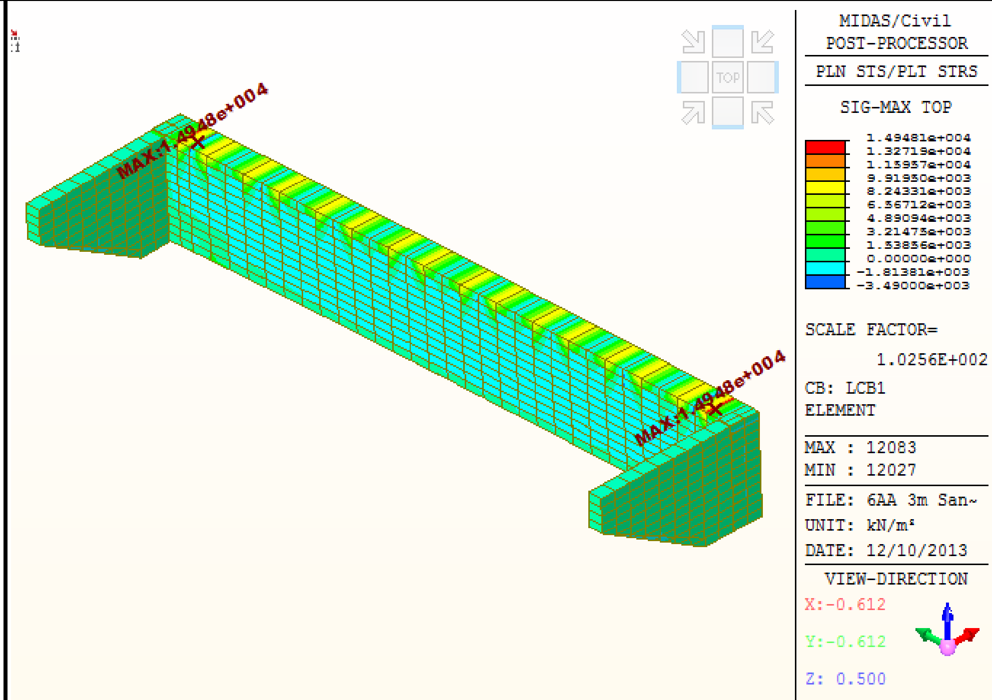
</td></tr>
<tr><td rowspan="2">Abutment</td><td colspan="2">Abutment Stress (weak-axis) Unit: kN/m^2</td></tr>
<tr><td>LCB1 (Expansion)</td><td>1.628E+04</td></tr>
<tr><td>4 m-Tall</td><td colspan="2">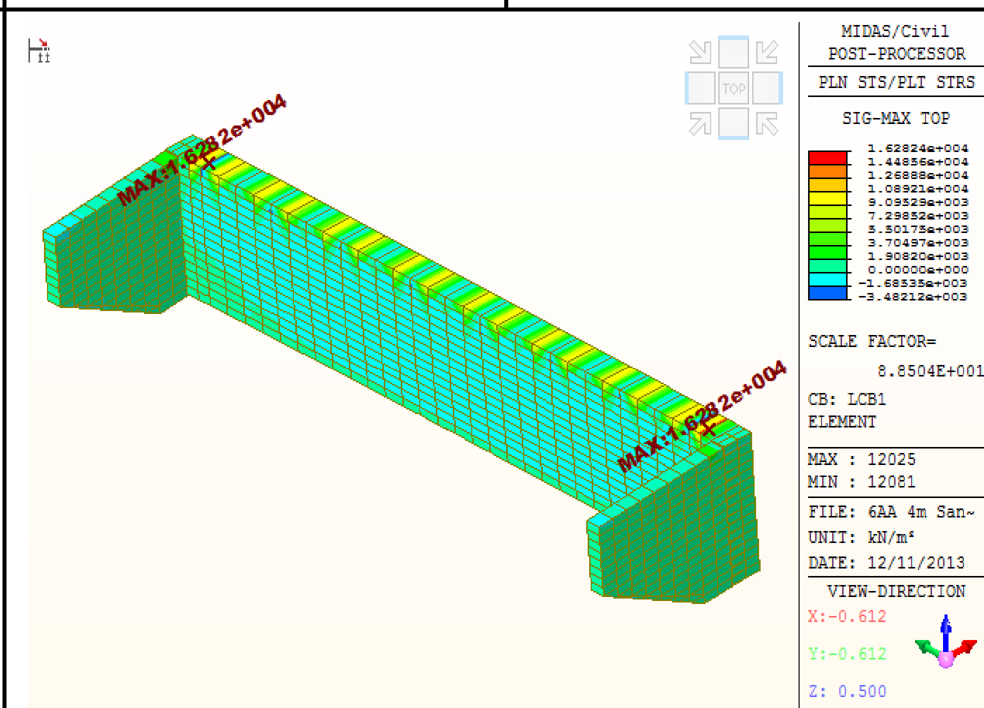
</td></tr>
</table>

Abutment	Abutment Stress (weak-axis) Unit: kN/m^2	
	LCB1 (Expansion)	1.664E+04
5 m-Tall	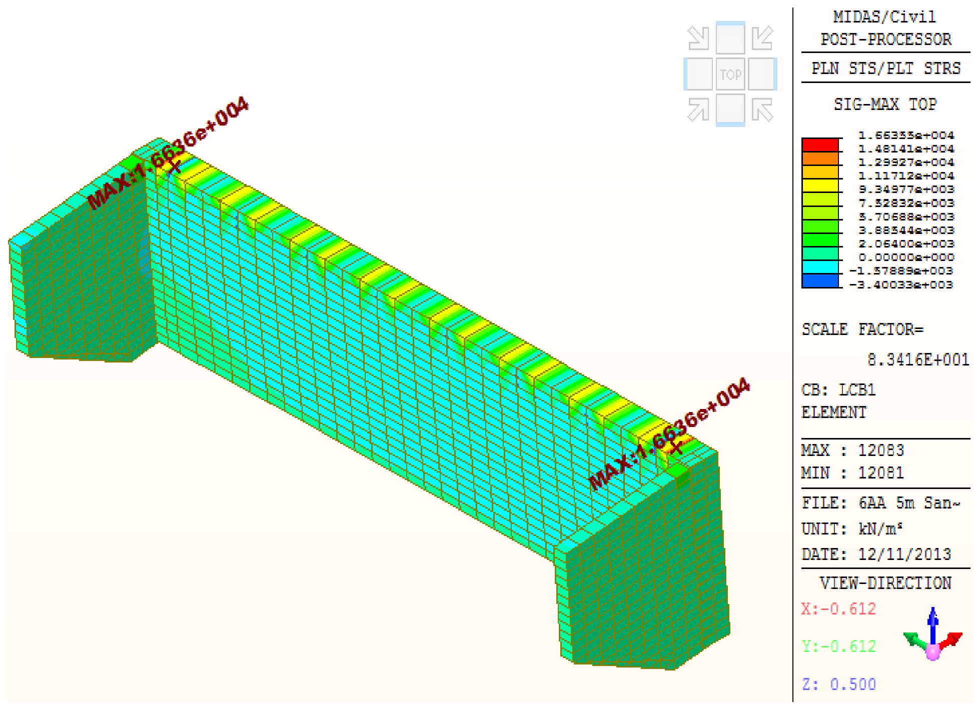	

Abutment	Abutment Stress (weak-axis) Unit: kN/m^2	
	LCB1 (Expansion)	1.664E+04
6 m-Tall	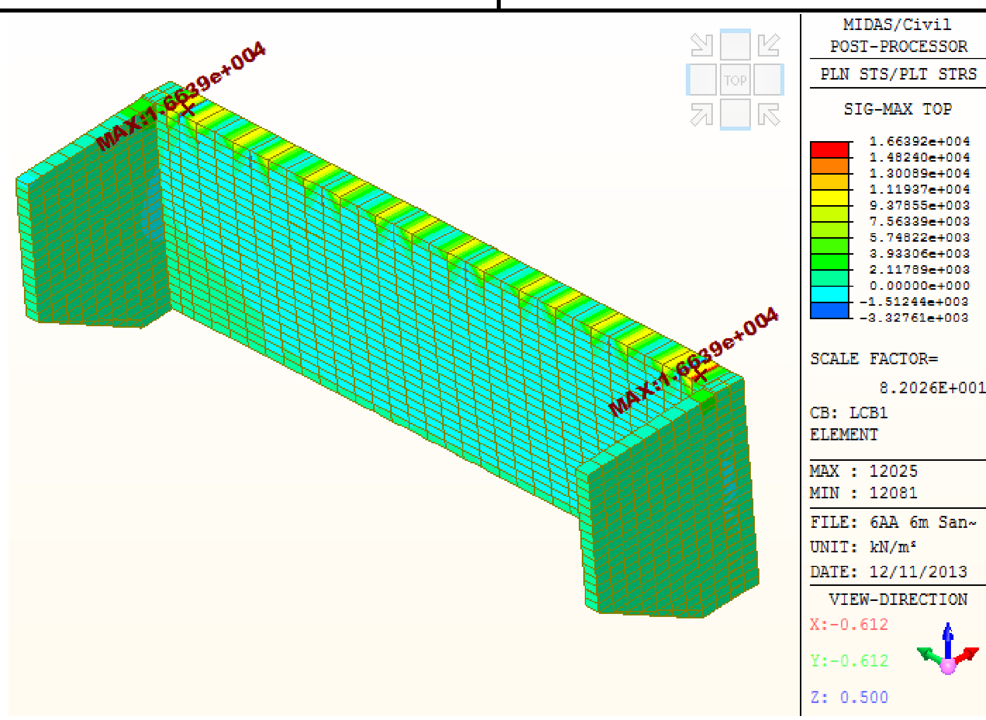	

Abutment	Abutment Stress (weak-axis) Unit: kN/m^2	
	LCB1 (Expansion)	1.651E+04

7 m-Tall

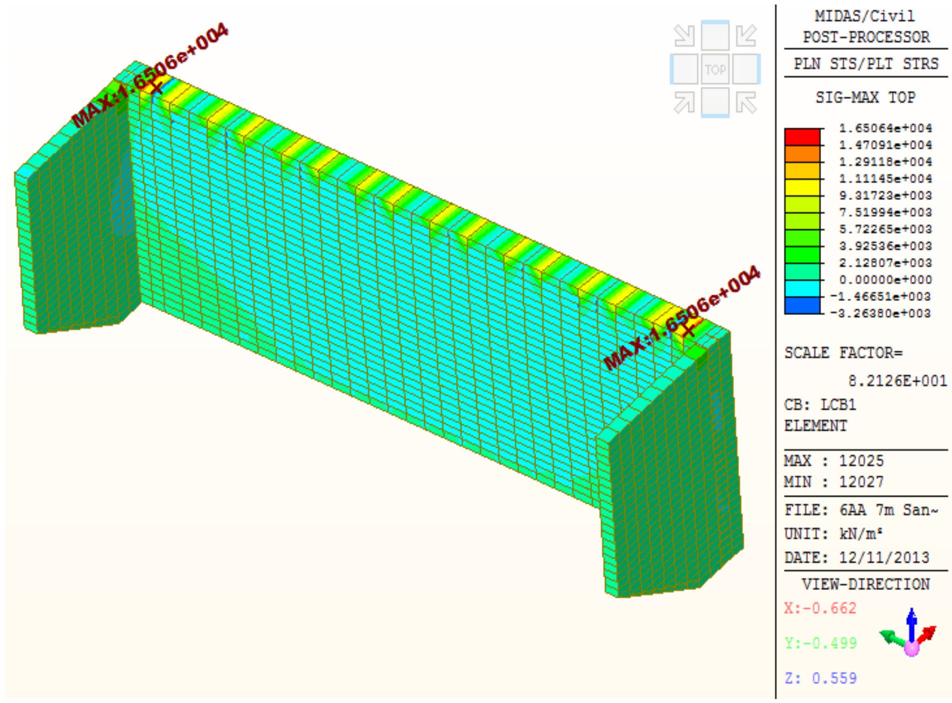

Abutment	Abutment Stress (weak-axis) Unit: kN/m^2	
	LCB1 (Expansion)	1.633E+04

8 m-Tall

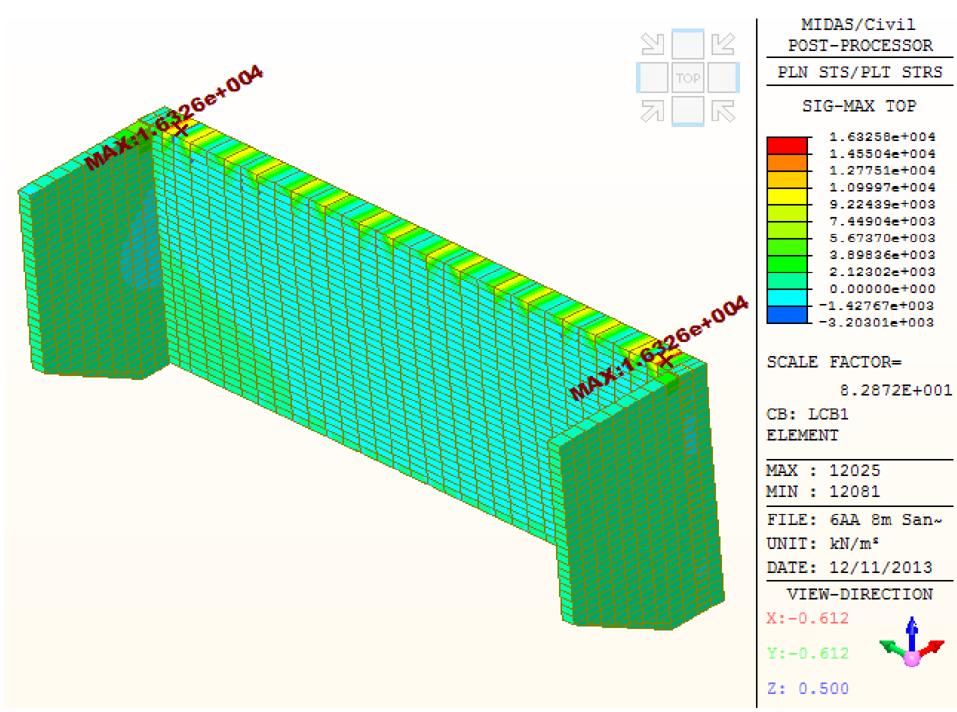

1. The Effects depending on Abutment Height

1.8. Abutment Stress (Pile Orientation: Weak-Axis, Contraction Case)

Abutment Stress (weak-axis) LCB2 (Contraction Case) Unit: kN/m^2	
3 m-Tall	4883
4 m-Tall	6522
5 m-Tall	7782
6 m-Tall	8703
7 m-Tall	9385
8 m-Tall	9911

<table>
<tr><td rowspan="2">Abutment</td><td colspan="2">Abutment Stress (weak-axis) Unit: kN/m^2</td></tr>
<tr><td>LCB2 (Contraction)</td><td>4.883E+03</td></tr>
<tr><td>3 m-Tall</td><td colspan="2">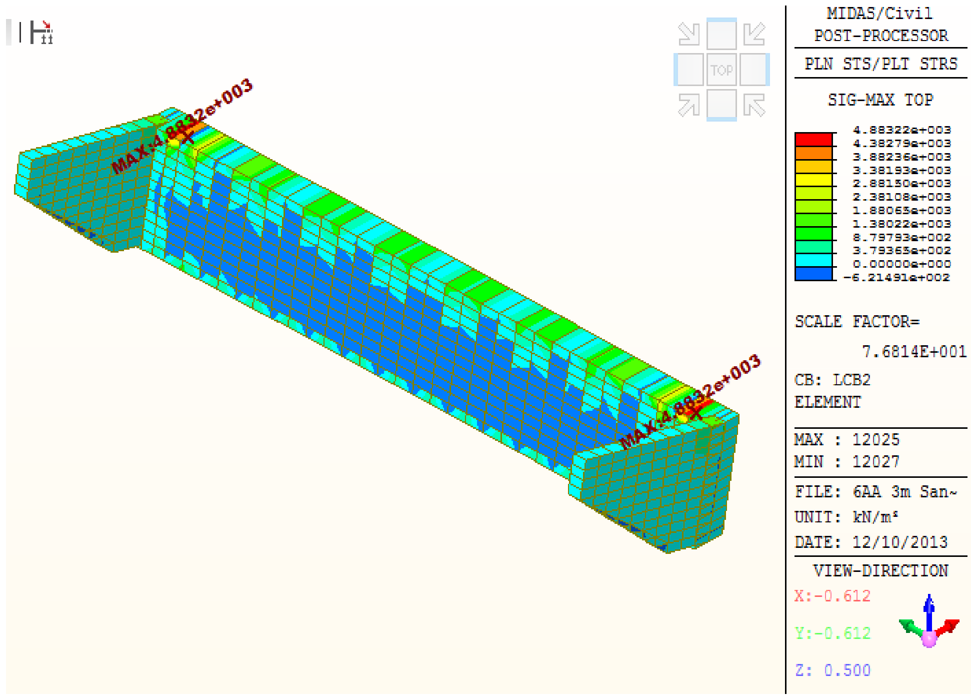
</td></tr>
<tr><td rowspan="2">Abutment</td><td colspan="2">Abutment Stress (weak-axis) Unit: kN/m^2</td></tr>
<tr><td>LCB2 (Contraction)</td><td>6.522E+03</td></tr>
<tr><td>4 m-Tall</td><td colspan="2">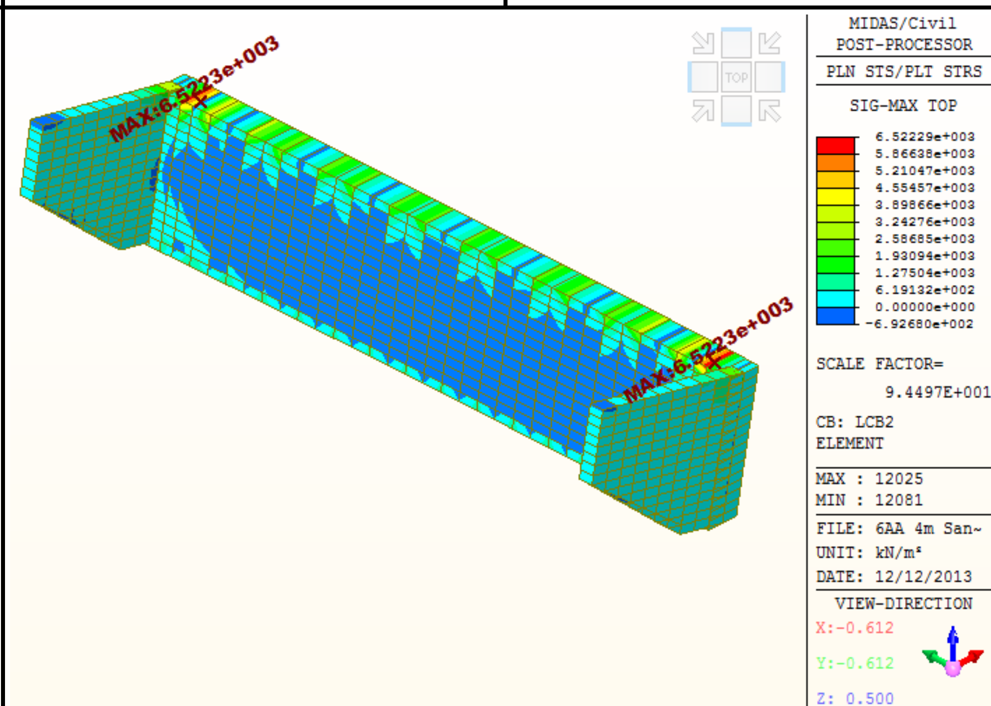
</td></tr>
</table>

<table>
<tr><td rowspan="2">Abutment</td><td colspan="2">Abutment Stress (weak-axis) Unit: kN/m^2</td></tr>
<tr><td>LCB2 (Contraction)</td><td>7.782E+03</td></tr>
<tr><td>5 m-Tall</td><td colspan="2">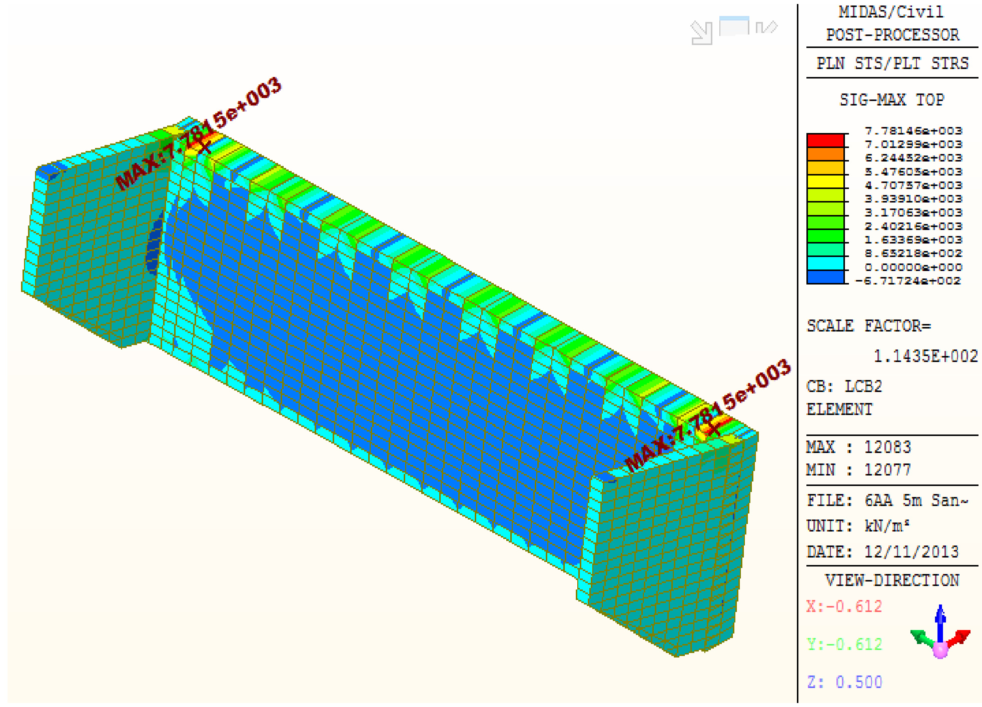
</td></tr>
<tr><td rowspan="2">Abutment</td><td colspan="2">Abutment Stress (weak-axis) Unit: kN/m^2</td></tr>
<tr><td>LCB2 (Contraction)</td><td>8.703E+03</td></tr>
<tr><td>6 m-Tall</td><td colspan="2">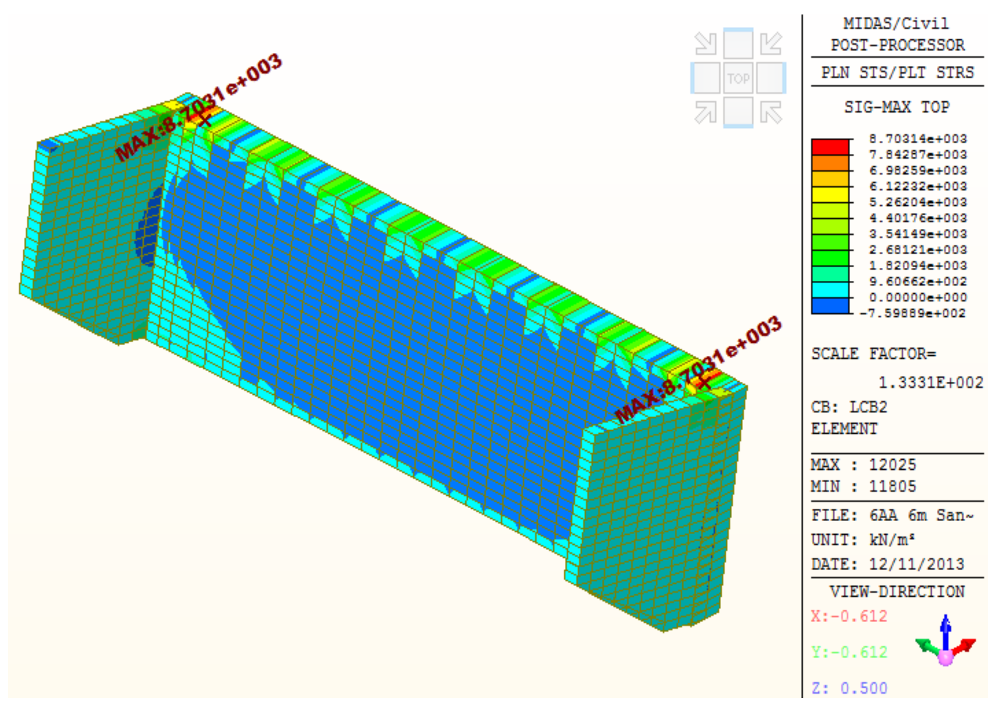
</td></tr>
</table>

<table>
<tr><td rowspan="2">Abutment</td><td colspan="2">Abutment Stress (weak-axis) Unit: kN/m^2</td></tr>
<tr><td>LCB2 (Contraction)</td><td>9.385E+03</td></tr>
<tr><td>7 m-Tall</td><td colspan="2">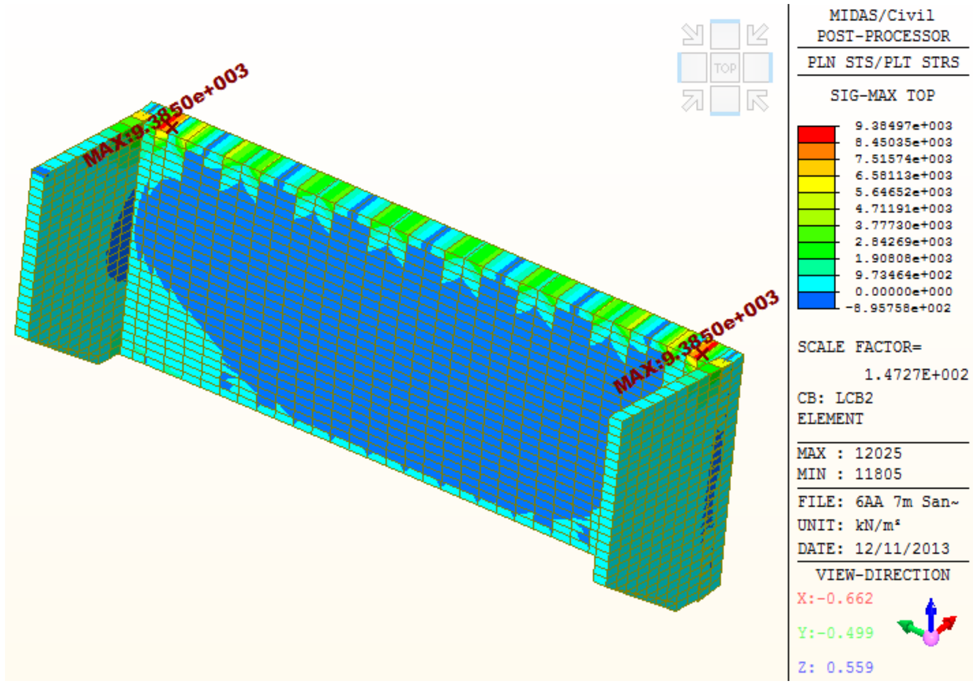
</td></tr>
<tr><td rowspan="2">Abutment</td><td colspan="2">Abutment Stress (weak-axis) Unit: kN/m^2</td></tr>
<tr><td>LCB2 (Contraction)</td><td>9.911E+03</td></tr>
<tr><td>8 m-Tall</td><td colspan="2">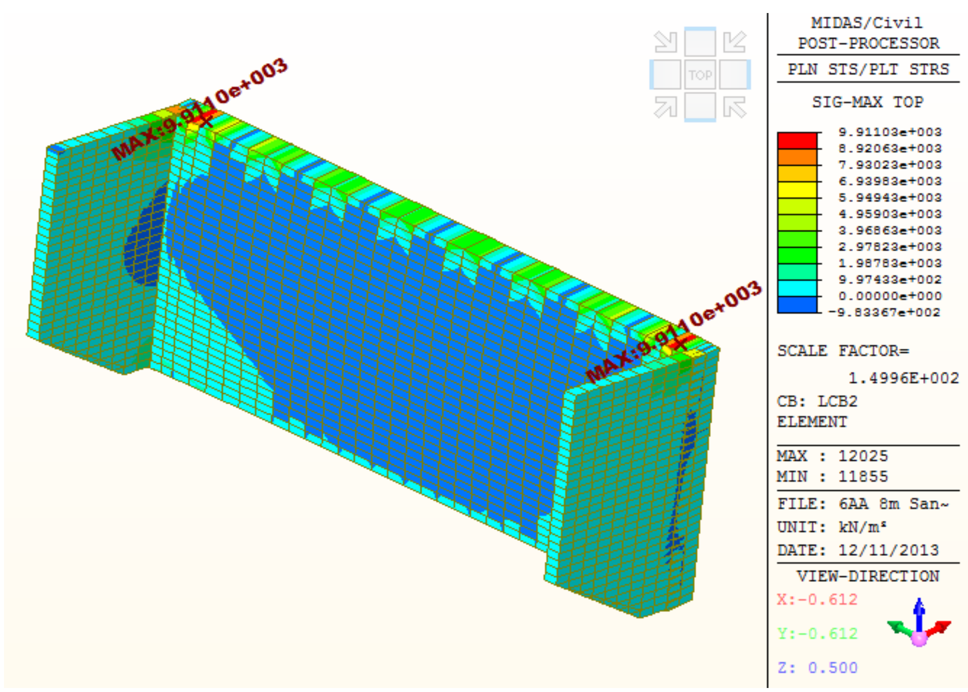
</td></tr>
</table>

1. The Effects depending on Abutment Height

1.9. Pile Moment (Pile Orientation: Strong-Axis, Expansion Case)

Pile Moment (strong-axis) LCB1 (Expansion Case) Unit: kN·m	
3 m-Tall	-250.1
4 m-Tall	-150.1
5 m-Tall	-82.54
6 m-Tall	43.97
7 m-Tall	44.17
8 m-Tall	50.82

<table>
<tr><td rowspan="2">Abutment</td><td colspan="2">Pile Moment (strong-axis) Unit: kN·m</td></tr>
<tr><td>LCB1 (Expansion)</td><td>-2.501E+02</td></tr>
<tr><td>3 m-Tall</td><td colspan="2">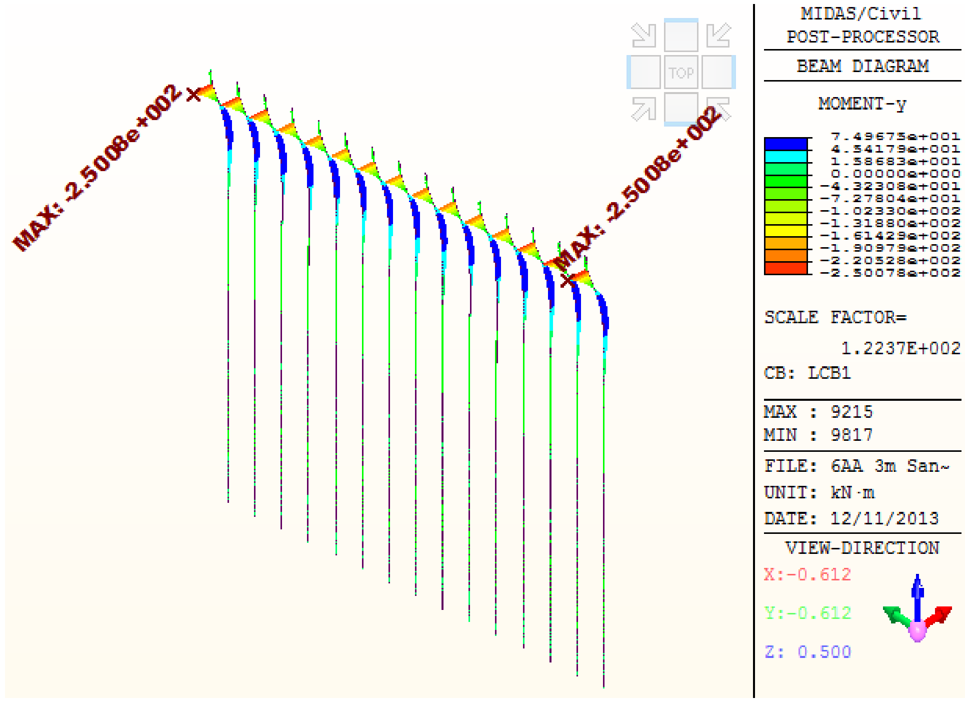</td></tr>
<tr><td rowspan="2">Abutment</td><td colspan="2">Pile Moment (strong-axis) Unit: kN·m</td></tr>
<tr><td>LCB1 (Expansion)</td><td>-1.501E+02</td></tr>
<tr><td>4 m-Tall</td><td colspan="2">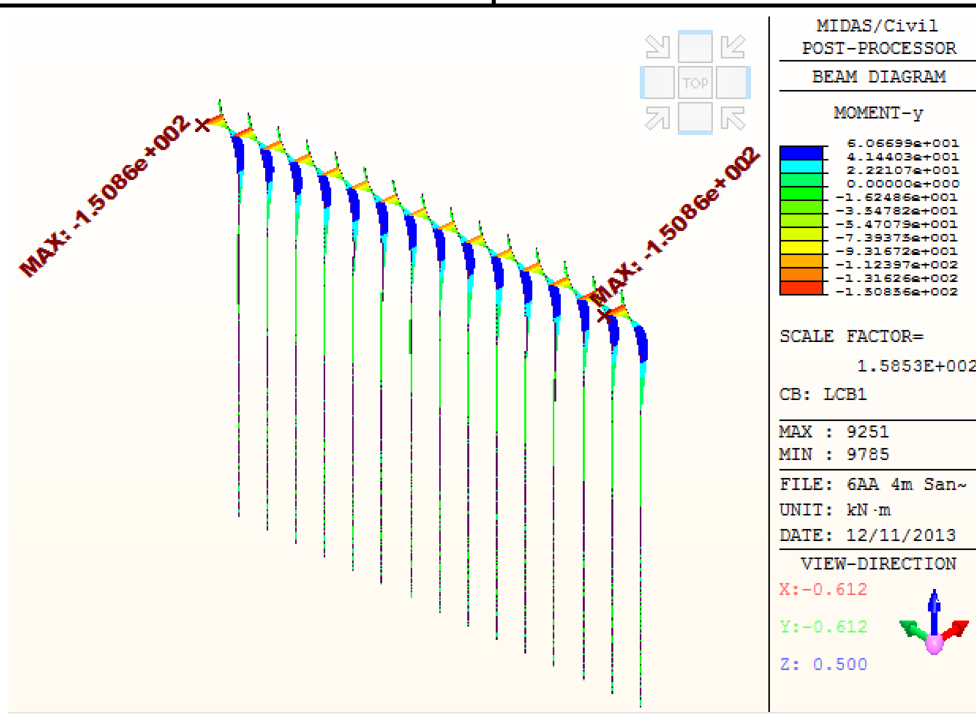</td></tr>
</table>

Abutment	Pile Moment (strong-axis) Unit: kN·m	
	LCB1 (Expansion)	-8.254E+01
5 m-Tall	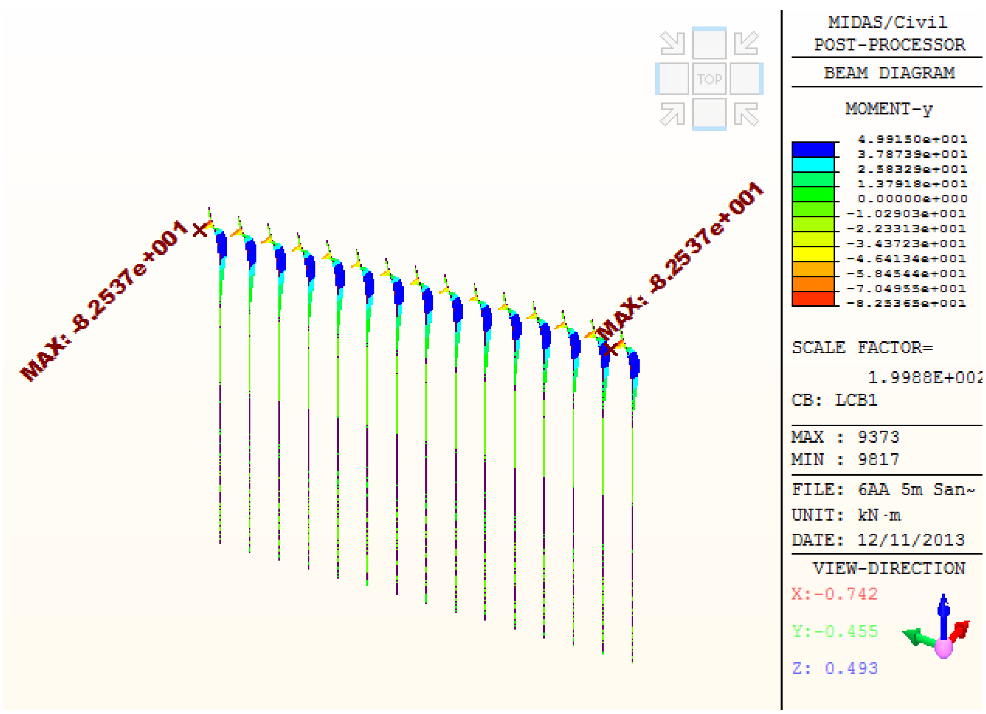	

Abutment	Pile Moment (strong-axis) Unit: kN·m	
	LCB1 (Expansion)	4.397E+01
6 m-Tall	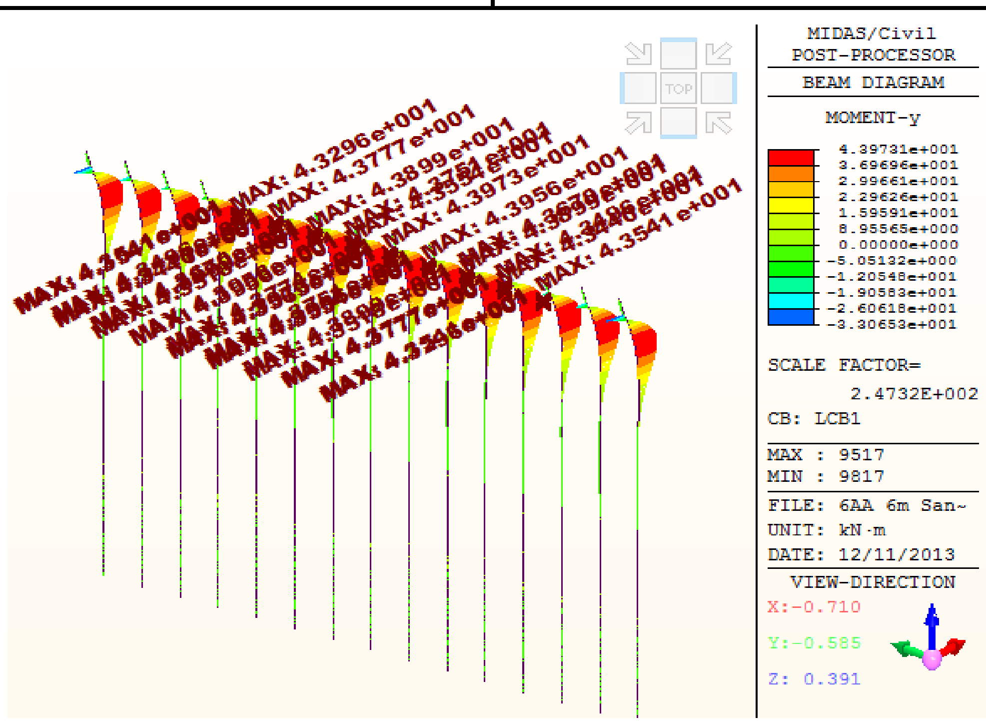	

<table>
<tr><td rowspan="2">Abutment</td><td colspan="2">Pile Moment (strong-axis) Unit: kN·m</td></tr>
<tr><td>LCB1 (Expansion)</td><td>4.417E+01</td></tr>
<tr><td>7 m-Tall</td><td colspan="2">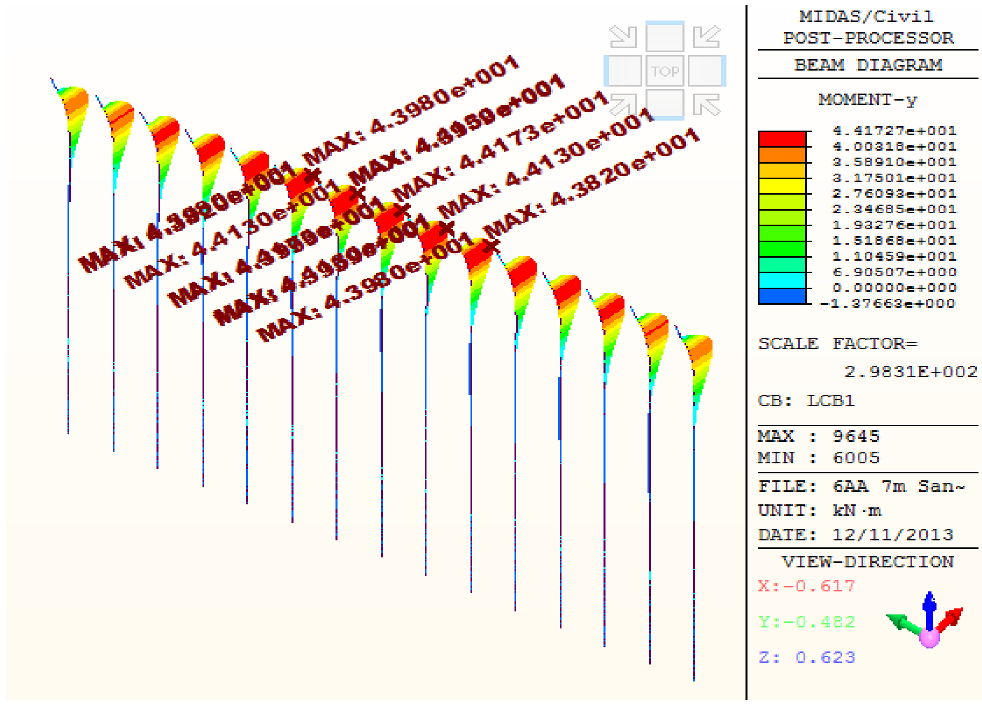
</td></tr>
<tr><td rowspan="2">Abutment</td><td colspan="2">Pile Moment (strong-axis) Unit: kN·m</td></tr>
<tr><td>LCB1 (Expansion)</td><td>5.082E+01</td></tr>
<tr><td>8 m-Tall</td><td colspan="2">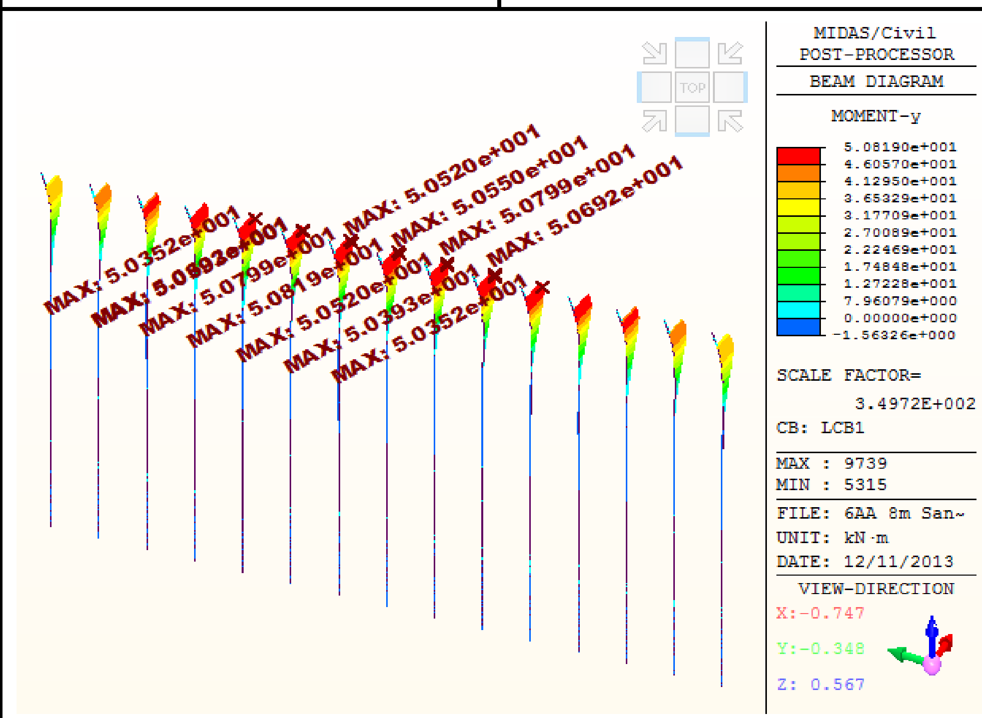
</td></tr>
</table>

1. The Effects depending on Abutment Height

1.10. Pile Moment (Pile Orientation: Strong-Axis, Contraction Case)

Pile Moment (strong-axis) LCB2 (Contraction Case) Unit: kN·m	
3 m-Tall	-169.2
4 m-Tall	-164.3
5 m-Tall	-147.1
6 m-Tall	-126.3
7 m-Tall	-106
8 m-Tall	-87.19

Abutment	Pile Moment (strong-axis) Unit: kN·m	
	LCB2 (Contraction)	-1.692E+02
3 m-Tall	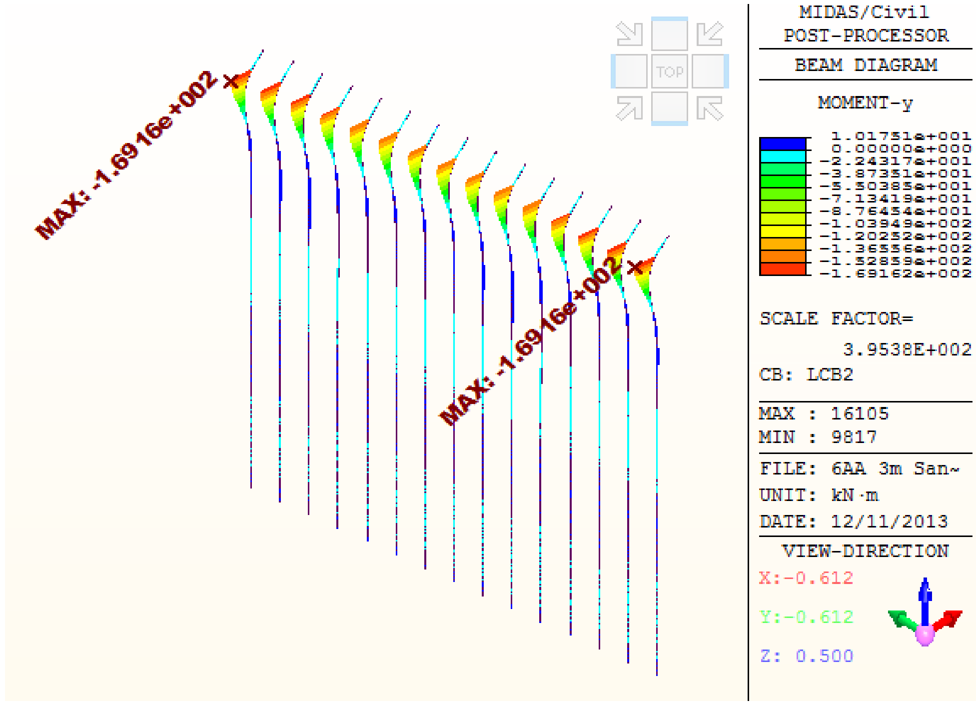	

Abutment	Pile Moment (strong-axis) Unit: kN·m	
	LCB2 (Contraction)	-1.643E+02
4 m-Tall	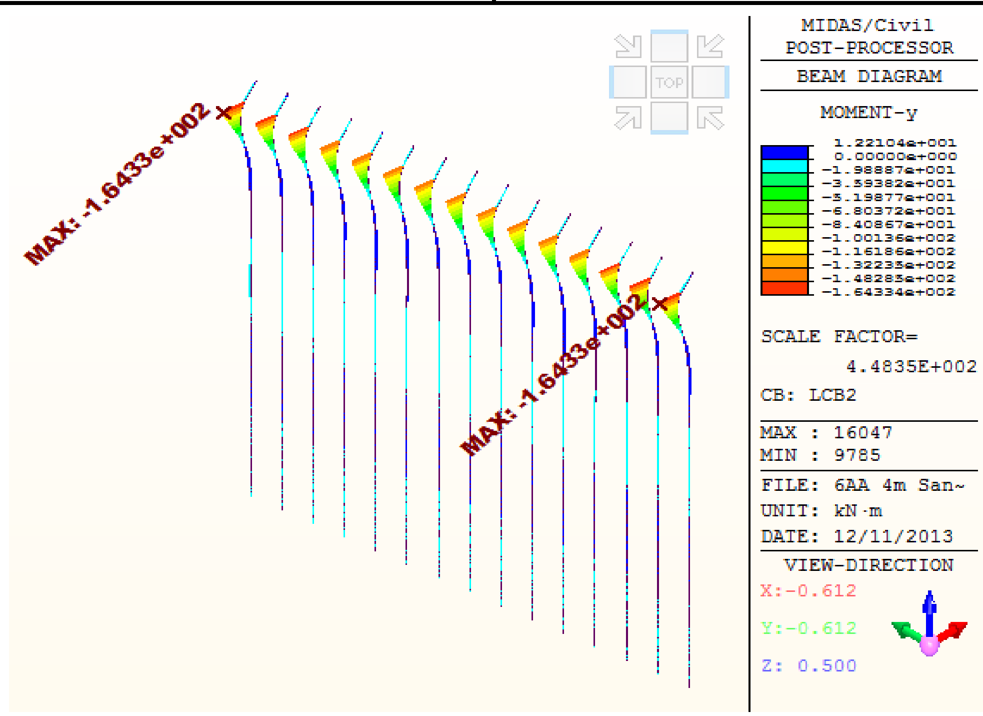	

Abutment	Pile Moment (strong-axis) Unit: kN·m	
	LCB2 (Contraction)	-1.471E+02
5 m-Tall	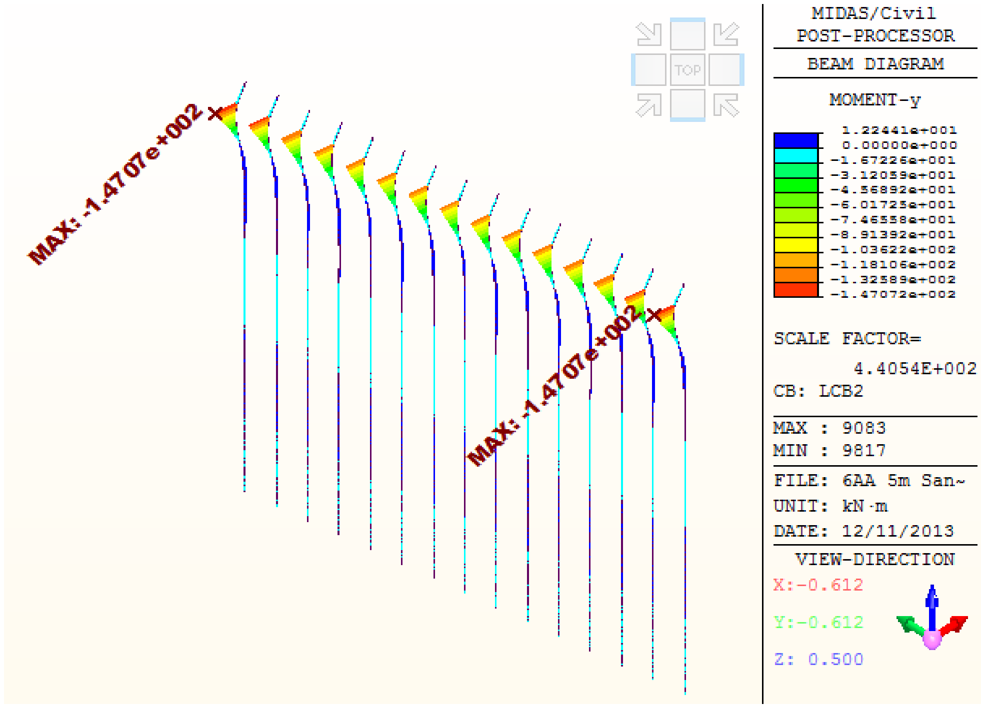	
Abutment	Pile Moment (strong-axis) Unit: kN·m	
	LCB2 (Contraction)	-1.263E+02
6 m-Tall	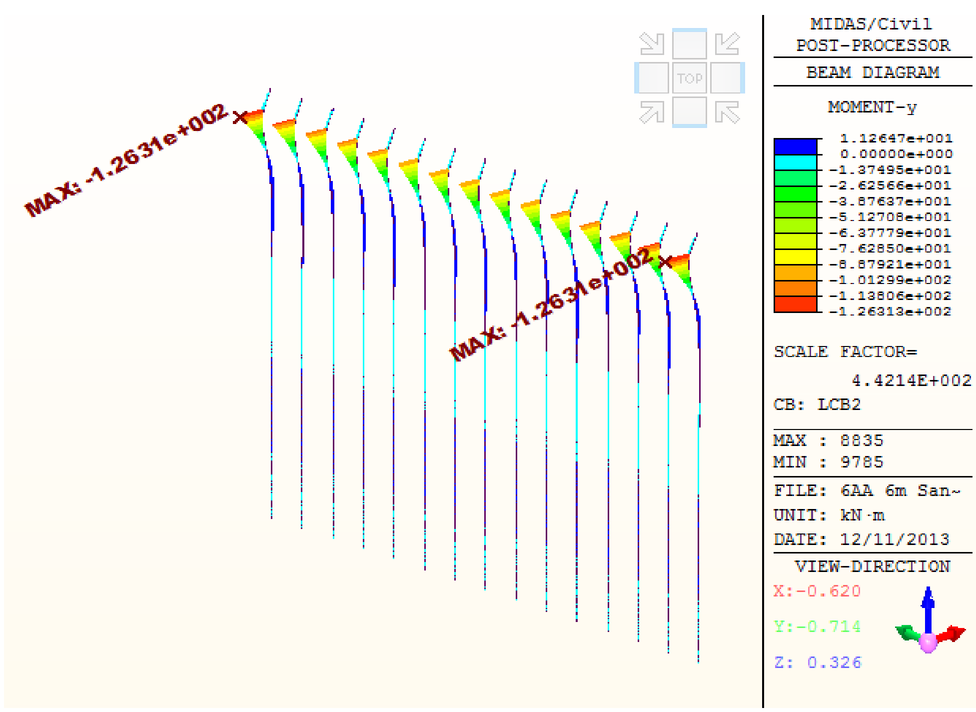	

<table>
<tr><td rowspan="2">Abutment</td><td colspan="2">Pile Moment (strong-axis) Unit: kN·m</td></tr>
<tr><td>LCB2 (Contraction)</td><td>-1.060E+02</td></tr>
<tr><td>7 m-Tall</td><td colspan="2">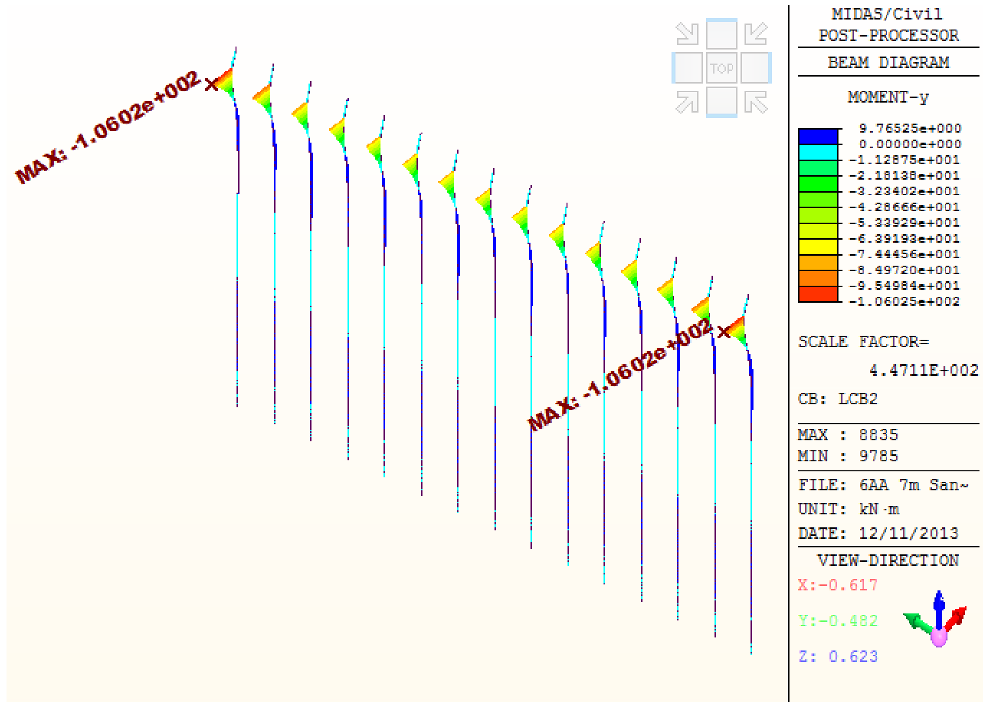
</td></tr>
<tr><td rowspan="2">Abutment</td><td colspan="2">Pile Moment (strong-axis) Unit: kN·m</td></tr>
<tr><td>LCB2 (Contraction)</td><td>-8.719E+01</td></tr>
<tr><td>8 m-Tall</td><td colspan="2">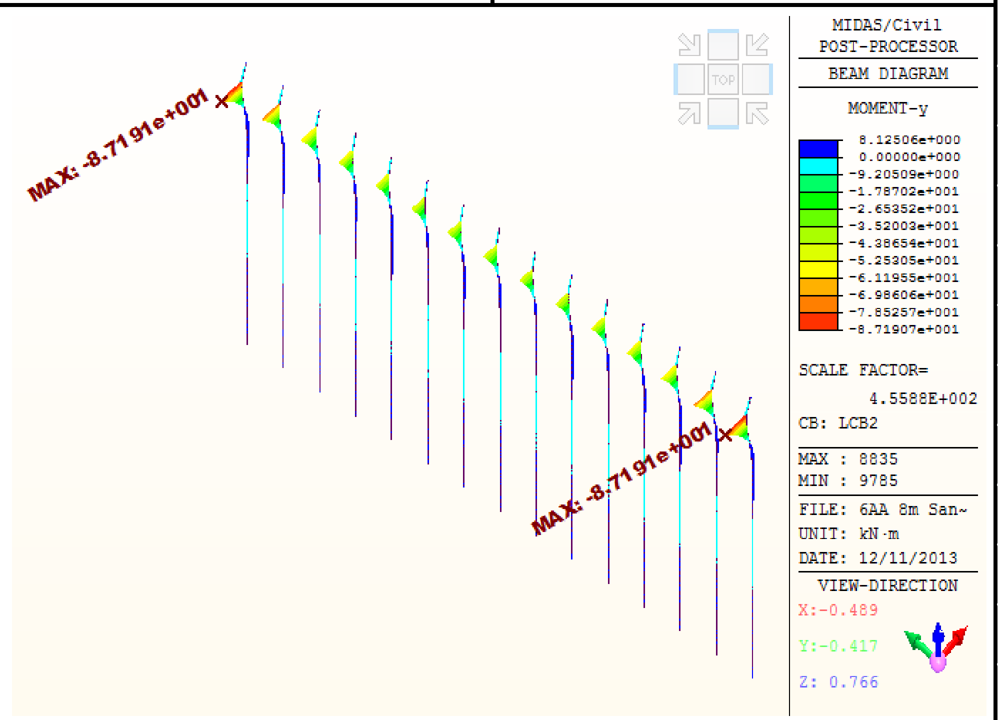
</td></tr>
</table>

1. The Effects depending on Abutment Height

1.11. Pile Moment (Pile Orientation: Weak-Axis, Expansion Case)

Pile Moment (weak-axis) LCB1 (Expansion Case) Unit: kN m	
3 m-Tall	-7.498
4 m-Tall	-5.461
5 m-Tall	-4.154
6 m-Tall	-3.321
7 m-Tall	-2.813
8 m-Tall	-2.521

<table>
<tr><td rowspan="2">Abutment</td><td colspan="2">Pile Moment (weak-axis) Unit: kN·m</td></tr>
<tr><td>LCB1 (Expansion)</td><td>-7.498E+00</td></tr>
<tr><td>3 m-Tall</td><td colspan="2">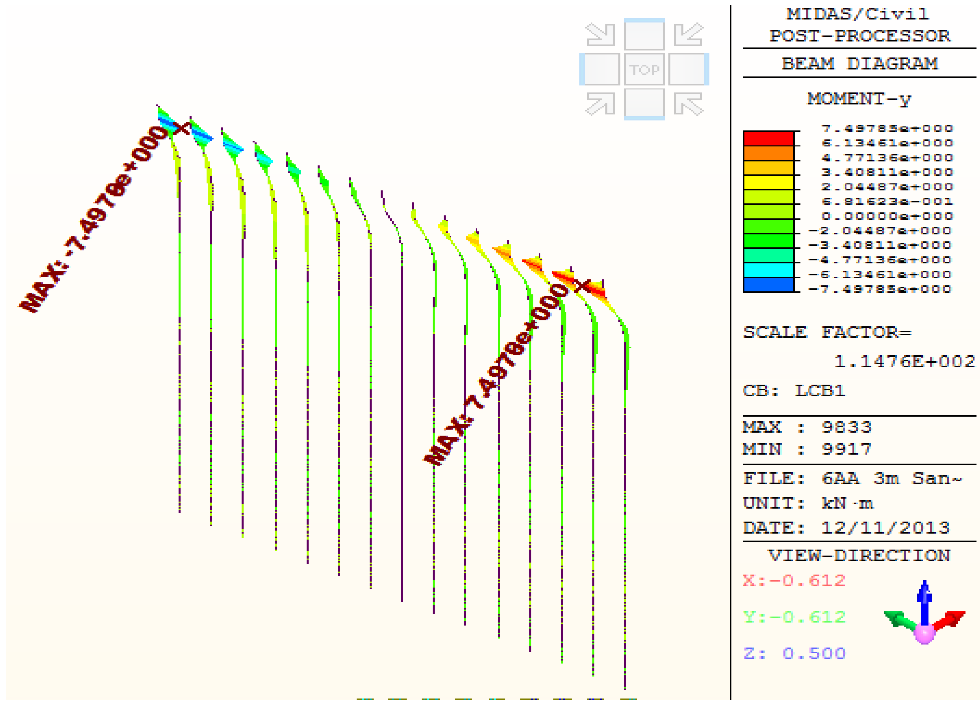
</td></tr>
<tr><td rowspan="2">Abutment</td><td colspan="2">Pile Moment (weak-axis) Unit: kN·m</td></tr>
<tr><td>LCB1 (Expansion)</td><td>-5.461E+00</td></tr>
<tr><td>4 m-Tall</td><td colspan="2">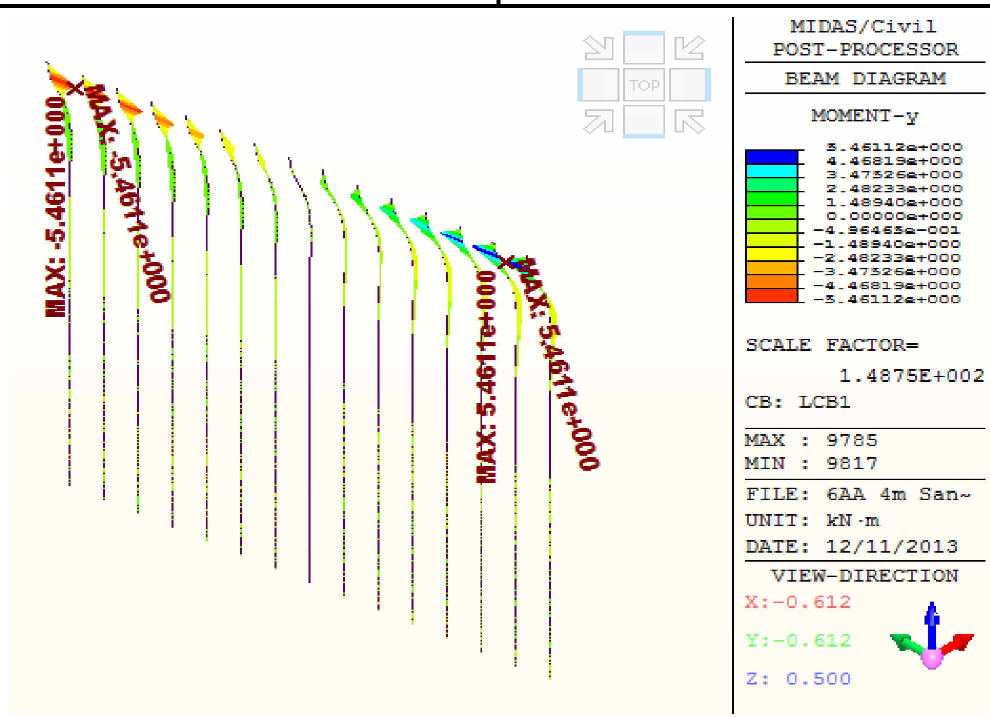
</td></tr>
</table>

<table>
<tr><th rowspan="2">Abutment</th><th colspan="2">Pile Moment (weak-axis) Unit: kN·m</th></tr>
<tr><th>LCB1 (Expansion)</th><th>-4.154E+00</th></tr>
<tr><td>5 m-Tall</td><td colspan="2">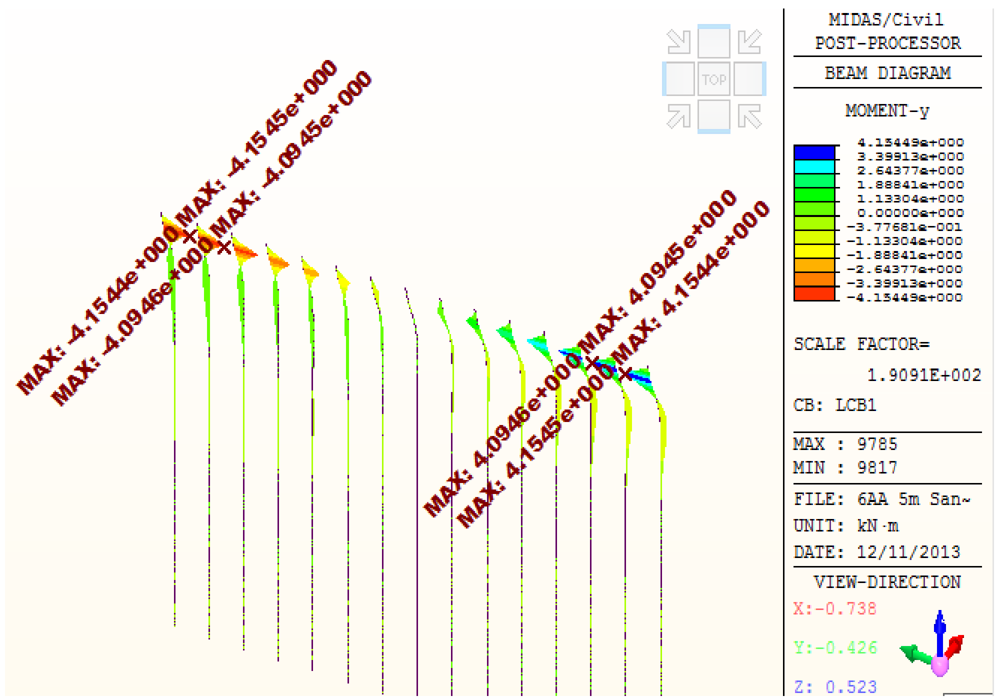
</td></tr>
<tr><th rowspan="2">Abutment</th><th colspan="2">Pile Moment (weak-axis) Unit: kN·m</th></tr>
<tr><th>LCB1 (Expansion)</th><th>-3.321E+00</th></tr>
<tr><td>6 m-Tall</td><td colspan="2">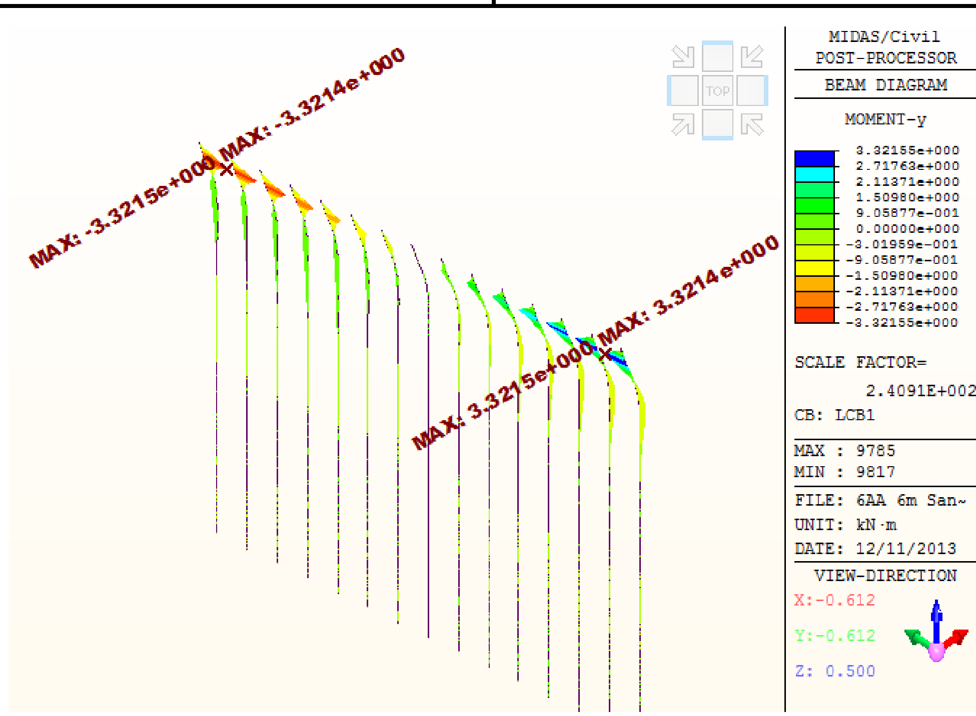
</td></tr>
</table>

<table>
<tr><td rowspan="2">Abutment</td><td colspan="2">Pile Moment (weak-axis) Unit: kN·m</td></tr>
<tr><td>LCB1 (Expansion)</td><td>-2.813E+00</td></tr>
<tr><td>7 m-Tall</td><td colspan="2">
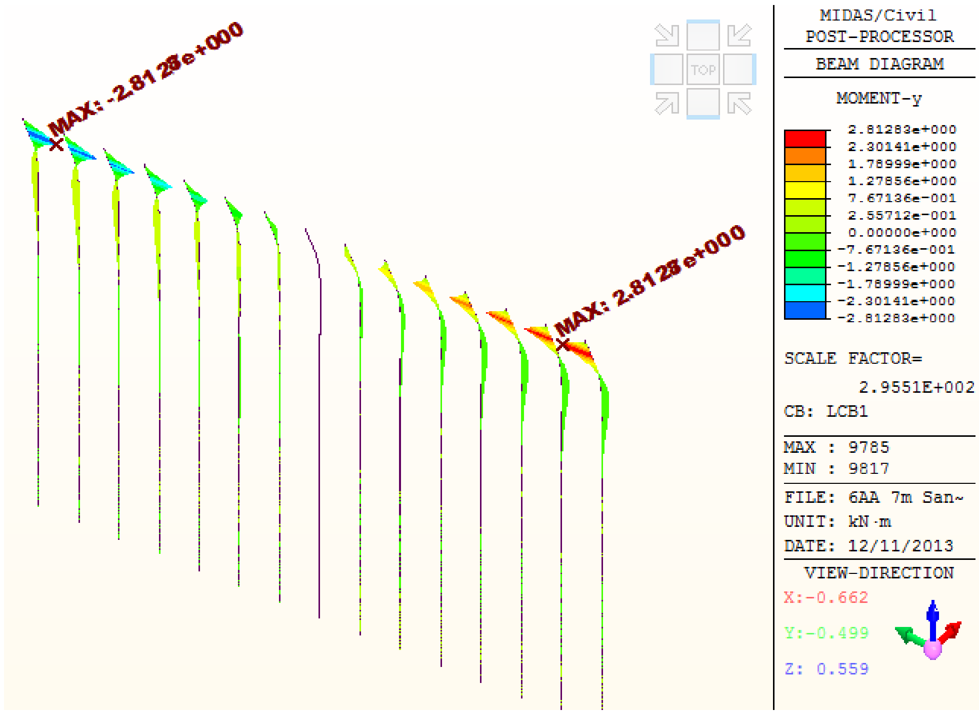

</td></tr>
<tr><td rowspan="2">Abutment</td><td colspan="2">Pile Moment (weak-axis) Unit: kN·m</td></tr>
<tr><td>LCB1 (Expansion)</td><td>-2.521E+00</td></tr>
<tr><td>8 m-Tall</td><td colspan="2">
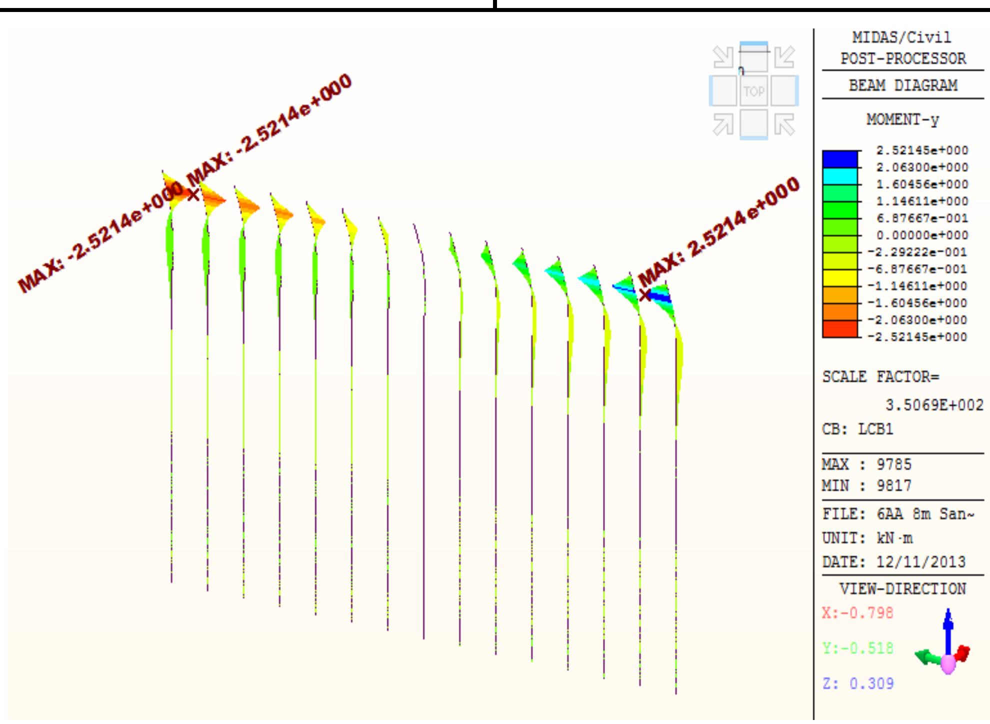

</td></tr>
</table>

1. The Effects depending on Abutment Height

1.12. Pile Moment (Pile Orientation: Weak-Axis, Contraction Case)

Pile Moment (weak-axis) LCB2 (Contraction Case) Unit: kN m	
3 m-Tall	-7.575
4 m-Tall	-5.631
5 m-Tall	-4.319
6 m-Tall	-3.383
7 m-Tall	-2.692
8 m-Tall	-2.16

<table>
<tr><th rowspan="2">Abutment</th><th colspan="2">Pile Moment (weak-axis) Unit: kN·m</th></tr>
<tr><th>LCB2 (Contraction)</th><th>-7.575E+00</th></tr>
<tr><td>3 m-Tall</td><td colspan="2">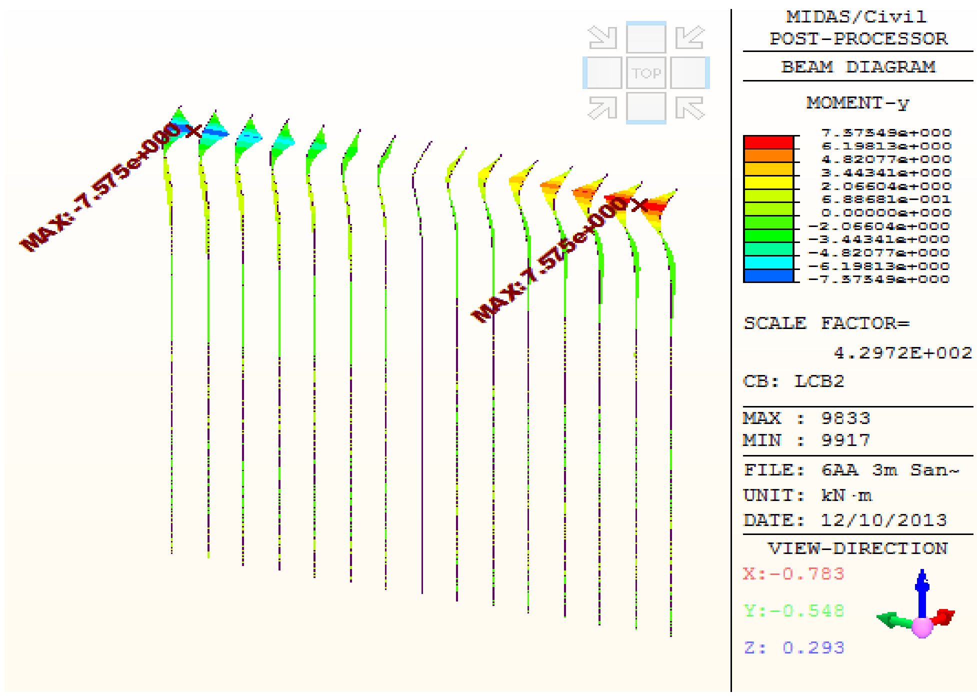
</td></tr>
<tr><th rowspan="2">Abutment</th><th colspan="2">Pile Moment (weak-axis) Unit: kN·m</th></tr>
<tr><th>LCB2 (Contraction)</th><th>-5.631E+00</th></tr>
<tr><td>4 m-Tall</td><td colspan="2">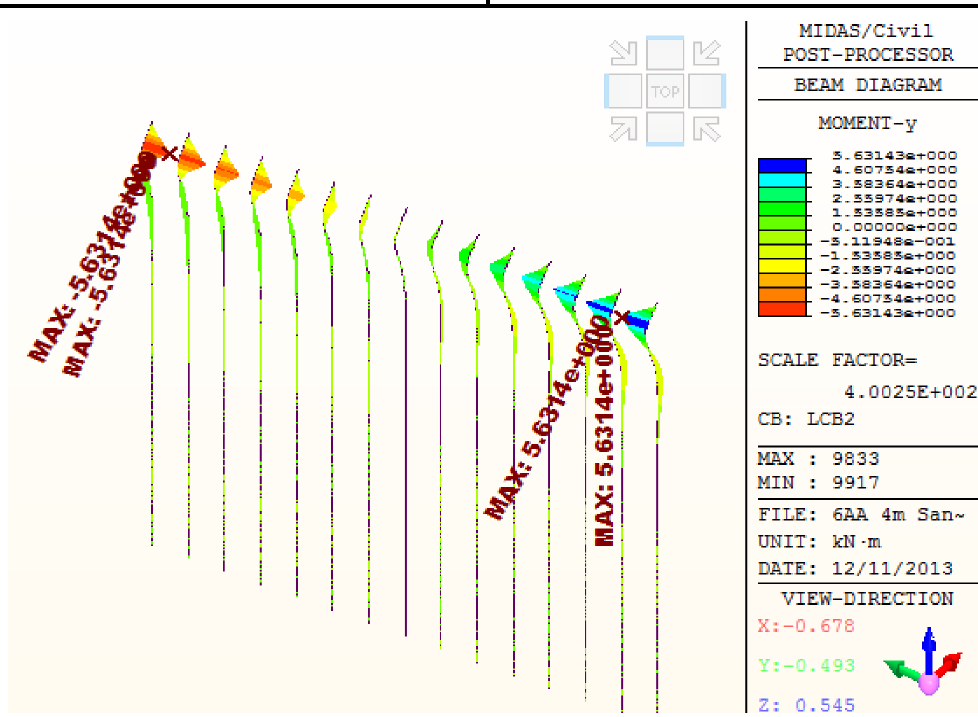
</td></tr>
</table>

<table>
<tr><th rowspan="2">Abutment</th><th colspan="2">Pile Moment (weak-axis) Unit: kN·m</th></tr>
<tr><th>LCB2 (Contraction)</th><th>-4.319E+00</th></tr>
<tr><td>5 m-Tall</td><td colspan="2">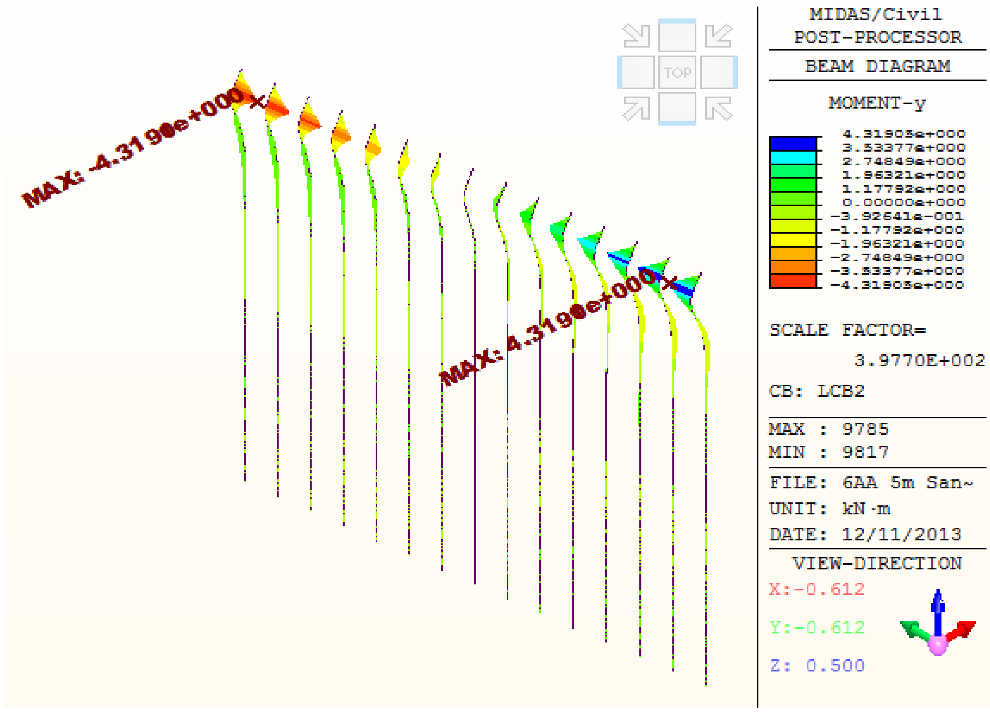
</td></tr>
<tr><th rowspan="2">Abutment</th><th colspan="2">Pile Moment (weak-axis) Unit: kN·m</th></tr>
<tr><th>LCB2 (Contraction)</th><th>-3.383E+00</th></tr>
<tr><td>6 m-Tall</td><td colspan="2">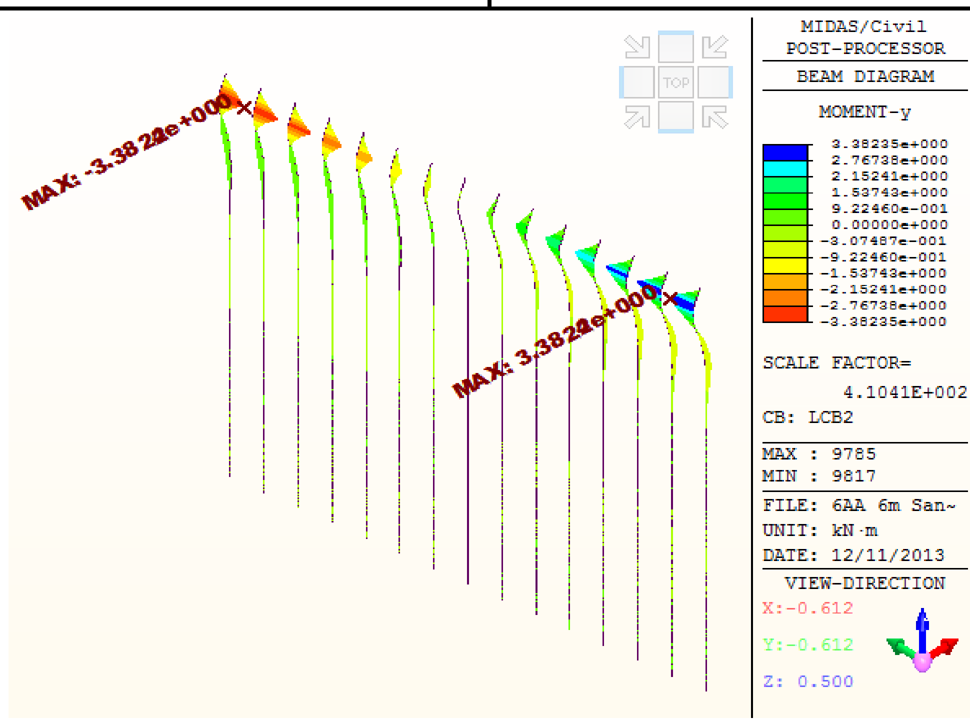
</td></tr>
</table>

<table>
<tr><td rowspan="2">Abutment</td><td colspan="2">Pile Moment (weak-axis) Unit: kN·m</td></tr>
<tr><td>LCB2 (Contraction)</td><td>-2.692E+00</td></tr>
<tr><td>7 m-Tall</td><td colspan="2">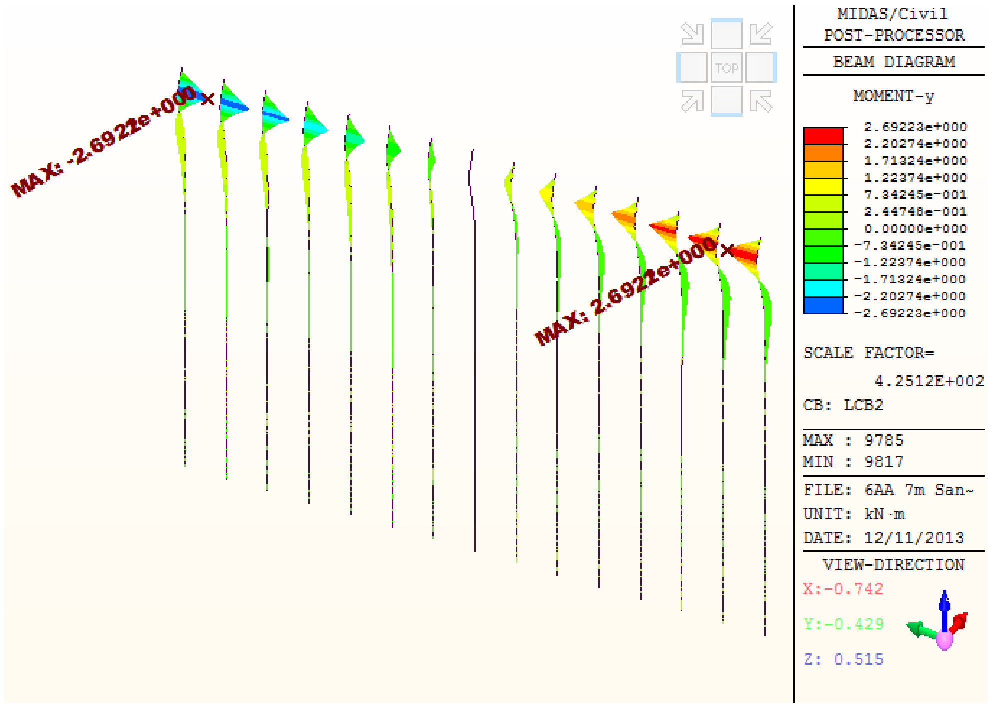
</td></tr>
</table>

<table>
<tr><td rowspan="2">Abutment</td><td colspan="2">Pile Moment (weak-axis) Unit: kN·m</td></tr>
<tr><td>LCB2 (Contraction)</td><td>-2.160E+00</td></tr>
<tr><td>8 m-Tall</td><td colspan="2">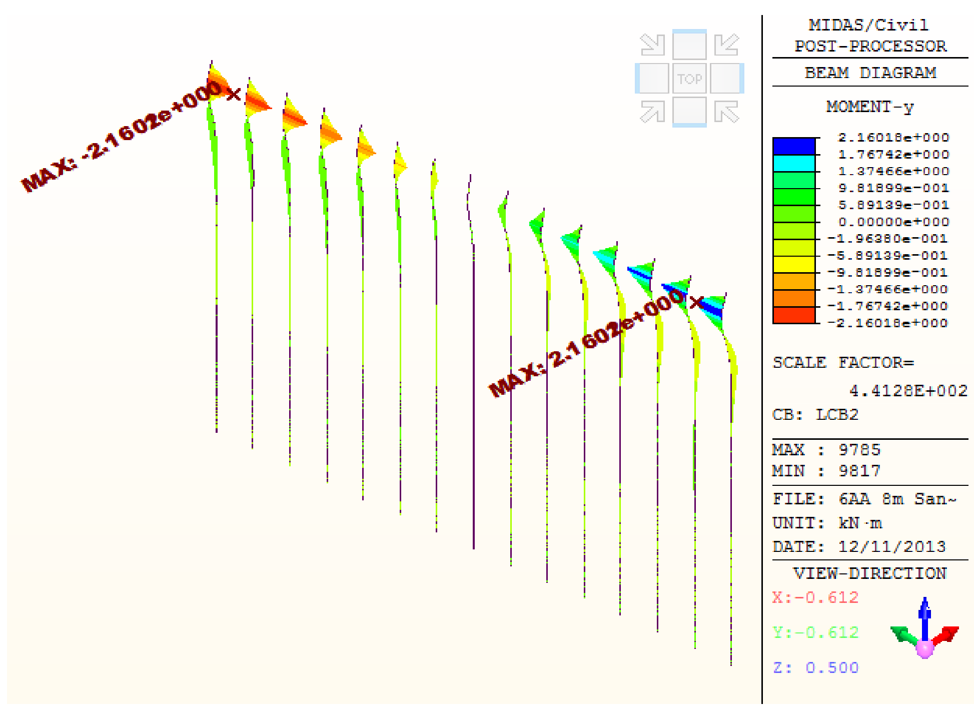
</td></tr>
</table>

1. The Effects depending on Abutment Height

1.13. Pile Stress (Pile Orientation: Strong-Axis, Expansion Case)

Pile Stress (strong-axis) LCB1 (Expansion Case) Unit: kN/m^2	
3 m-Tall	-178800
4 m-Tall	-120800
5 m-Tall	-81580
6 m-Tall	-55700
7 m-Tall	-56770
8 m-Tall	-64180

<table>
<tr><td rowspan="2">Abutment</td><td colspan="2">Pile Stress (strong-axis) Unit: kN/m²</td></tr>
<tr><td>LCB1 (Expansion)</td><td>-1.788E+05</td></tr>
<tr><td>3 m-Tall</td><td colspan="2">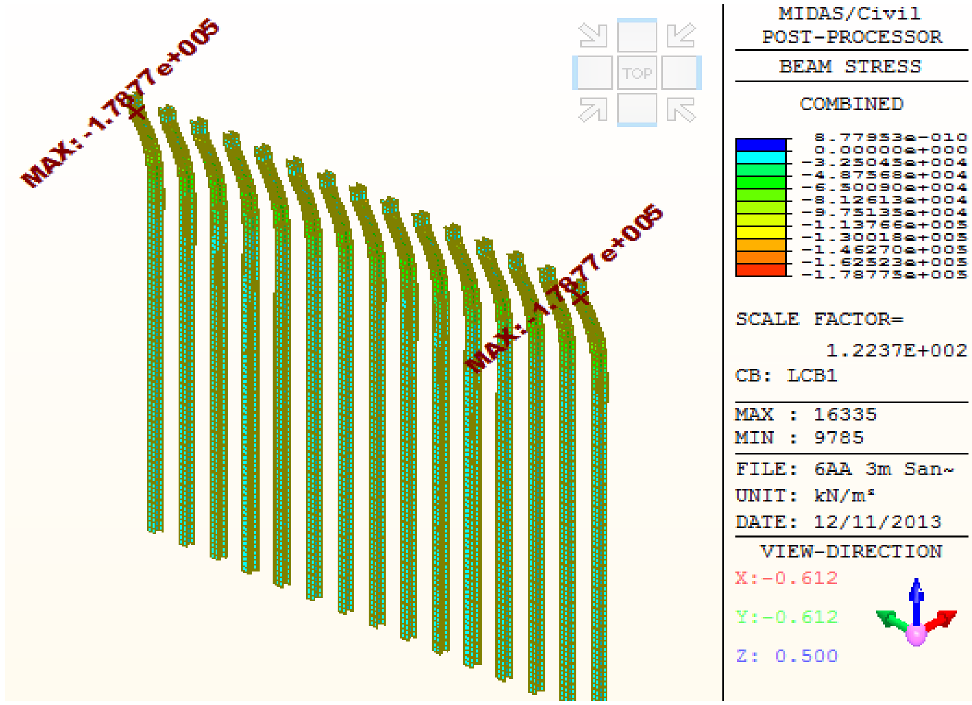
</td></tr>
<tr><td rowspan="2">Abutment</td><td colspan="2">Pile Stress (strong-axis) Unit: kN/m²</td></tr>
<tr><td>LCB1 (Expansion)</td><td>-1.208E+05</td></tr>
<tr><td>4 m-Tall</td><td colspan="2">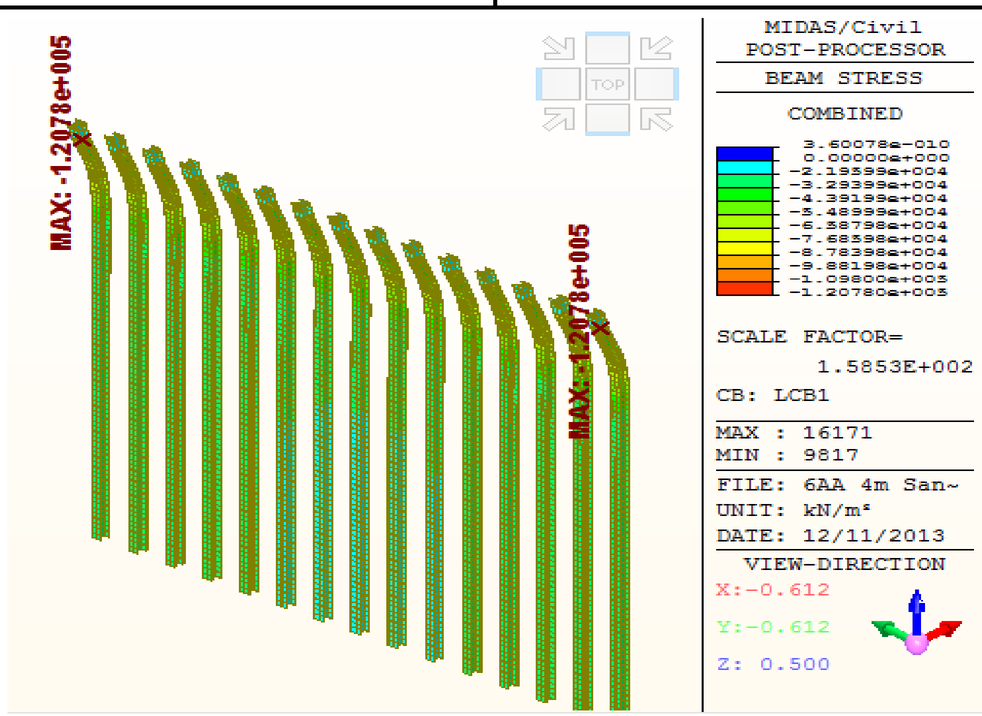
</td></tr>
</table>

<table>
<tr><td rowspan="2">Abutment</td><td colspan="2">Pile Stress (strong-axis) Unit: kN/m^2</td></tr>
<tr><td>LCB1 (Expansion)</td><td>-8.158E+04</td></tr>
<tr><td>5 m-Tall</td><td colspan="2">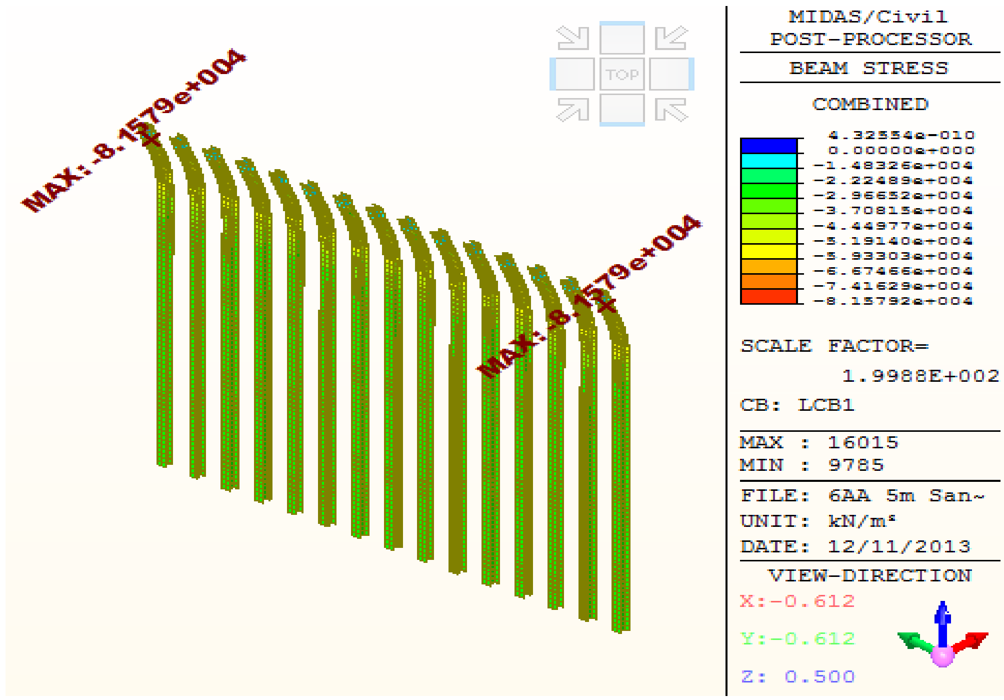
</td></tr>
<tr><td rowspan="2">Abutment</td><td colspan="2">Pile Stress (strong-axis) Unit: kN/m^2</td></tr>
<tr><td>LCB1 (Expansion)</td><td>-5.570E+04</td></tr>
<tr><td>6 m-Tall</td><td colspan="2">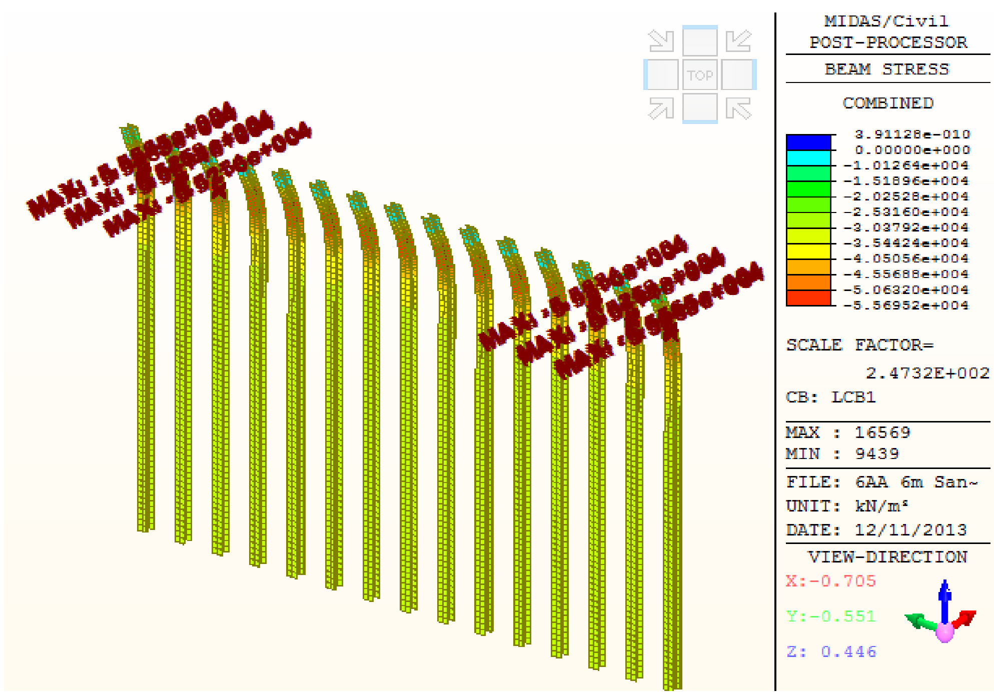
</td></tr>
</table>

Abutment	Pile Stress (strong-axis) Unit: kN/m^2	
	LCB1 (Expansion)	-5.677E+04
7 m-Tall	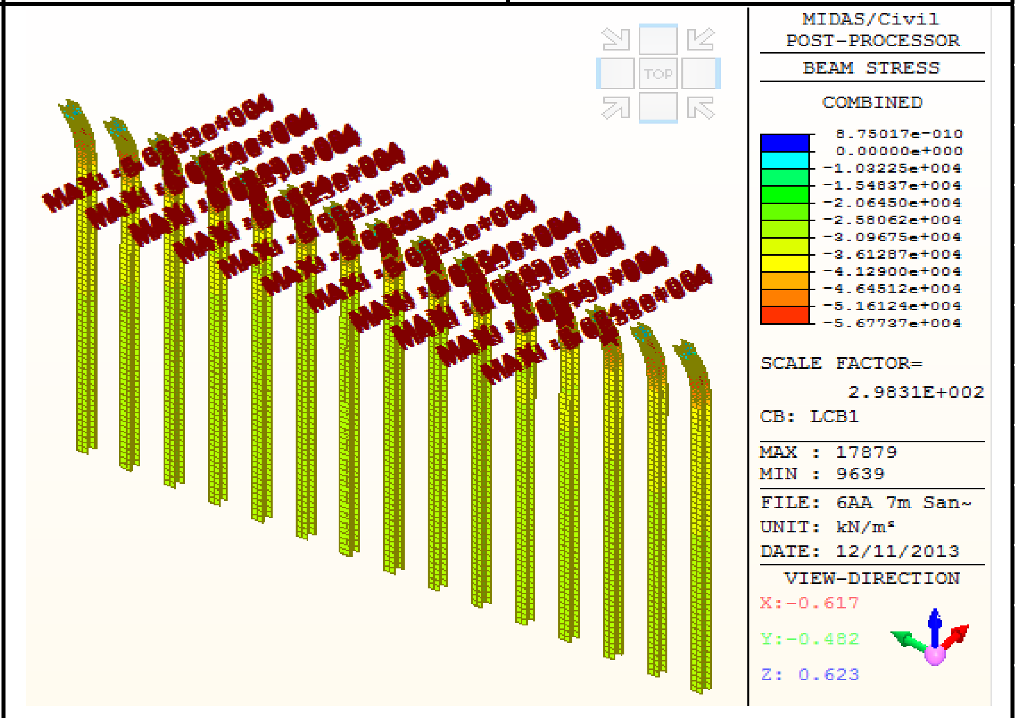	

Abutment	Pile Stress (strong-axis) Unit: kN/m^2	
	LCB1 (Expansion)	-6.418E+04
8 m-Tall	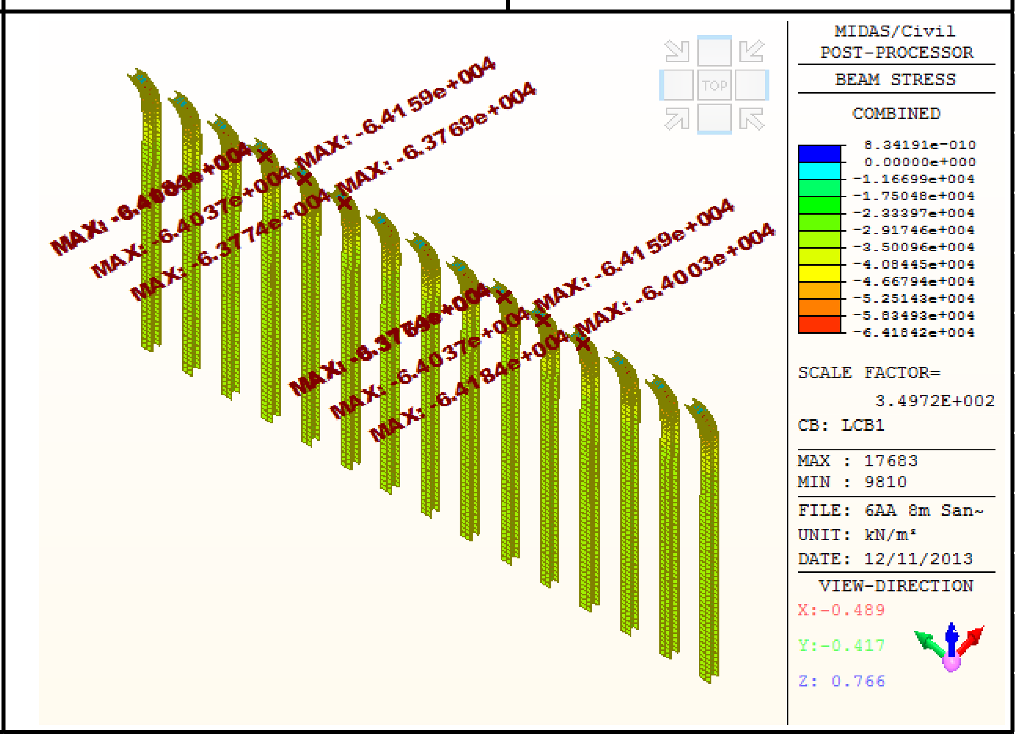	

1. The Effects depending on Abutment Height

1.14. Pile Stress (Pile Orientation: Strong-Axis, Contraction Case)

Pile Stress (strong-axis) LCB2 (Contraction Case) Unit: kN/m^2	
3 m-Tall	-129400
4 m-Tall	-126300
5 m-Tall	-116800
6 m-Tall	-105900
7 m-Tall	-95620
8 m-Tall	-86340

<table>
<tr><td rowspan="2">Abutment</td><td colspan="2">Pile Stress (strong-axis) Unit: kN/m^2</td></tr>
<tr><td>LCB2 (Contraction)</td><td>-1.294E+05</td></tr>
<tr><td>3 m-Tall</td><td colspan="2">
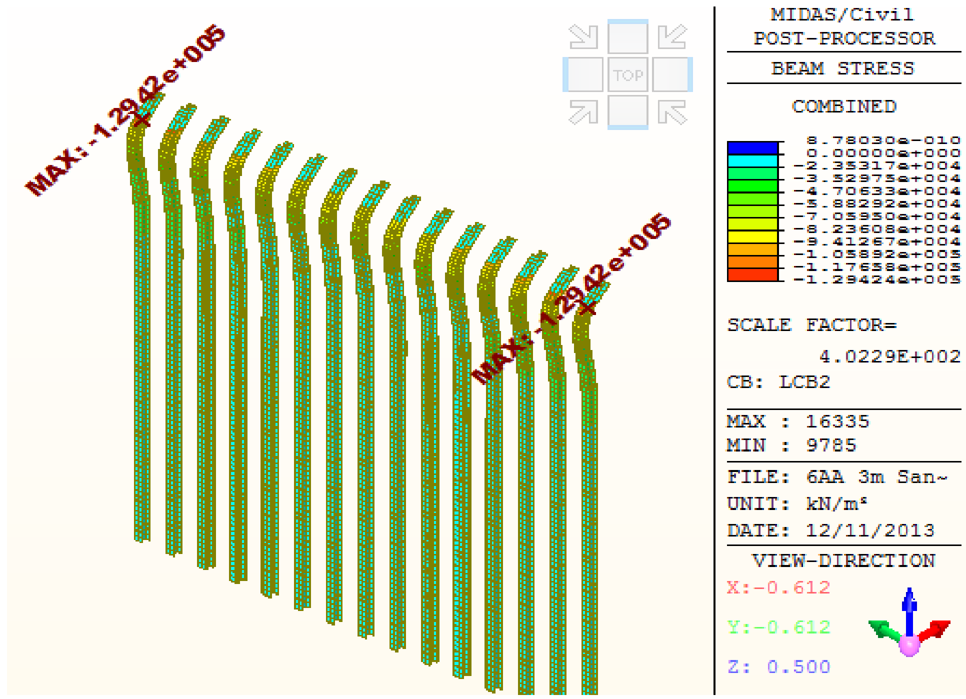

</td></tr>
<tr><td rowspan="2">Abutment</td><td colspan="2">Pile Stress (strong-axis) Unit: kN/m^2</td></tr>
<tr><td>LCB2 (Contraction)</td><td>-1.263E+05</td></tr>
<tr><td>4 m-Tall</td><td colspan="2">
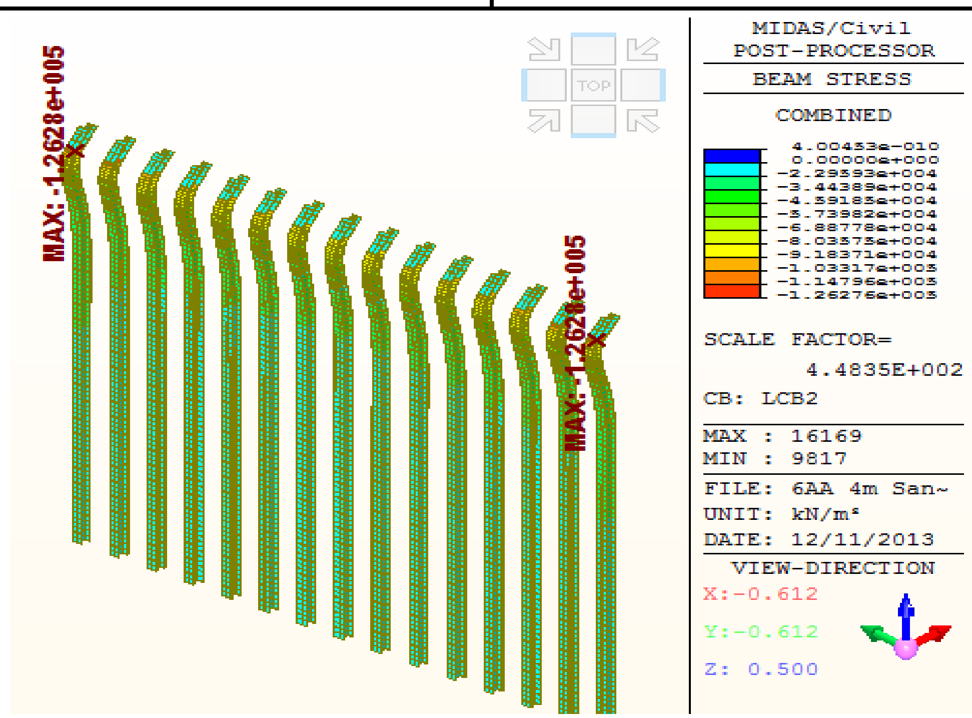

</td></tr>
</table>

<table>
<tr><td rowspan="2">Abutment</td><td colspan="2">Pile Stress (strong-axis) Unit: kN/m^2</td></tr>
<tr><td>LCB2 (Contraction)</td><td>-1.168E+05</td></tr>
<tr><td>5 m-Tall</td><td colspan="2">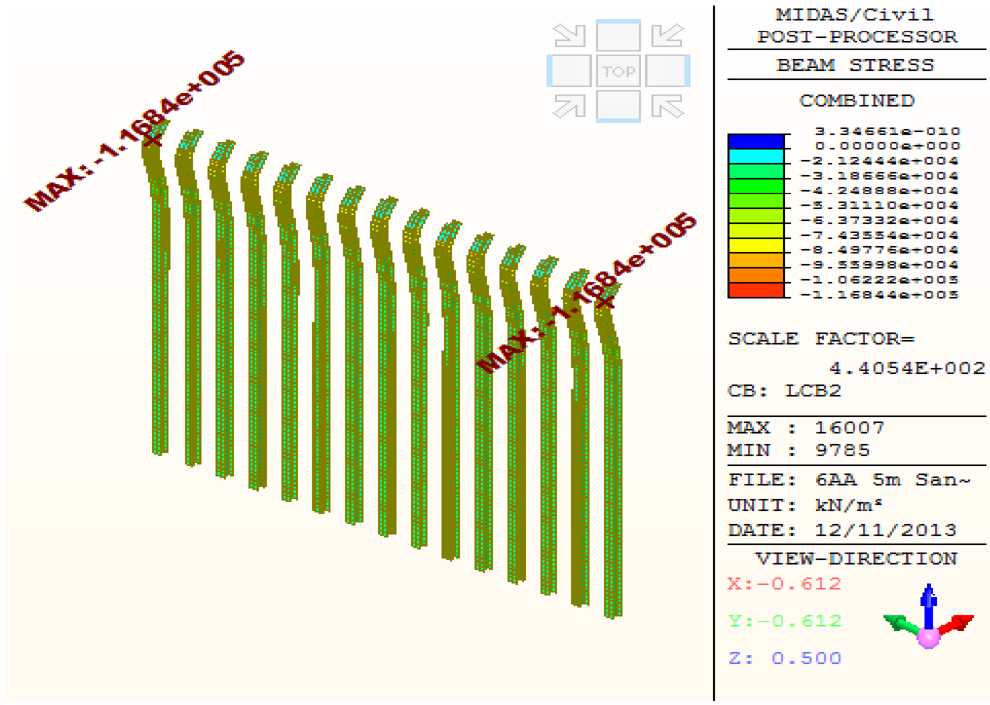
</td></tr>
<tr><td rowspan="2">Abutment</td><td colspan="2">Pile Stress (strong-axis) Unit: kN/m^2</td></tr>
<tr><td>LCB2 (Contraction)</td><td>-1.059E+05</td></tr>
<tr><td>6 m-Tall</td><td colspan="2">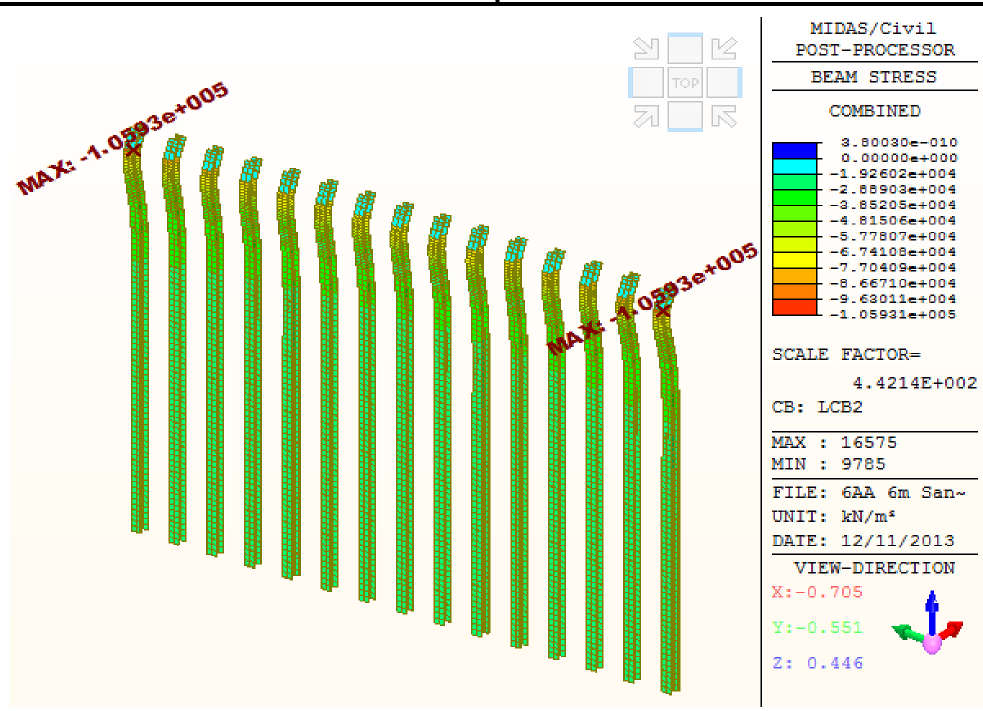
</td></tr>
</table>

Abutment	Pile Stress (strong-axis) Unit: kN/m^2	
	LCB2 (Contraction)	-9.562E+04
7 m-Tall	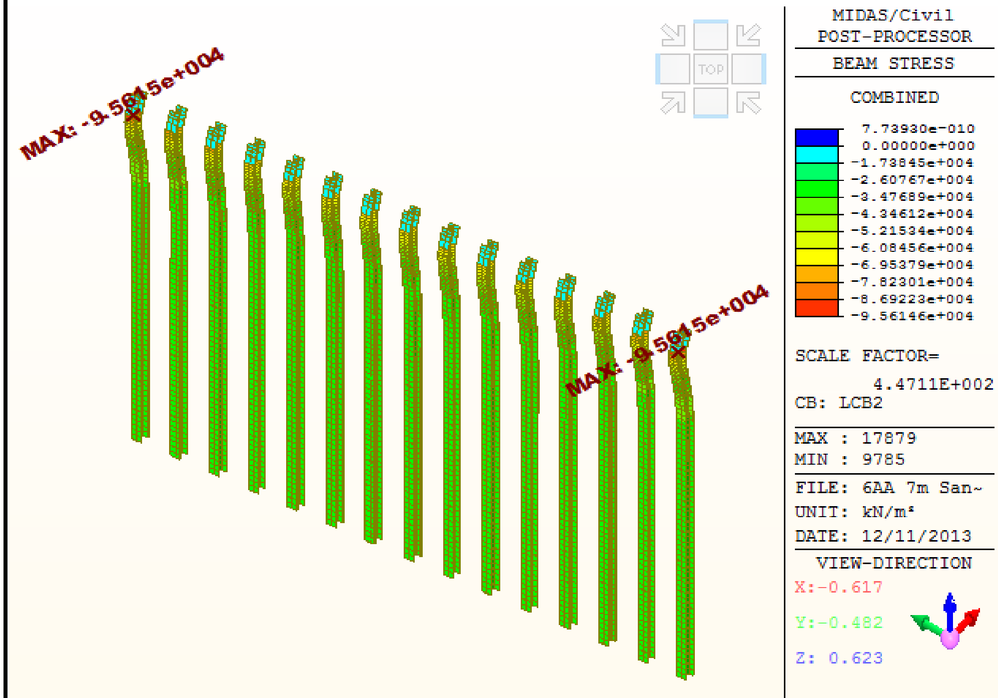	

Abutment	Pile Stress (strong-axis) Unit: kN/m^2	
	LCB2 (Contraction)	-8.634E+04
8 m-Tall	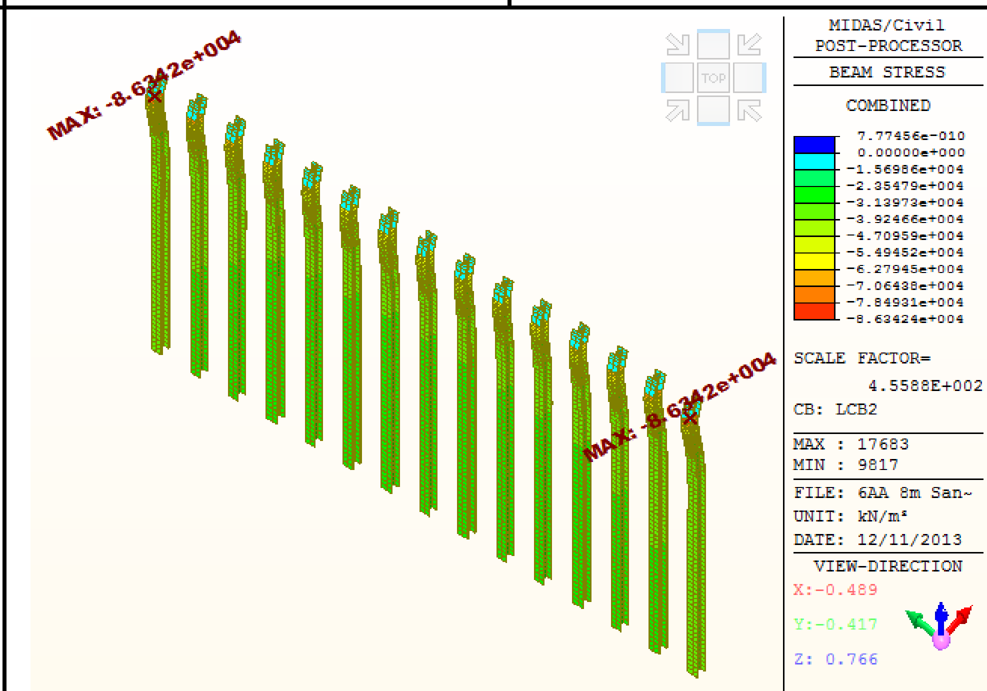	

1. The Effects depending on Abutment Height

1.15. Pile Stress (Pile Orientation: Weak-Axis, Expansion Case)

Pile Stress (weak-axis) LCB1 (Expansion Case) Unit: kN/m^2	
3 m-Tall	-382200
4 m-Tall	-263600
5 m-Tall	-176400
6 m-Tall	-111800
7 m-Tall	-64720
8 m-Tall	-70940

<table>
<tr><th rowspan="2">Abutment</th><th colspan="2">Pile Stress (weak-axis) Unit: kN/m^2</th></tr>
<tr><th>LCB1 (Expansion)</th><th>-3.822E+05</th></tr>
<tr><td>3 m-Tall</td><td colspan="2">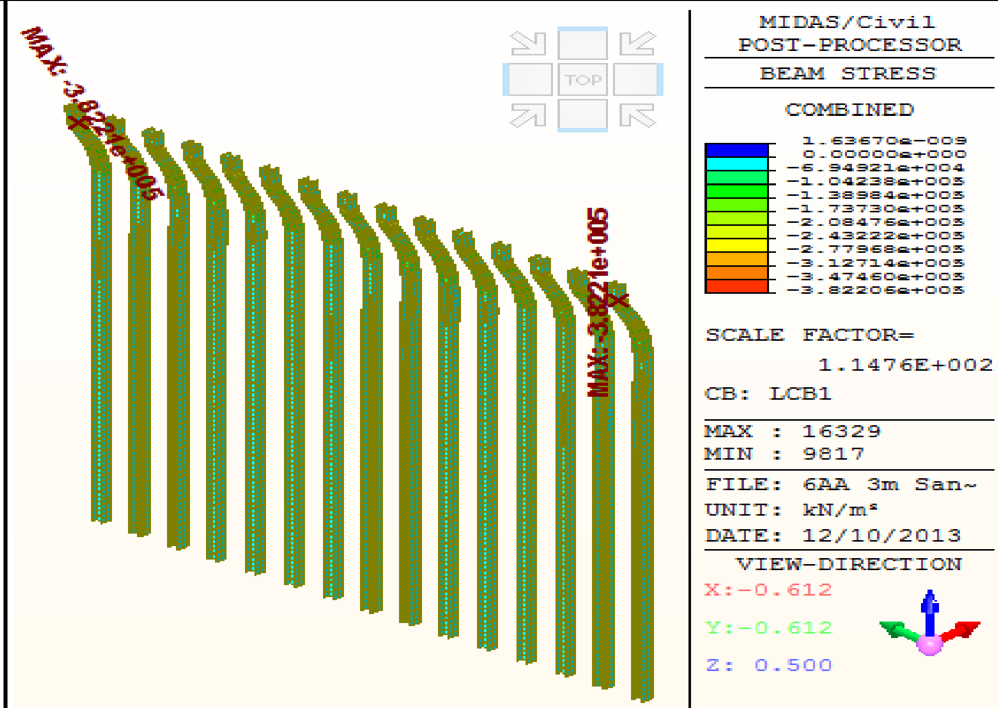
</td></tr>
</table>

<table>
<tr><th rowspan="2">Abutment</th><th colspan="2">Pile Stress (weak-axis) Unit: kN/m^2</th></tr>
<tr><th>LCB1 (Expansion)</th><th>-2.636E+05</th></tr>
<tr><td>4 m-Tall</td><td colspan="2">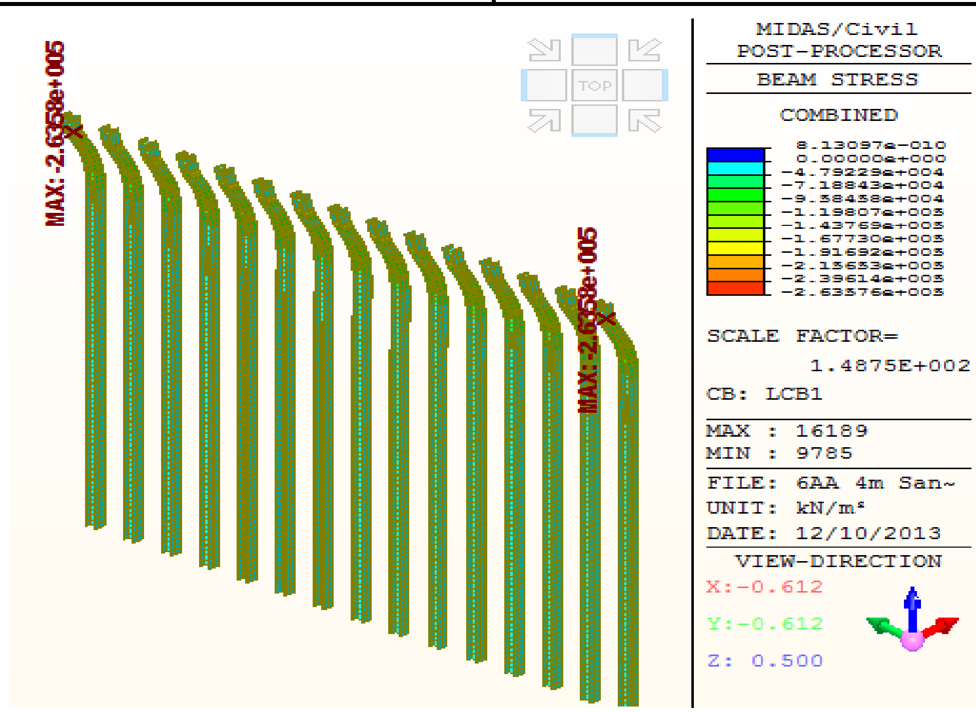
</td></tr>
</table>

<table>
<tr><td rowspan="2">Abutment</td><td colspan="2">Pile Stress (weak-axis)   Unit: kN/m^2</td></tr>
<tr><td>LCB1 (Expansion)</td><td>-1.764E+05</td></tr>
<tr><td>5 m-Tall</td><td colspan="2">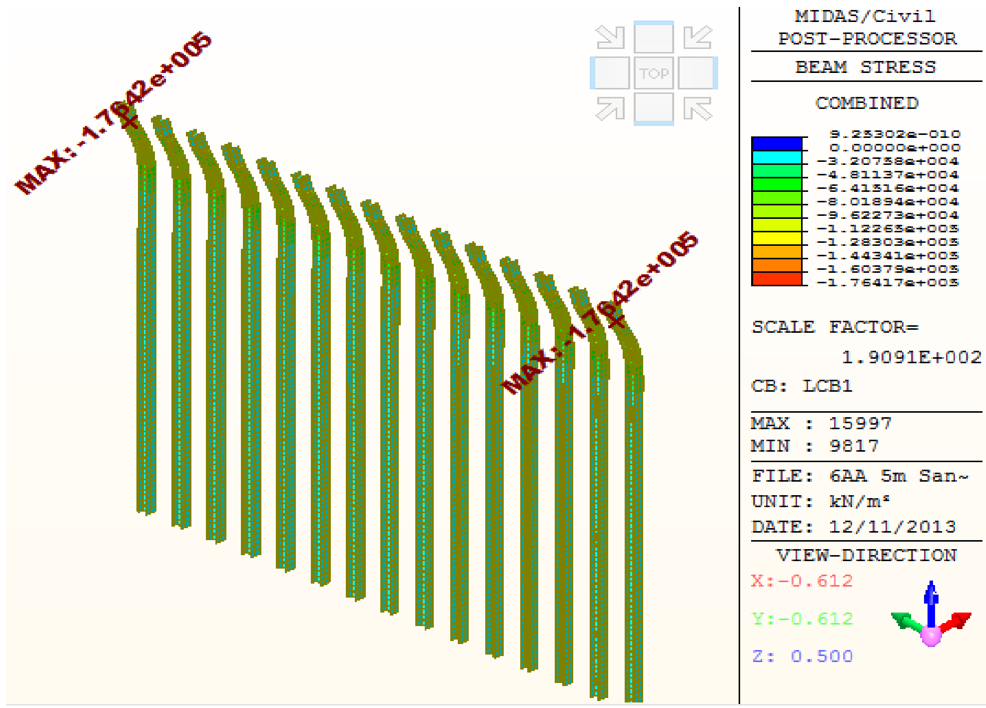
</td></tr>
<tr><td rowspan="2">Abutment</td><td colspan="2">Pile Stress (weak-axis)   Unit: kN/m^2</td></tr>
<tr><td>LCB1 (Expansion)</td><td>-1.118E+05</td></tr>
<tr><td>6 m-Tall</td><td colspan="2">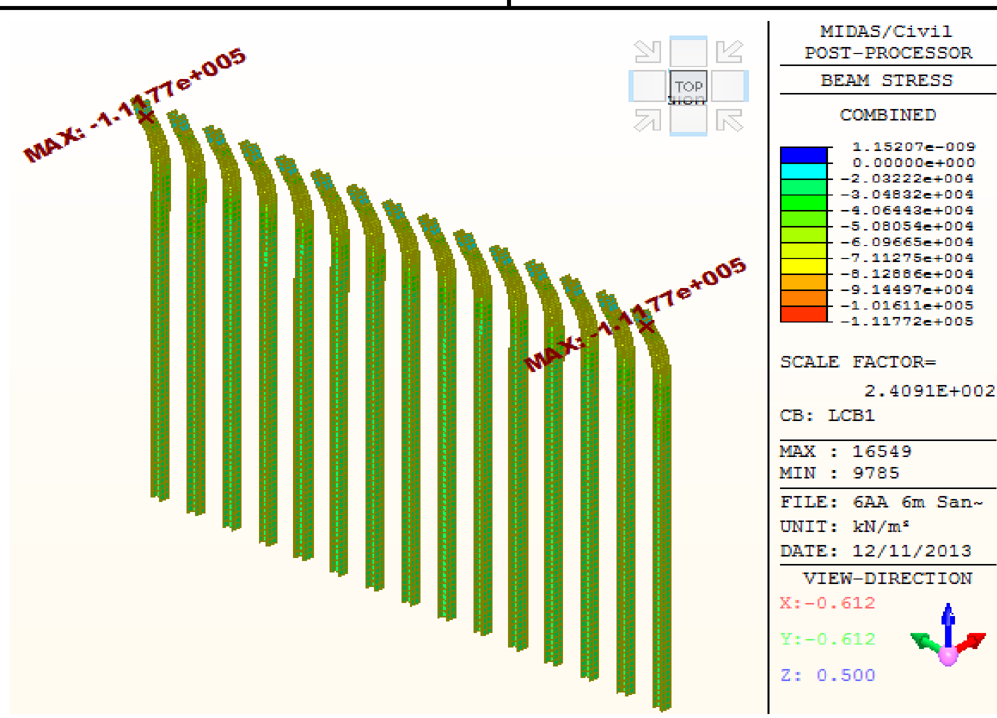
</td></tr>
</table>

<table>
<tr><td rowspan="2">Abutment</td><td colspan="2">Pile Stress (weak-axis) Unit: kN/m^2</td></tr>
<tr><td>LCB1 (Expansion)</td><td>-6.472E+04</td></tr>
<tr><td>7 m-Tall</td><td colspan="2">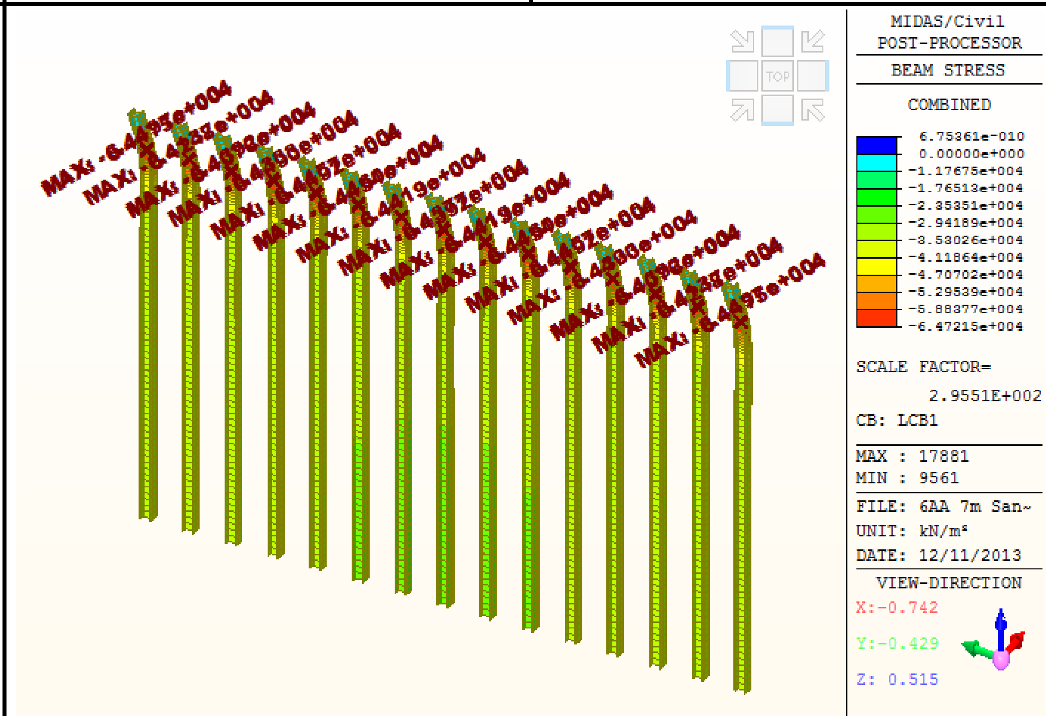
</td></tr>
<tr><td rowspan="2">Abutment</td><td colspan="2">Pile Stress (weak-axis) Unit: kN/m^2</td></tr>
<tr><td>LCB1 (Expansion)</td><td>-7.094E+04</td></tr>
<tr><td>8 m-Tall</td><td colspan="2">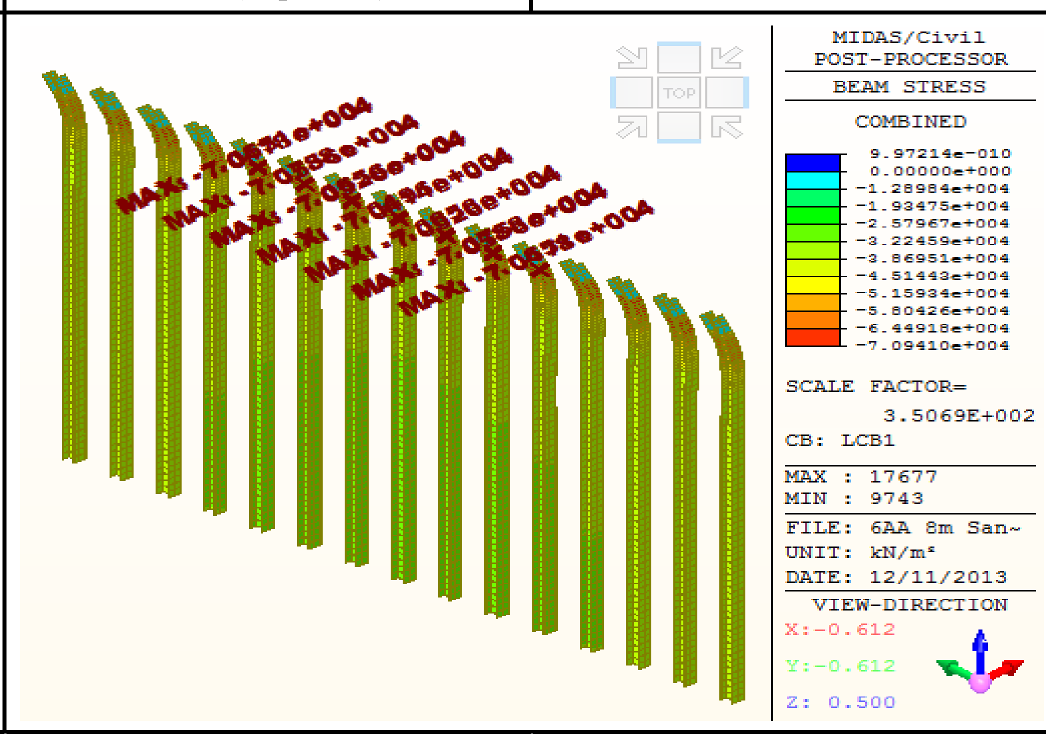
</td></tr>
</table>

1. The Effects depending on Abutment Height

1.16. Pile Stress (Pile Orientation: Weak-Axis, Contraction Case)

Pile Stress (weak-axis) LCB2 (Contraction Case) Unit: kN/m^2	
3 m-Tall	-210400
4 m-Tall	-215800
5 m-Tall	-200700
6 m-Tall	-179800
7 m-Tall	-159100
8 m-Tall	-139600

<table>
<tr><td rowspan="2">Abutment</td><td colspan="2">Pile Stress (weak-axis) Unit: kN/m^2</td></tr>
<tr><td>LCB2 (Contraction)</td><td>-2.104E+05</td></tr>
<tr><td>3 m-Tall</td><td colspan="2">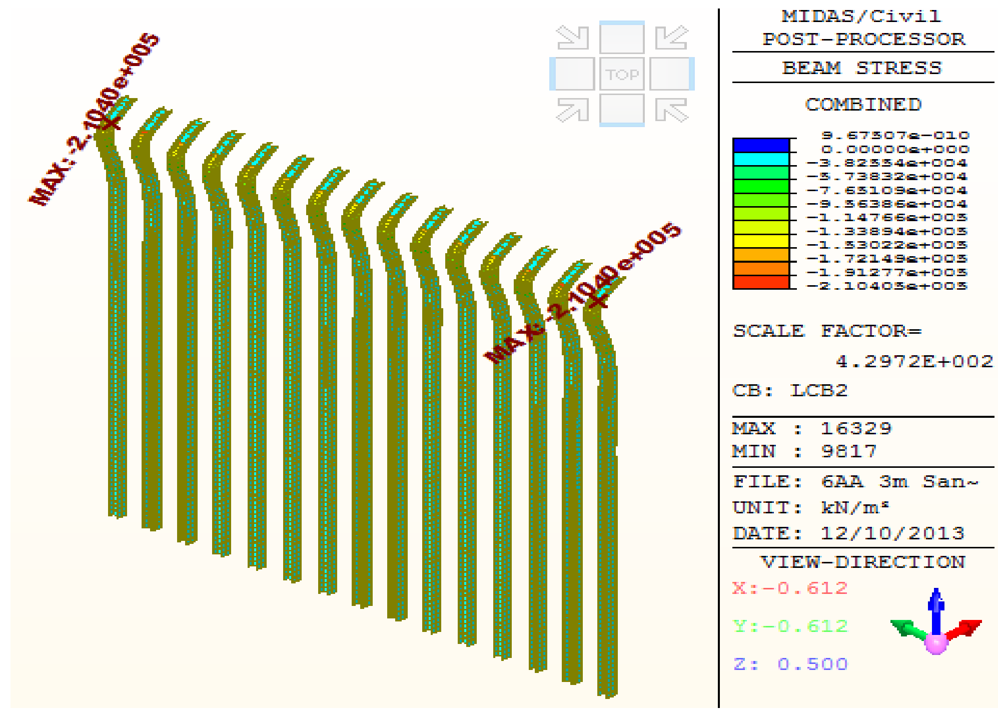
</td></tr>
<tr><td rowspan="2">Abutment</td><td colspan="2">Pile Stress (weak-axis) Unit: kN/m^2</td></tr>
<tr><td>LCB2 (Contraction)</td><td>-2.158E+05</td></tr>
<tr><td>4 m-Tall</td><td colspan="2">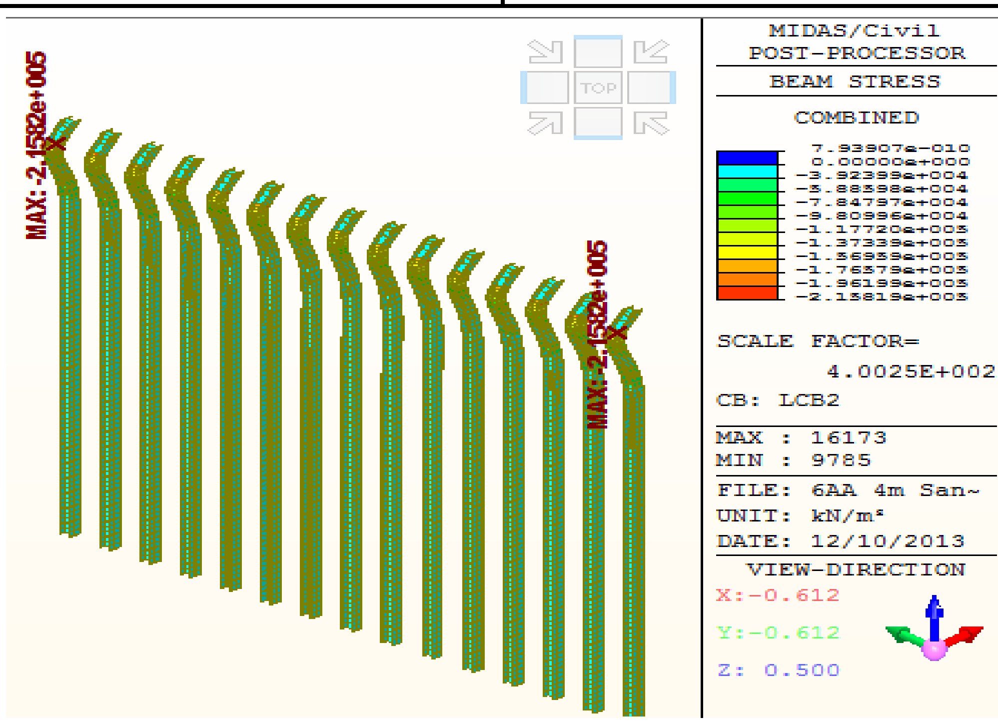
</td></tr>
</table>

<table>
<tr><td rowspan="2">Abutment</td><td colspan="2">Pile Stress (weak-axis) Unit: kN/m^2</td></tr>
<tr><td>LCB2 (Contraction)</td><td>-2.007E+05</td></tr>
<tr><td>5 m-Tall</td><td colspan="2">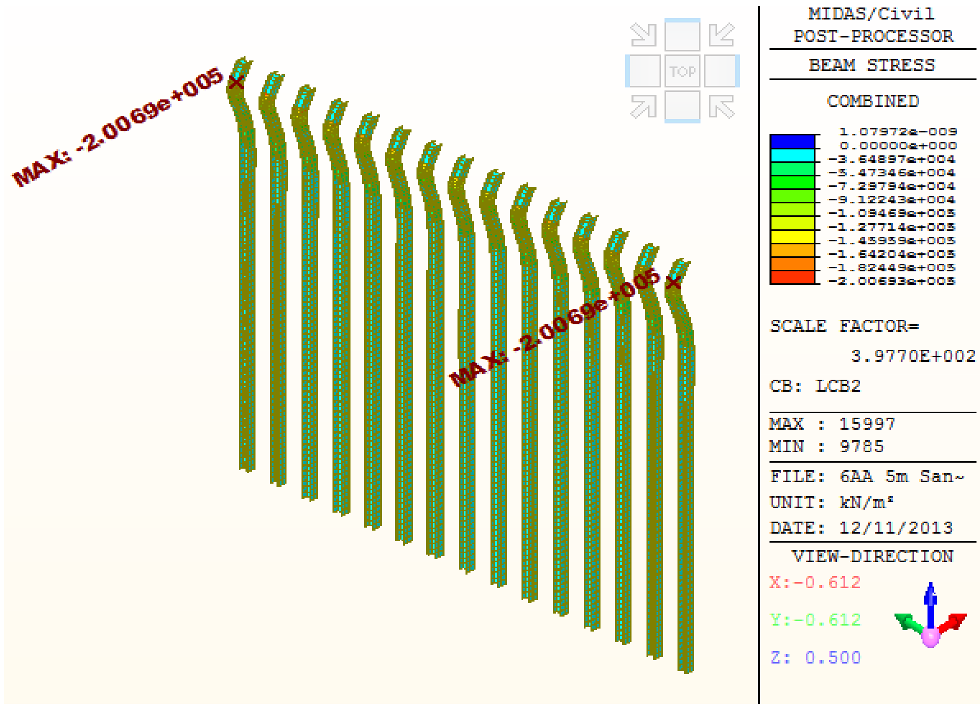
</td></tr>
</table>

<table>
<tr><td rowspan="2">Abutment</td><td colspan="2">Pile Stress (weak-axis) Unit: kN/m^2</td></tr>
<tr><td>LCB2 (Contraction)</td><td>-1.798E+05</td></tr>
<tr><td>6 m-Tall</td><td colspan="2">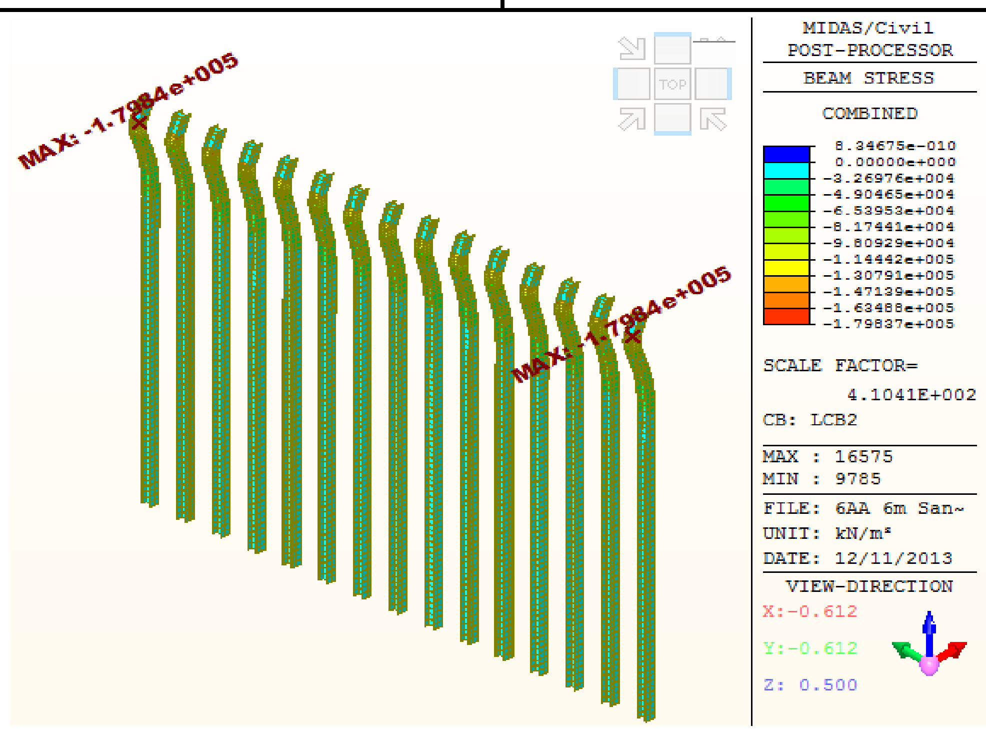
</td></tr>
</table>

Abutment	Pile Stress (weak-axis) Unit: kN/m^2	
	LCB2 (Contraction)	-1.591E+05
7 m-Tall	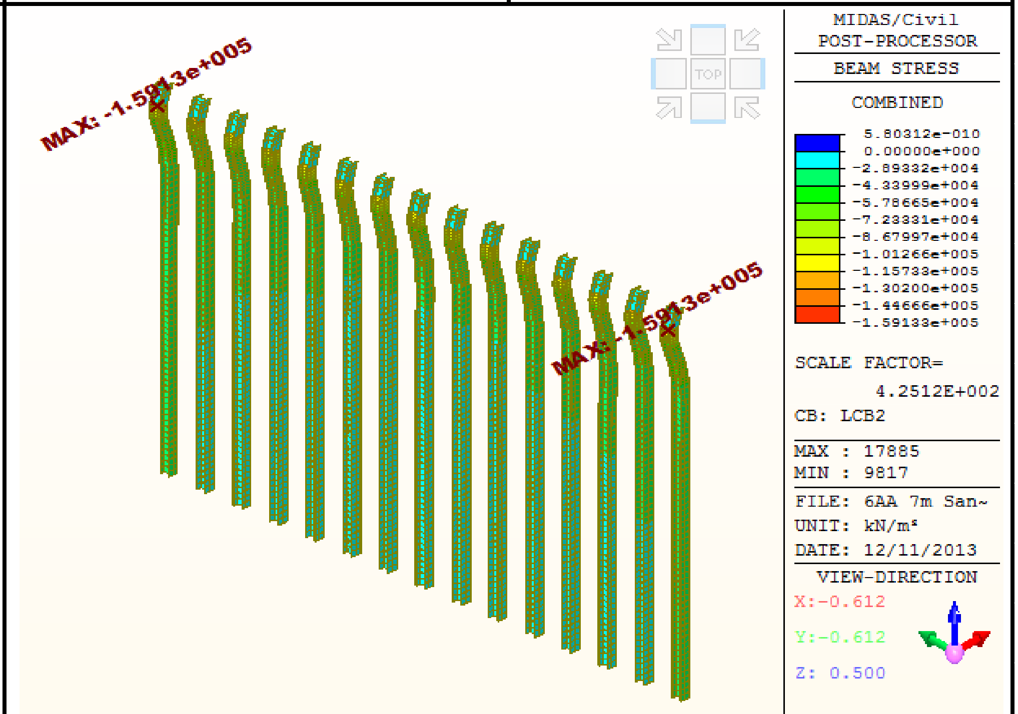	

Abutment	Pile Stress (weak-axis) Unit: kN/m^2	
	LCB2 (Contraction)	-1.396E+05
8 m-Tall	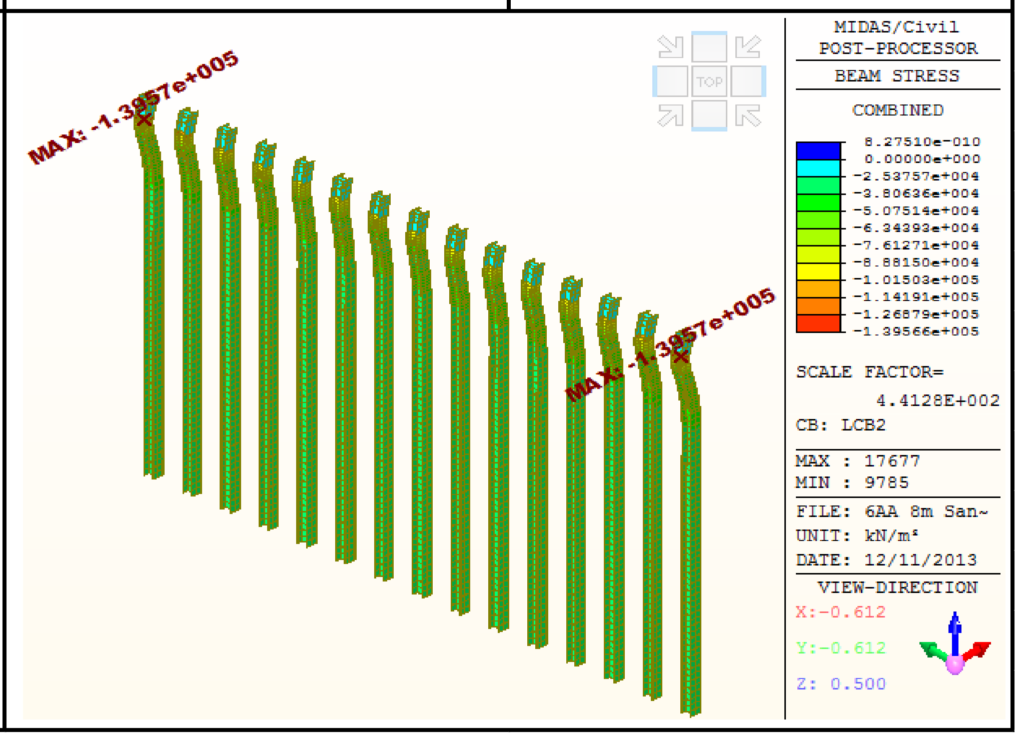	

1. The Effects depending on Abutment Height

1.17. Pile Head Displacement (Pile Orientation: Strong-Axis, Expansion Case)

Pile Head Displacement (strong-axis) LCB1 (Expansion Case) Unit: m	
3 m-Tall	-0.007005
4 m-Tall	-0.005355
5 m-Tall	-0.004057
6 m-Tall	-0.003044
7 m-Tall	-0.00225
8 m-Tall	-0.001641

<table>
<tr><th rowspan="2">Abutment</th><th colspan="2">Pile Head Displacement (strong-axis) Unit: m</th></tr>
<tr><th>LCB1 (Expansion)</th><th>-7.005E-03</th></tr>
<tr><td>3 m-Tall</td><td colspan="2">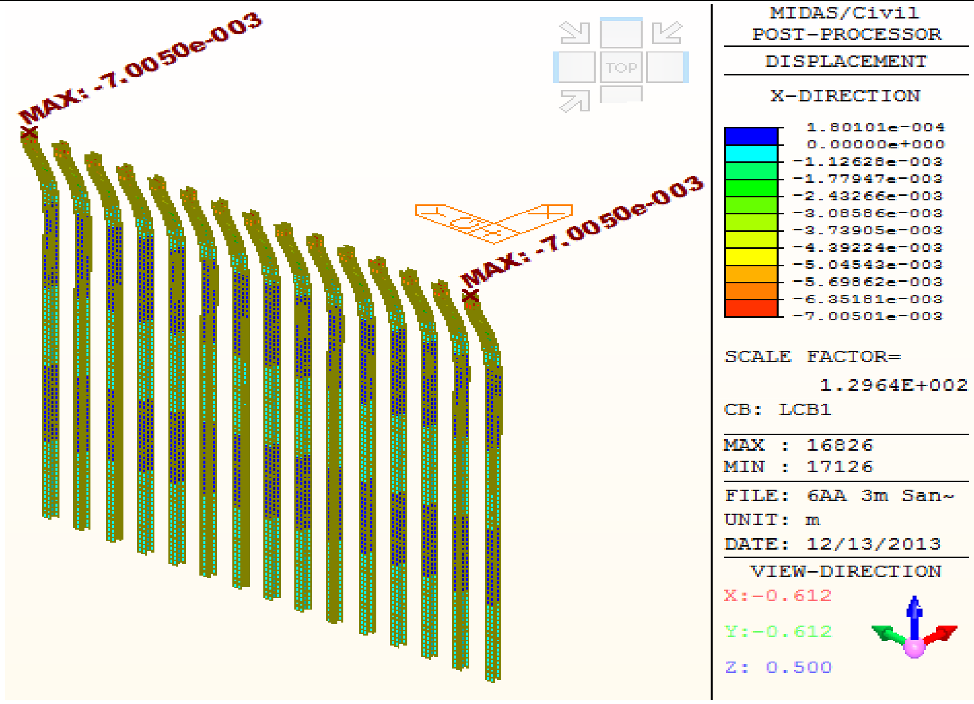
</td></tr>
<tr><th rowspan="2">Abutment</th><th colspan="2">Pile Head Displacement (strong-axis) Unit: m</th></tr>
<tr><th>LCB1 (Expansion)</th><th>-5.355E-03</th></tr>
<tr><td>4 m-Tall</td><td colspan="2">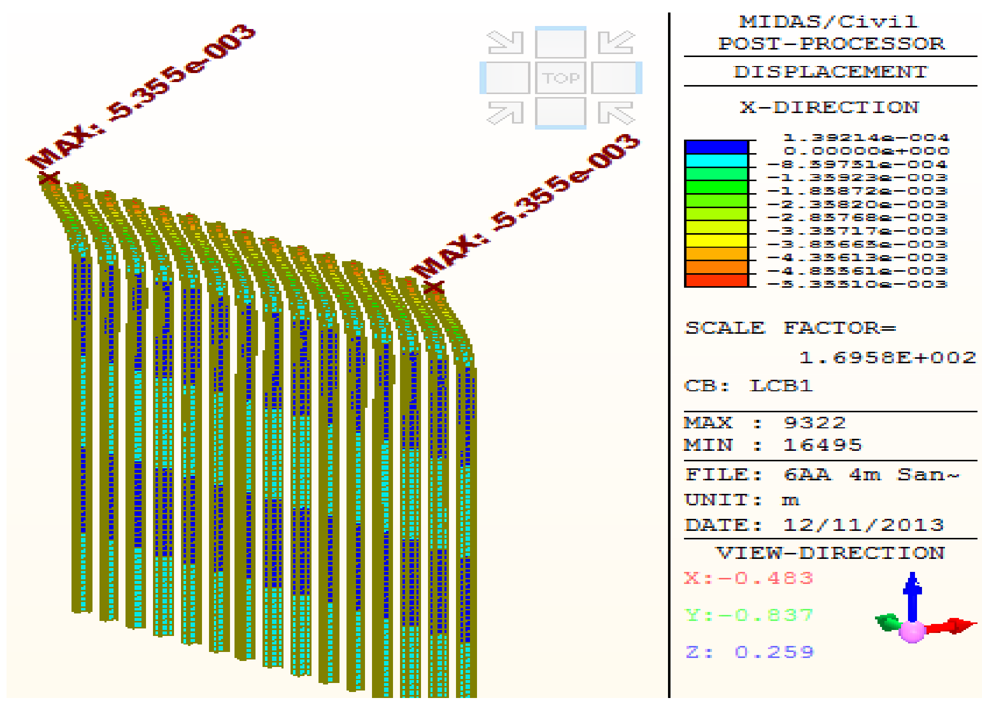
</td></tr>
</table>

<table>
<tr><td rowspan="2">Abutment</td><td colspan="2">Pile Head Displacement (strong-axis) Unit: m</td></tr>
<tr><td>LCB1 (Expansion)</td><td>-4.057E-03</td></tr>
<tr><td>5 m-Tall</td><td colspan="2">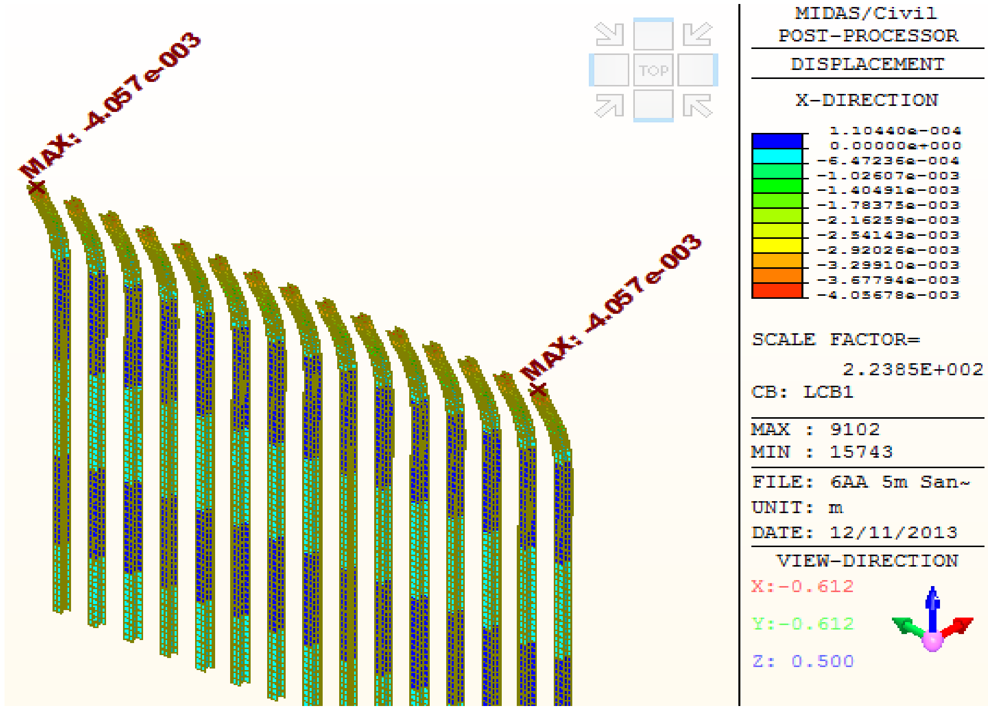
</td></tr>
<tr><td rowspan="2">Abutment</td><td colspan="2">Pile Head Displacement (strong-axis) Unit: m</td></tr>
<tr><td>LCB1 (Expansion)</td><td>-3.044E-03</td></tr>
<tr><td>6 m-Tall</td><td colspan="2">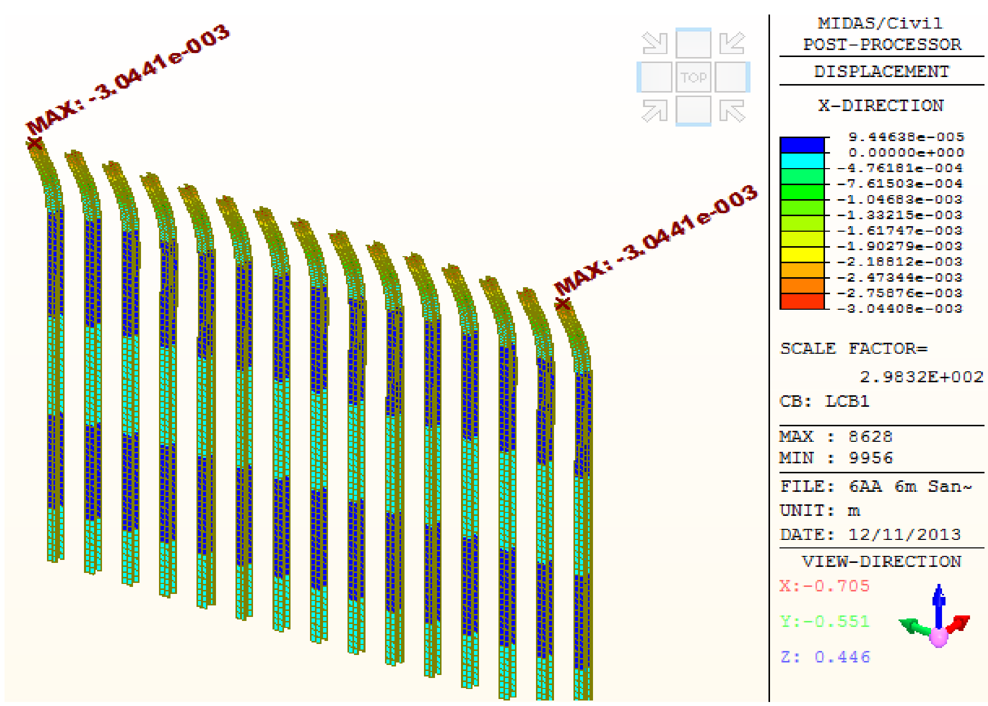
</td></tr>
</table>

<table>
<tr><td rowspan="2">Abutment</td><td colspan="2">Pile Head Displacement (strong-axis) Unit: m</td></tr>
<tr><td>LCB1 (Expansion)</td><td>-2.250E-03</td></tr>
<tr><td>7 m-Tall</td><td colspan="2">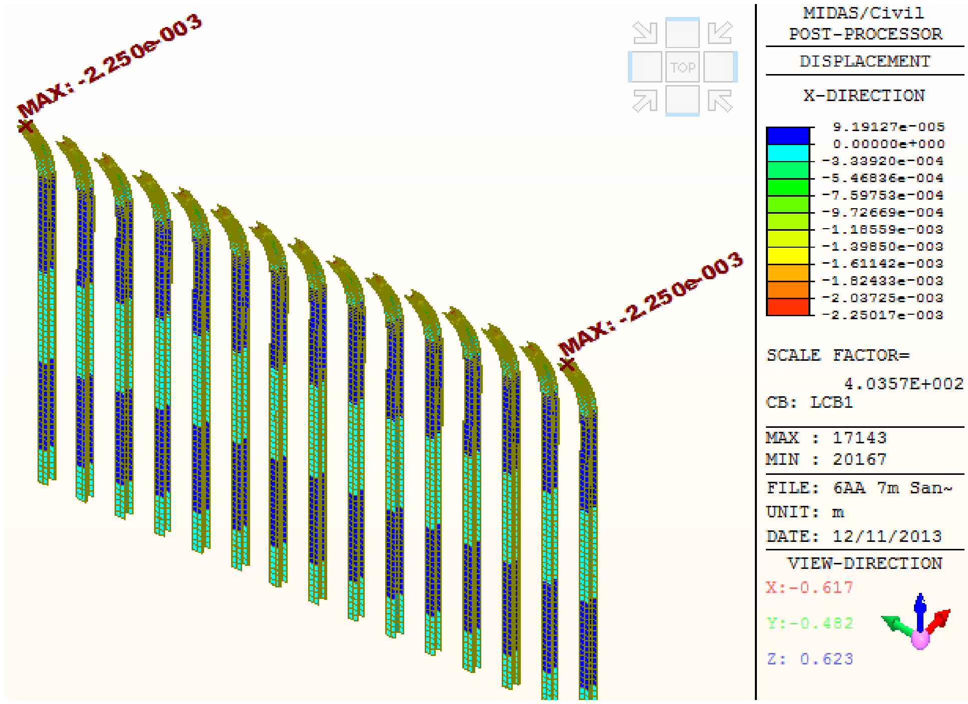
</td></tr>
<tr><td rowspan="2">Abutment</td><td colspan="2">Pile Head Displacement (strong-axis) Unit: m</td></tr>
<tr><td>LCB1 (Expansion)</td><td>-1.641E-03</td></tr>
<tr><td>8 m-Tall</td><td colspan="2">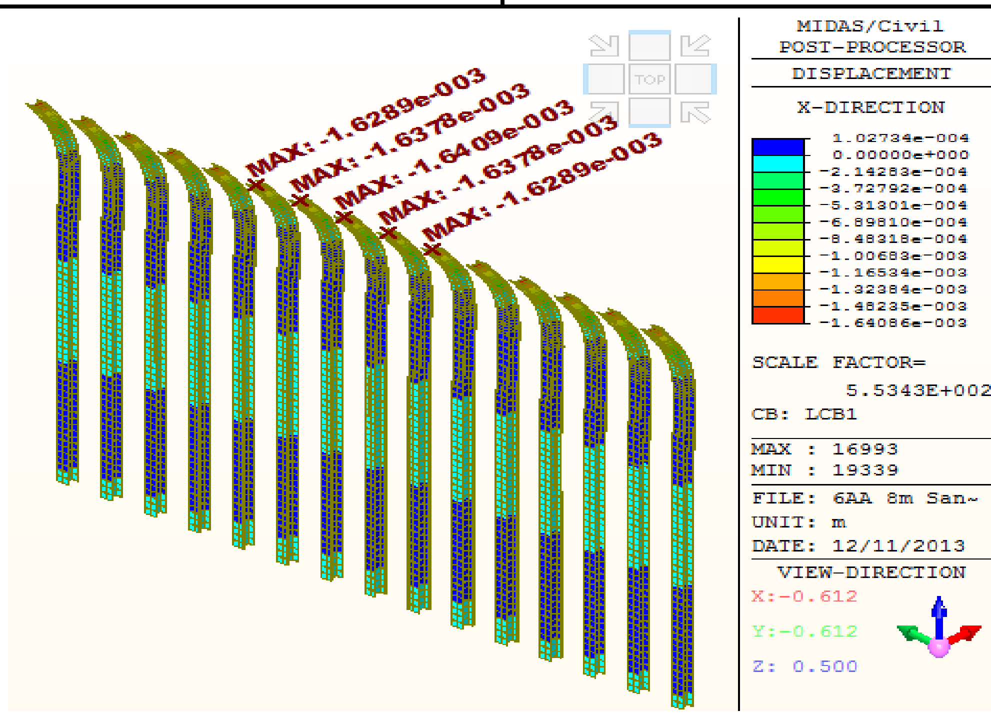
</td></tr>
</table>

1. The Effects depending on Abutment Height

1.18. Pile Head Displacement (Pile Orientation: Strong-Axis, Contraction Case)

Pile Head Displacement (strong-axis) LCB2 (Contraction Case) Unit: m	
3 m-Tall	0.001595
4 m-Tall	0.0006689
5 m-Tall	0.0002291
6 m-Tall	0.00002341
7 m-Tall	-0.0001818
8 m-Tall	-0.0001668

<table>
<tr><td rowspan="2">Abutment</td><td colspan="2">Pile Head Displacement (strong-axis) Unit: m</td></tr>
<tr><td>LCB2 (Contraction)</td><td>1.595E-03</td></tr>
<tr><td>3 m-Tall</td><td colspan="2">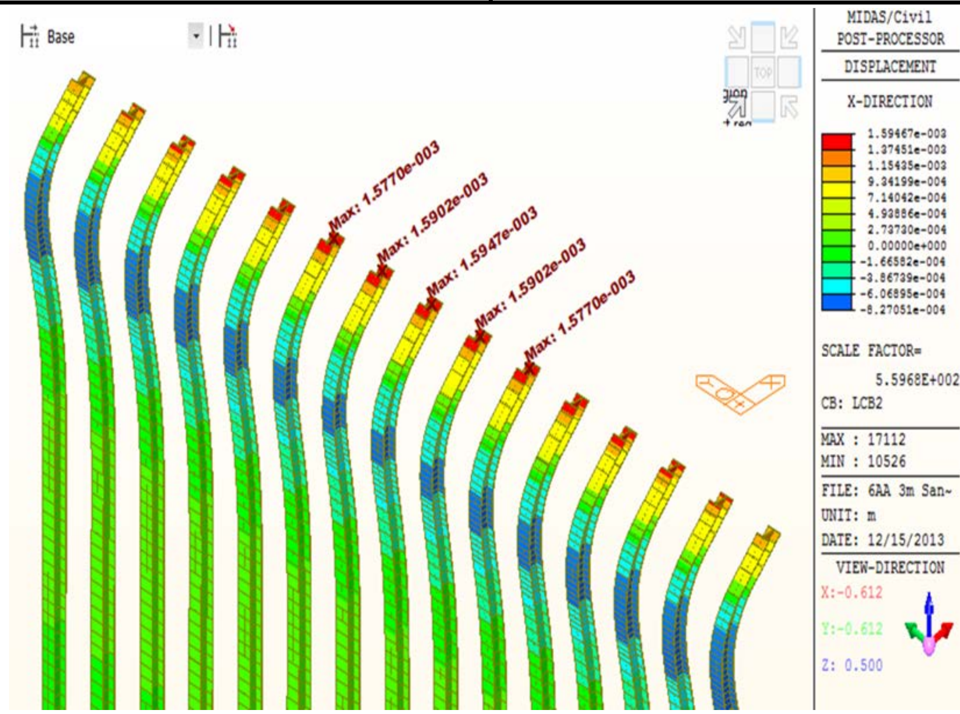</td></tr>
<tr><td rowspan="2">Abutment</td><td colspan="2">Pile Head Displacement (strong-axis) Unit: m</td></tr>
<tr><td>LCB2 (Contraction)</td><td>6.689E-04</td></tr>
<tr><td>4 m-Tall</td><td colspan="2">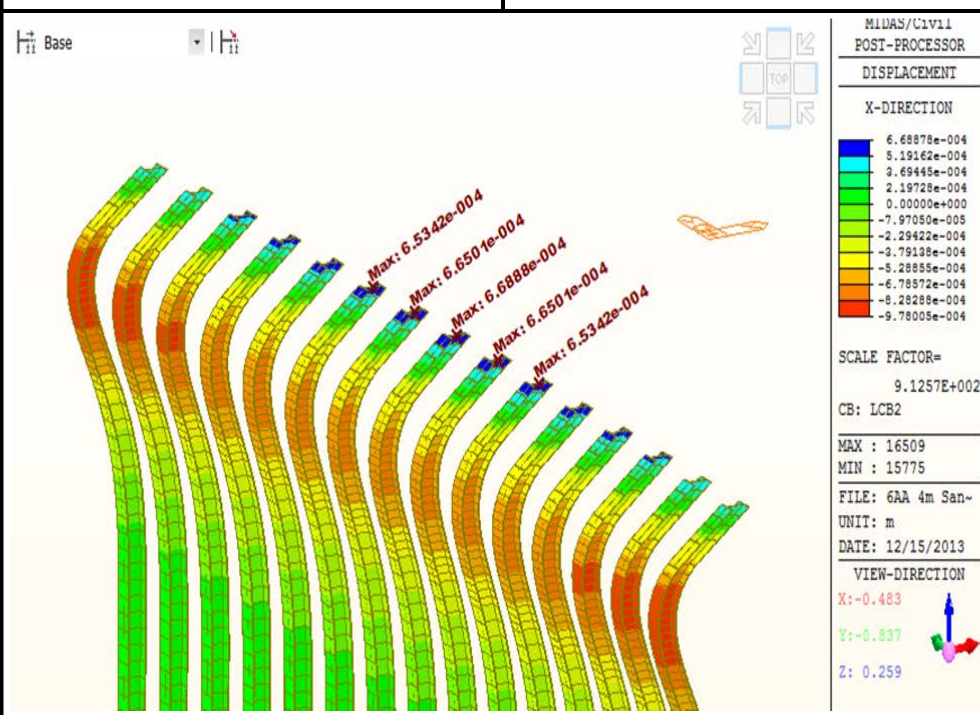</td></tr>
</table>

Abutment	Pile Head Displacement (strong-axis) Unit: m	
	LCB2 (Contraction)	2.291E-04
5 m-Tall		

Abutment	Pile Head Displacement (strong-axis) Unit: m	
	LCB2 (Contraction)	2.341E-05
6 m-Tall	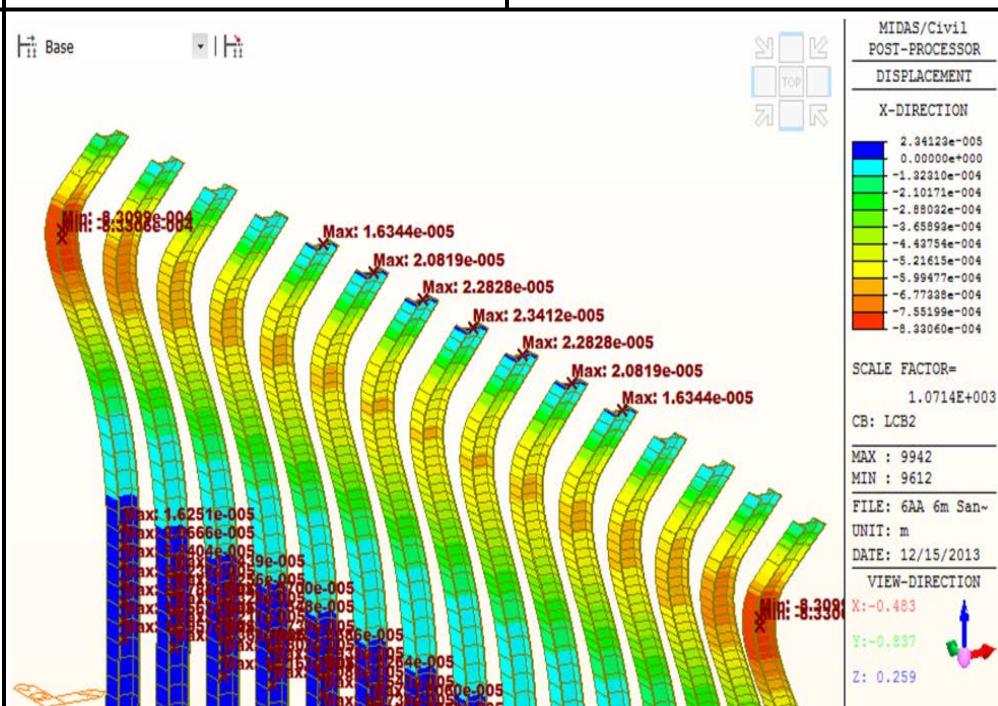	

<table>
<tr><td rowspan="2">Abutment</td><td colspan="2">Pile Head Displacement (strong-axis) Unit: m</td></tr>
<tr><td>LCB2 (Contraction)</td><td>-1.818E-04</td></tr>
<tr><td>7 m-Tall</td><td colspan="2">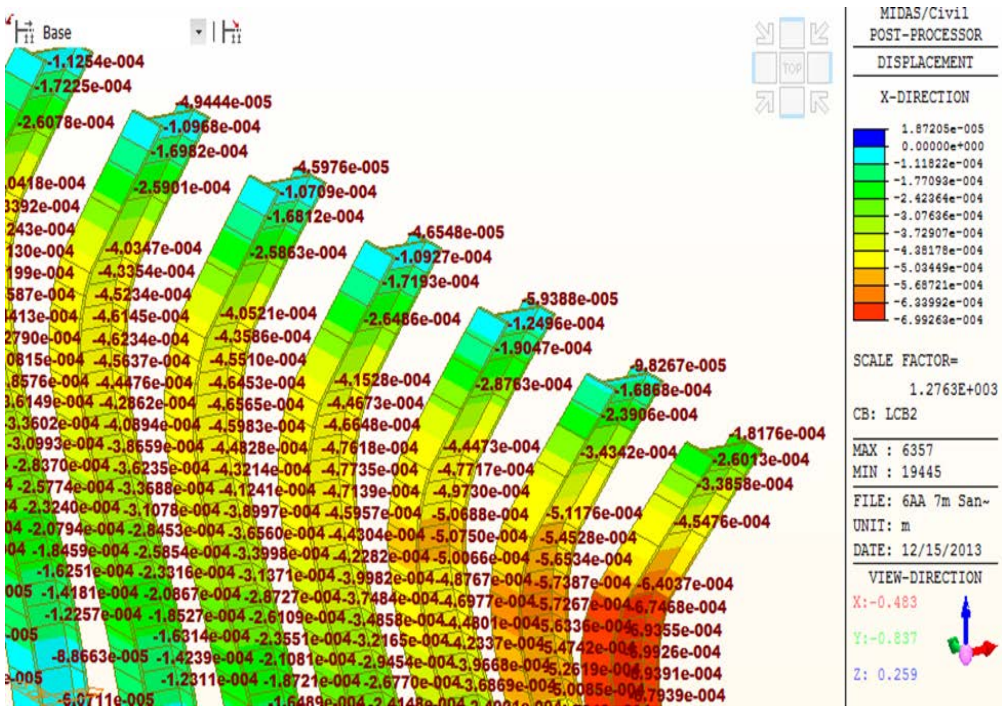
</td></tr>
</table>

<table>
<tr><td rowspan="2">Abutment</td><td colspan="2">Pile Head Displacement (strong-axis) Unit: m</td></tr>
<tr><td>LCB2 (Contraction)</td><td>-1.668E-04</td></tr>
<tr><td>8 m-Tall</td><td colspan="2">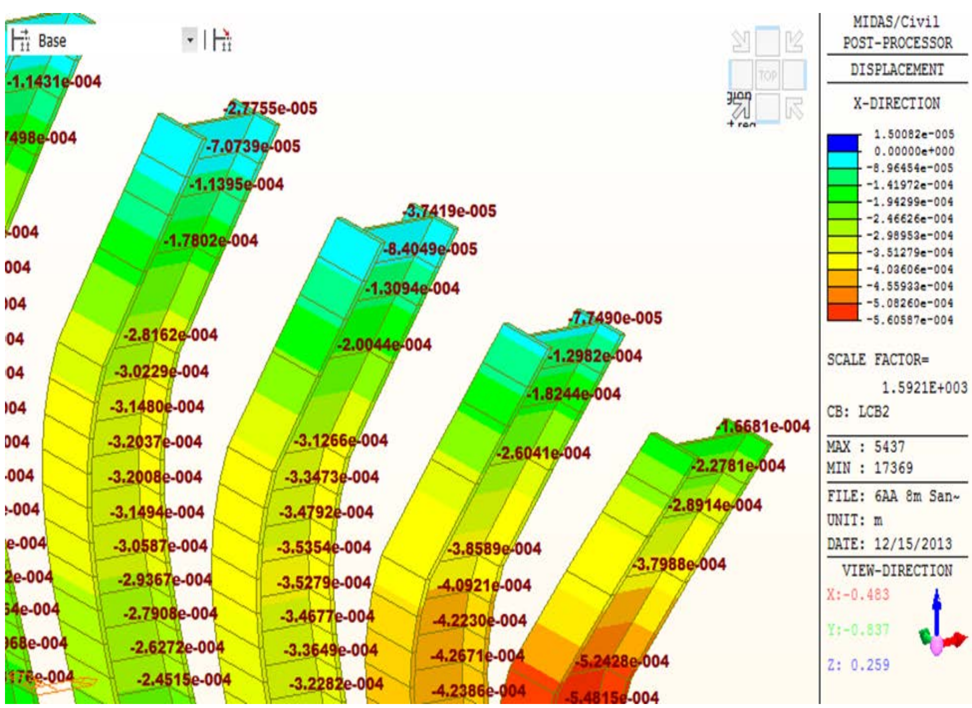
</td></tr>
</table>

1. The Effects depending on Abutment Height

1.19. Pile Head Displacement (Pile Orientation: Weak-Axis, Expansion Case)

Pile Head Displacement (weak-axis) LCB1 (Expansion Case) Unit: m	
3 m-Tall	-0.007656
4 m-Tall	-0.00577
5 m-Tall	-0.004296
6 m-Tall	-0.003162
7 m-Tall	-0.00229
8 m-Tall	-0.001606

Abutment	Pile Head Displacement (weak-axis) Unit: m	
	LCB1 (Expansion)	-7.656E-03
3 m-Tall	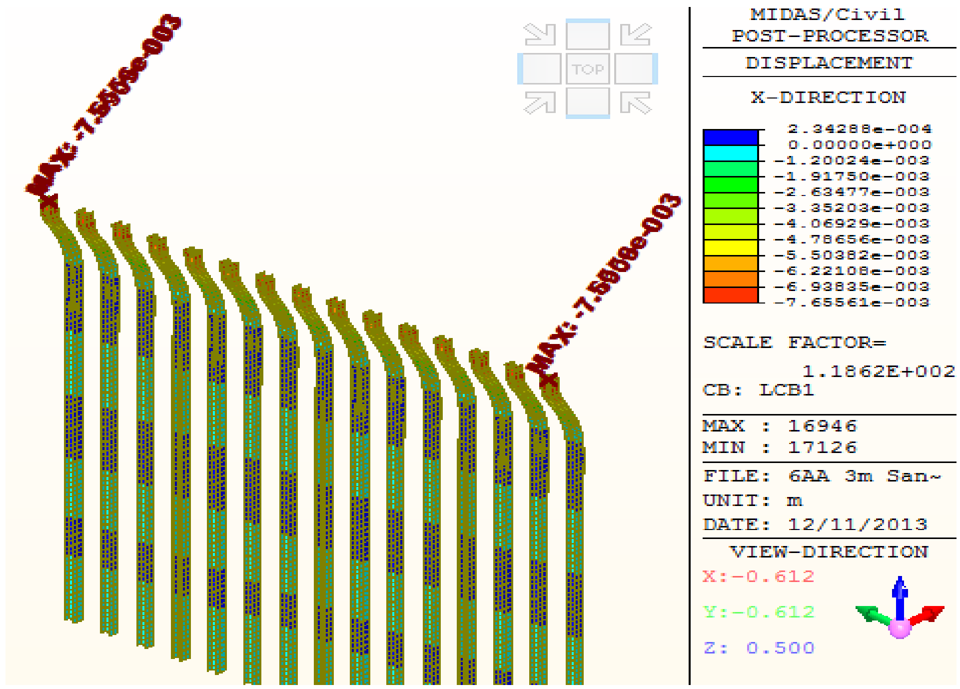	
Abutment	Pile Head Displacement (weak-axis) Unit: m	
	LCB1 (Expansion)	-5.770E-03
4 m-Tall	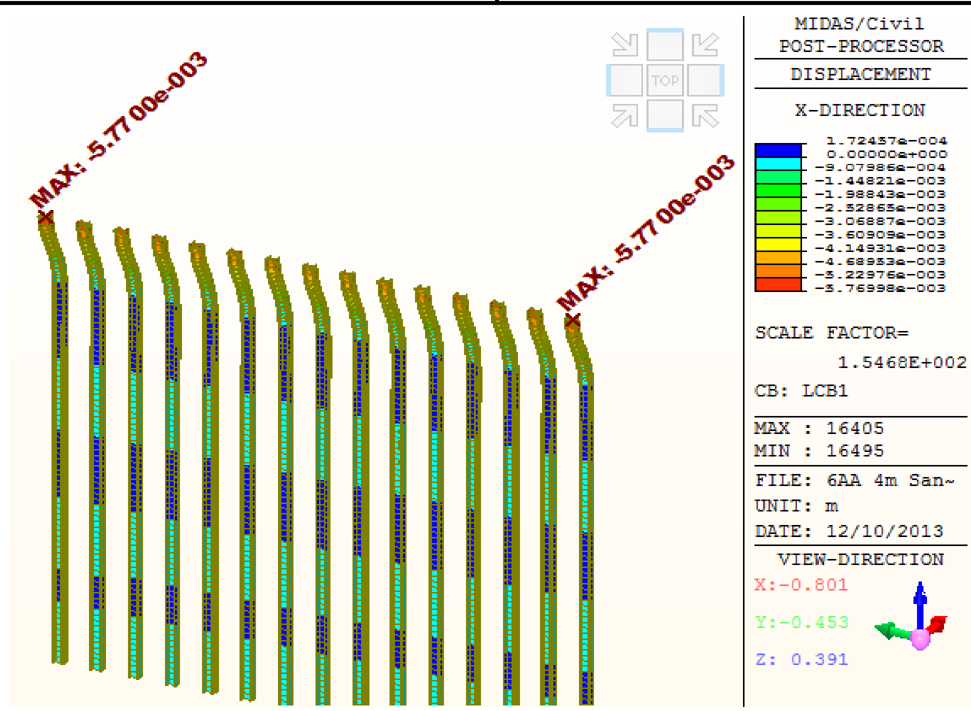	

<table>
<tr><td rowspan="2">Abutment</td><td colspan="2">Pile Head Displacement (weak-axis) Unit: m</td></tr>
<tr><td>LCB1 (Expansion)</td><td>-4.296E-03</td></tr>
<tr><td>5 m-Tall</td><td colspan="2">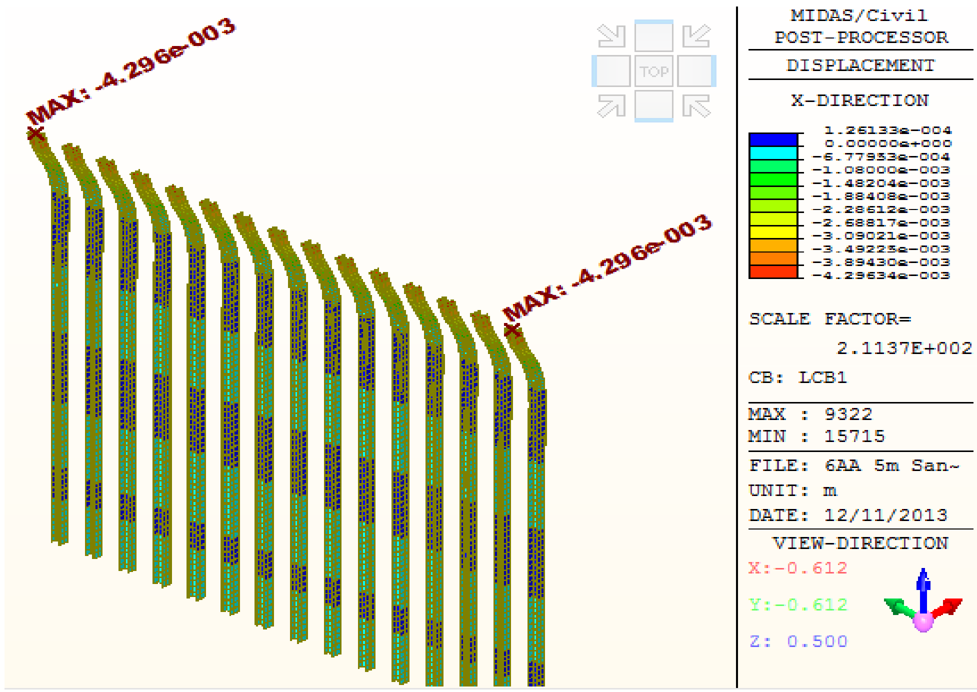
</td></tr>
<tr><td rowspan="2">Abutment</td><td colspan="2">Pile Head Displacement (weak-axis) Unit: m</td></tr>
<tr><td>LCB1 (Expansion)</td><td>-3.162E-03</td></tr>
<tr><td>6 m-Tall</td><td colspan="2">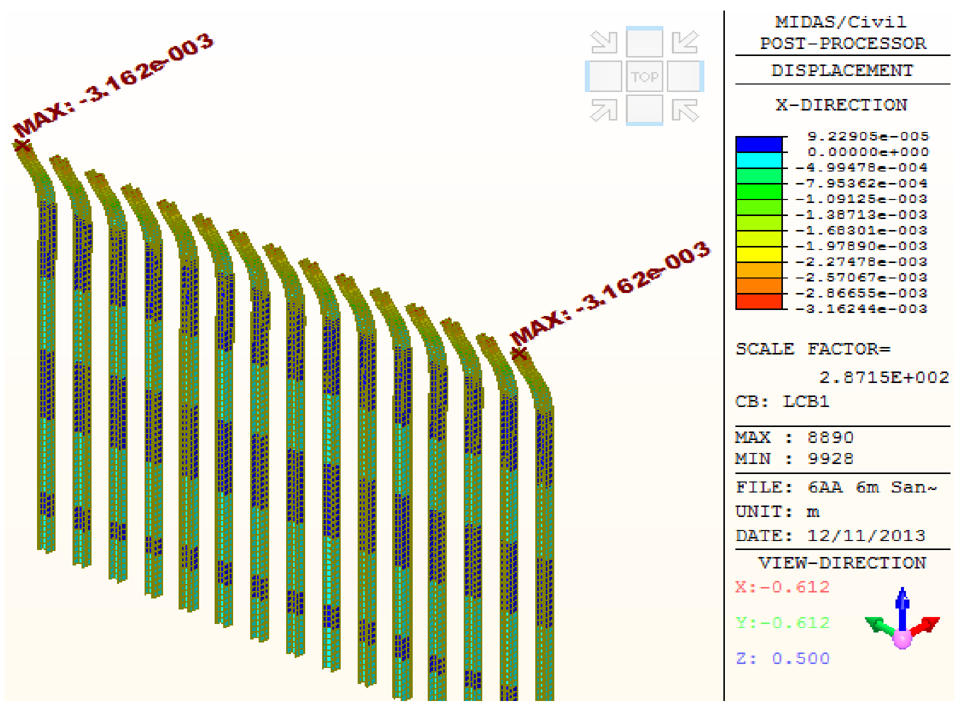
</td></tr>
</table>

Abutment	Pile Head Displacement (weak-axis) Unit: m	
	LCB1 (Expansion)	-2.290E-03
7 m-Tall	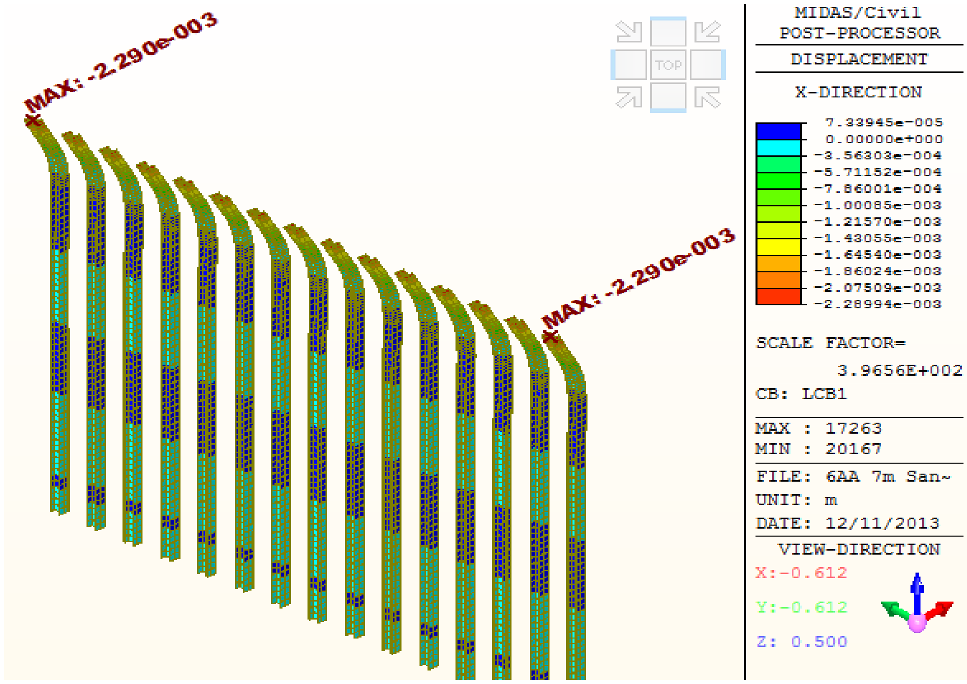	

Abutment	Pile Head Displacement (weak-axis) Unit: m	
	LCB1 (Expansion)	-1.606E-03
8 m-Tall	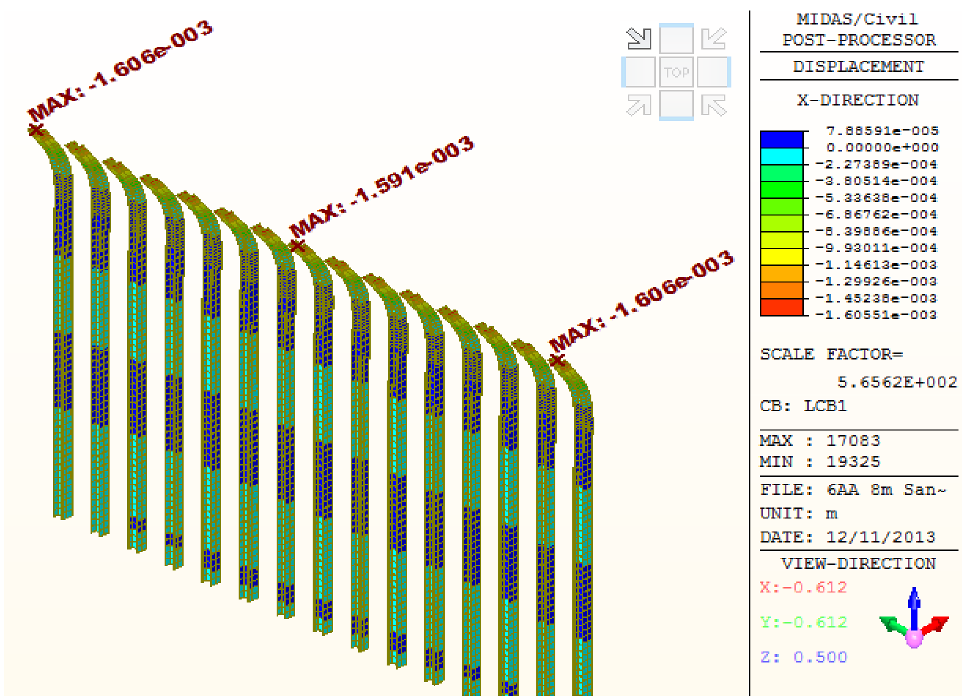	

1. The Effects depending on Abutment Height

1.20. Pile Head Displacement (Pile Orientation: Weak-Axis, Contraction Case)

Pile Head Displacement (weak-axis) LCB2 (Contraction Case) Unit: m	
3 m-Tall	0.00113
4 m-Tall	0.0002383
5 m-Tall	-0.0003409
6 m-Tall	-0.0004306
7 m-Tall	-0.000418
8 m-Tall	-0.0003556

<table>
<tr><td rowspan="2">Abutment</td><td colspan="2">Pile Head Displacement (weak-axis) Unit: m</td></tr>
<tr><td>LCB2 (Contraction)</td><td>1.130E-03</td></tr>
<tr><td>3 m-Tall</td><td colspan="2">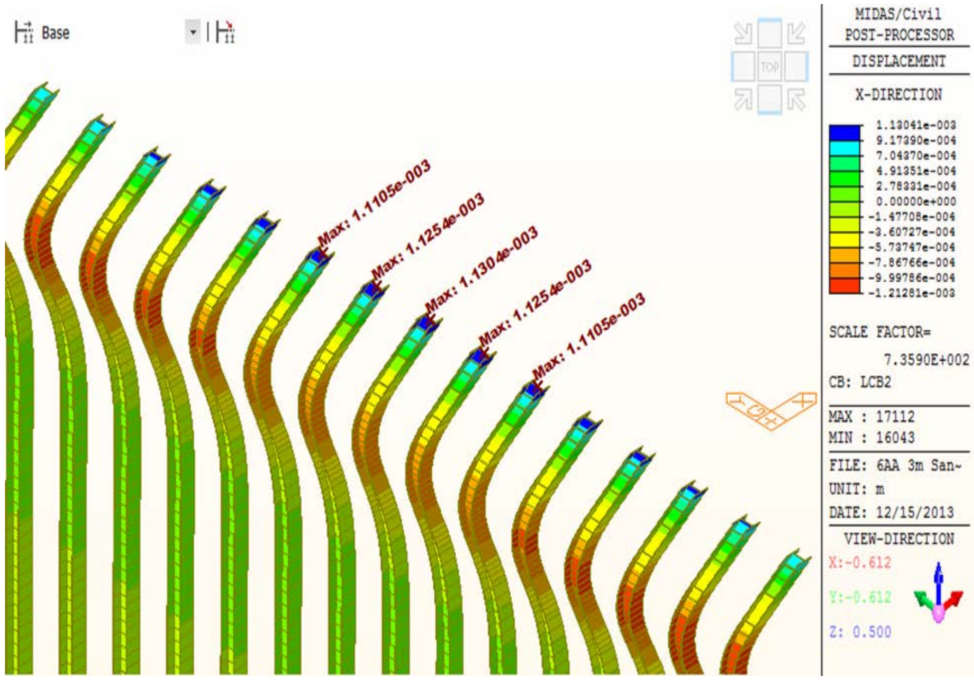
</td></tr>
<tr><td rowspan="2">Abutment</td><td colspan="2">Pile Head Displacement (weak-axis) Unit: m</td></tr>
<tr><td>LCB2 (Contraction)</td><td>2.383E-04</td></tr>
<tr><td>4 m-Tall</td><td colspan="2">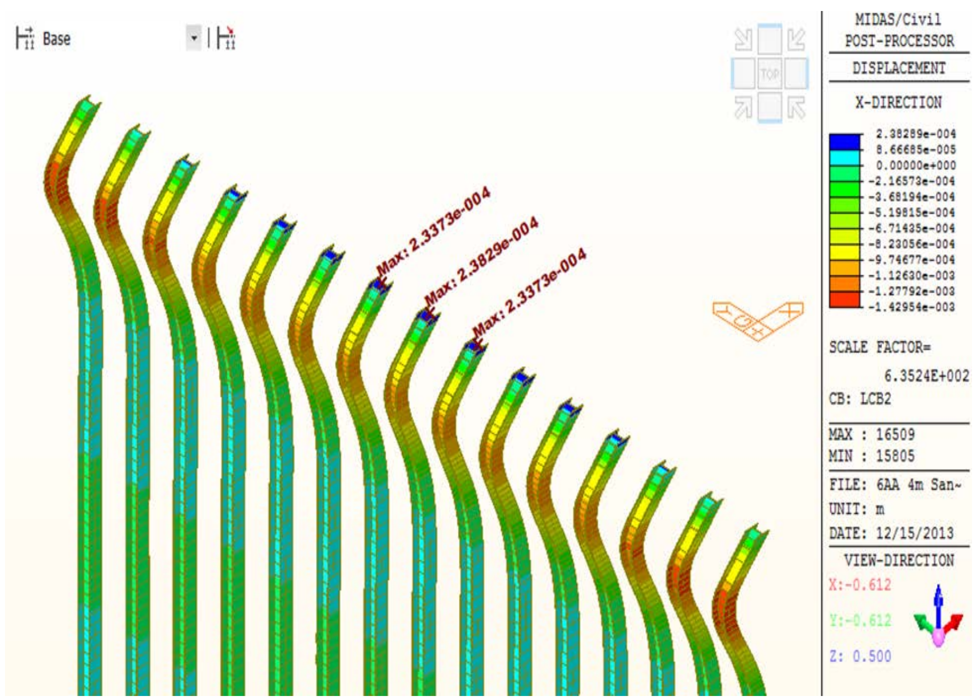
</td></tr>
</table>

Abutment	Pile Head Displacement (weak-axis) Unit: m	
	LCB2 (Contraction)	-3.409E-04
5 m-Tall	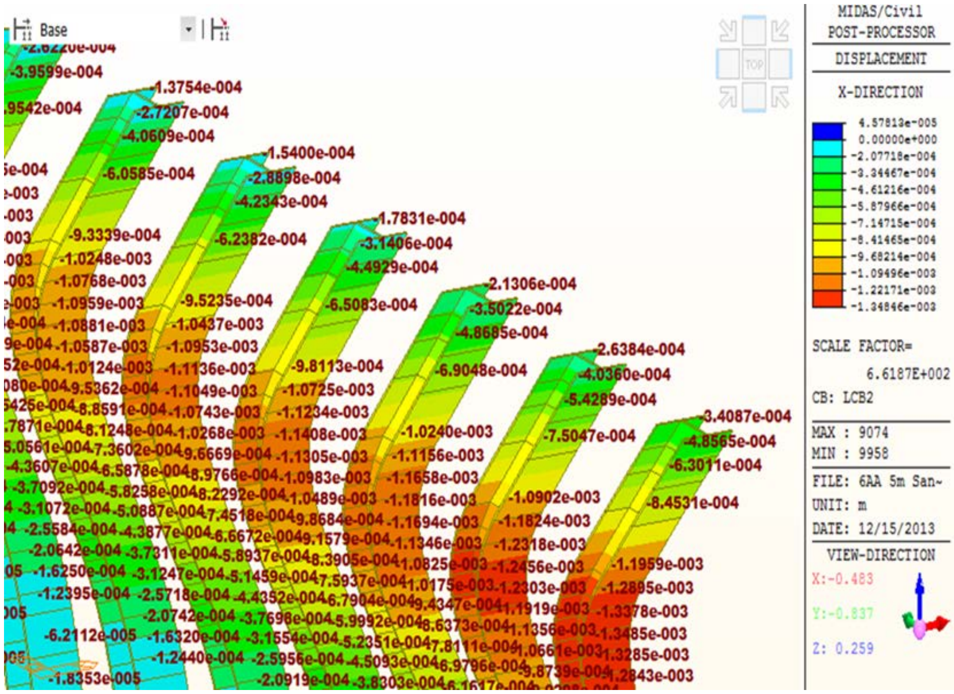	
Abutment	Pile Head Displacement (weak-axis) Unit: m	
	LCB2 (Contraction)	-4.306E-04
6 m-Tall	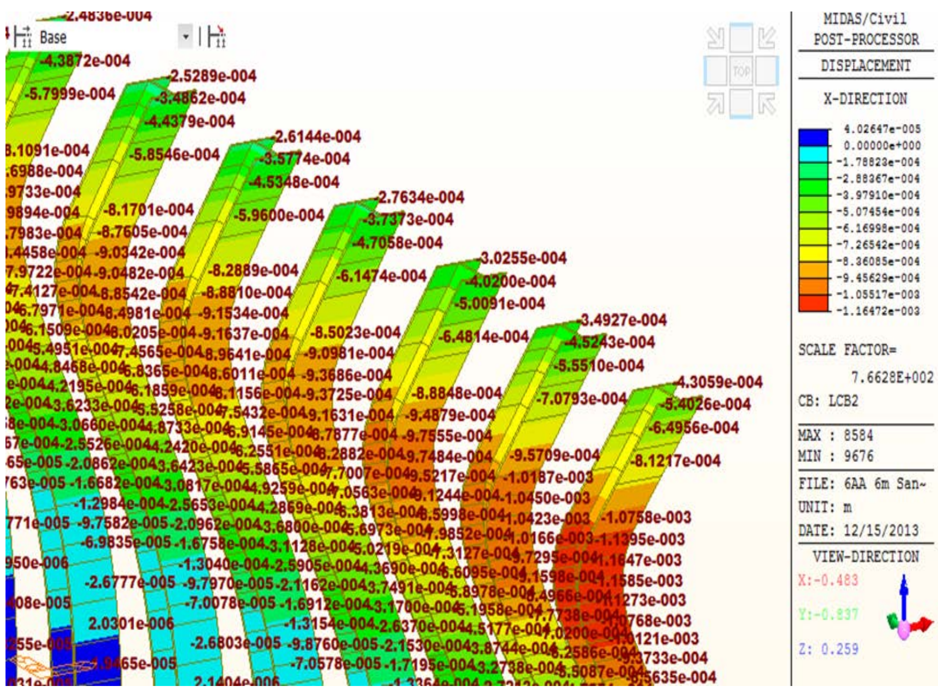	

Abutment	Pile Head Displacement (weak-axis) Unit: m	
	LCB2 (Contraction)	-4.180E-04
7 m-Tall	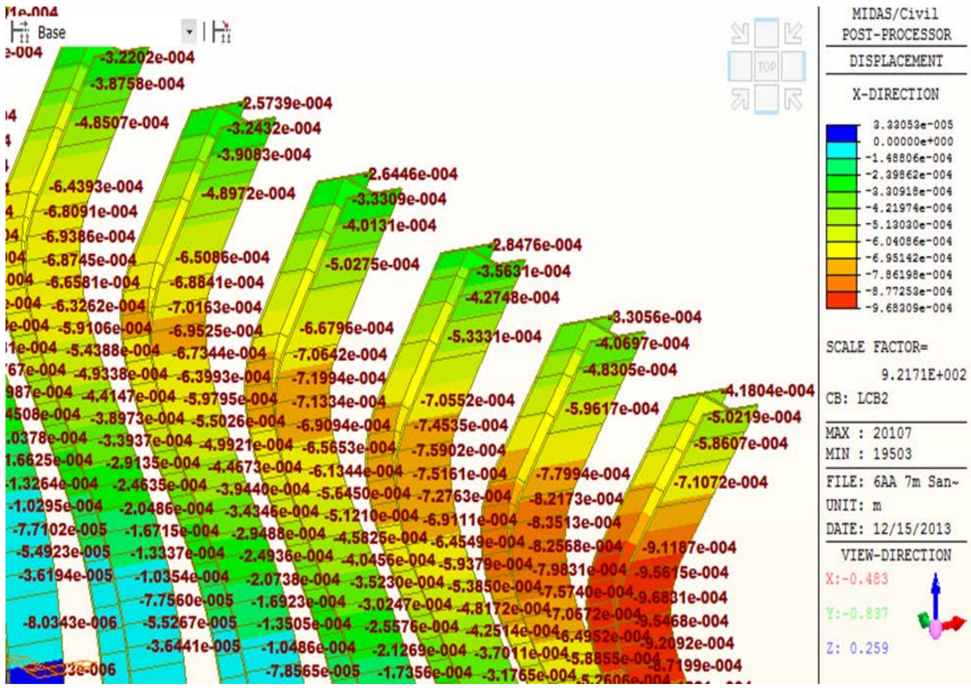	
Abutment	Pile Head Displacement (weak-axis) Unit: m	
	LCB2 (Contraction)	-3.556E-04
8 m-Tall	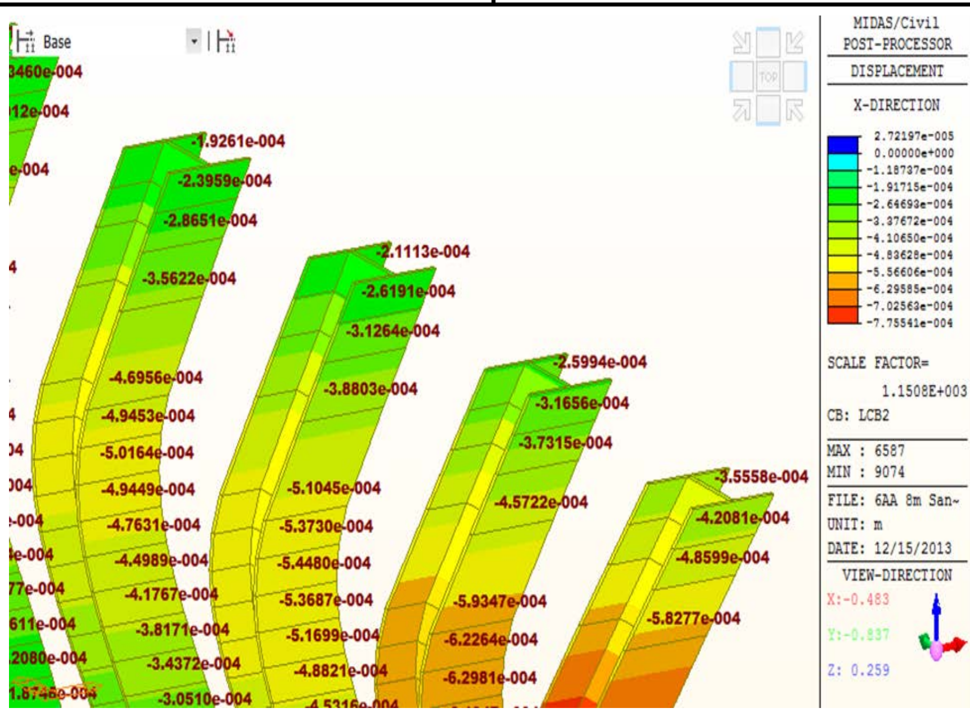	

2. The Effects depending on Soil Types

2.1. Girder Stress (Pile Orientation: Strong-Axis, Expansion Case)

Girder Stress (strong-axis) LCB1 (Expansion Case) Unit: kN/m^2	
Sand 1	-14410
Sand 2	-14240
Clay 1	-15110
Clay 2	-14650

<table>
<tr><td rowspan="2">Abutment</td><td colspan="2">Girder Stress (strong-axis) Unit: kN/m^2</td></tr>
<tr><td>LCB1 (Expansion)</td><td>-1.441E+04</td></tr>
<tr><td>Sand 1</td><td colspan="2">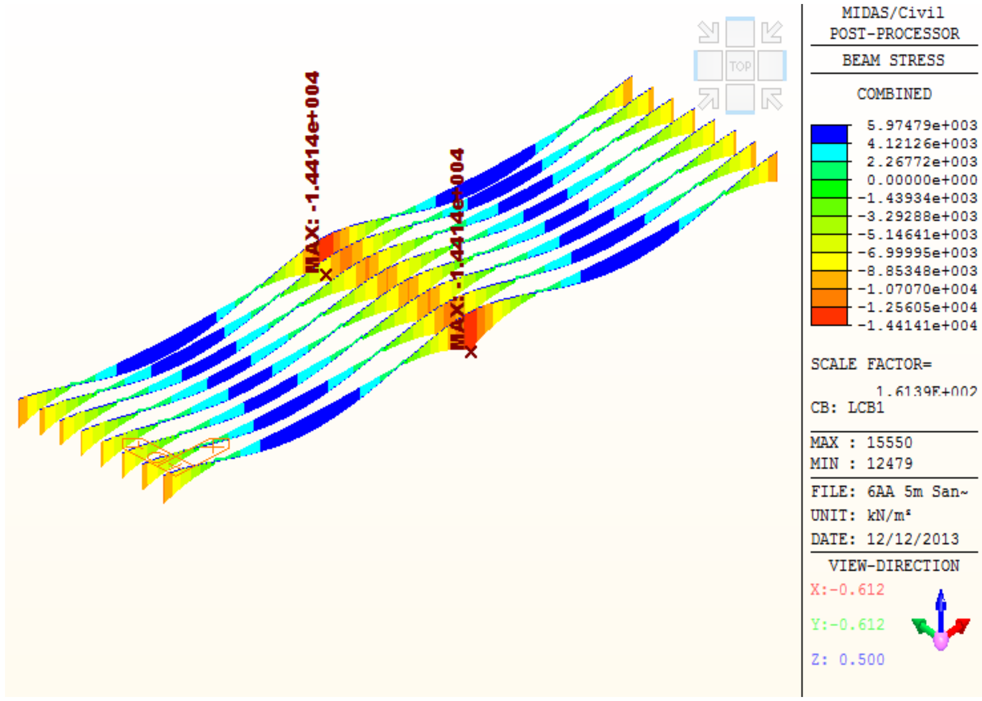
</td></tr>
<tr><td rowspan="2">Abutment</td><td colspan="2">Girder Stress (strong-axis) Unit: kN/m^2</td></tr>
<tr><td>LCB1 (Expansion)</td><td>-1.424E+04</td></tr>
<tr><td>Sand 2</td><td colspan="2">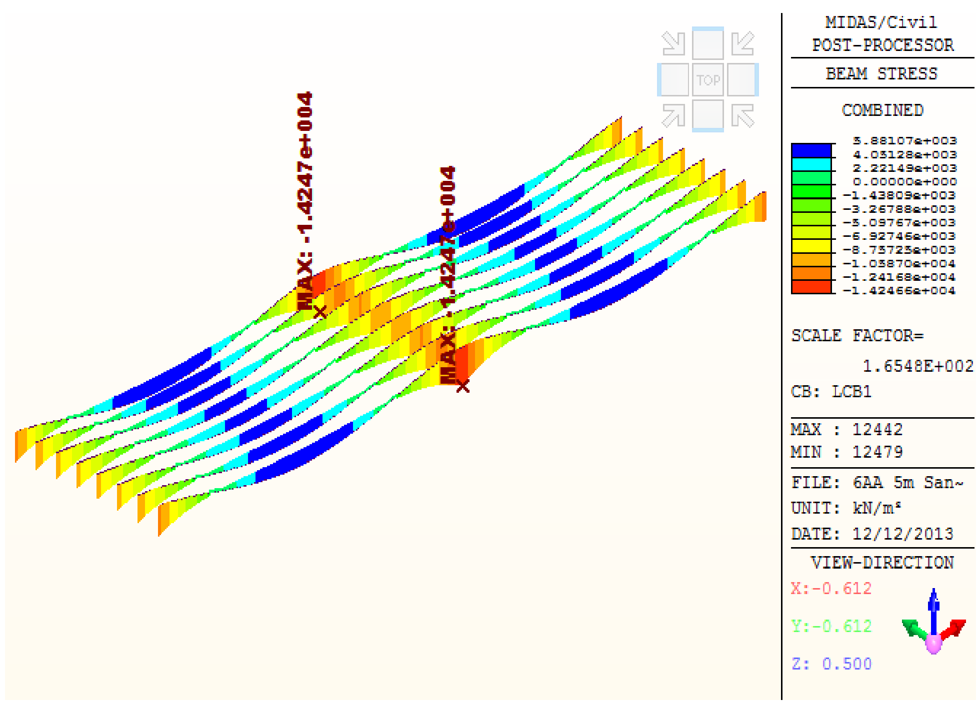
</td></tr>
</table>

<table>
<tr><td rowspan="2">Abutment</td><td colspan="2">Girder Stress (strong-axis) Unit: kN/m²</td></tr>
<tr><td>LCB1 (Expansion)</td><td>-1.511E+04</td></tr>
<tr><td>Clay 1</td><td colspan="2">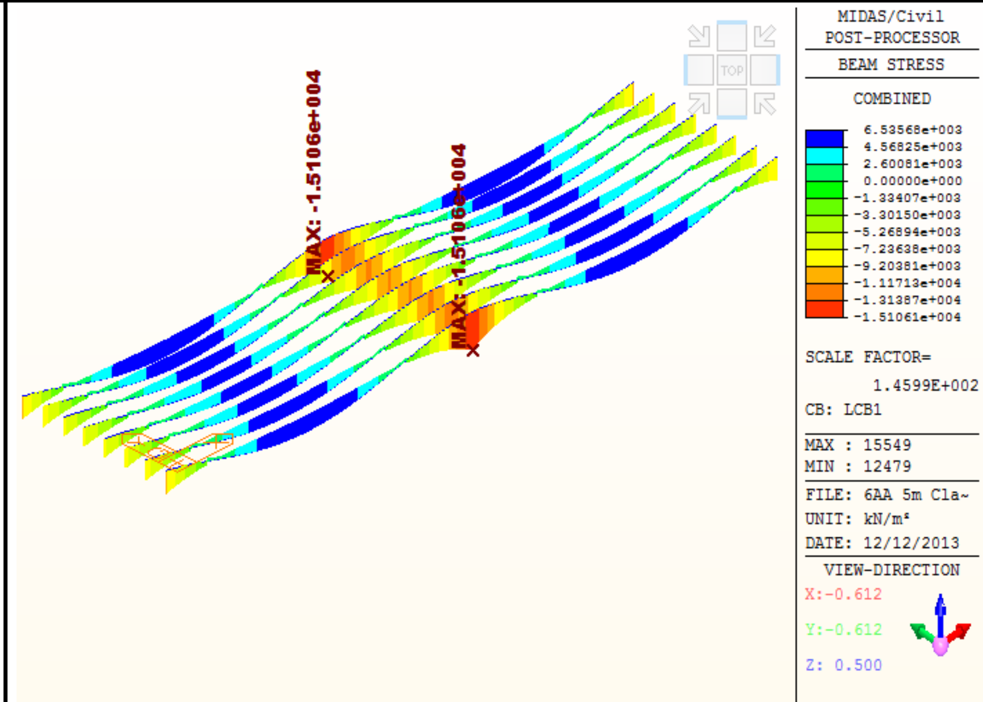
</td></tr>
<tr><td rowspan="2">Abutment</td><td colspan="2">Girder Stress (strong-axis) Unit: kN/m²</td></tr>
<tr><td>LCB1 (Expansion)</td><td>-1.465E+04</td></tr>
<tr><td>Clay 2</td><td colspan="2">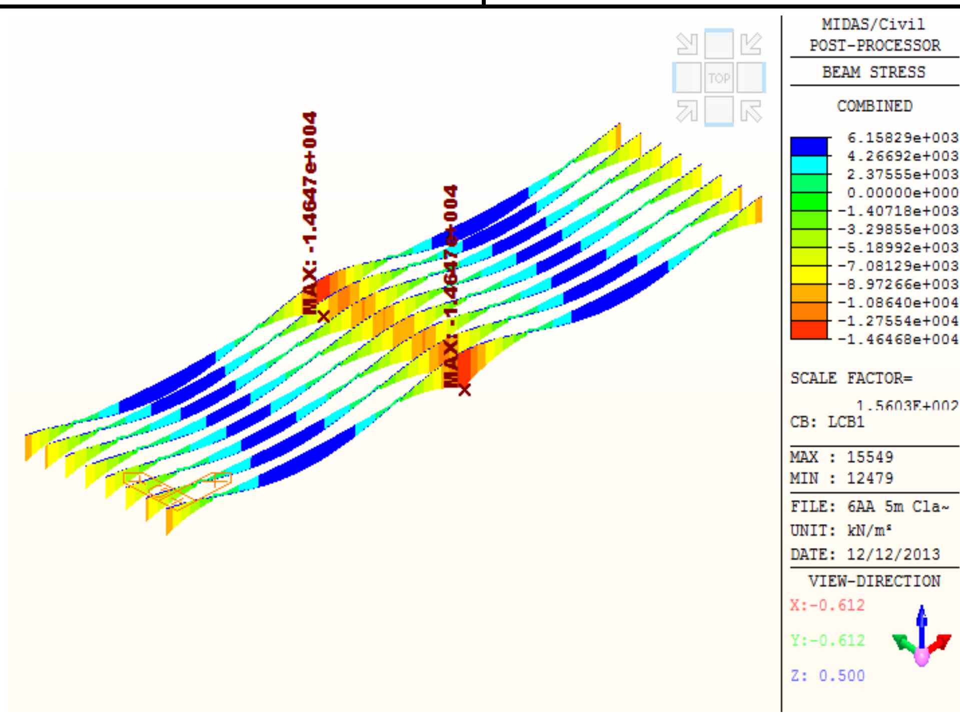
</td></tr>
</table>

2. The Effects depending on Soil Types

2.2. Girder Stress (Pile Orientation: Strong-Axis, Contraction Case)

Girder Stress (strong-axis) LCB2 (Contraction Case) Unit: kN/m^2	
Sand 1	-16310
Sand 2	-16070
Clay 1	-16770
Clay 2	-16420

<table>
<tr><th rowspan="2">Abutment</th><th colspan="2">Girder Stress (strong-axis) Unit: kN/m^2</th></tr>
<tr><th>LCB2 (Contraction)</th><th>-1.631E+04</th></tr>
<tr><td>Sand 1</td><td colspan="2">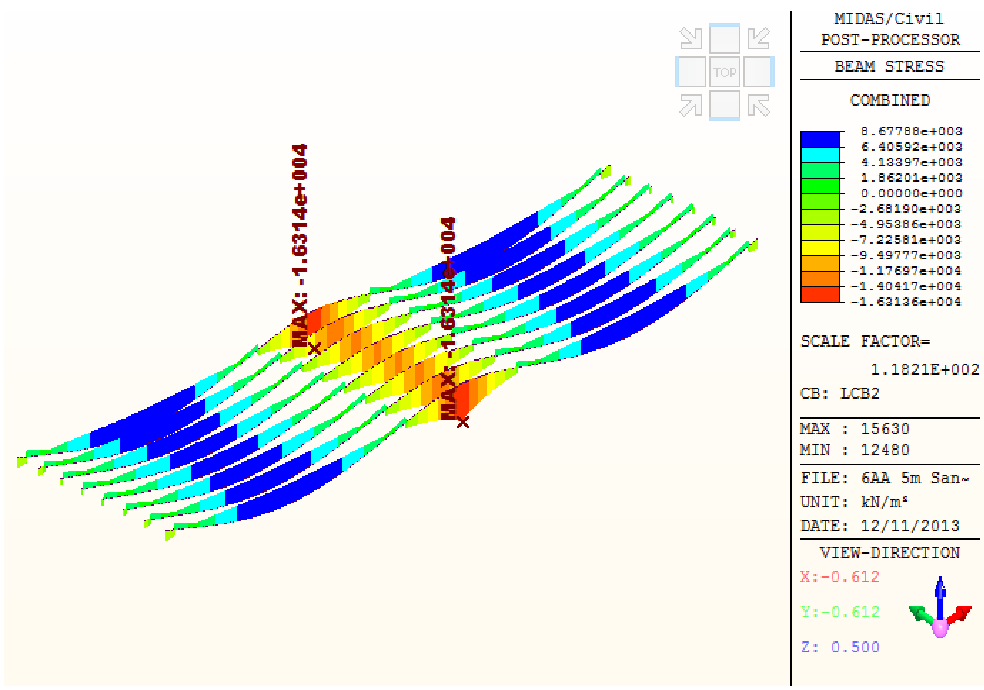
</td></tr>
<tr><th rowspan="2">Abutment</th><th colspan="2">Girder Stress (strong-axis) Unit: kN/m^2</th></tr>
<tr><th>LCB2 (Contraction)</th><th>-1.607E+04</th></tr>
<tr><td>Sand 2</td><td colspan="2">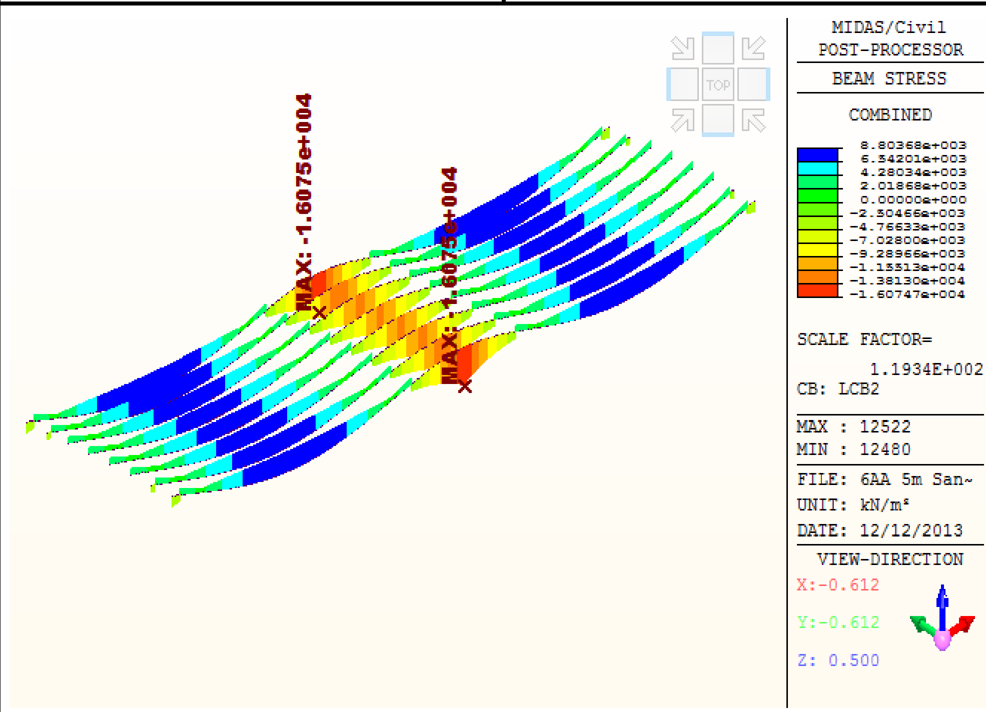
</td></tr>
</table>

Abutment	Girder Stress (strong-axis) Unit: kN/m^2	
	LCB2 (Contraction)	-1.677E+04
Clay 1	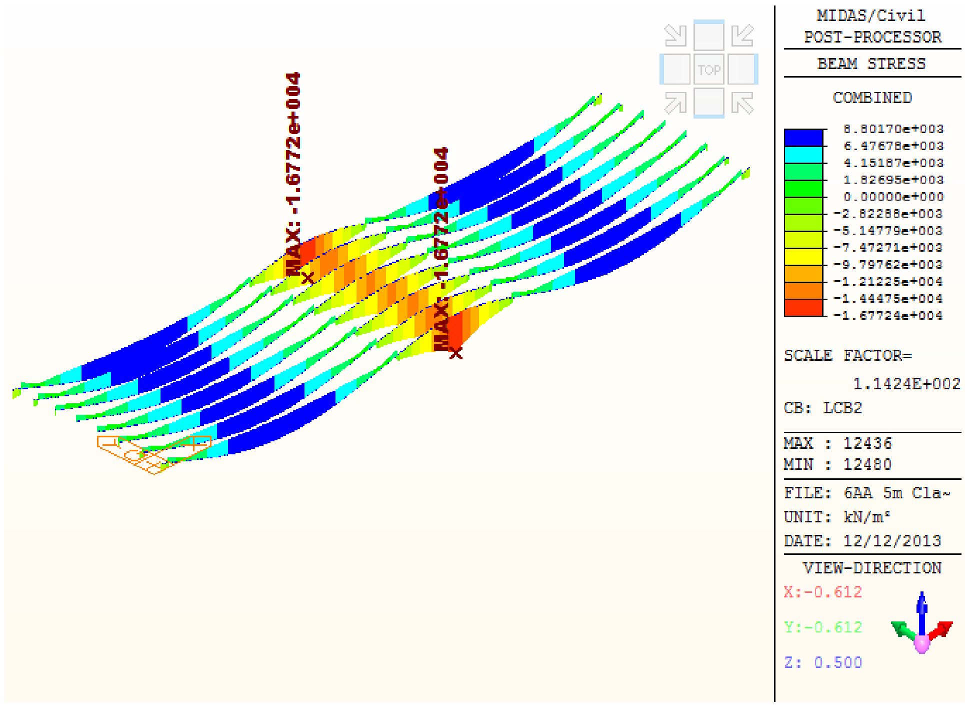	
Abutment	Girder Stress (strong-axis) Unit: kN/m^2	
	LCB2 (Contraction)	-1.642E+04
Clay 2	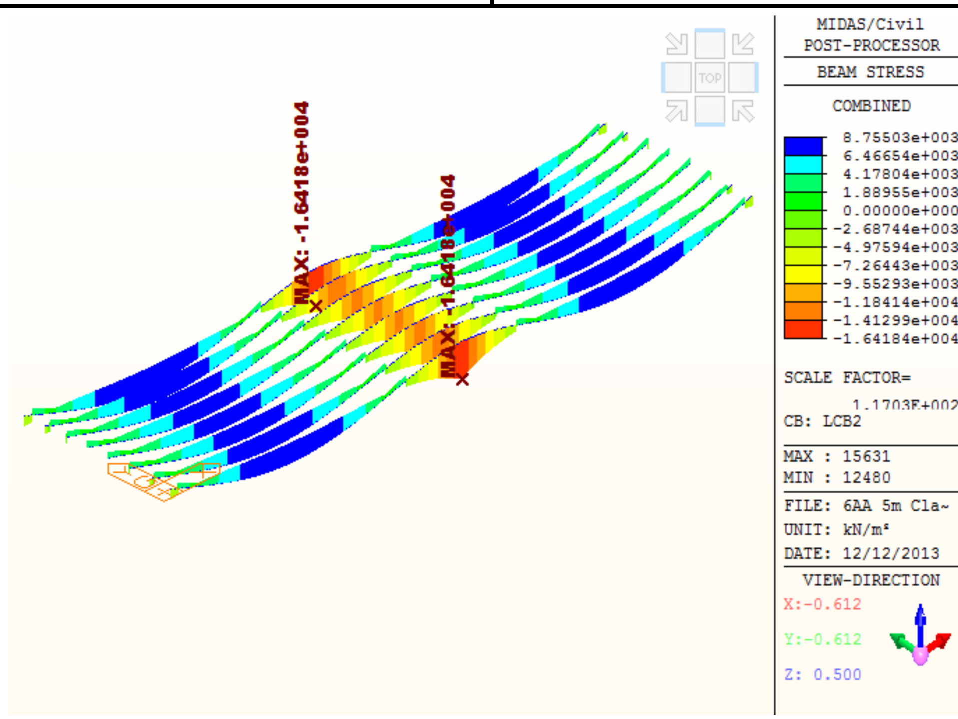	

2. The Effects depending on Soil Types

2.3. Girder Stress (Pile Orientation: Weak-Axis, Expansion Case)

Girder Stress (weak-axis) LCB1 (Expansion Case) Unit: kN/m^2	
Sand 1	-14460
Sand 2	-14260
Clay 1	-15380
Clay 2	-14800

Abutment	Girder Stress (weak-axis) Unit: kN/m^2	
	LCB1 (Expansion)	-1.446E+04
Sand 1		

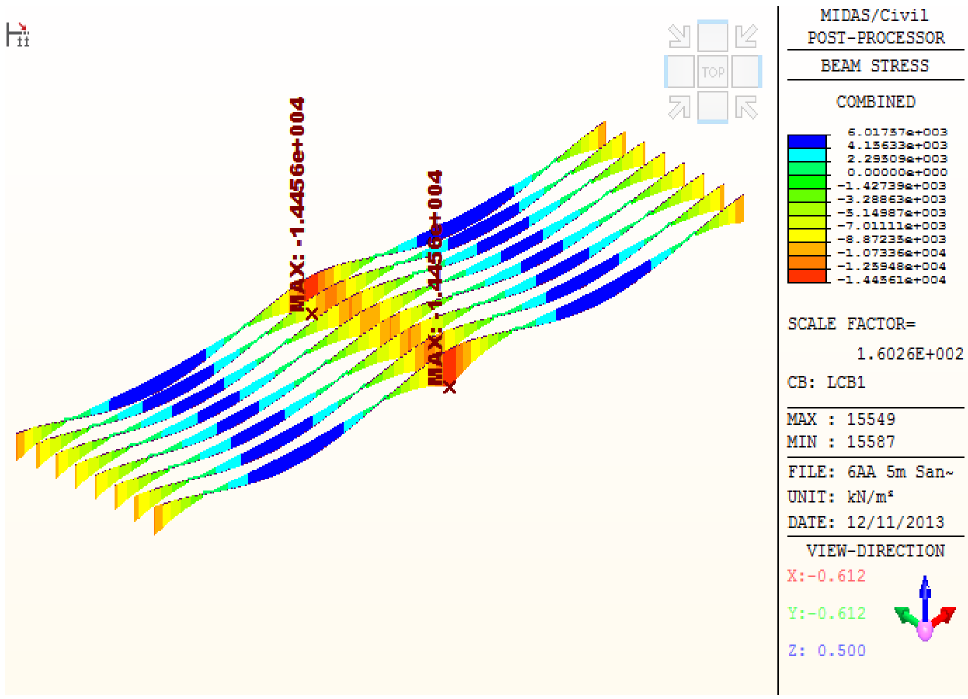

Abutment	Girder Stress (weak-axis) Unit: kN/m^2	
	LCB1 (Expansion)	-1.426E+04
Sand 2		

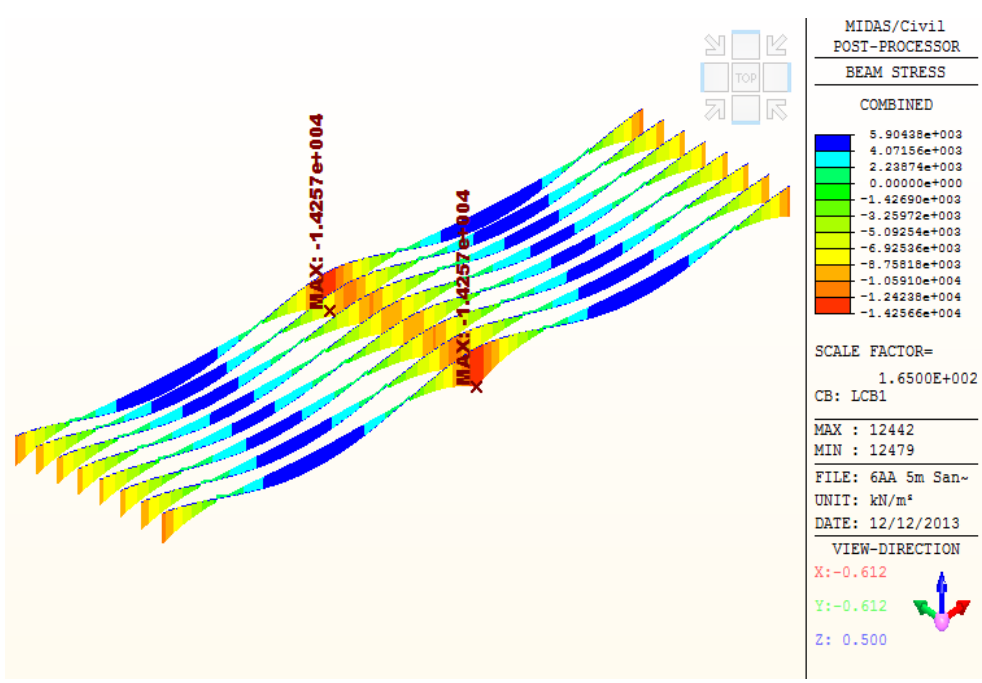

<table>
<tr><td rowspan="2">Abutment</td><td colspan="2">Girder Stress (weak-axis) Unit: kN/m^2</td></tr>
<tr><td>LCB1 (Expansion)</td><td>-1.538E+04</td></tr>
<tr><td>Clay 1</td><td colspan="2">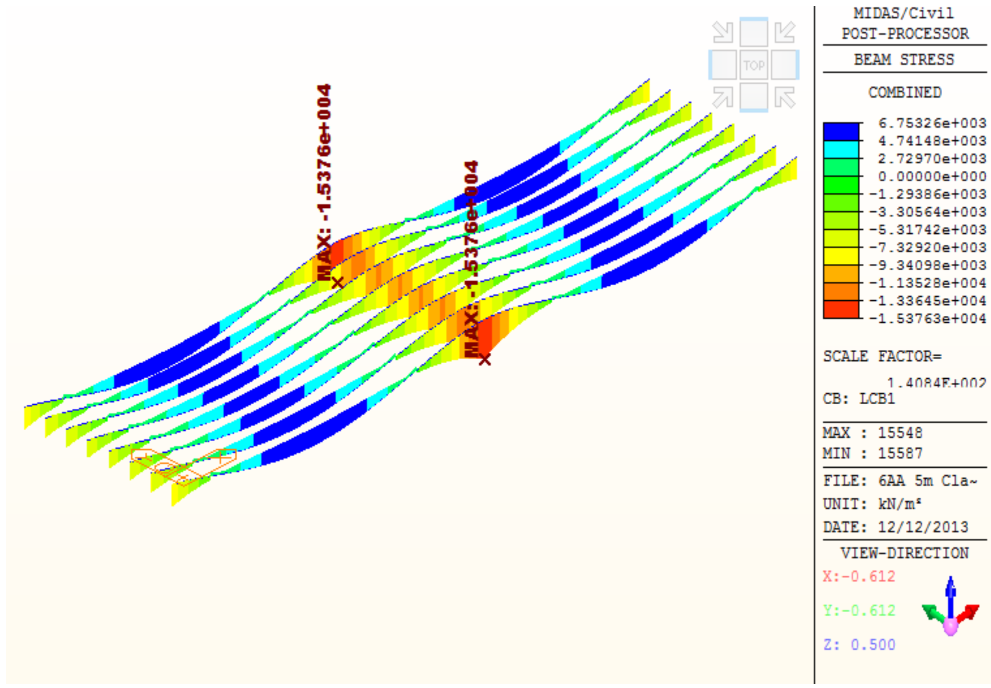
</td></tr>
</table>

<table>
<tr><td rowspan="2">Abutment</td><td colspan="2">Girder Stress (weak-axis) Unit: kN/m^2</td></tr>
<tr><td>LCB1 (Expansion)</td><td>-1.480E+04</td></tr>
<tr><td>Clay 2</td><td colspan="2">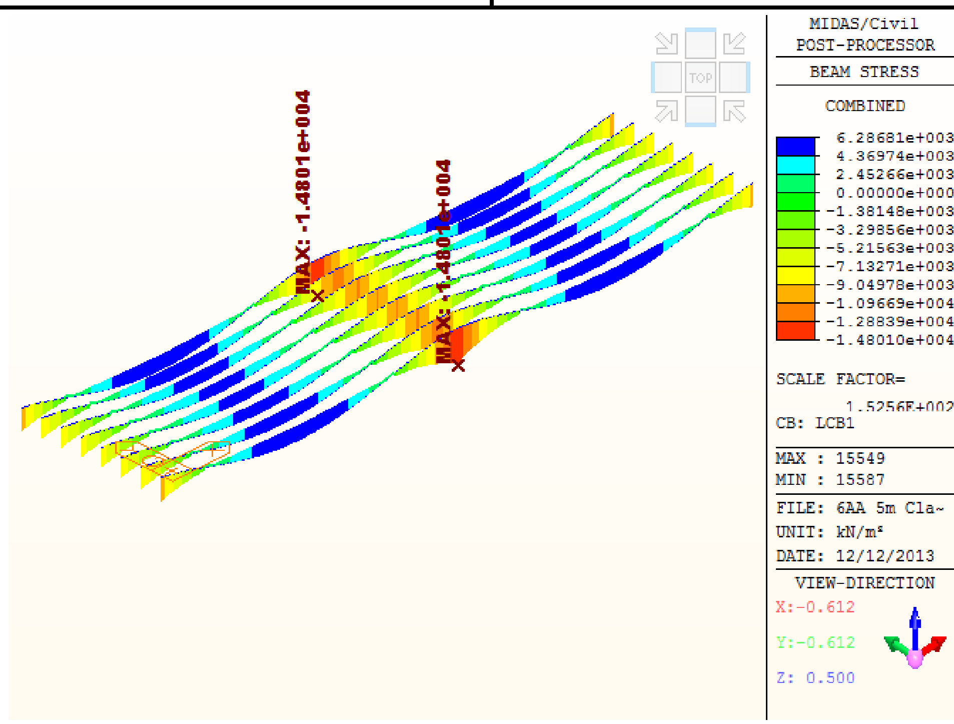
</td></tr>
</table>

2. The Effects depending on Soil Types

2.4. Girder Stress (Pile Orientation: Weak-Axis, Contraction Case)

Girder Stress (weak-axis) LCB2 (Contraction Case) Unit: kN/m^2	
Sand 1	-16410
Sand 2	-16150
Clay 1	-17020
Clay 2	-16600

Abutment	Girder Stress (weak-axis) Unit: kN/m^2	
	LCB2 (Contraction)	-1.641E+04
Sand 1	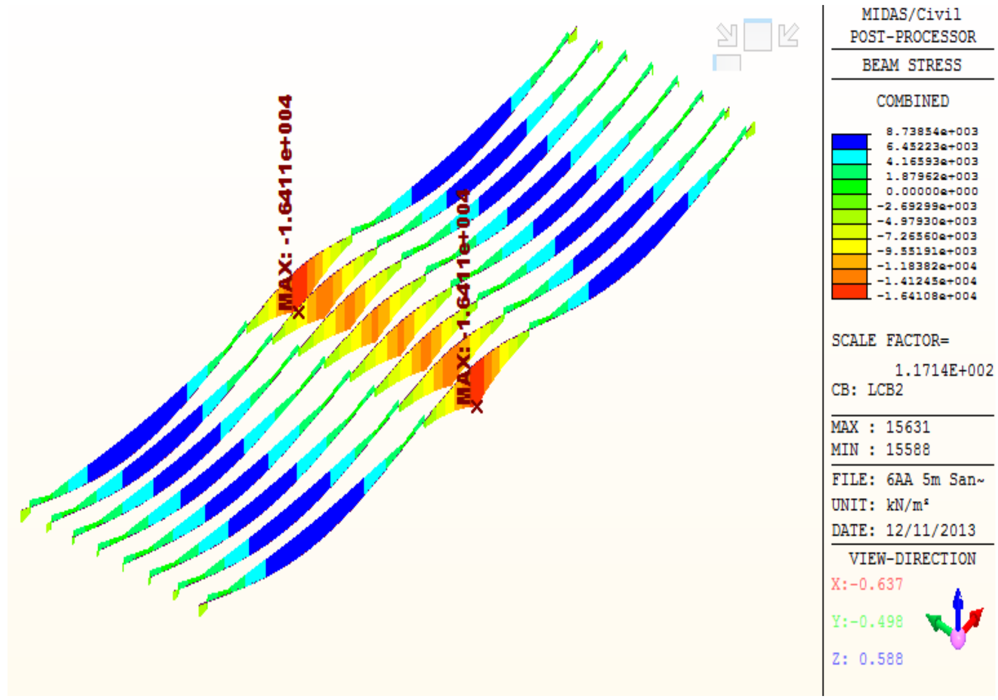	
Abutment	Girder Stress (weak-axis) Unit: kN/m^2	
	LCB2 (Contraction)	-1.615E+04
Sand 2	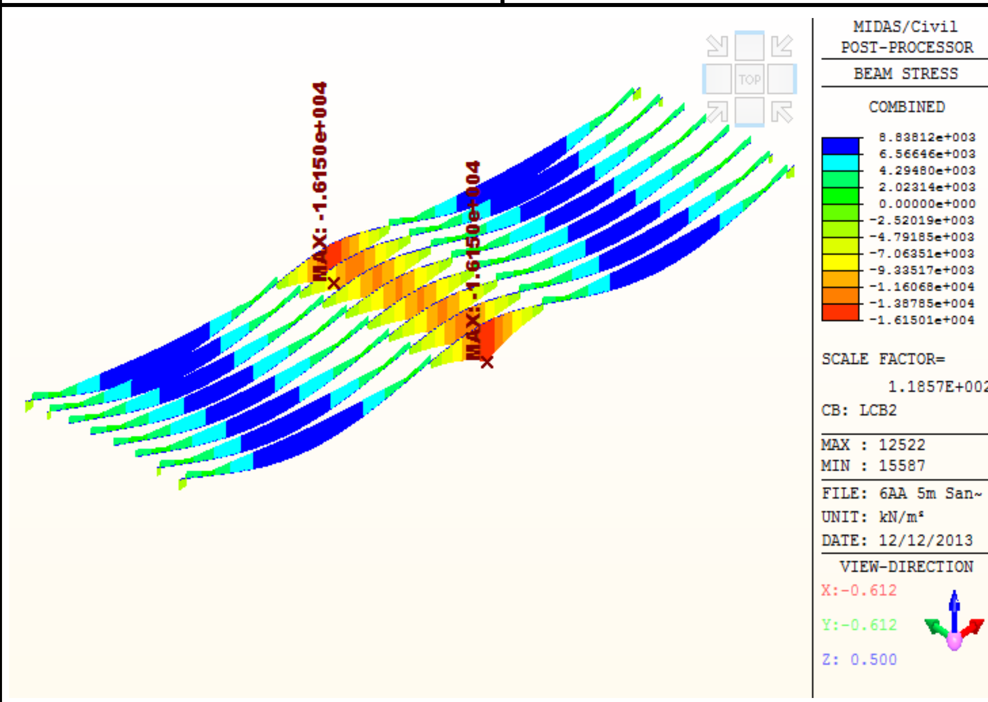	

<table>
<tr><td rowspan="2">Abutment</td><td colspan="2">Girder Stress (weak-axis) Unit: kN/m^2</td></tr>
<tr><td>LCB2 (Contraction)</td><td>-1.702E+04</td></tr>
<tr><td>Clay 1</td><td colspan="2">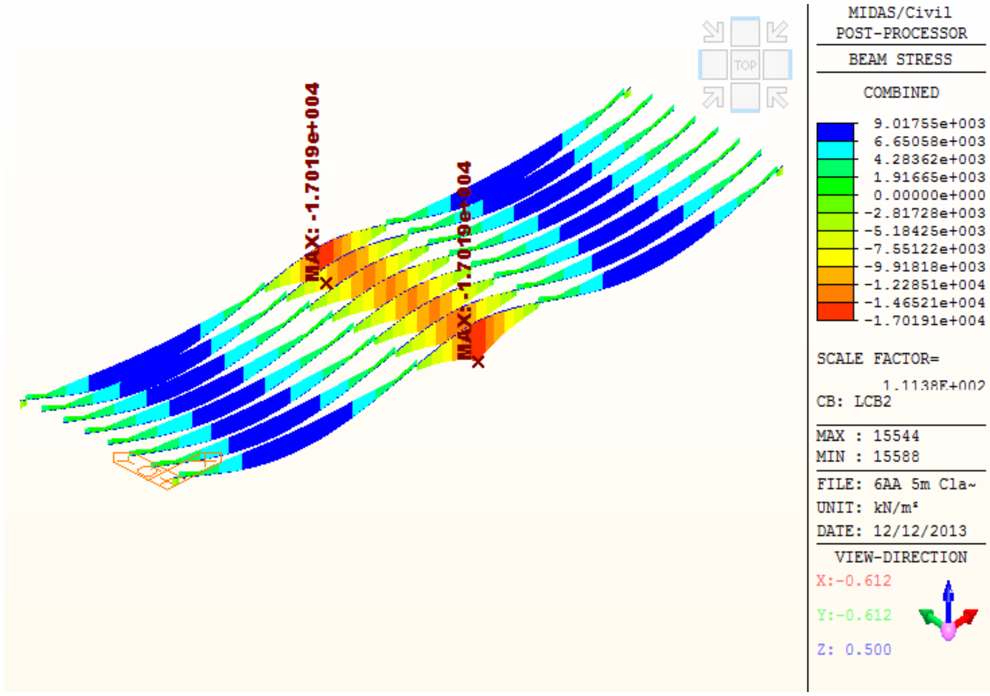
</td></tr>
<tr><td rowspan="2">Abutment</td><td colspan="2">Girder Stress (weak-axis) Unit: kN/m^2</td></tr>
<tr><td>LCB2 (Contraction)</td><td>-1.660E+04</td></tr>
<tr><td>Clay 2</td><td colspan="2">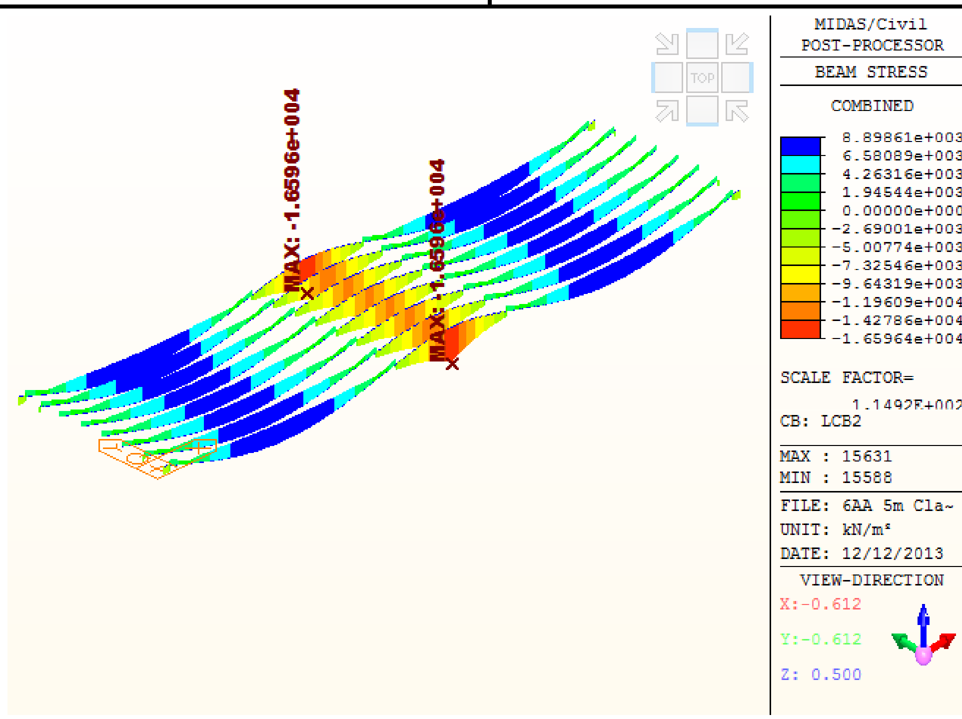
</td></tr>
</table>

2. The Effects depending on Soil Types

2.5. Abutment Stress (Pile Orientation: Strong-Axis, Expansion Case)

Abutment Stress (strong-axis) LCB1 (Expansion Case) Unit: kN/m^2	
Sand 1	16800
Sand 2	17280
Clay 1	14400
Clay 2	15990

<table>
<tr><th rowspan="2">Abutment</th><th colspan="2">Abutment Stress (strong-axis) Unit: kN/m^2</th></tr>
<tr><th>LCB1 (Expansion)</th><th>1.680E+04</th></tr>
<tr><td>Sand 1</td><td colspan="2">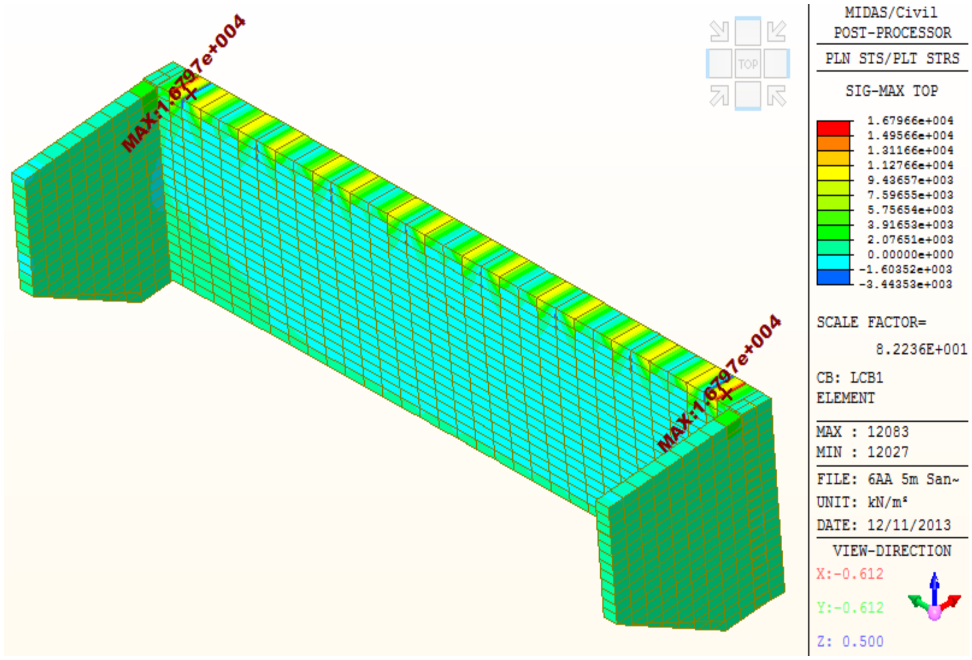
</td></tr>
<tr><th rowspan="2">Abutment</th><th colspan="2">Abutment Stress (strong-axis) Unit: kN/m^2</th></tr>
<tr><th>LCB1 (Expansion)</th><th>1.728E+04</th></tr>
<tr><td>Sand 2</td><td colspan="2">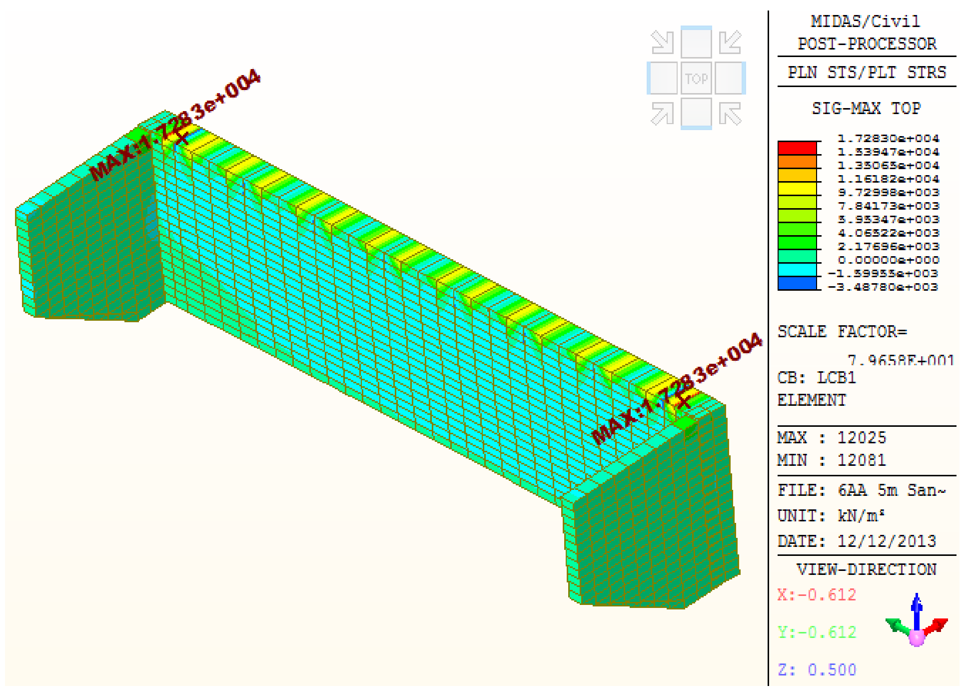
</td></tr>
</table>

<table>
<tr><td rowspan="2">Abutment</td><td colspan="2">Abutment Stress (strong-axis) Unit: kN/m^2</td></tr>
<tr><td>LCB1 (Expansion)</td><td>1.440E+04</td></tr>
<tr><td>Clay 1</td><td colspan="2">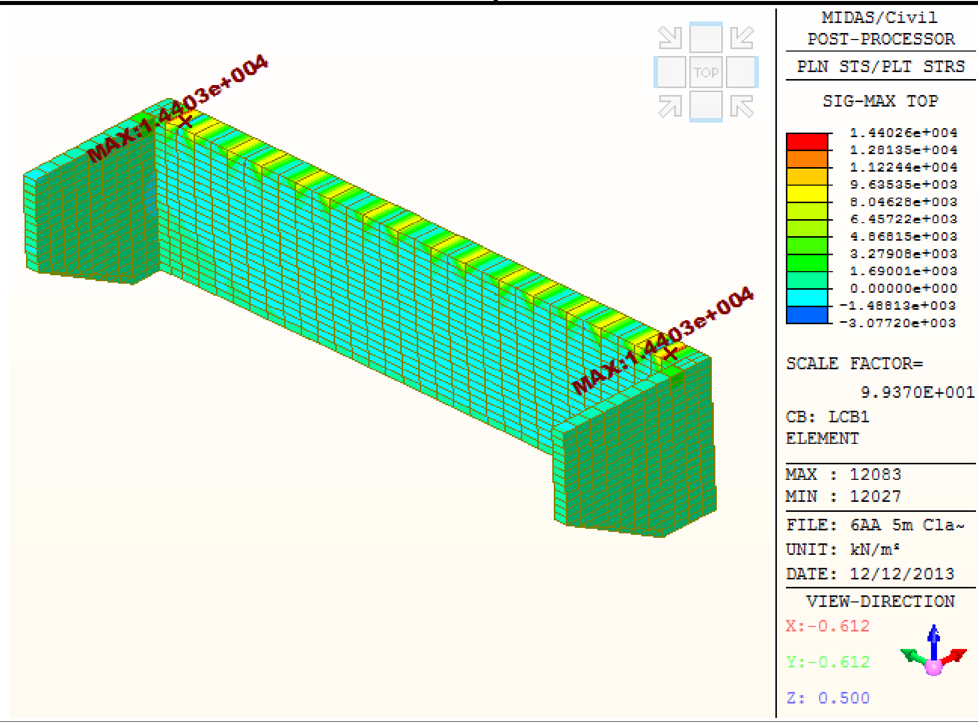
</td></tr>
<tr><td rowspan="2">Abutment</td><td colspan="2">Abutment Stress (strong-axis) Unit: kN/m^2</td></tr>
<tr><td>LCB1 (Expansion)</td><td>1.599E+04</td></tr>
<tr><td>Clay 2</td><td colspan="2">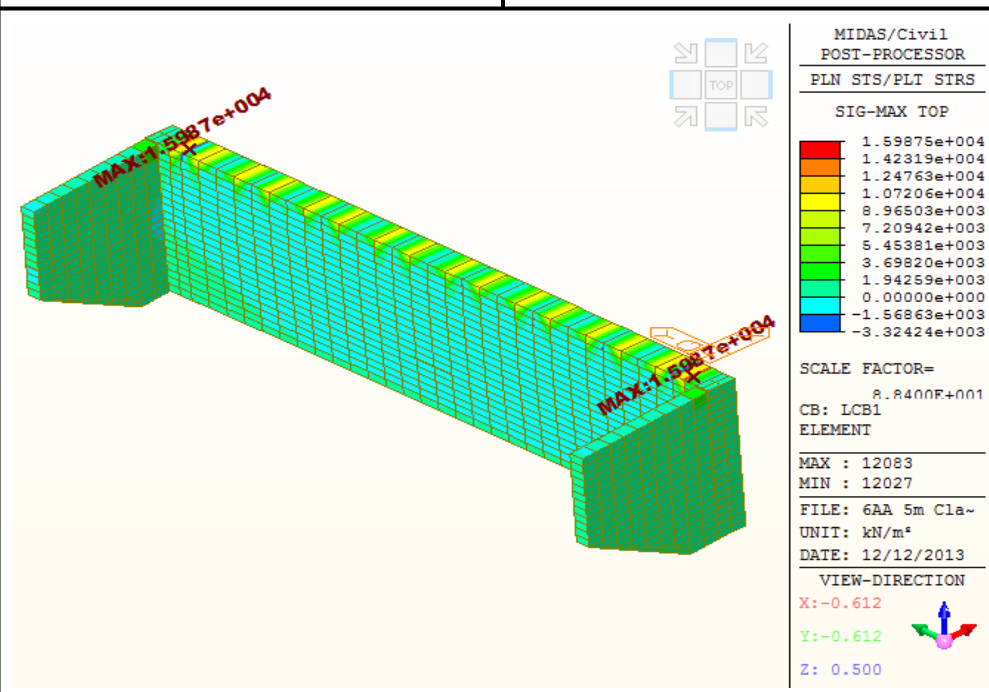
</td></tr>
</table>

2. The Effects depending on Soil Types

2.6. Abutment Stress (Pile Orientation: Strong-Axis, Contraction Case)

Abutment Stress (strong-axis) LCB2 (Contraction Case) Unit: kN/m^2	
Sand 1	8046
Sand 2	8138
Clay 1	7149
Clay 2	7738

<table>
<tr><td rowspan="2">Abutment</td><td colspan="2">Abutment Stress (strong-axis) Unit: kN/m^2</td></tr>
<tr><td>LCB2 (Contraction)</td><td>8.046E+03</td></tr>
<tr><td>Sand 1</td><td colspan="2">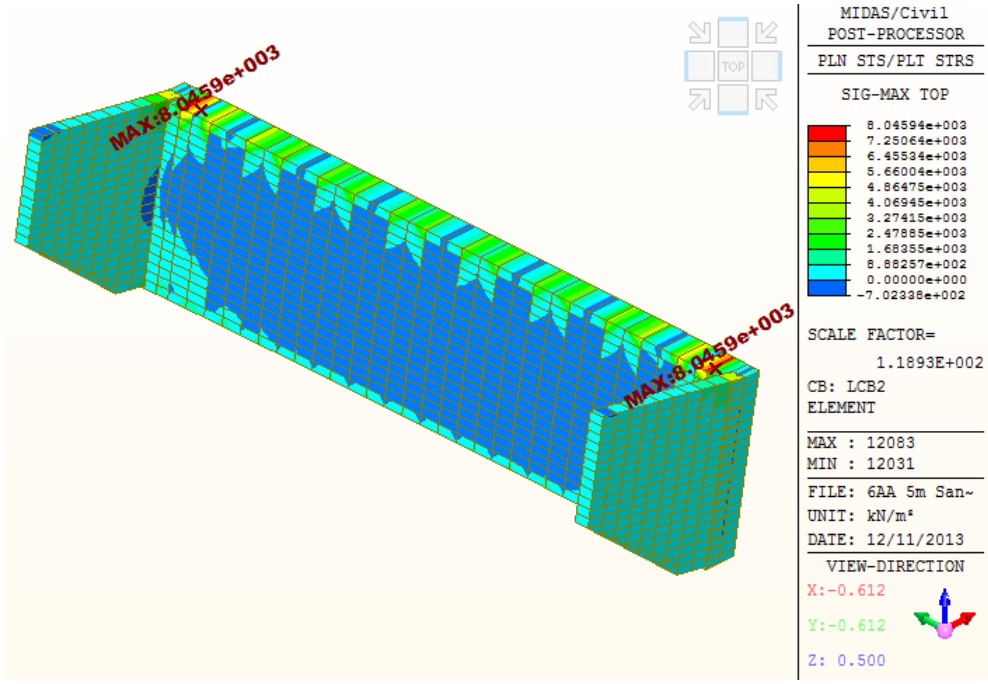
</td></tr>
</table>

<table>
<tr><td rowspan="2">Abutment</td><td colspan="2">Abutment Stress (strong-axis) Unit: kN/m^2</td></tr>
<tr><td>LCB2 (Contraction)</td><td>8.138E+03</td></tr>
<tr><td>Sand 2</td><td colspan="2">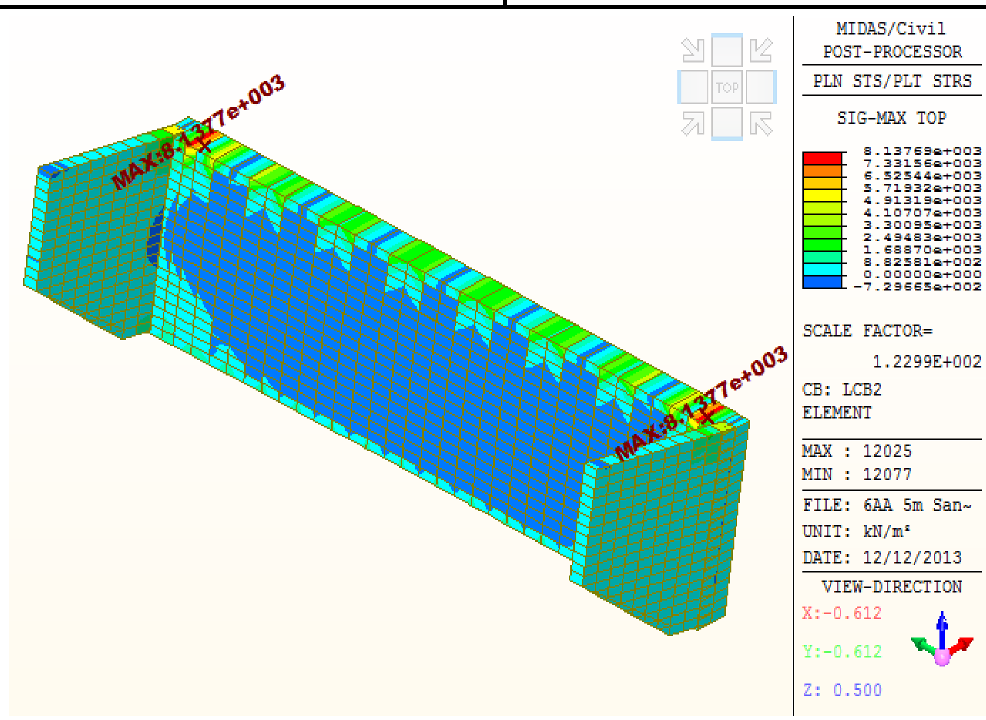
</td></tr>
</table>

<table>
<tr><td rowspan="2">Abutment</td><td colspan="2">Abutment Stress (strong-axis) Unit: kN/m^2</td></tr>
<tr><td>LCB2 (Contraction)</td><td>7.149E+03</td></tr>
<tr><td>Clay 1</td><td colspan="2">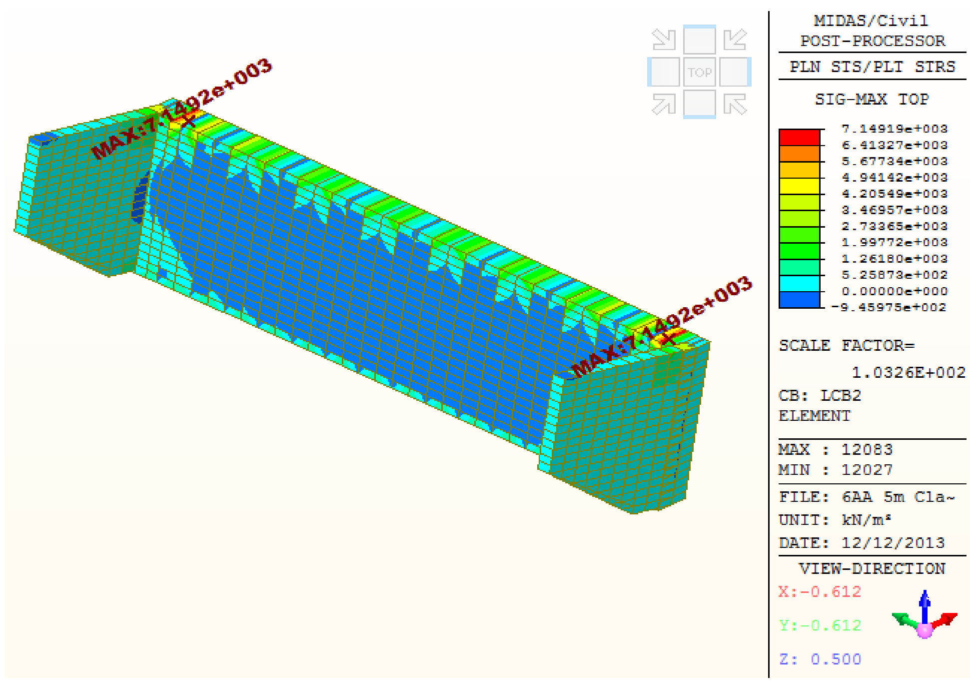
</td></tr>
<tr><td rowspan="2">Abutment</td><td colspan="2">Abutment Stress (strong-axis) Unit: kN/m^2</td></tr>
<tr><td>LCB2 (Contraction)</td><td>7.738E+03</td></tr>
<tr><td>Clay 2</td><td colspan="2">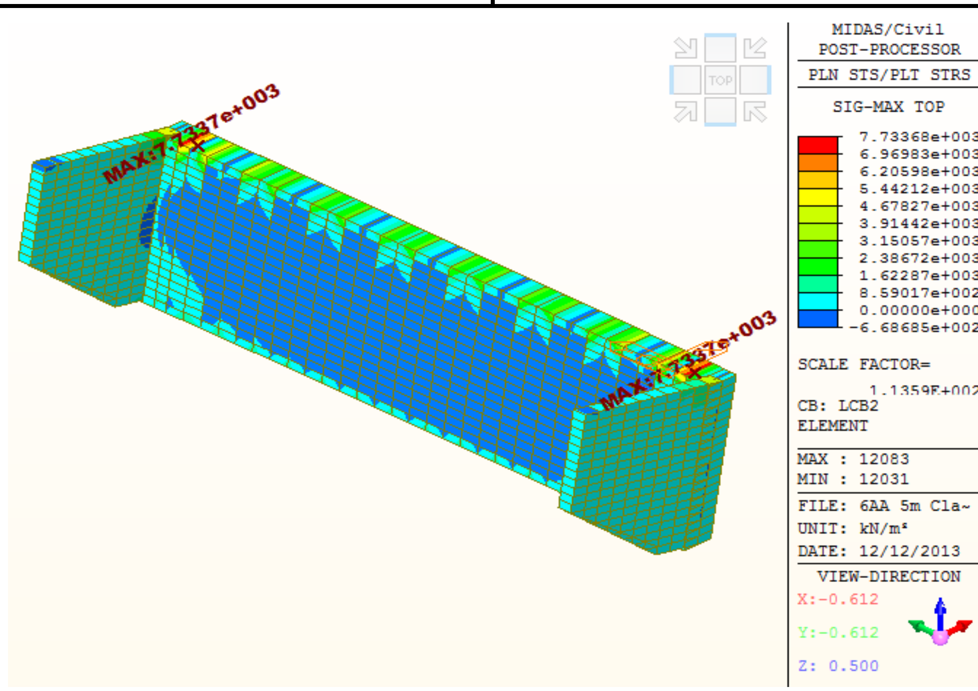
</td></tr>
</table>

2. The Effects depending on Soil Types

2.7. Abutment Stress (Pile Orientation: Weak-Axis, Expansion Case)

Abutment Stress (weak-axis) LCB1 (Expansion Case) Unit: kN/m^2	
Sand 1	**16640**
Sand 2	**17220**
Clay 1	**13480**
Clay 2	**15450**

<table>
<tr><td rowspan="2">Abutment</td><td colspan="2">Abutment Stress (weak-axis) Unit: kN/m^2</td></tr>
<tr><td>LCB1 (Expansion)</td><td>1.664E+04</td></tr>
<tr><td>Sand 1</td><td colspan="2">
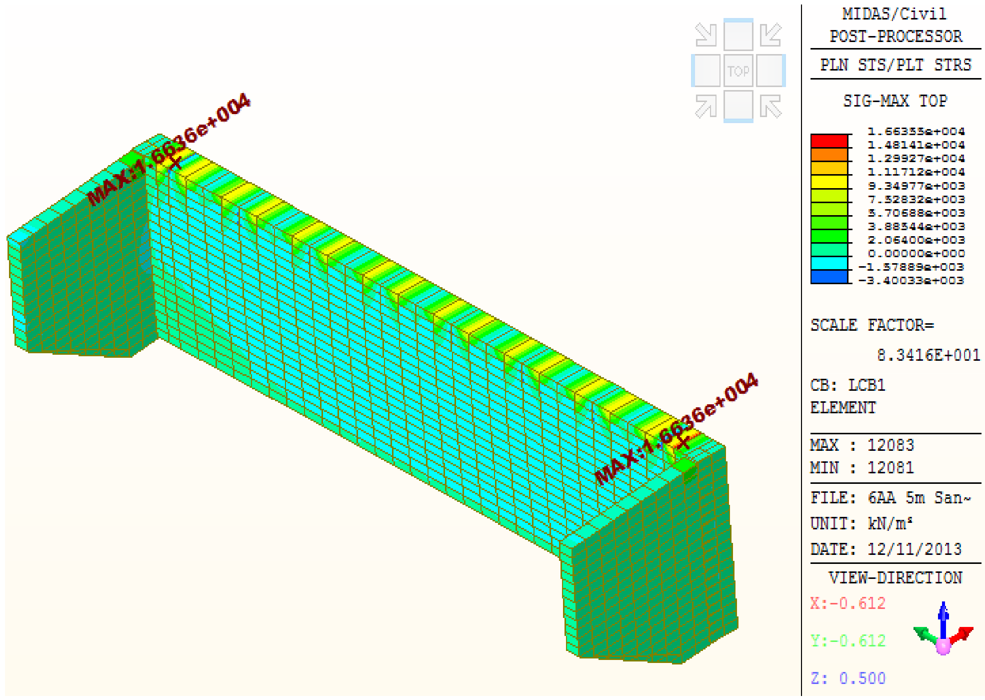

</td></tr>
<tr><td rowspan="2">Abutment</td><td colspan="2">Abutment Stress (weak-axis) Unit: kN/m^2</td></tr>
<tr><td>LCB1 (Expansion)</td><td>1.722E+04</td></tr>
<tr><td>Sand 2</td><td colspan="2">
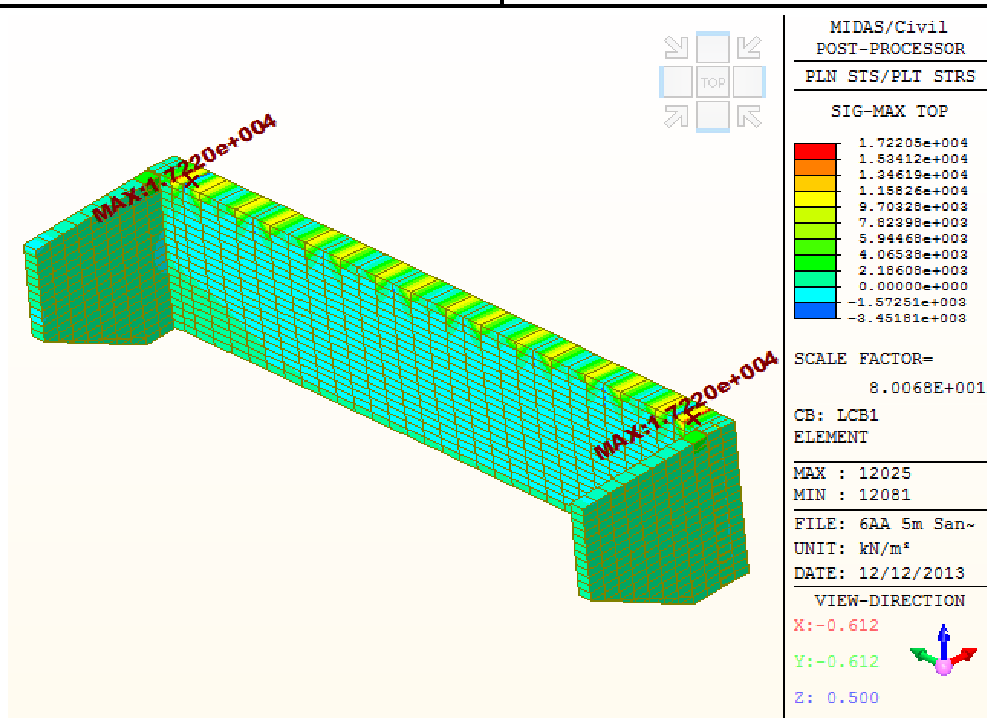

</td></tr>
</table>

<table>
<tr><td rowspan="2">Abutment</td><td colspan="2">Abutment Stress (weak-axis) Unit: kN/m²</td></tr>
<tr><td>LCB1 (Expansion)</td><td>1.348E+04</td></tr>
<tr><td>Clay 1</td><td colspan="2">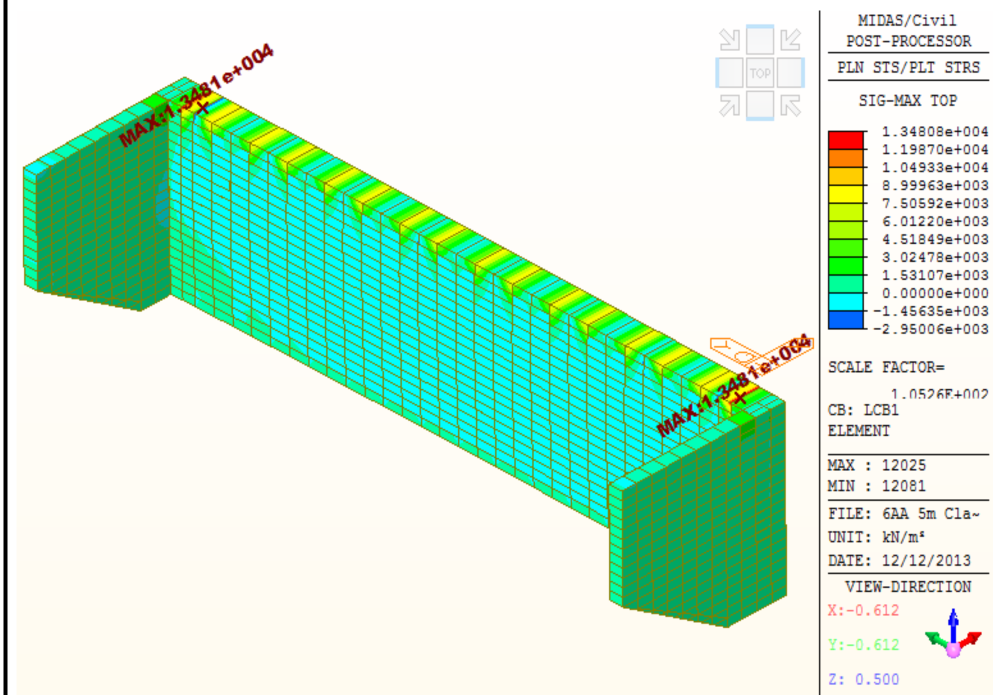
</td></tr>
<tr><td rowspan="2">Abutment</td><td colspan="2">Abutment Stress (weak-axis) Unit: kN/m²</td></tr>
<tr><td>LCB1 (Expansion)</td><td>1.545E+04</td></tr>
<tr><td>Clay 2</td><td colspan="2">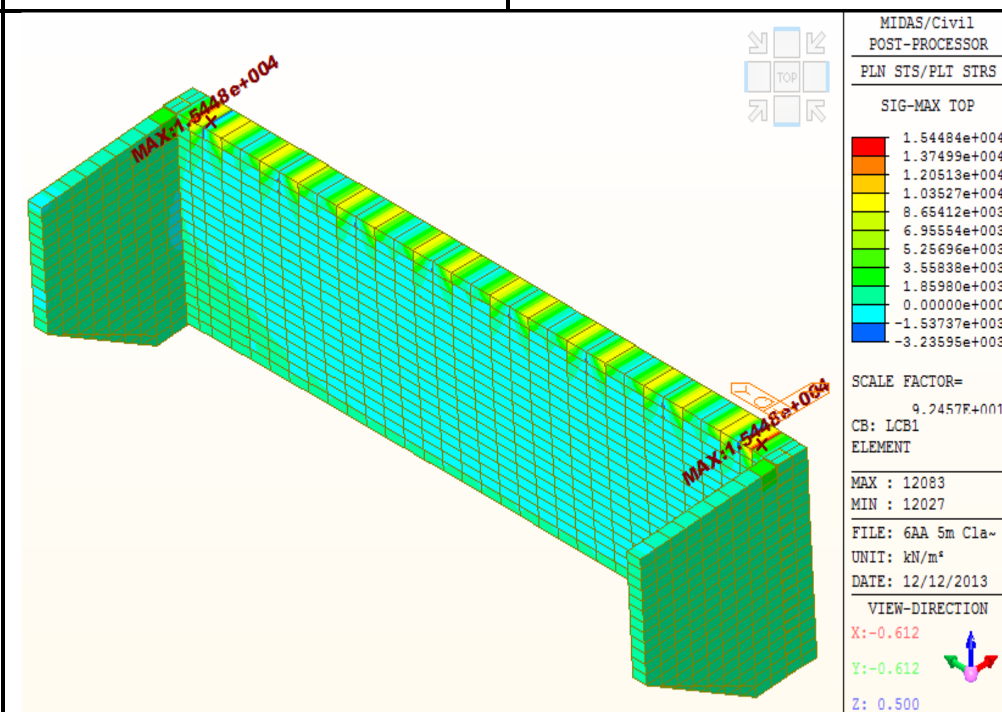
</td></tr>
</table>

2. The Effects depending on Soil Types

2.8. Abutment Stress (Pile Orientation: Weak-Axis, Contraction Case)

Abutment Stress (weak-axis) LCB2 (Contraction Case) Unit: kN/m^2	
Sand 1	7782
Sand 2	7953
Clay 1	6374
Clay 2	7195

<table>
<tr><td rowspan="2">Abutment</td><td colspan="2">Abutment Stress (weak-axis) Unit: kN/m^2</td></tr>
<tr><td>LCB2 (Contraction)</td><td>7.782E+03</td></tr>
<tr><td>Sand 1</td><td colspan="2">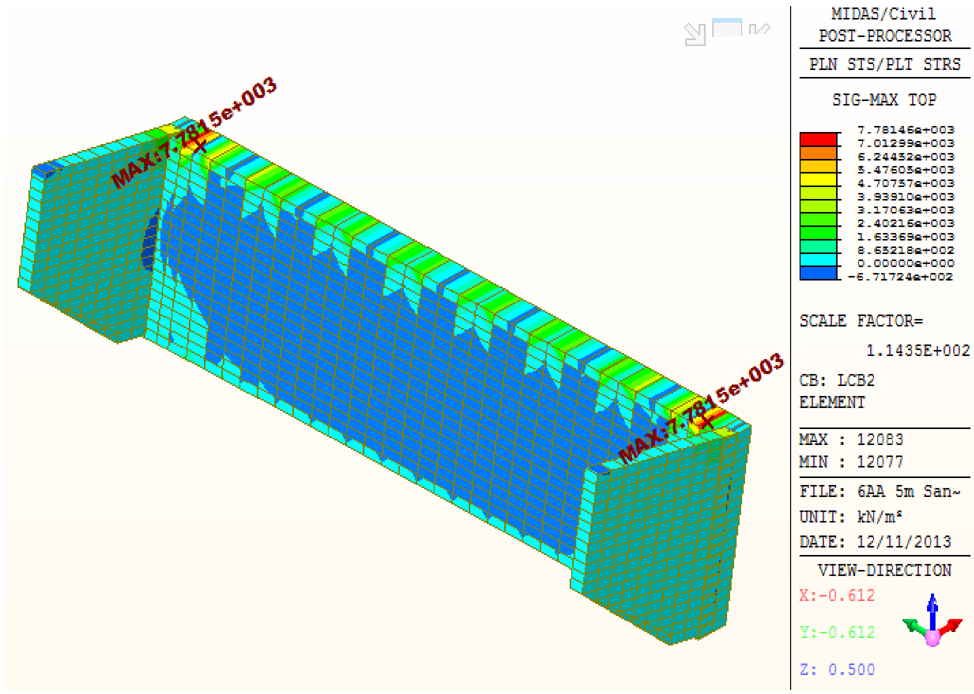
</td></tr>
<tr><td rowspan="2">Abutment</td><td colspan="2">Abutment Stress (weak-axis) Unit: kN/m^2</td></tr>
<tr><td>LCB2 (Contraction)</td><td>7.953E+03</td></tr>
<tr><td>Sand 2</td><td colspan="2">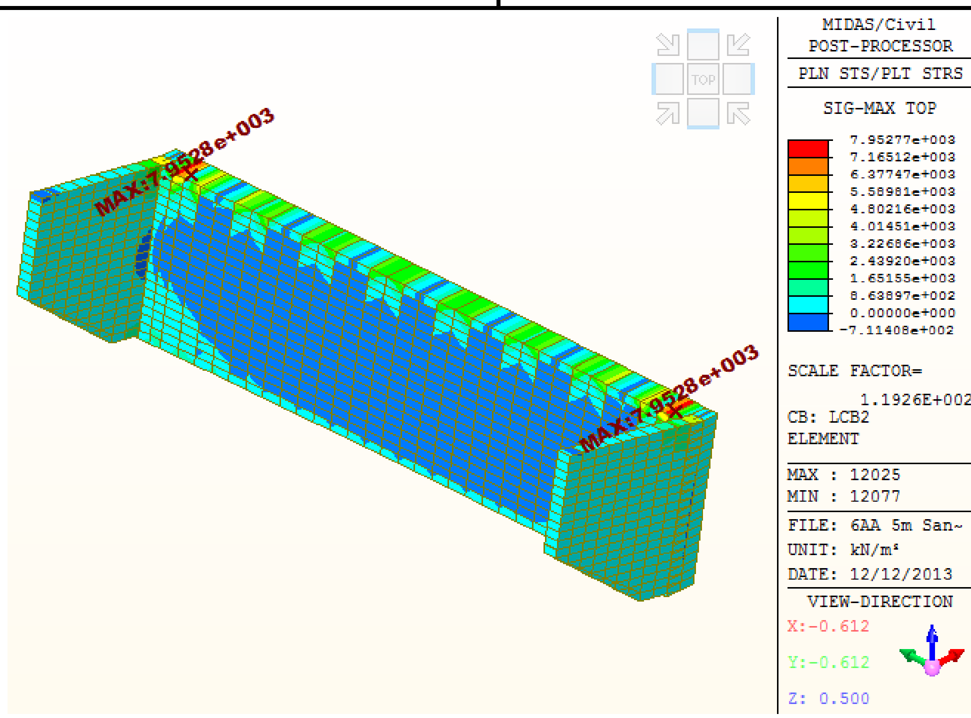
</td></tr>
</table>

Abutment	Abutment Stress (weak-axis) Unit: kN/m^2	
	LCB2 (Contraction)	6.374E+03
Clay 1	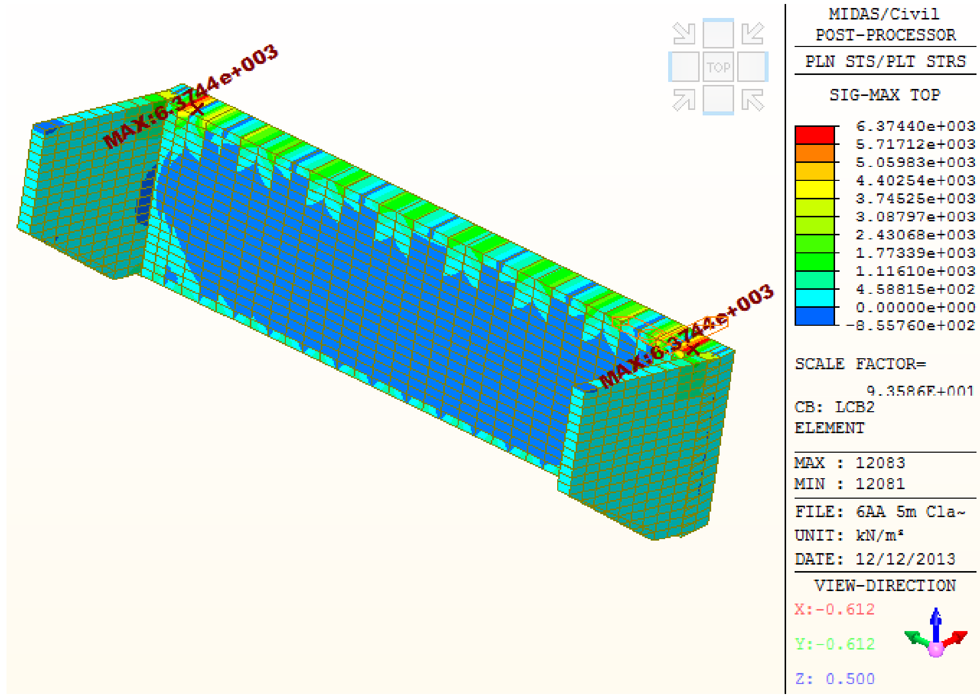	
Abutment	Abutment Stress (weak-axis) Unit: kN/m^2	
	LCB2 (Contraction)	7.195E+03
Clay 2	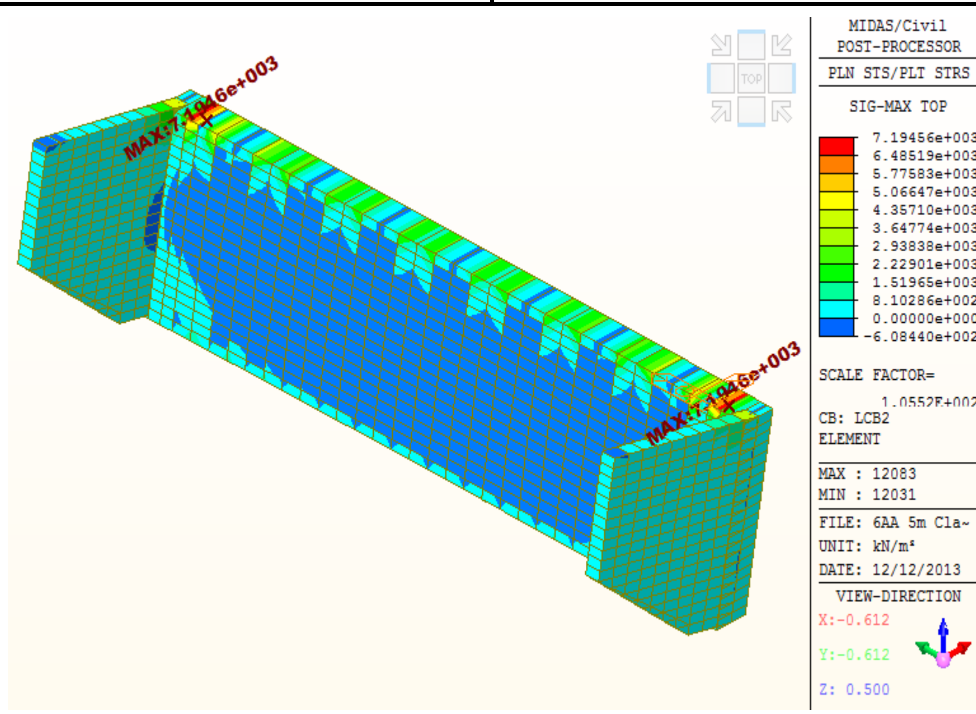	

2. The Effects depending on Soil Types

2.9. Pile Moment (Pile Orientation: Strong-Axis, Expansion Case)

Pile Moment (strong-axis) LCB1 (Expansion Case) Unit: kN·m	
Sand 1	-82.54
Sand 2	-58.73
Clay 1	-135.8
Clay 2	-111.6

Abutment	Pile Moment (strong-axis) Unit: kN·m	
	LCB1 (Expansion)	-8.254E+01
Sand 1	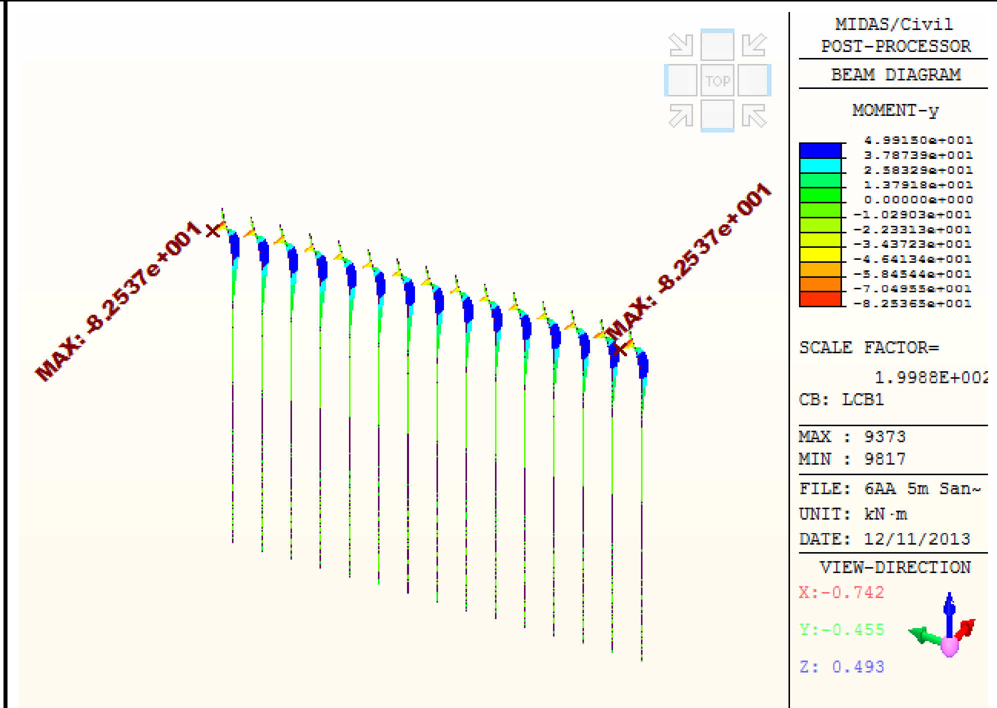	

Abutment	Pile Moment (strong-axis) Unit: kN·m	
	LCB1 (Expansion)	-5.873E+01
Sand 2	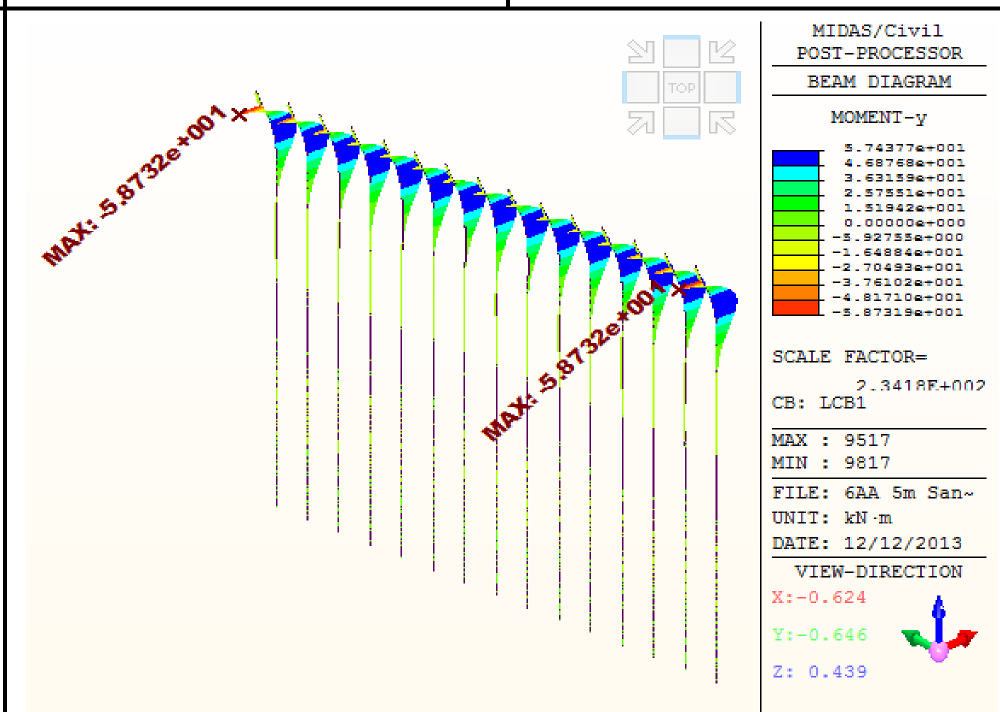	

<table>
<tr><td rowspan="2">Abutment</td><td colspan="2">Pile Moment (strong-axis) Unit: kN·m</td></tr>
<tr><td>LCB1 (Expansion)</td><td>-1.358E+02</td></tr>
<tr><td>Clay 1</td><td colspan="2">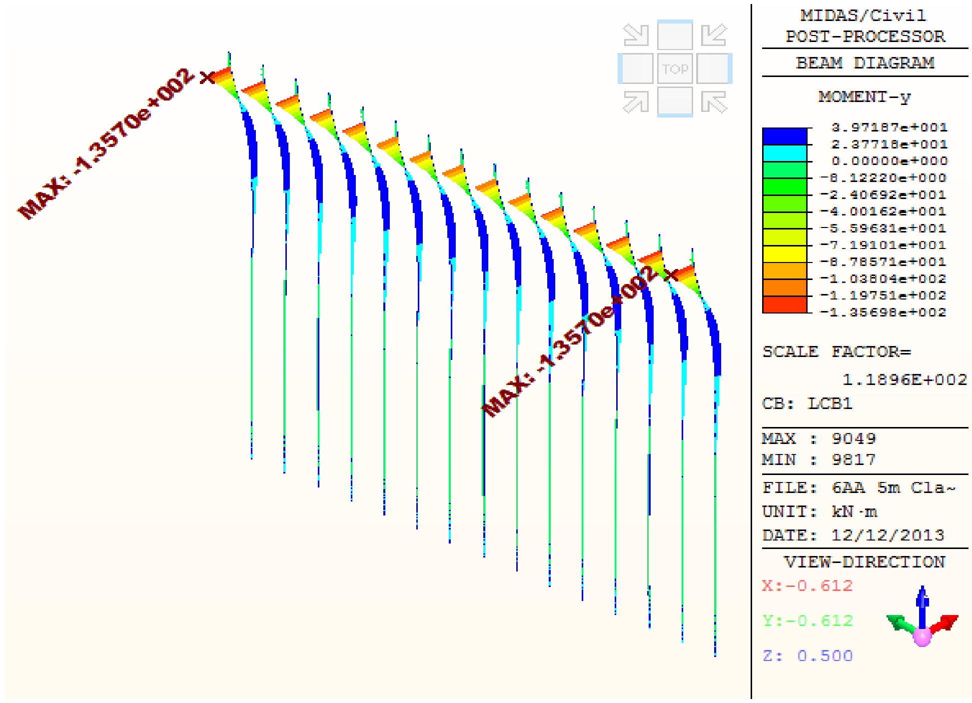
</td></tr>
<tr><td rowspan="2">Abutment</td><td colspan="2">Pile Moment (strong-axis) Unit: kN·m</td></tr>
<tr><td>LCB1 (Expansion)</td><td>-1.116E+02</td></tr>
<tr><td>Clay 2</td><td colspan="2">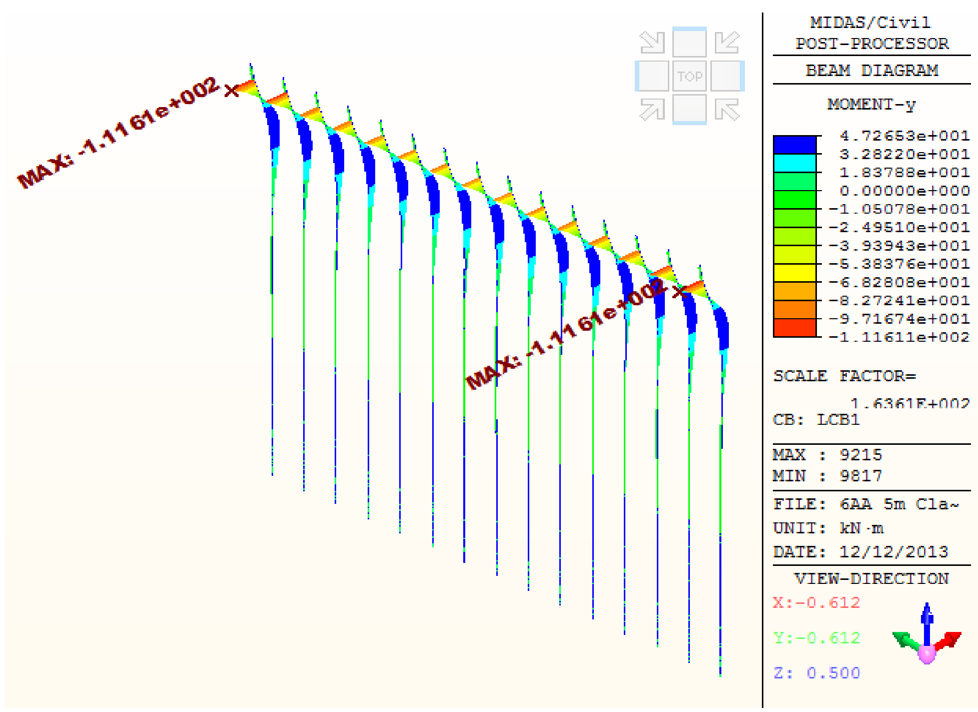
</td></tr>
</table>

2. The Effects depending on Soil Types

2.10. Pile Moment (Pile Orientation: Strong-Axis, Contraction Case)

Pile Moment (strong-axis) LCB2 (Contraction Case) Unit: kN·m	
Sand 1	-147.1
Sand 2	-161.8
Clay 1	-134.6
Clay 2	-147.8

<table>
<tr><td rowspan="2">Abutment</td><td colspan="2">Pile Moment (strong-axis)   Unit: kN·m</td></tr>
<tr><td>LCB2 (Contraction)</td><td>-1.471E+02</td></tr>
<tr><td>Sand 1</td><td colspan="2">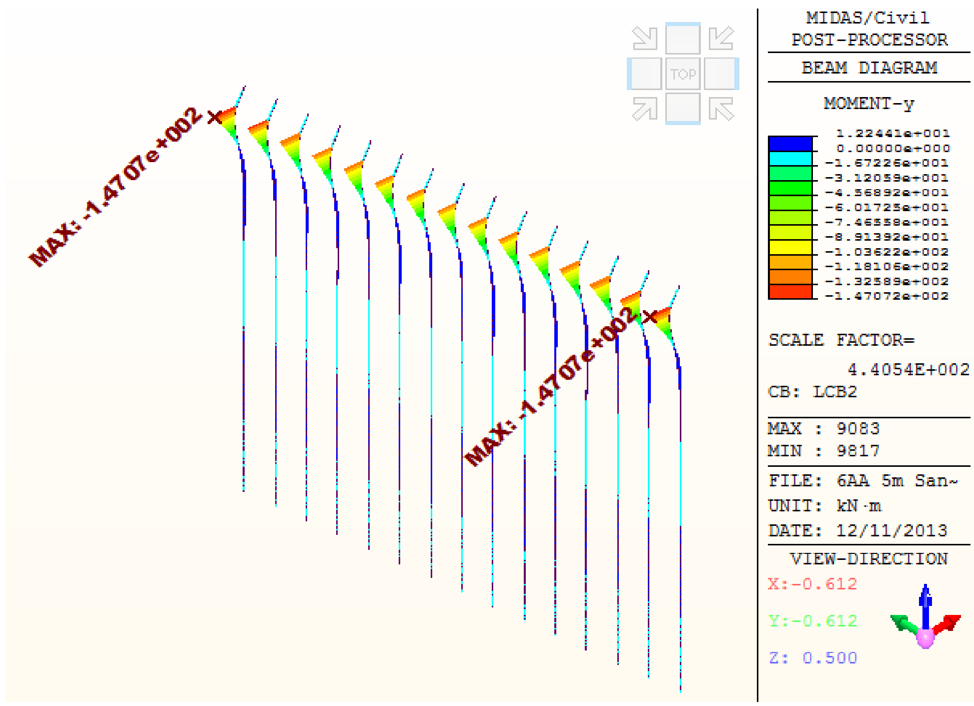
</td></tr>
<tr><td rowspan="2">Abutment</td><td colspan="2">Pile Moment (strong-axis)   Unit: kN·m</td></tr>
<tr><td>LCB2 (Contraction)</td><td>-1.618E+02</td></tr>
<tr><td>Sand 2</td><td colspan="2">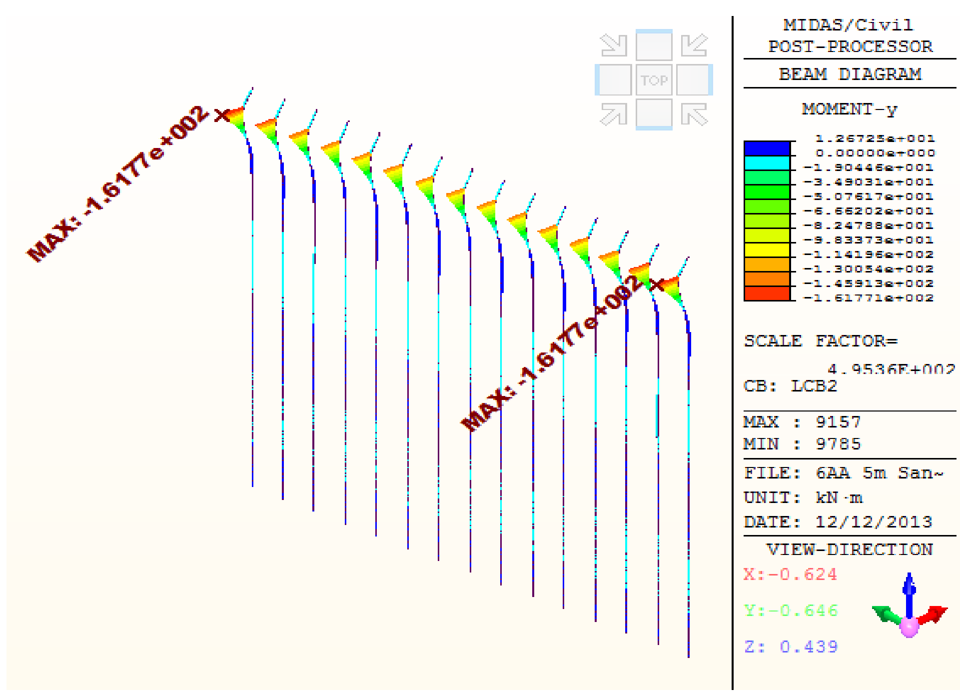
</td></tr>
</table>

<table>
<tr><td rowspan="2">Abutment</td><td colspan="2">Pile Moment (strong-axis)   Unit: kN·m</td></tr>
<tr><td>LCB2 (Contraction)</td><td>-1.346E+02</td></tr>
<tr><td>Clay 1</td><td colspan="2">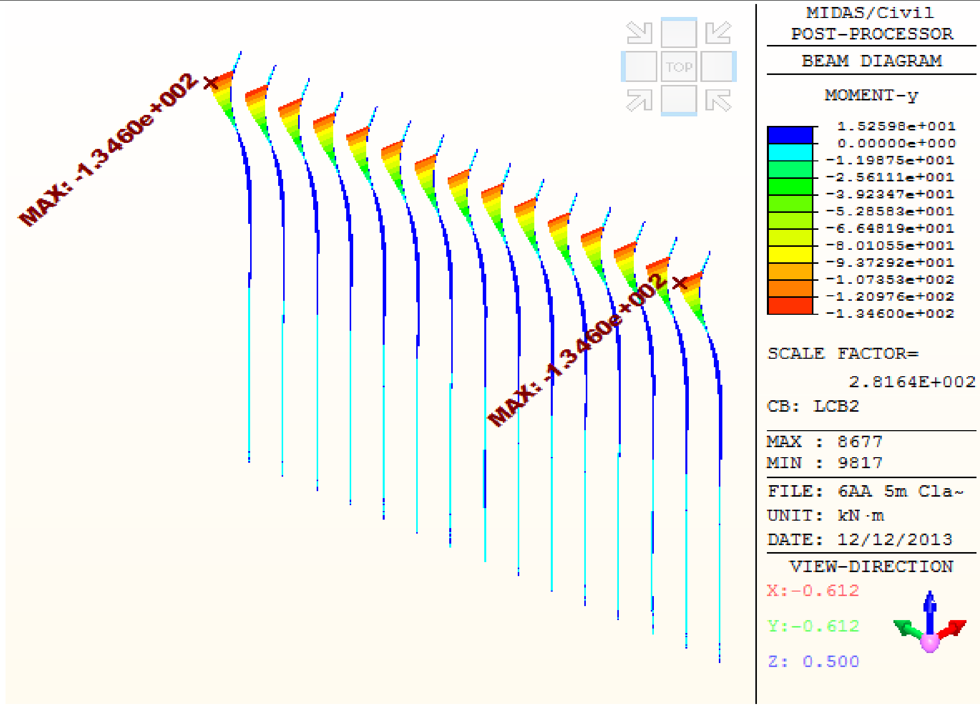
</td></tr>
<tr><td rowspan="2">Abutment</td><td colspan="2">Pile Moment (strong-axis)   Unit: kN·m</td></tr>
<tr><td>LCB2 (Contraction)</td><td>-1.478E+02</td></tr>
<tr><td>Clay 2</td><td colspan="2">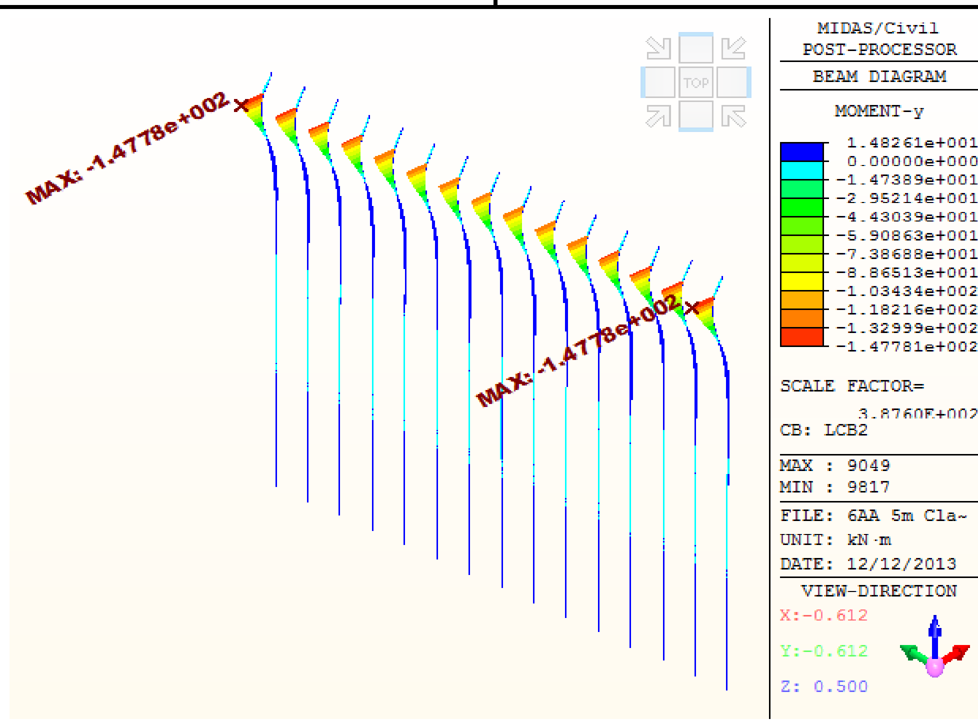
</td></tr>
</table>

2. The Effects depending on Soil Types

2.11. Pile Moment (Pile Orientation: Weak-Axis, Expansion Case)

Pile Moment (weak-axis) LCB1 (Expansion Case) Unit: kN m	
Sand 1	**-4.154**
Sand 2	**-4.72**
Clay 1	**-2.793**
Clay 2	**-3.688**

<table>
<tr><td rowspan="2">Abutment</td><td colspan="2">Pile Moment (weak-axis) Unit: kN·m</td></tr>
<tr><td>LCB1 (Expansion)</td><td>-4.154E+00</td></tr>
<tr><td>Sand 1</td><td colspan="2">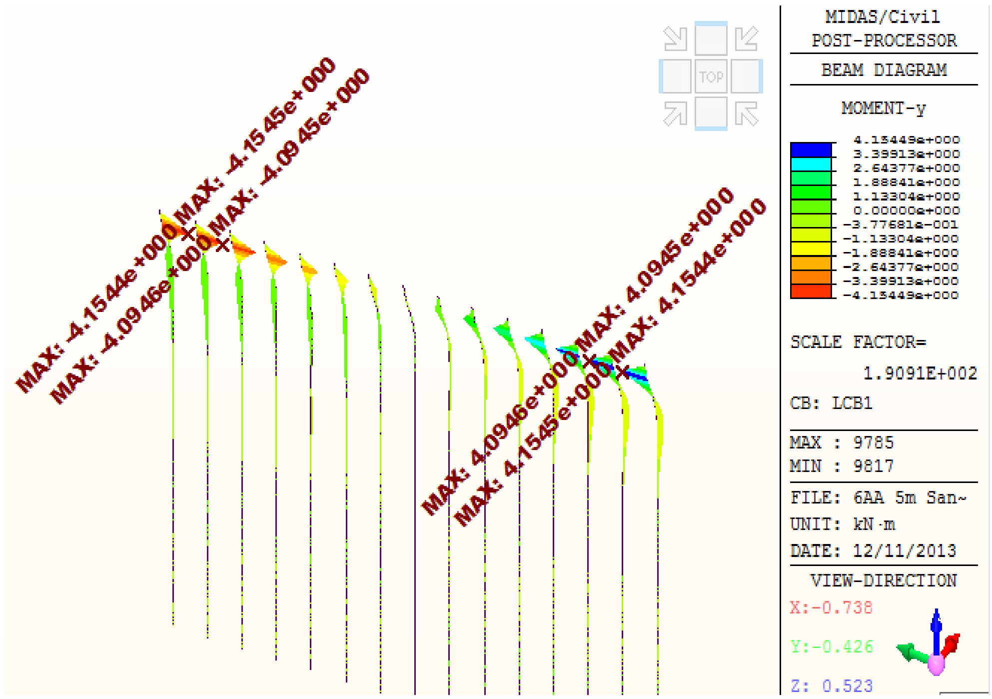
</td></tr>
<tr><td rowspan="2">Abutment</td><td colspan="2">Pile Moment (weak-axis) Unit: kN·m</td></tr>
<tr><td>LCB1 (Expansion)</td><td>-4.720E+00</td></tr>
<tr><td>Sand 2</td><td colspan="2">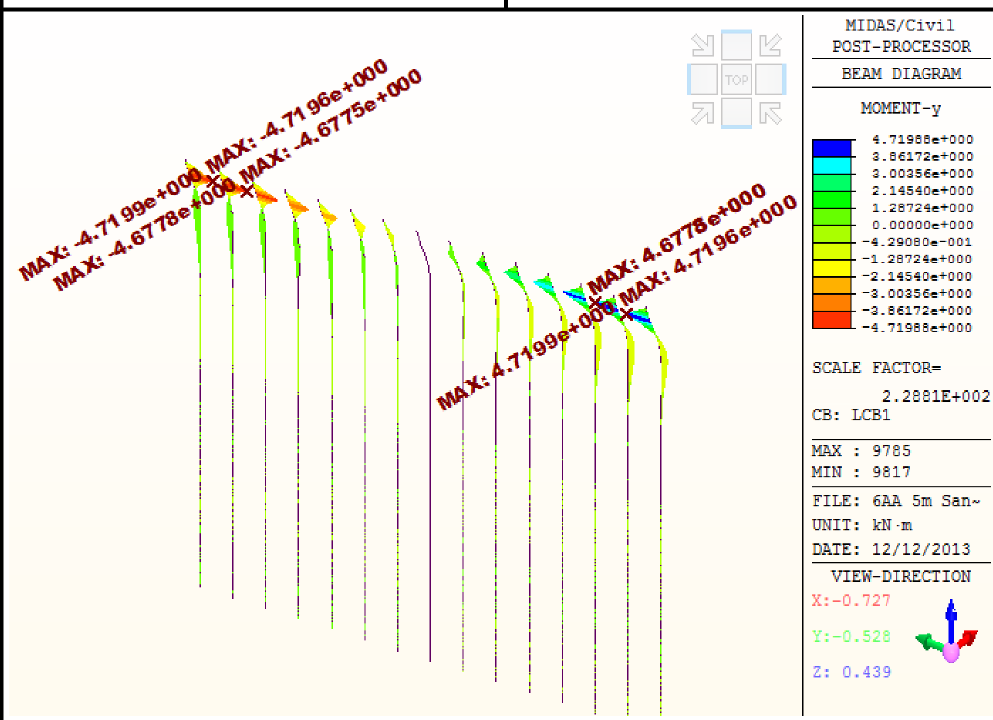
</td></tr>
</table>

Abutment	Pile Moment (weak-axis) Unit: kN·m	
	LCB1 (Expansion)	-2.793E+00
Clay 1	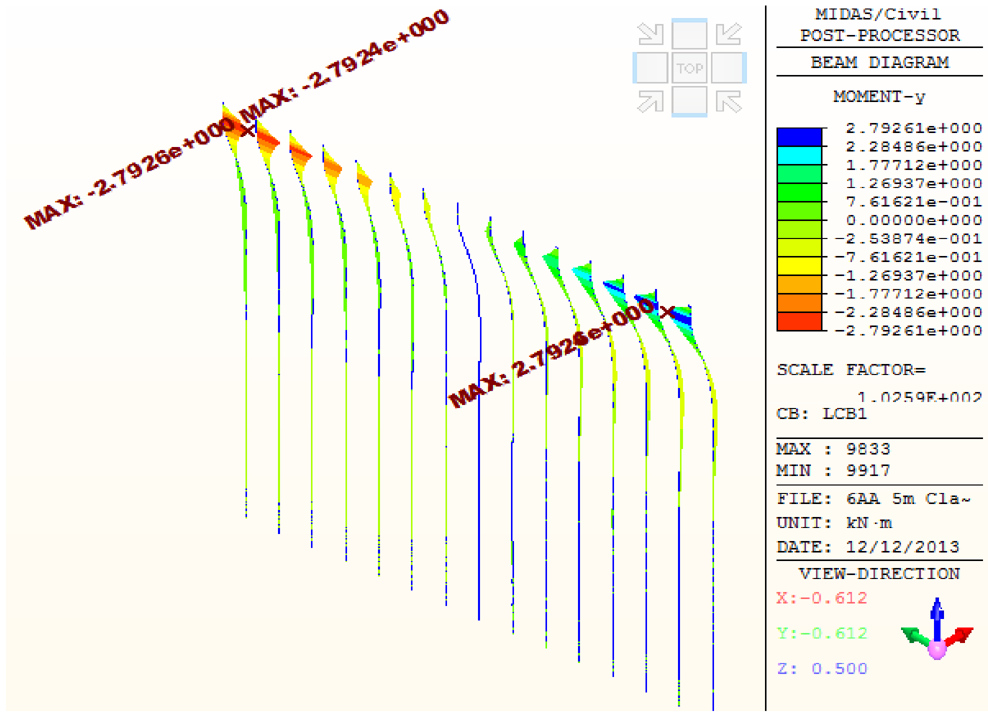	

Abutment	Pile Moment (weak-axis) Unit: kN·m	
	LCB1 (Expansion)	-3.688E+00
Clay 2	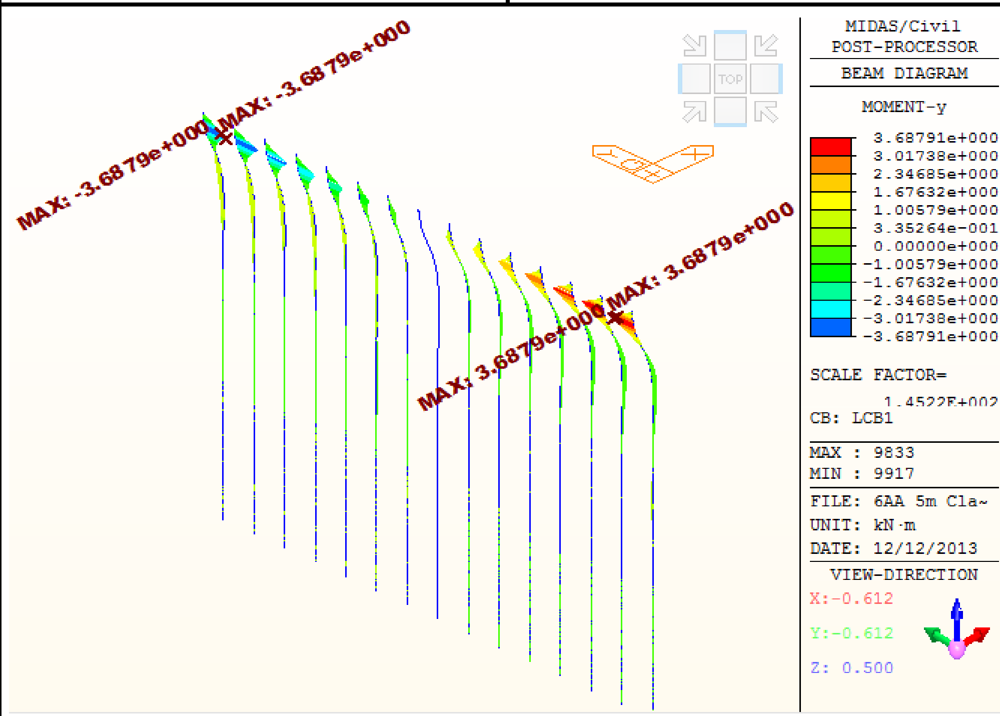	

2. The Effects depending on Soil Types

2.12. Pile Moment (Pile Orientation: Weak-Axis, Contraction Case)

Pile Moment (weak-axis) LCB2 (Contraction Case) Unit: kN m	
Sand 1	**-4.319**
Sand 2	**-4.85**
Clay 1	**-2.907**
Clay 2	**-3.826**

<table>
<tr><td rowspan="2">Abutment</td><td colspan="2">Pile Moment (weak-axis) Unit: kN·m</td></tr>
<tr><td>LCB2 (Contraction)</td><td>-4.319E+00</td></tr>
<tr><td>Sand 1</td><td colspan="2">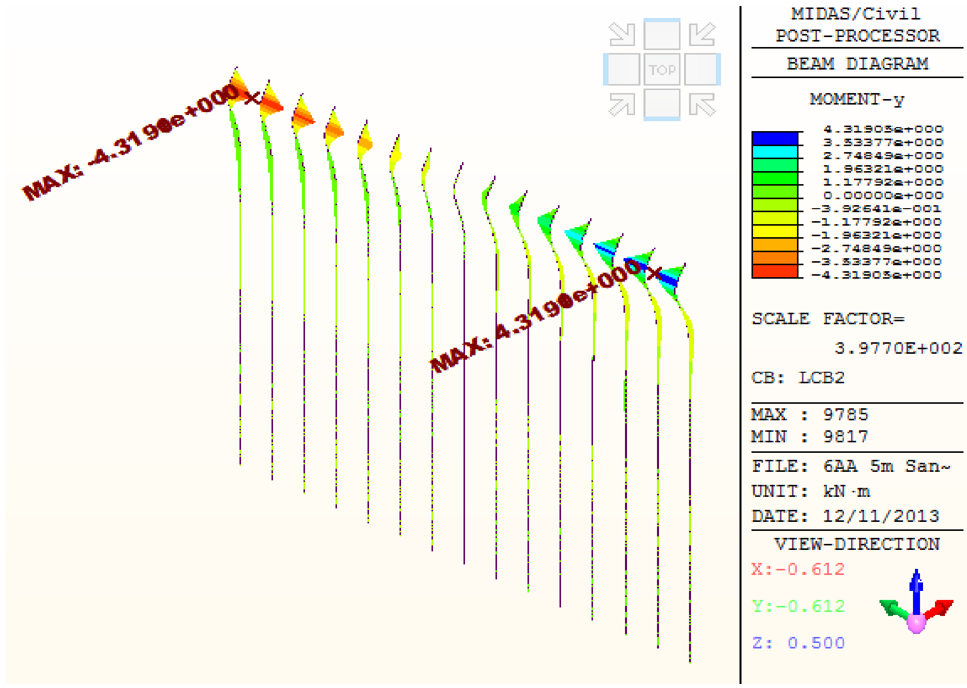
</td></tr>
<tr><td rowspan="2">Abutment</td><td colspan="2">Pile Moment (weak-axis) Unit: kN·m</td></tr>
<tr><td>LCB2 (Contraction)</td><td>-4.850E+00</td></tr>
<tr><td>Sand 2</td><td colspan="2">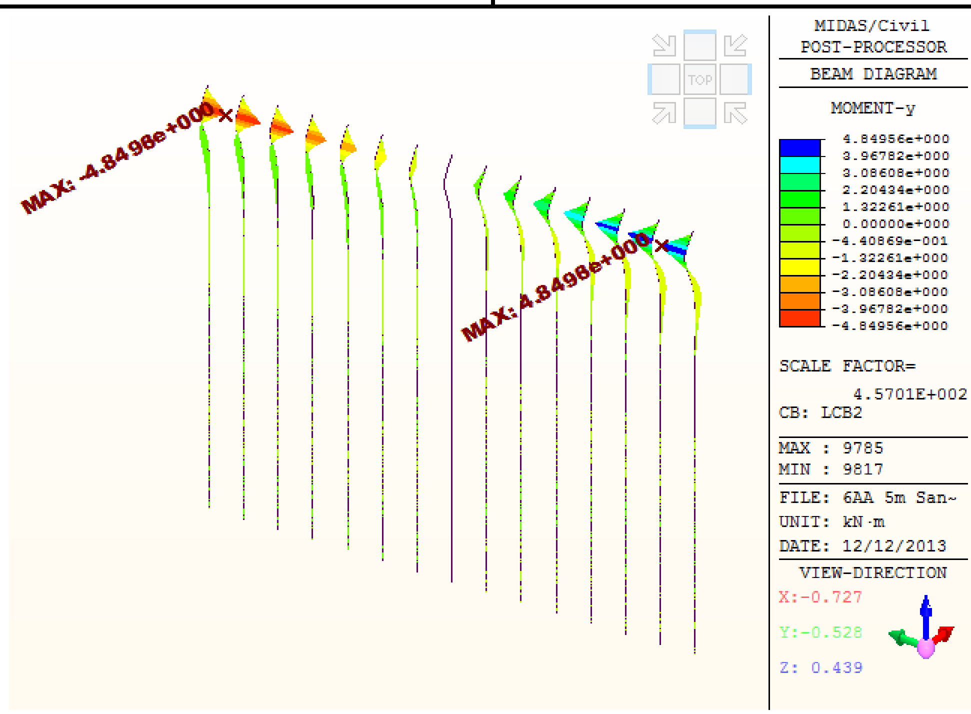
</td></tr>
</table>

<table>
<tr><td rowspan="2">Abutment</td><td colspan="2">Pile Moment (weak-axis) Unit: kN·m</td></tr>
<tr><td>LCB2 (Contraction)</td><td>-2.907E+00</td></tr>
<tr><td>Clay 1</td><td colspan="2">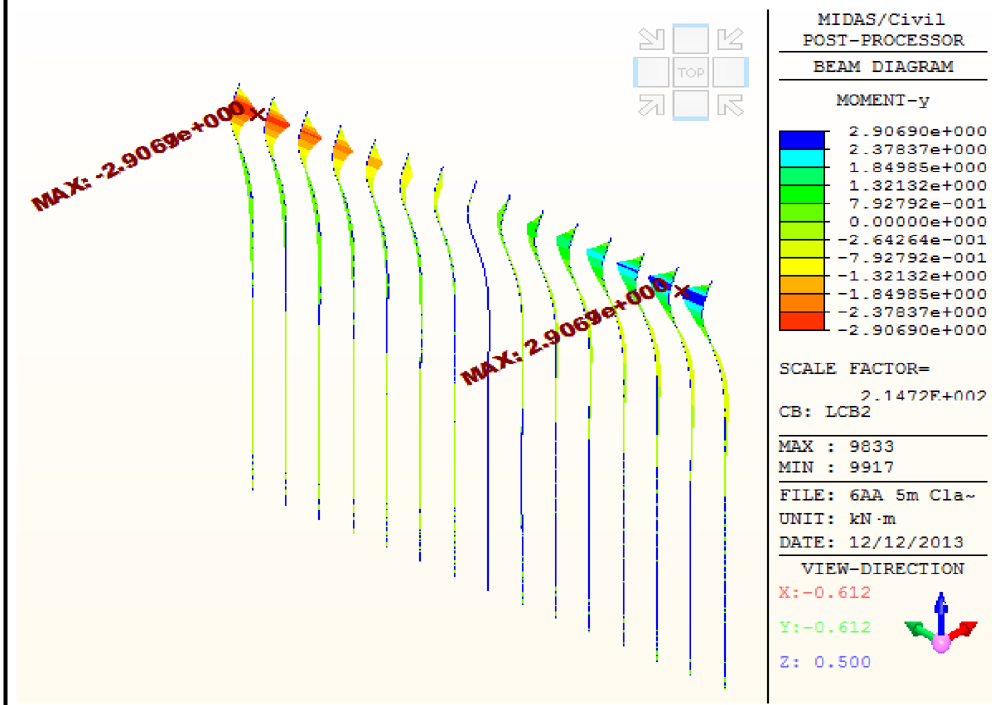
</td></tr>
<tr><td rowspan="2">Abutment</td><td colspan="2">Pile Moment (weak-axis) Unit: kN·m</td></tr>
<tr><td>LCB2 (Contraction)</td><td>-3.826E+00</td></tr>
<tr><td>Clay 2</td><td colspan="2">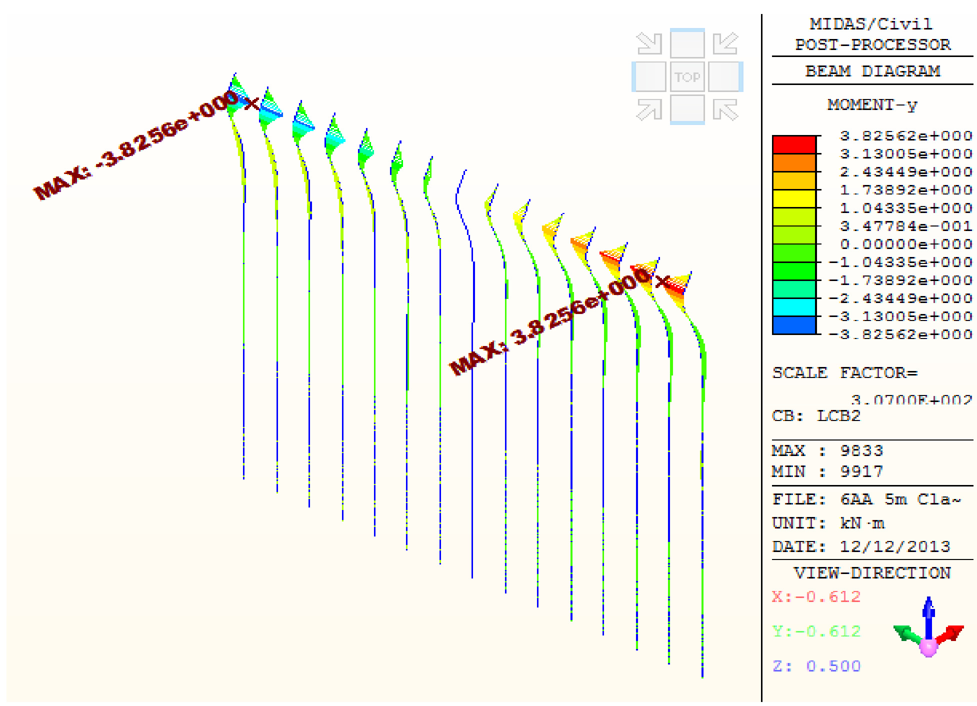
</td></tr>
</table>

2. The Effects depending on Soil Types

2.13. Pile Stress (Pile Orientation: Strong-Axis, Expansion Case)

Pile Stress (strong-axis) LCB1 (Expansion Case) Unit: kN/m^2	
Sand 1	-81580
Sand 2	-69050
Clay 1	-109700
Clay 2	-97490

Abutment	Pile Stress (strong-axis) Unit: kN/m^2	
	LCB1 (Expansion)	-8.158E+04
Sand 1	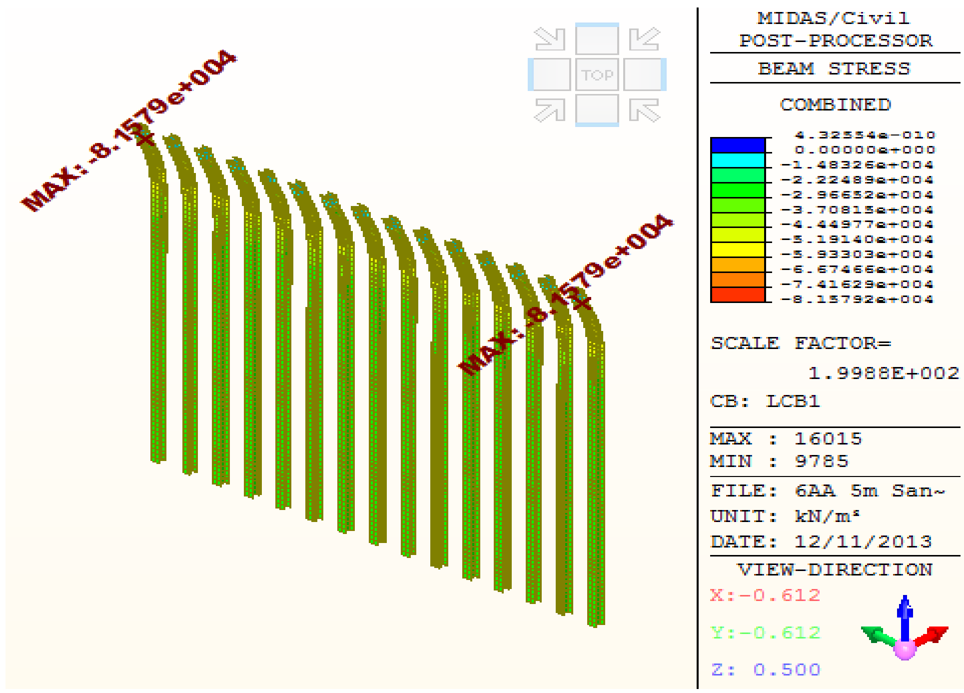	

Abutment	Pile Stress (strong-axis) Unit: kN/m^2	
	LCB1 (Expansion)	-6.905E+04
Sand 2	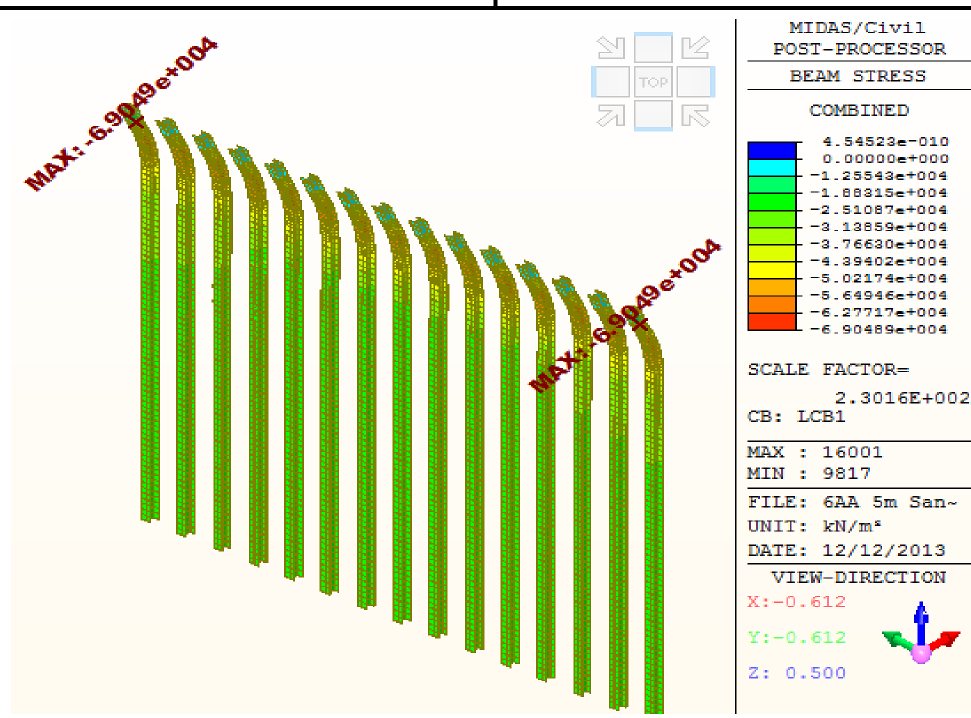	

<table>
<tr><td rowspan="2">Abutment</td><td colspan="2">Pile Stress (strong-axis) Unit: kN/m^2</td></tr>
<tr><td>LCB1 (Expansion)</td><td>-1.097E+05</td></tr>
<tr><td>Clay 1</td><td colspan="2">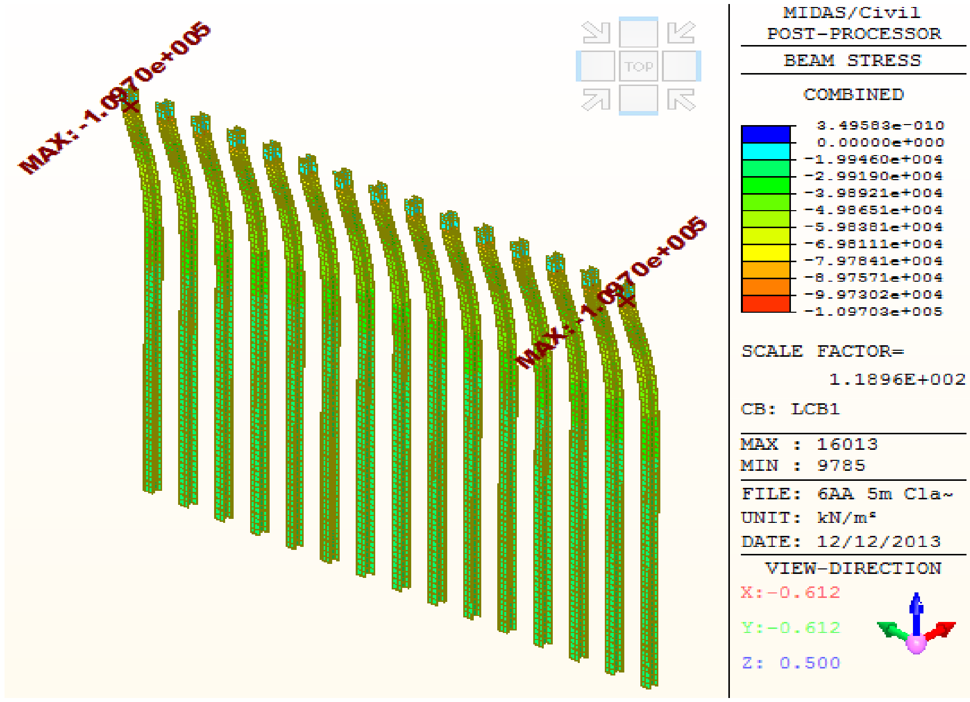
</td></tr>
<tr><td rowspan="2">Abutment</td><td colspan="2">Pile Stress (strong-axis) Unit: kN/m^2</td></tr>
<tr><td>LCB1 (Expansion)</td><td>-9.749E+04</td></tr>
<tr><td>Clay 2</td><td colspan="2">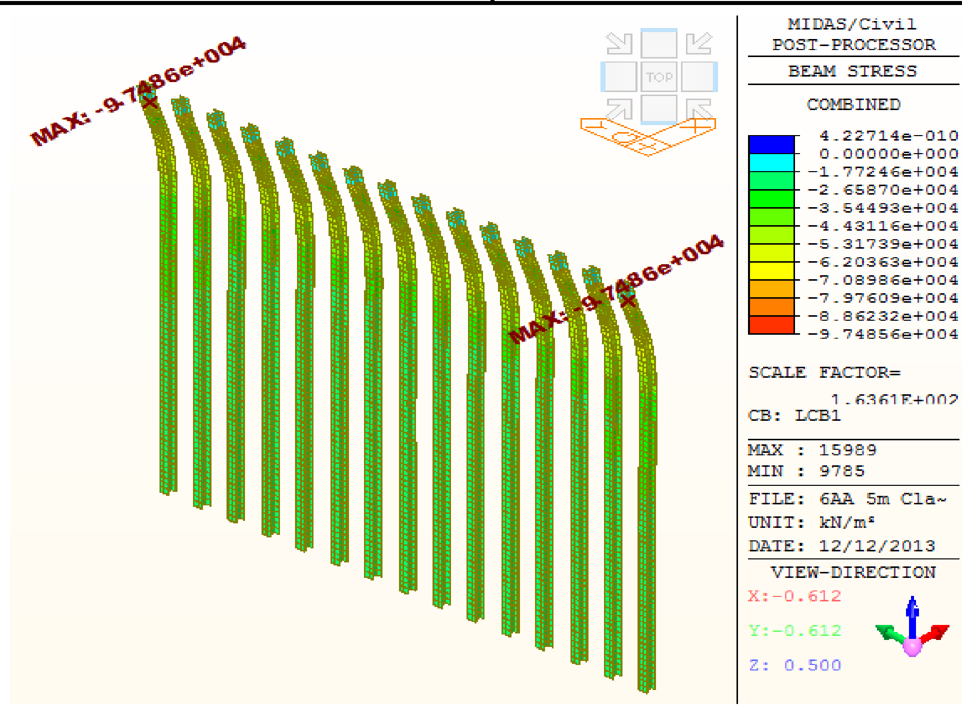
</td></tr>
</table>

2. The Effects depending on Soil Types

2.14. Pile Stress (Pile Orientation: Strong-Axis, Contraction Case)

Pile Stress (strong-axis) LCB2 (Contraction Case) Unit: kN/m^2	
Sand 1	-116800
Sand 2	-126400
Clay 1	-107400
Clay 2	-116500

<table>
<tr><th rowspan="2">Abutment</th><th colspan="2">Pile Stress (strong-axis) Unit: kN/m^2</th></tr>
<tr><th>LCB2 (Contraction)</th><th>-1.168E+05</th></tr>
<tr><td>Sand 1</td><td colspan="2">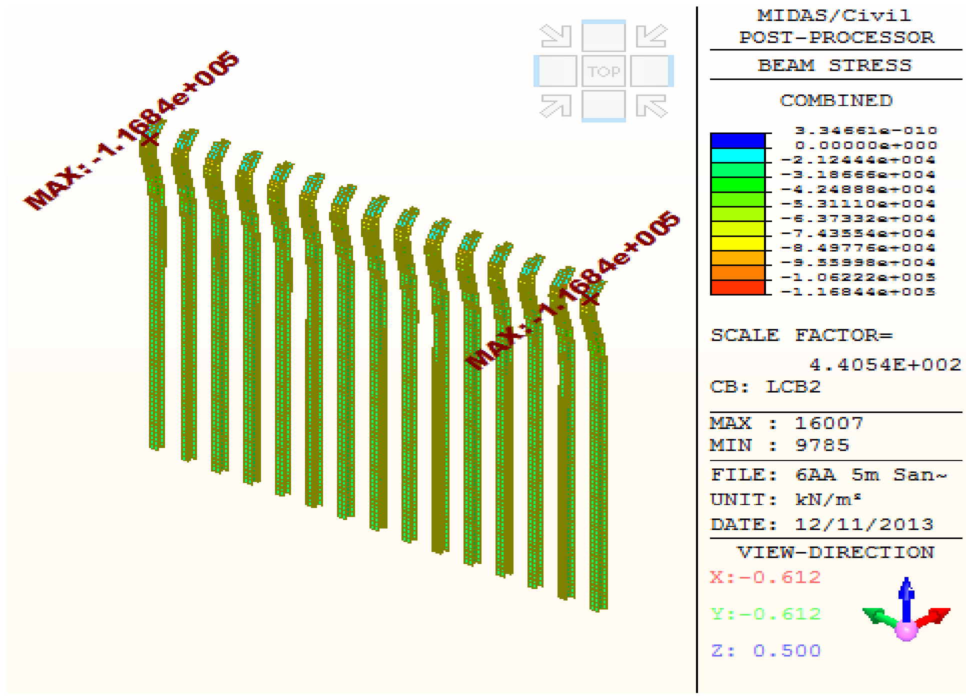
</td></tr>
<tr><th rowspan="2">Abutment</th><th colspan="2">Pile Stress (strong-axis) Unit: kN/m^2</th></tr>
<tr><th>LCB2 (Contraction)</th><th>-1.264E+05</th></tr>
<tr><td>Sand 2</td><td colspan="2">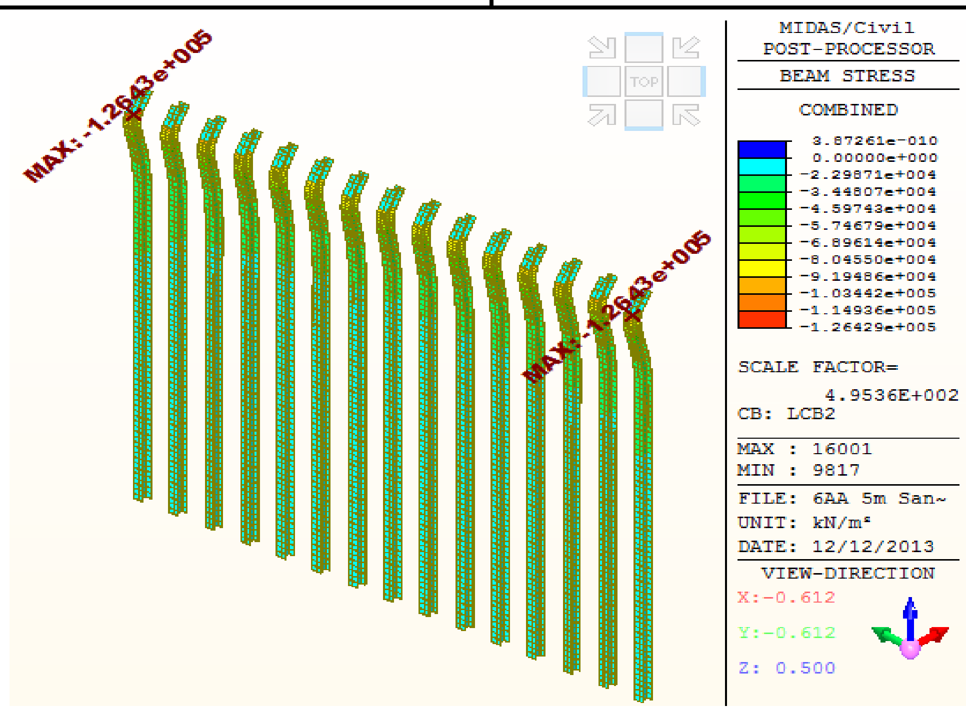
</td></tr>
</table>

<table>
<tr><td rowspan="2">Abutment</td><td colspan="2">Pile Stress (strong-axis) Unit: kN/m^2</td></tr>
<tr><td>LCB2 (Contraction)</td><td>-1.074E+05</td></tr>
<tr><td>Clay 1</td><td colspan="2">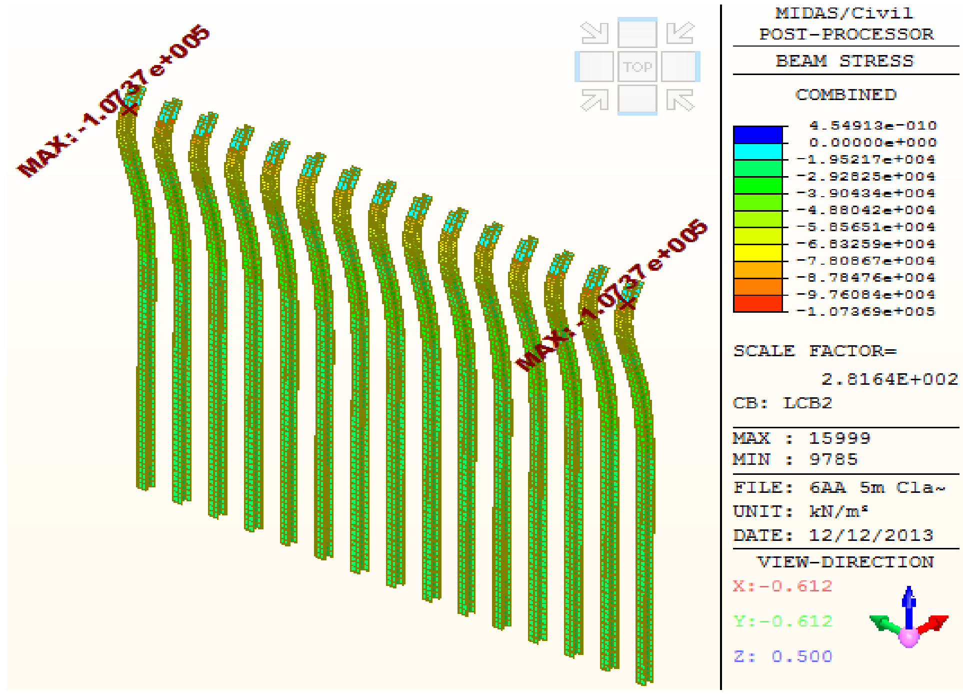
</td></tr>
</table>

<table>
<tr><td rowspan="2">Abutment</td><td colspan="2">Pile Stress (strong-axis) Unit: kN/m^2</td></tr>
<tr><td>LCB2 (Contraction)</td><td>-1.165E+05</td></tr>
<tr><td>Clay 2</td><td colspan="2">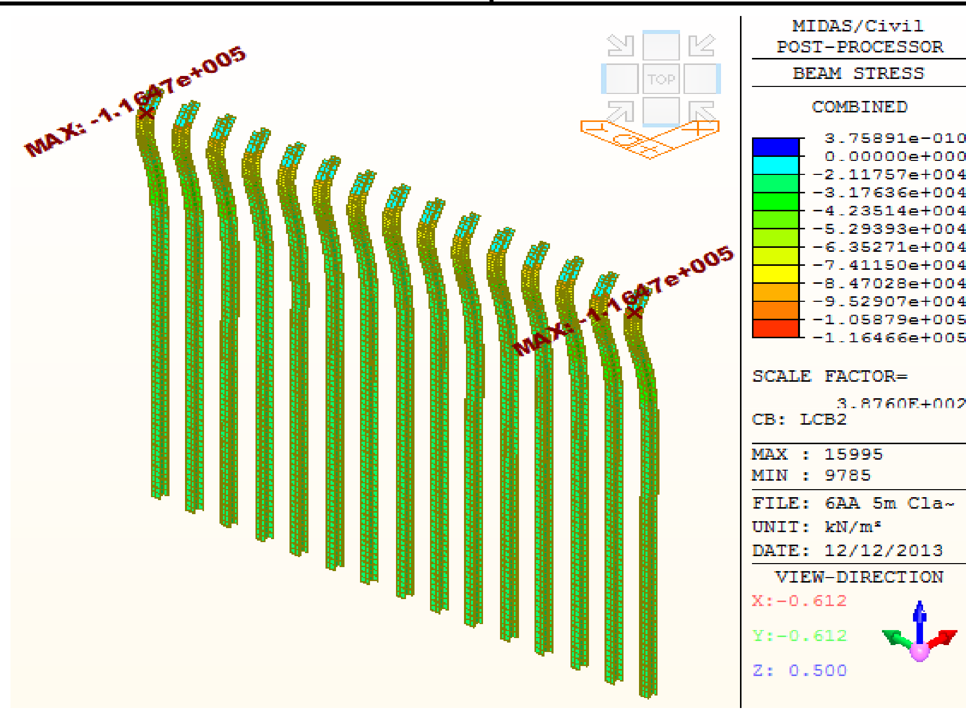
</td></tr>
</table>

2. The Effects depending on Soil Types

2.15. Pile Stress (Pile Orientation: Weak-Axis, Expansion Case)

Pile Stress (weak-axis) LCB1 (Expansion Case) Unit: kN/m^2	
Sand 1	-176400
Sand 2	-154700
Clay 1	-219000
Clay 2	-207600

<table>
<tr><td rowspan="2">Abutment</td><td colspan="2">Pile Stress (weak-axis) Unit: kN/m²</td></tr>
<tr><td>LCB1 (Expansion)</td><td>-1.764E+05</td></tr>
<tr><td>Sand 1</td><td colspan="2">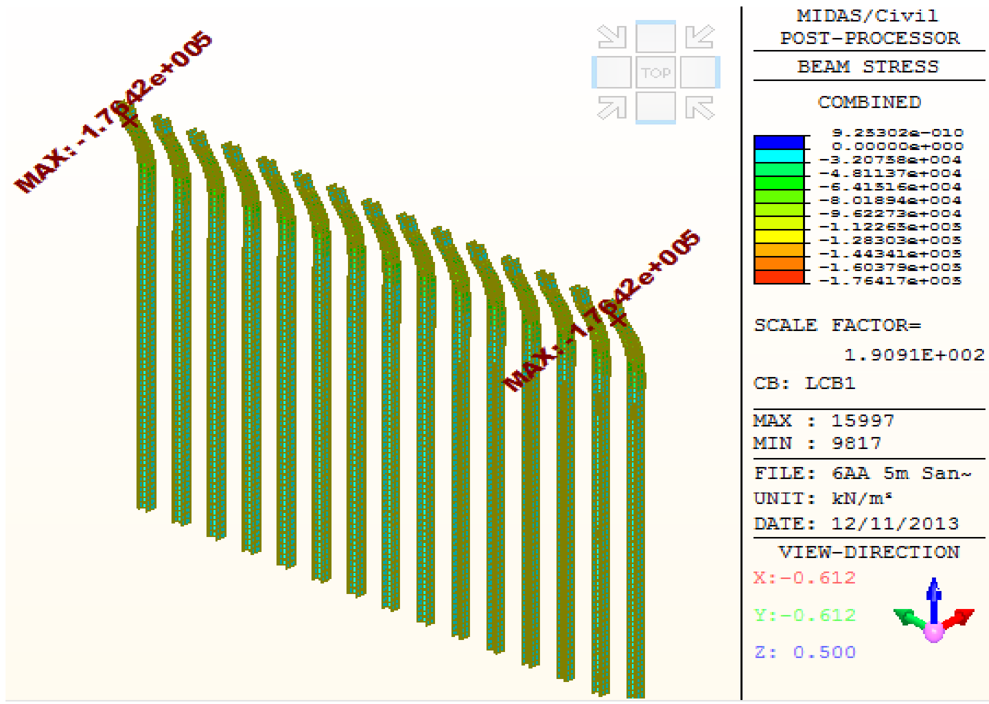
</td></tr>
<tr><td rowspan="2">Abutment</td><td colspan="2">Pile Stress (weak-axis) Unit: kN/m²</td></tr>
<tr><td>LCB1 (Expansion)</td><td>-1.547E+05</td></tr>
<tr><td>Sand 2</td><td colspan="2">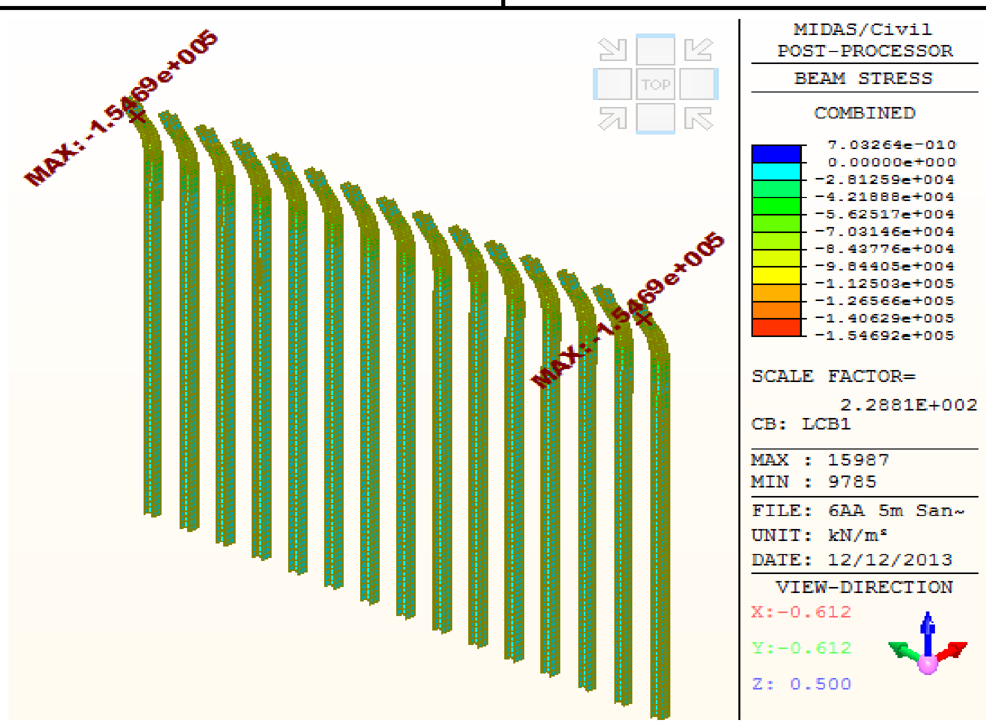
</td></tr>
</table>

<table>
<tr><td rowspan="2">Abutment</td><td colspan="2">Pile Stress (weak-axis) Unit: kN/m^2</td></tr>
<tr><td>LCB1 (Expansion)</td><td>-2.190E+05</td></tr>
<tr><td>Clay 1</td><td colspan="2">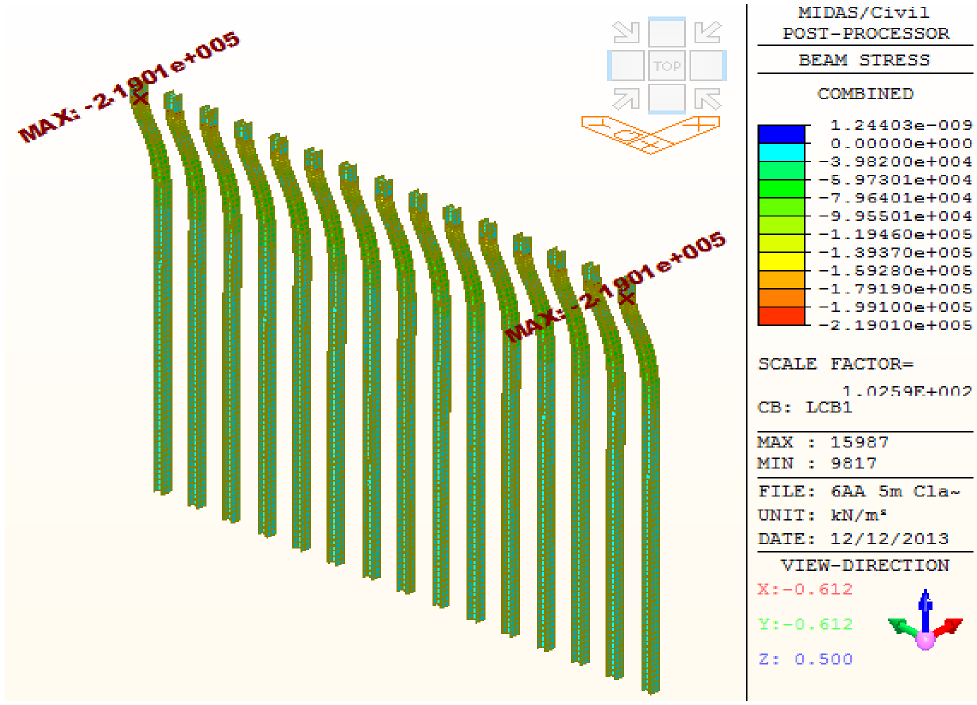
</td></tr>
<tr><td rowspan="2">Abutment</td><td colspan="2">Pile Stress (weak-axis) Unit: kN/m^2</td></tr>
<tr><td>LCB1 (Expansion)</td><td>-2.076E+05</td></tr>
<tr><td>Clay 2</td><td colspan="2">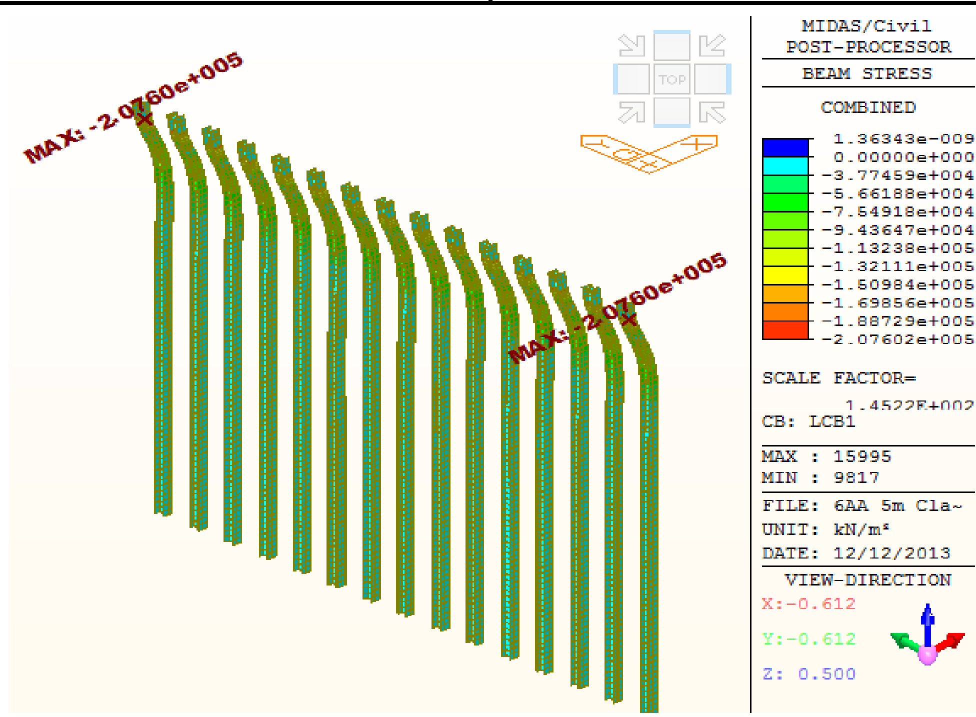
</td></tr>
</table>

2. The Effects depending on Soil Types

2.16. Pile Stress (Pile Orientation: Weak-Axis, Contraction Case)

Pile Stress (weak-axis) LCB2 (Contraction Case) Unit: kN/m^2	
Sand 1	-200700
Sand 2	-220400
Clay 1	-182000
Clay 2	-204400

Abutment	Pile Stress (weak-axis) Unit: kN/m²	
	LCB2 (Contraction)	-2.007E+05
Sand 1	see figure below	

Sand 1

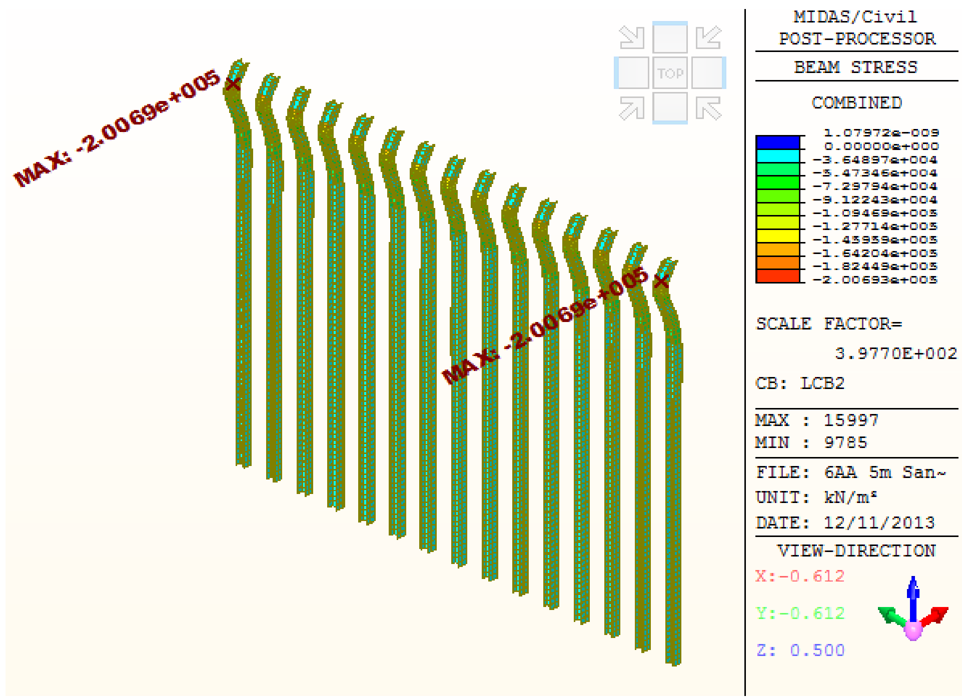

Abutment	Pile Stress (weak-axis) Unit: kN/m²	
	LCB2 (Contraction)	-2.204E+05
Sand 2	see figure below	

Sand 2

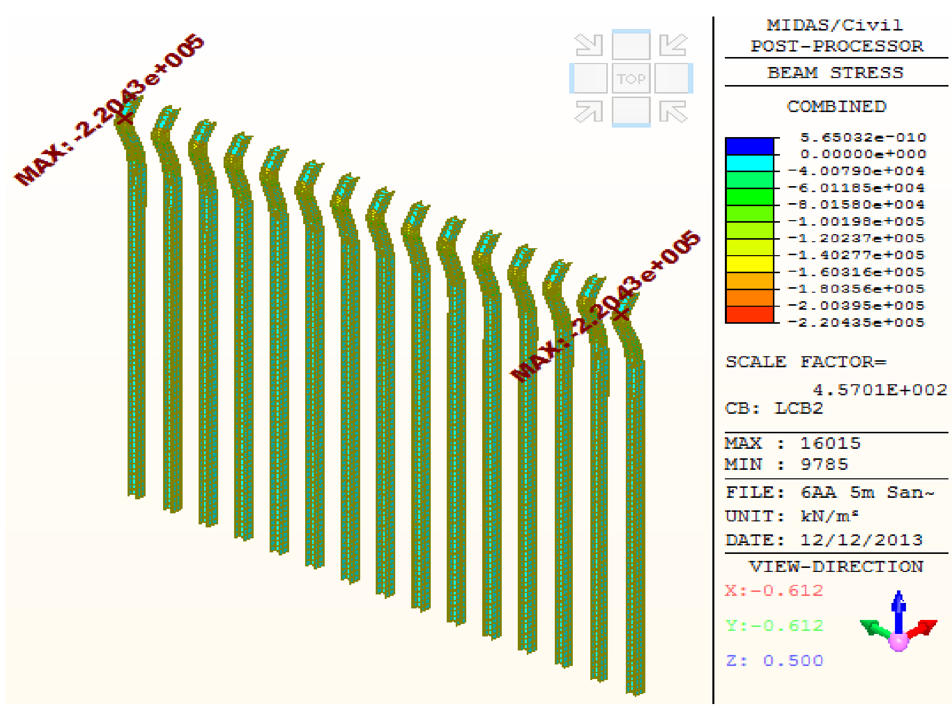

Abutment	Pile Stress (weak-axis) Unit: kN/m^2	
	LCB2 (Contraction)	-1.820E+05
Clay 1	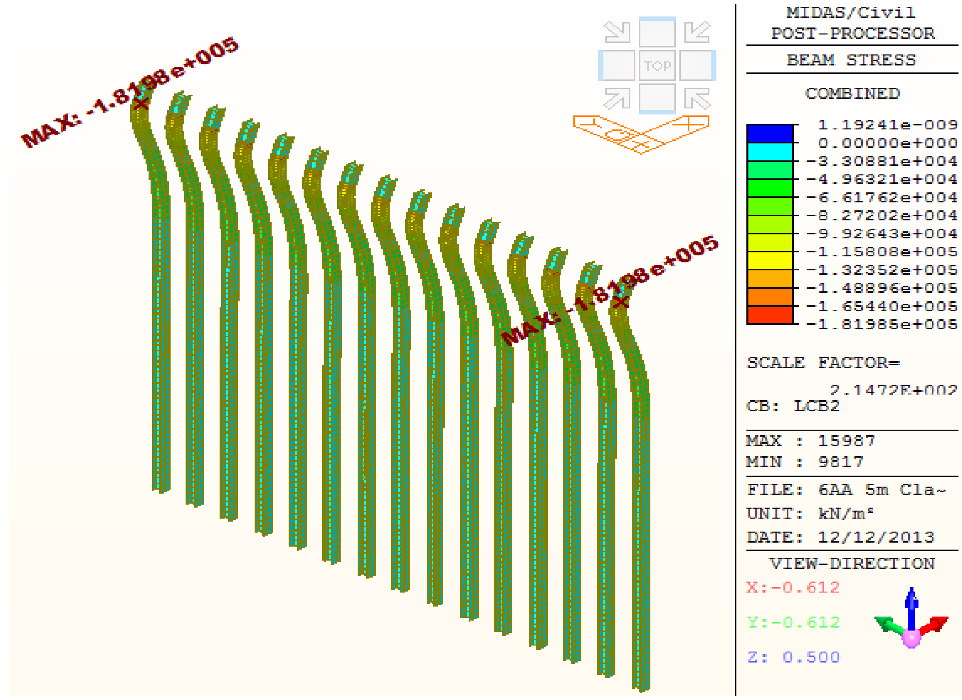	

Abutment	Pile Stress (weak-axis) Unit: kN/m^2	
	LCB2 (Contraction)	-2.044E+05
Clay 2	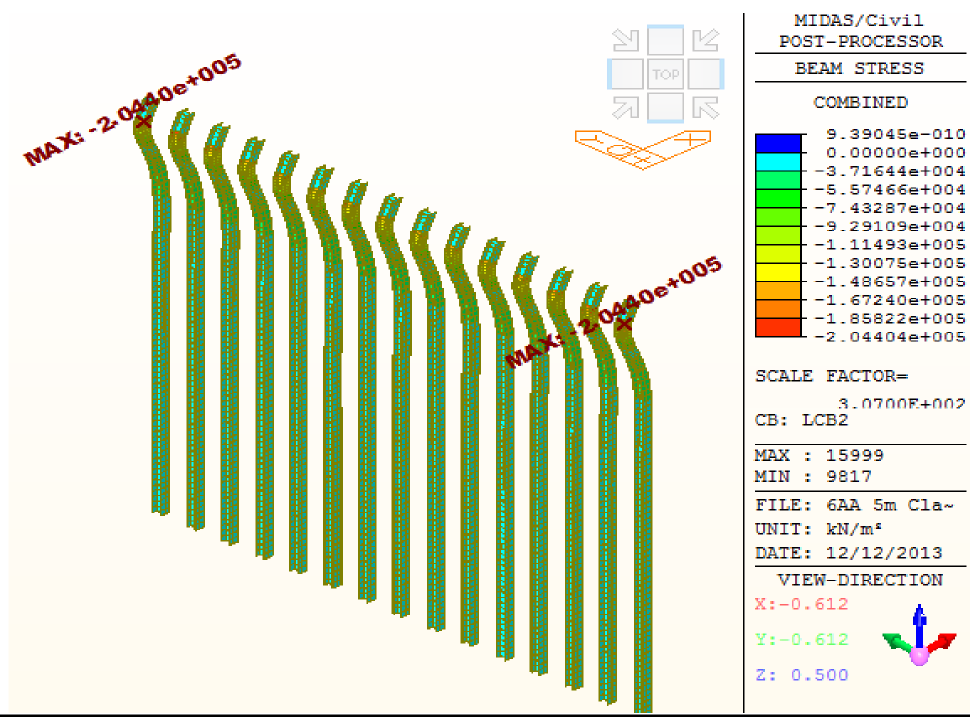	

2. The Effects depending on Soil Types

2.17. Pile Head Displacement (Pile Orientation: Strong-Axis, Expansion Case)

Pile Head Displacement (strong-axis) LCB1 (Expansion Case) Unit: m	
Sand 1	**-0.004057**
Sand 2	**-0.003411**
Clay 1	**-0.007345**
Clay 2	**-0.005178**

<table>
<tr><td rowspan="2">Abutment</td><td colspan="2">Pile Head Displacement (strong-axis) Unit: m</td></tr>
<tr><td>LCB1 (Expansion)</td><td>-4.057E-03</td></tr>
<tr><td>Sand 1</td><td colspan="2">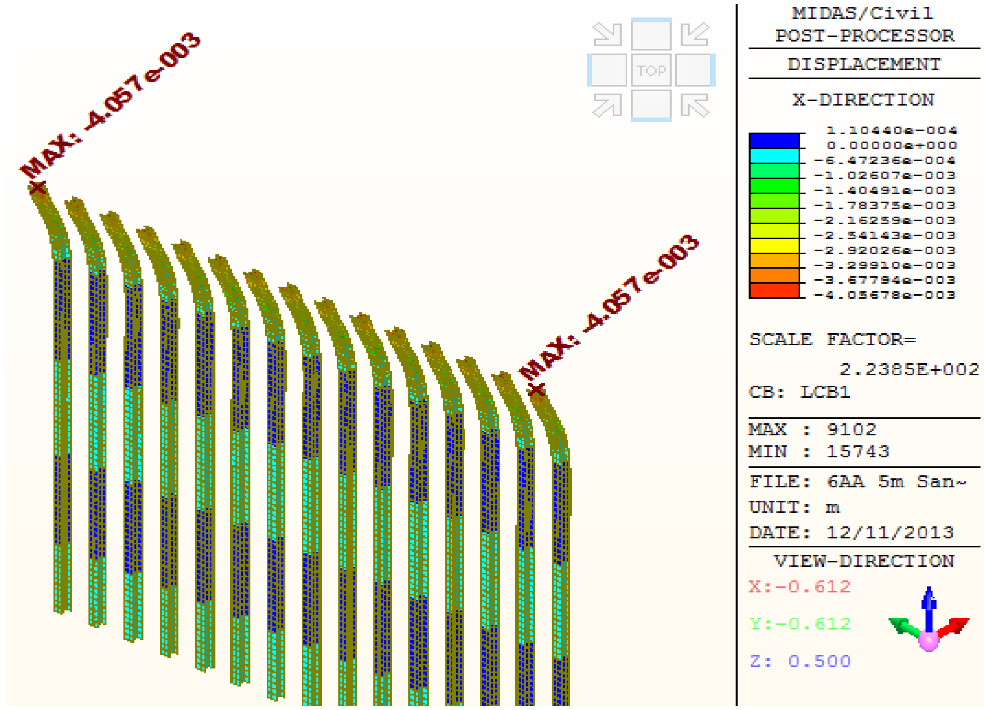
</td></tr>
<tr><td rowspan="2">Abutment</td><td colspan="2">Pile Head Displacement (strong-axis) Unit: m</td></tr>
<tr><td>LCB1 (Expansion)</td><td>-3.411E-03</td></tr>
<tr><td>Sand 2</td><td colspan="2">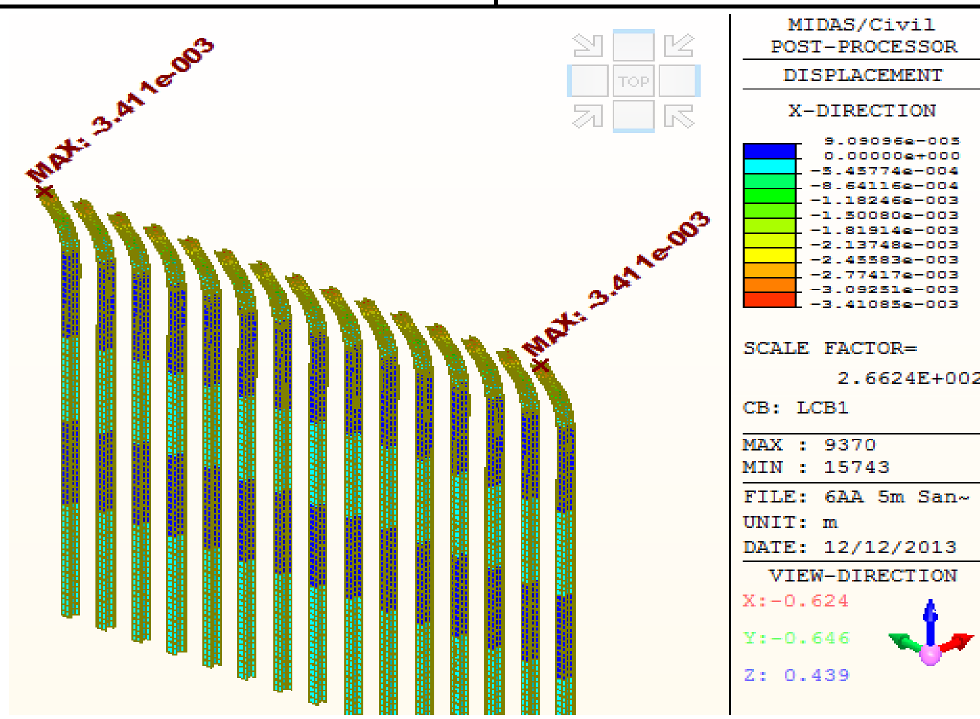
</td></tr>
</table>

<table>
<tr><td rowspan="2">Abutment</td><td colspan="2">Pile Head Displacement (strong-axis)   Unit: m</td></tr>
<tr><td>LCB1 (Expansion)</td><td>-7.345E-03</td></tr>
<tr><td>Clay 1</td><td colspan="2">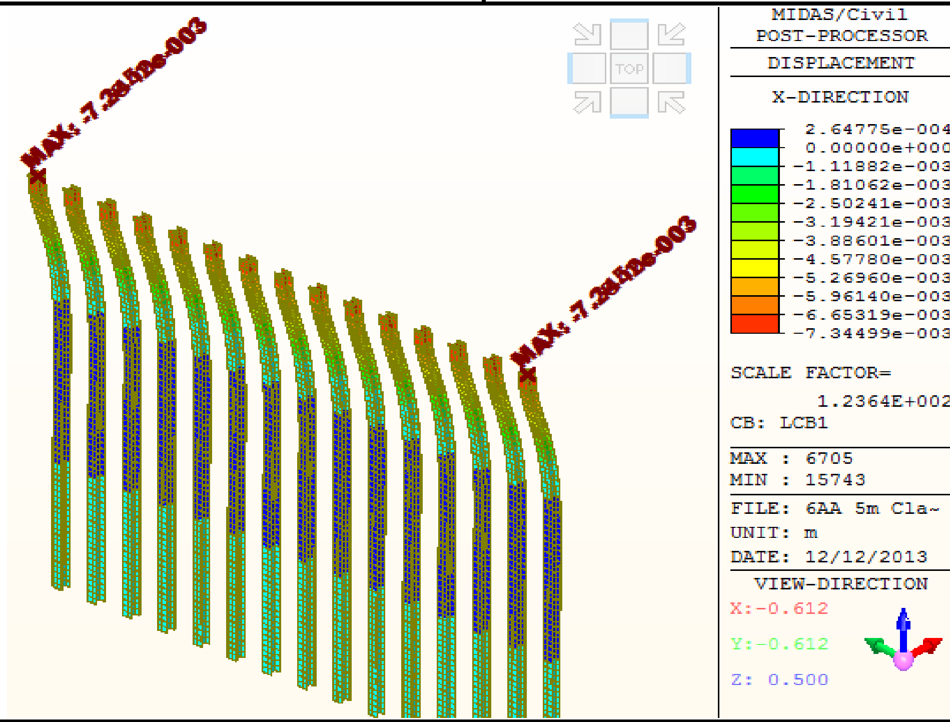
</td></tr>
<tr><td rowspan="2">Abutment</td><td colspan="2">Pile Head Displacement (strong-axis)   Unit: m</td></tr>
<tr><td>LCB1 (Expansion)</td><td>-5.178E-03</td></tr>
<tr><td>Clay 2</td><td colspan="2">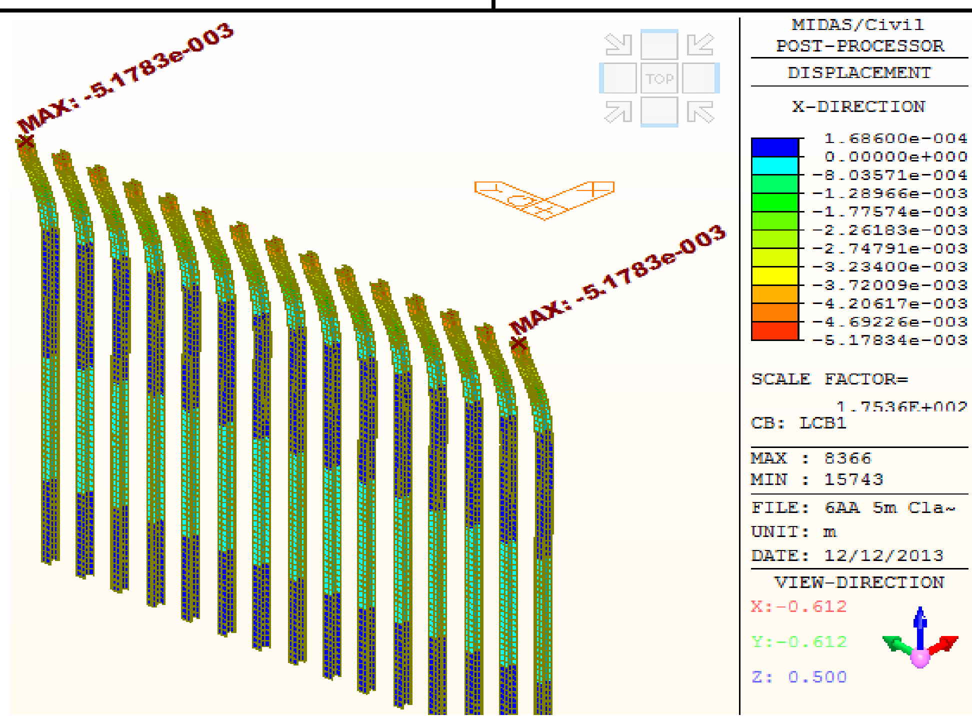
</td></tr>
</table>

2. The Effects depending on Soil Types

2.18. Pile Head Displacement (Pile Orientation: Strong-Axis, Contraction Case)

Pile Head Displacement (strong-axis) LCB2 (Contraction Case) Unit: m	
Sand 1	0.0002291
Sand 2	0.000241
Clay 1	-0.001136
Clay 2	-0.0004021

Abutment	Pile Head Displacement (strong-axis) Unit: m	
	LCB2 (Contraction)	2.291E-04
Sand 1	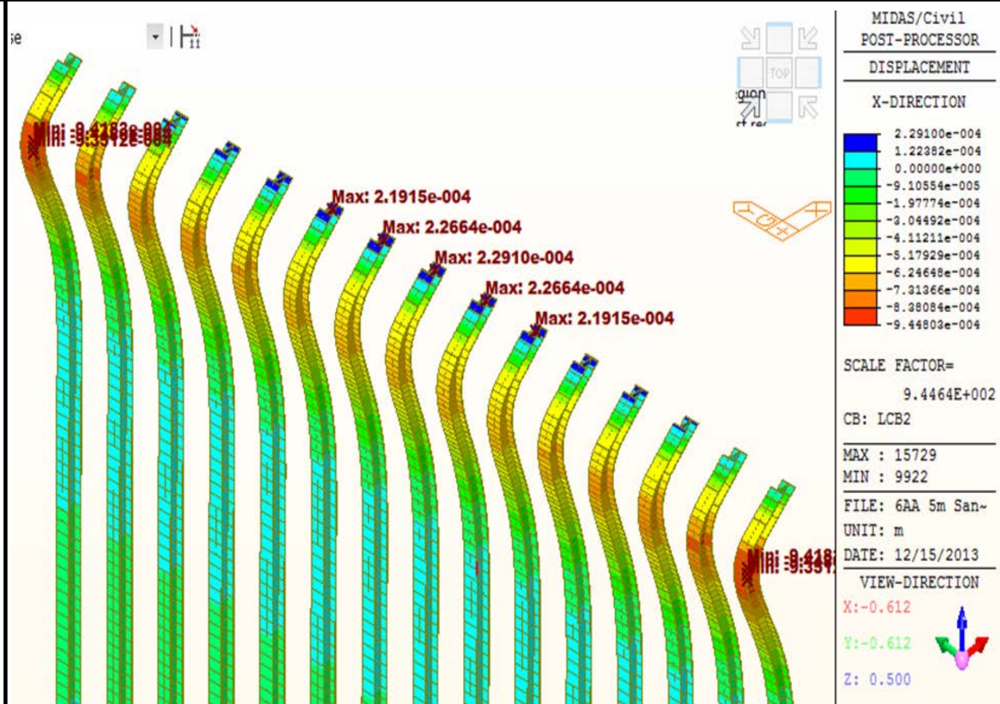	

Abutment	Pile Head Displacement (strong-axis) Unit: m	
	LCB2 (Contraction)	2.410E-04
Sand 2	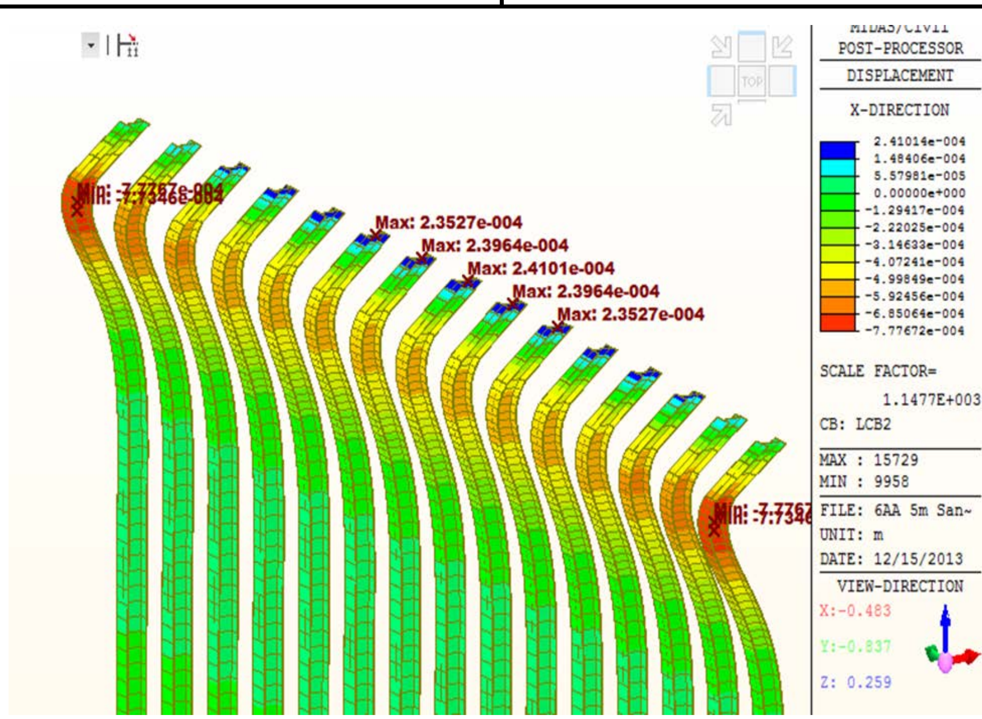	

<table>
<tr><td rowspan="2">Abutment</td><td colspan="2">Pile Head Displacement (strong-axis) Unit: m</td></tr>
<tr><td>LCB2 (Contraction)</td><td>-1.136E-03</td></tr>
<tr><td>Clay 1</td><td colspan="2">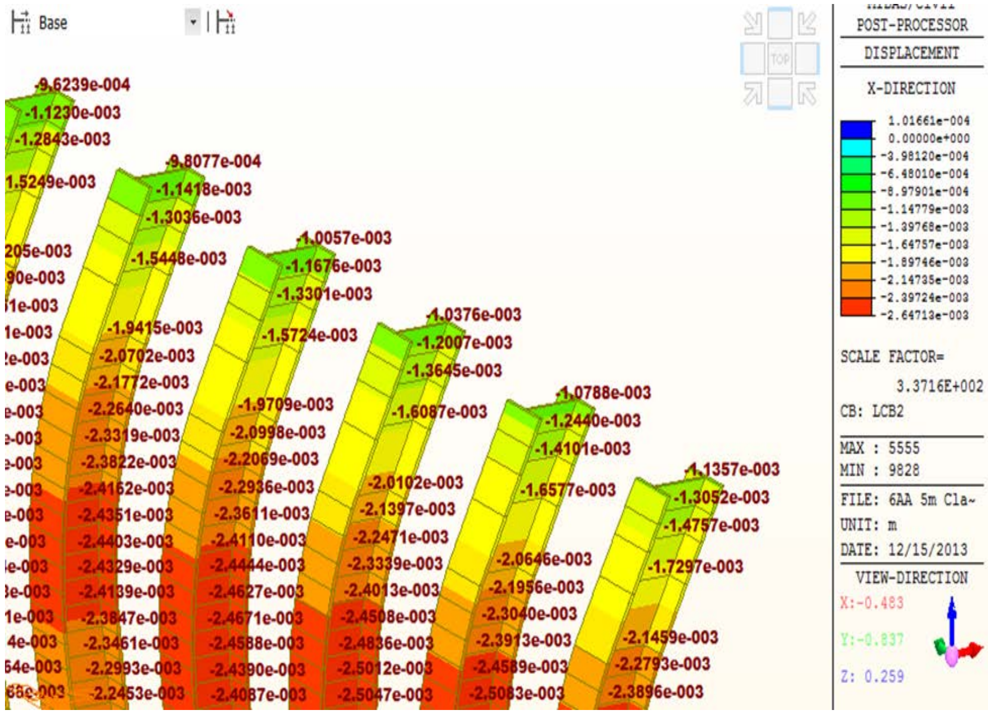
</td></tr>
<tr><td rowspan="2">Abutment</td><td colspan="2">Pile Head Displacement (strong-axis) Unit: m</td></tr>
<tr><td>LCB2 (Contraction)</td><td>-4.021E-04</td></tr>
<tr><td>Clay 2</td><td colspan="2">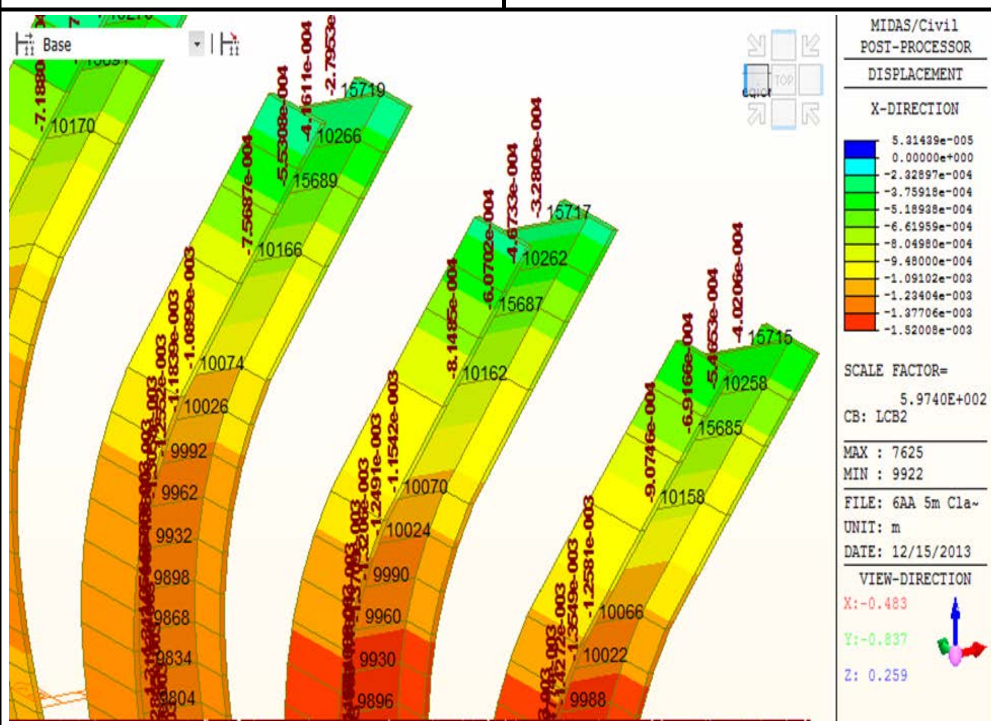
</td></tr>
</table>

2. The Effects depending on Soil Types

2.19. Pile Head Displacement (Pile Orientation: Weak-Axis, Expansion Case)

Pile Head Displacement (weak-axis) LCB1 (Expansion Case) Unit: m	
Sand 1	-0.004296
Sand 2	-0.003515
Clay 1	-0.008608
Clay 2	-0.005929

Abutment	Pile Head Displacement (weak-axis) Unit: m	
	LCB1 (Expansion)	-4.296E-03
Sand 1	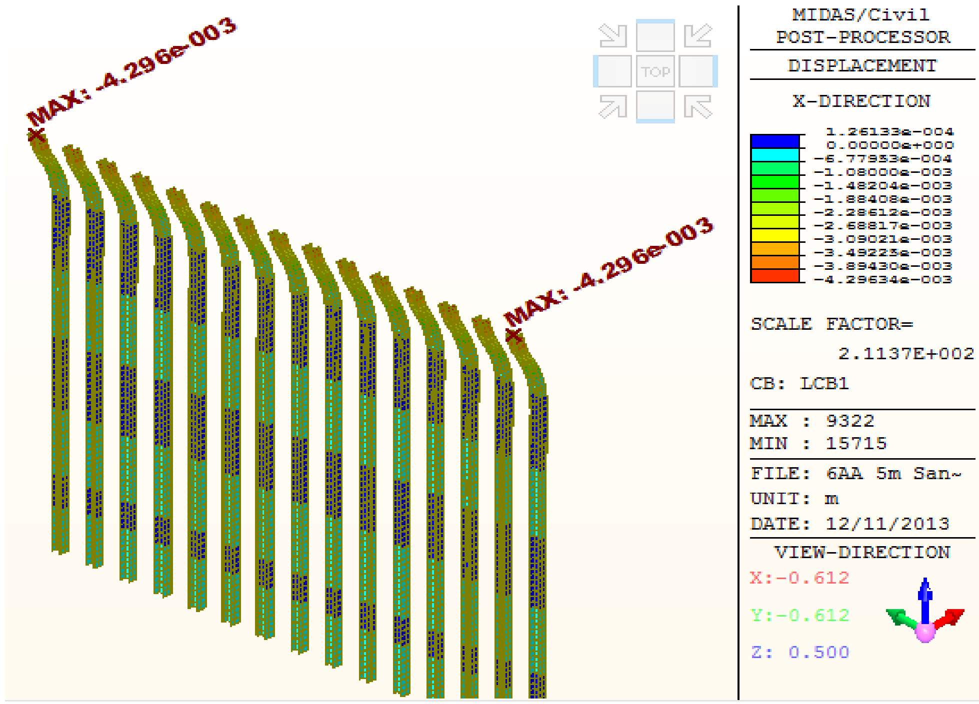	

Abutment	Pile Head Displacement (weak-axis) Unit: m	
	LCB1 (Expansion)	-3.515E-03
Sand 2	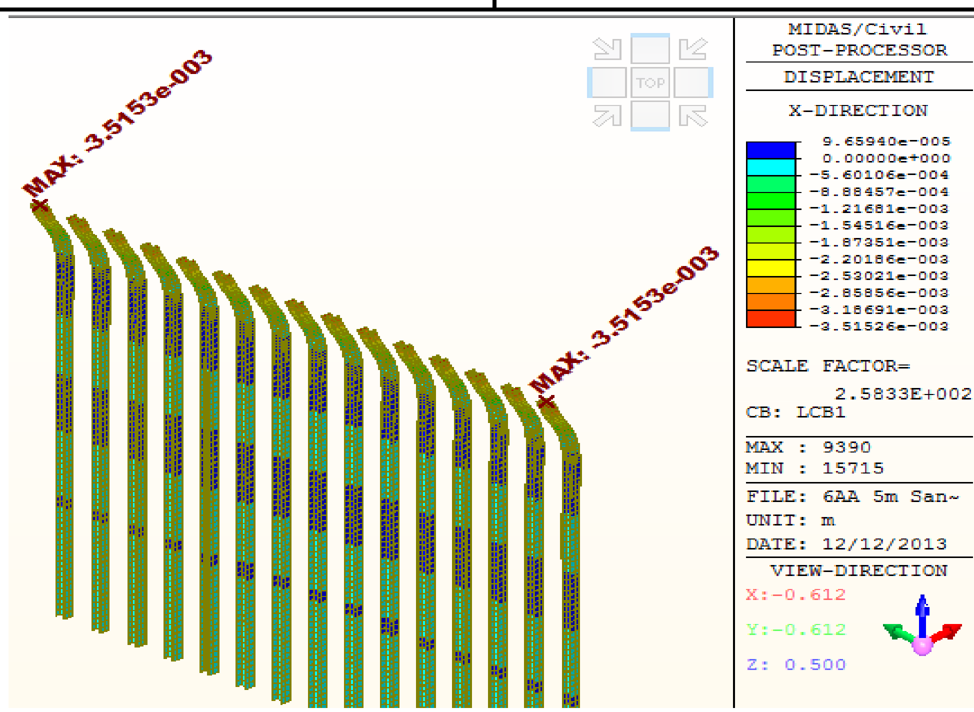	

<table>
<tr><td rowspan="2">Abutment</td><td colspan="2">Pile Head Displacement (weak-axis) Unit: m</td></tr>
<tr><td>LCB1 (Expansion)</td><td>-8.608E-03</td></tr>
<tr><td>Clay 1</td><td colspan="2">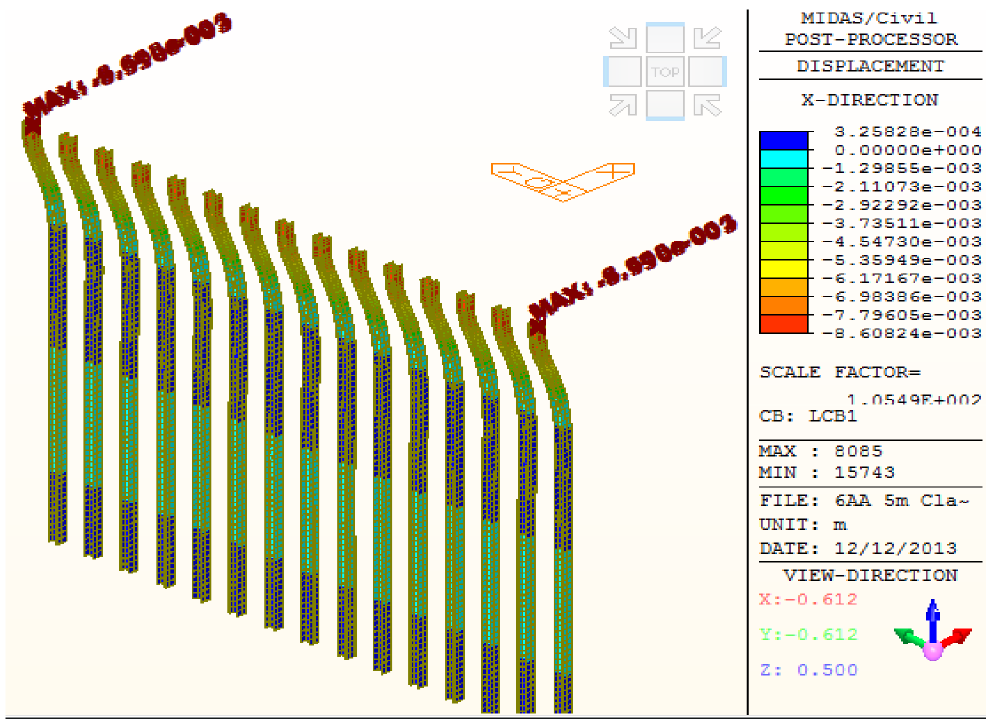
</td></tr>
<tr><td rowspan="2">Abutment</td><td colspan="2">Pile Head Displacement (weak-axis) Unit: m</td></tr>
<tr><td>LCB1 (Expansion)</td><td>-5.929E-03</td></tr>
<tr><td>Clay 2</td><td colspan="2">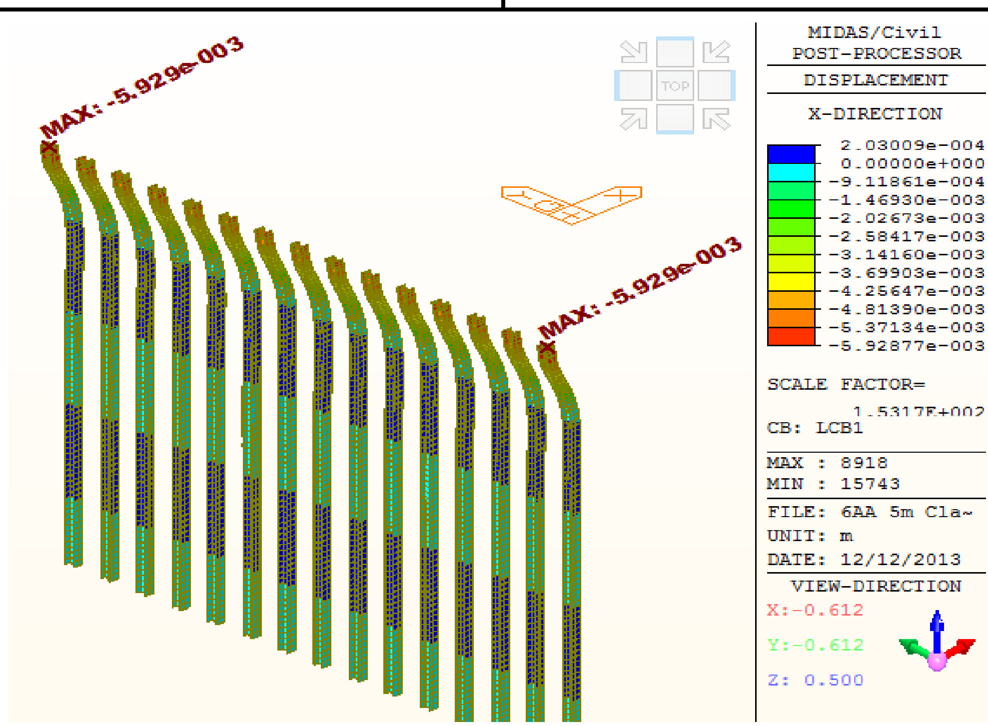
</td></tr>
</table>

2. The Effects depending on Soil Types

2.20. Pile Head Displacement (Pile Orientation: Weak-Axis, Contraction Case)

Pile Head Displacement (weak-axis) LCB2 (Contraction Case) Unit: m	
Sand 1	-0.0003409
Sand 2	-0.0002131
Clay 1	-0.00222
Clay 2	-0.001155

<table>
<tr><td rowspan="2">Abutment</td><td colspan="2">Pile Head Displacement (weak-axis)   Unit: m</td></tr>
<tr><td>LCB2 (Contraction)</td><td>-3.409E-04</td></tr>
<tr><td>Sand 1</td><td colspan="2">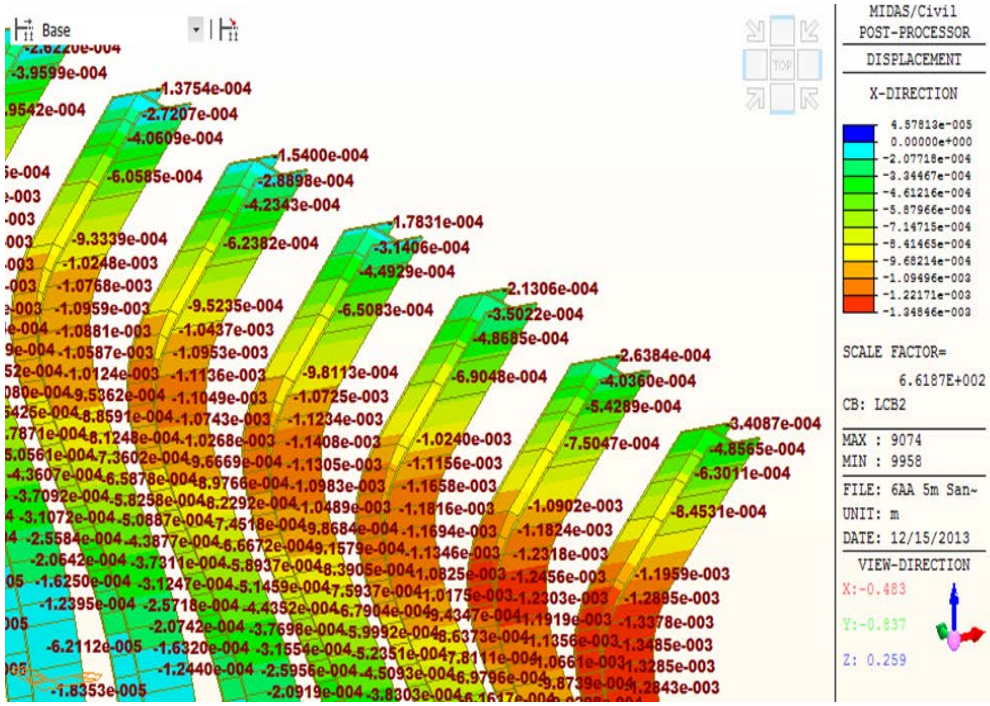
</td></tr>
<tr><td rowspan="2">Abutment</td><td colspan="2">Pile Head Displacement (weak-axis)   Unit: m</td></tr>
<tr><td>LCB2 (Contraction)</td><td>-2.131E-04</td></tr>
<tr><td>Sand 2</td><td colspan="2">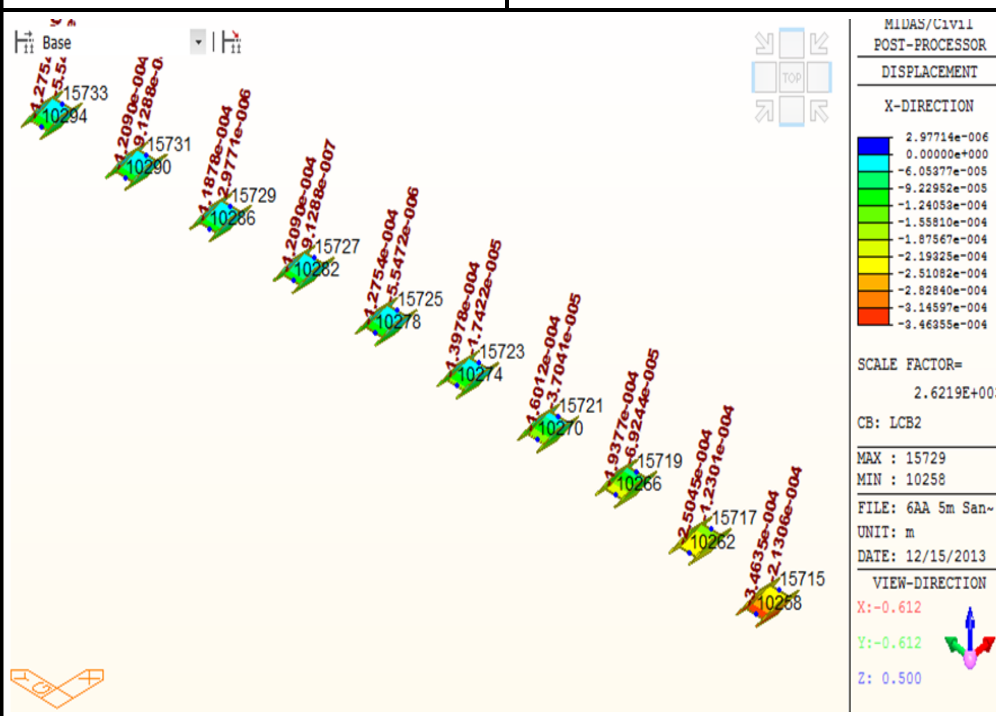
</td></tr>
</table>

<table>
<tr><td rowspan="2">Abutment</td><td colspan="2">Pile Head Displacement (weak-axis) Unit: m</td></tr>
<tr><td>LCB2 (Contraction)</td><td>-2.220E-03</td></tr>
<tr><td>Clay 1</td><td colspan="2">
</td></tr>
<tr><td rowspan="2">Abutment</td><td colspan="2">Pile Head Displacement (weak-axis) Unit: m</td></tr>
<tr><td>LCB2 (Contraction)</td><td>-1.155E-03</td></tr>
<tr><td>Clay 2</td><td colspan="2">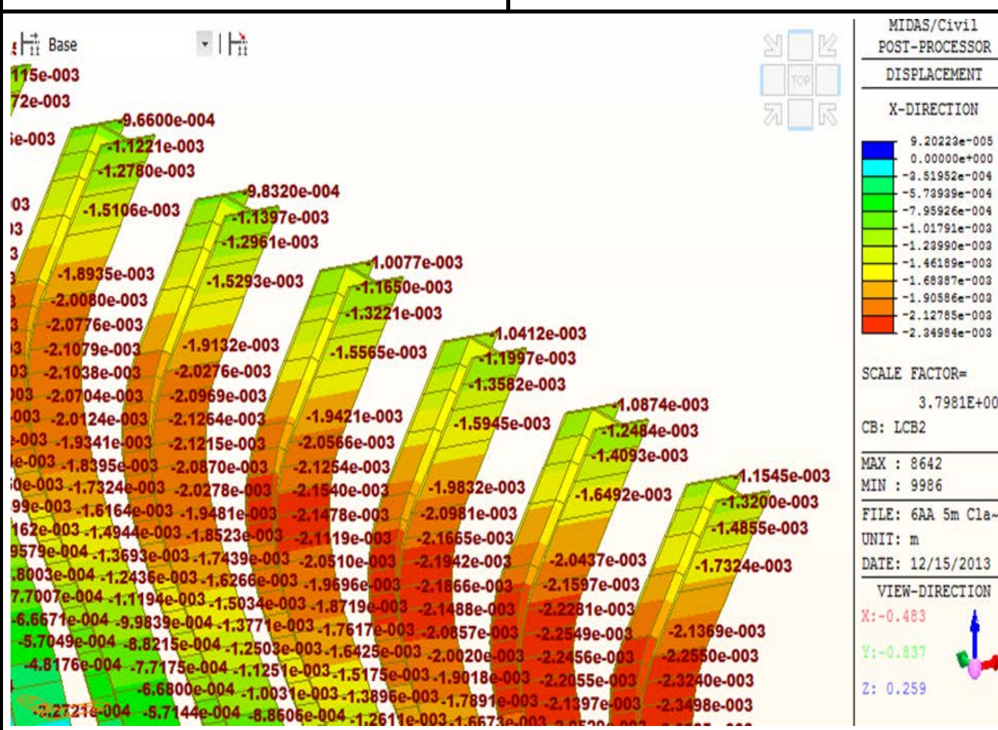
</td></tr>
</table>